Vol. 110 No. 1, October 1, 1979 ISSN 0003-2670

ANALYTICA CHIMICA ACTA

International journal devoted to all branches of analytical chemistry

ELSEVIER SCIENTIFIC PUBLISHING COMPANY

ANALYTICA CHIMICA ACTA

International journal devoted to all branches of analytical chemistry
Revue internationale consacrée à tous les domaines de la chimie analytique
Internationale Zeitschrift für alle Gebiete der analytischen Chemie

PUBLICATION SCHEDULE FOR 1979 (incorporating the section on Computer Techniques and Optimization).

	J	F	M	A	M	J	J	A	S	O	N	D
Analytica Chimica Acta	104/1	104/2	105	106/1	106/2	107	108	109/1	109/2	110/1	110/2	111
Section on Computer Techniques and Optimization			112/1			112/2			112/3			112/4

Scope. *Analytica Chimica Acta* publishes original papers, short communications, and reviews dealing with every aspect of modern chemical analysis, both fundamental and applied. The section on *Computer Techniques and Optimization* is devoted to new developments in chemical analysis by the application of computer techniques and by interdisciplinary approaches, including statistics, systems theory and operation research. The section deals with the following topics: Computerized acquisition, processing and evaluation of data. Computerized methods for the interpretation of analytical data including chemometrics, cluster analysis, and pattern recognition. Storage and retrieval systems. Optimization procedures and their application. Automated analysis for industrial processes and quality control. Organizational problems.

Submission of Papers. Manuscripts (three copies) should be submitted to:
for *Analytica Chimica Acta:* Dr. A. M. G. Macdonald, Department of Chemistry, The University, P.O. Box 363, Birmingham B15 2TT, England;
for the section on *Computer Techniques and Optimization:* Dr. J. T. Clerc, Universität Bern, Pharmazeutisches Institut, Sahlistrasse 10, CH-3012 Bern, Switzerland.

Information for Authors. Papers in English, French and German are published. There are no page charges. Manuscripts should conform in layout and style to the papers published in this Volume. Authors should consult Vol. 102, p. 253 for detailed information. Reprints of this information are available from the Editors or from: Elsevier Editorial Services Ltd., Mayfield House, 256 Banbury Road, Oxford OX2 7DE (Great Britain).

Reprints. Fifty reprints will be supplied free of charge. Additional reprints (minimum 100) can be ordered. An order form containing price quotations will be sent to the authors together with the proofs of their article.

Advertisements. Advertisement rates are available from the publisher.

Subscriptions. Subscriptions should be sent to: Elsevier Scientific Publishing Company, P.O. Box 211, 1000 AE Amsterdam, The Netherlands. The section on *Computer Techniques and Optimization* can be subscribed to separately.

Publication. *Analytica Chimica Acta* (including the section on *Computer Techniques and Optimization*) appears in 9 volumes in 1979. The subscription for 1979 (Vols. 104–112) is Dfl. 1179.00 plus Dfl. 135.00 (postage) (total approx. U.S. $641.00). The subscription for the *Computer Techniques and Optimization* section only (Vol. 112) is Dfl. 131.00 plus Dfl. 15.00 (postage) (total approx. U.S. $71.00). Journals are sent automatically by air mail to the U.S.A. and Canada at no extra cost and to Japan, Australia and New Zealand for a small additional postal charge. All earlier volumes (Vols. 1–95) except Vols. 23 and 28 are available at Dfl. 144.00 (U.S. $70.00), plus Dfl. 10.00 (U.S. $5.00) postage and handling, per volume.

Claims for issues not received should be made within three months of publication of the issue, otherwise they cannot be honoured free of charge.

Customers in the U.S.A. and Canada who wish to obtain additional bibliographic information on this and other Elsevier journals should contact Elsevier/North Holland Inc., Journal Information Center, 52 Vanderbilt Avenue, New York, NY 10017. Tel: (212) 867-9040.

ANALYTICA CHIMICA ACTA
VOL. 110 (1979)

ANALYTICA CHIMICA ACTA

International journal devoted to all branches of analytical chemistry

ELSEVIER SCIENTIFIC PUBLISHING COMPANY

Anal. Chim. Acta, Vol. 110 (1979)

Printed in The Netherlands.

Analytica Chimica Acta, 110 (1979) 1—7

COMBINED FURNACE—FLAME NON-DISPERSIVE ATOMIC FLUORESCENCE SPECTROMETRY FOR DIRECT SIMULTANEOUS MULTI-ELEMENT ANALYSIS OF AIR FILTERS

J. IP, Y. THOMASSEN,** L. R. P. BUTLER,*** B. RADZIUK, and J. C. VAN LOON*

Departments of Geology and Chemistry and Institute for Environmental Studies, University of Toronto, Toronto M5S 1A1 (Canada)

(Received 6th April 1979)

SUMMARY

Furnace volatilization followed by atomization in the flame of a non-dispersive atomic fluorescence spectrometer is used for the direct, simultaneous, multi-element determination of Zn, Cd, Pb and Fe on air filter papers. Standardization is done by using blank filter papers impregnated with standard metal solutions. The results agree well with those obtained by a standard atomic absorption procedure.

Two important goals for the elemental analysis of solids are the possibility of direct analysis of solids so as to avoid the time-consuming and error-prone steps of wet chemical sample preparation, and the capability for simultaneous multi-element analysis. For trace metals atomic absorption spectrometry (a.a.s.) is the analytical technique most commonly employed because of its relative simplicity of operation and low cost. However, commercially available a.a.s. equipment is usually capable of only single-element operation. In addition, analyses are generally done on liquid samples, the analysis of solids being difficult and error-prone.

Of the other atomic spectrometric techniques, arc or spark emission spectrometry can be used for multi-element analysis of solid samples. However, this is a more complicated technique, requiring the attention of a highly trained operator. In addition, the equipment and facilities are expensive.

Atomic fluorescence spectrometry (a.f.s.) has the same relative freedom from atomic spectral interferences as a.a.s. If non-dispersive a.f.s. is used, simultaneous multi-element analysis is possible and the cost of equipment is relatively low. However, a major potential drawback to non-dispersive a.f.s. is the scatter of incident radiation by particles in the atomizer.

In a.a.s. and a.f.s. there is no generally accepted, widely applicable method

---

**On leave from Institute of Occupational Health, Oslo, Norway.
***On leave from National Physical Research Laboratory, CSIR, Pretoria, South Africa.

for the direct analysis of solids. A slurry of solids has been successfully nebulized into the flame of an atomic absorption unit [1, 2] but this approach has not received widespread acceptance. Starting with L'vov [3], several reports have appeared on the direct analysis of solids by electrothermal a.a.s. However, the complex volatilization interferences and very large non-specific background effects are a serious drawback to this approach. L'vov [4] proposed a capsule-in-flame technique which reduces the magnitude of the background interferences, but this method requires a specially designed furnace which is not commercially available. Koop et al. [5] employed a combined furnace—flame a.a.s. approach to the analysis of solid samples; this takes advantage of the superiority of the flame as an atomizer while retaining the capability of the furnace to handle solid samples. Non-specific background interferences were found to be negligible. In the following report a combined furnace—flame, non-dispersive a.f.s. system is described and evaluated for the direct simultaneous determination of Pb, Cd, Zn and Fe on air filters.

EXPERIMENTAL

Equipment

A Perkin-Elmer HGA 2000 furnace is used to volatilize the solid sample which is carried as an aerosol in argon carrier gas into the flame of a non-dispersive atomic fluorescence spectrometer. The arrangement is shown in Fig. 1. A transfer tube (7 mm i.d., 12 cm long) extends from the end of the furnace into the flame. A Teflon O-ring is fitted over one of the Teflon end pieces of the furnace. A machined aluminium cap is constructed to seal over the O-ring. A small diameter aluminium tube, machined in the centre of the cap, is attached to Tygon tubing coming from the argon cylinder. A machined graphite plug is placed at the other end of the furnace. The quartz transfer tube is fitted with an O-ring seal into a hole drilled in the centre of this graphite plug.

Grooved tubes are used in the furnace. The grooves prevent the unvolatilized sample from being blown into the transfer line during the pressure pulse which occurs on heating. The sample is placed in the middle of the grooved tube with a Perkin-Elmer solid-sampling tool.

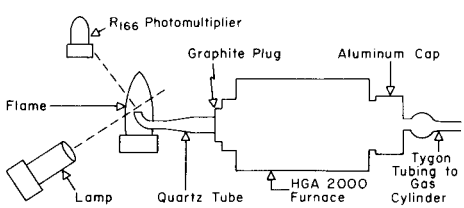

Fig. 1. Schematic diagram of instrumental arrangement.

The non-dispersive atomic fluorescence unit consists of a Perkin-Elmer Model 303 burner chamber—nebulizer system and gas box equipped with a circular sheathed burner head similar to that described by Larkins [6]. A nitrogen-separated air—acetylene flame was used. Hollow-cathode lamps (Perkin-Elmer) and electrodeless discharge lamps (Westinghouse and Perkin-Elmer) were pulsed in 1:16 and 1:8 duty cycles, respectively, synchronized with an 8-channel gated detector. Suprasil lenses (40 mm diameter, 50 mm focal length) were used. An R166 solar-blind photomultiplier was employed in the 200—300-nm wavelength range. Output was obtained on two dual-pen recorders.

Air filter samples were used for detailed study. Whatman no. 42 filter paper was used to trap air particulates (less than 10-μm particle size) from downtown air in Toronto. The filter head was pointed towards the ground to avoid catching large grains of particulate (blowing soil, etc.).

Reagents

A stock solution of mixed metals (Zn, Cd, Pb and Fe, 1000 $\mu g\ ml^{-1}$ each) was prepared by separately dissolving the pure metals in a minimum amount of nitric acid, combining the solutions and diluting to volume with distilled water. The final nitric acid content was 1%. Working standard solutions were prepared by appropriate dilution of the stock solution, the final acid content being maintained at 1%.

Recommended procedure for air filter analysis

Using a stainless steel office punch, obtain 3-mm discs from exposed or blank air filters. Place a clean filter paper over these air filters to minimize contamination during this operation. With plastic forceps transfer a disc to the solid sampling tool. Introduce the disc into the centre of the grooved graphite furnace tube. Cap the end of the furnace and initiate the argon carrier gas flow at 300 $cm^3\ min^{-1}$. Set the furnace power supply to give the following heating cycle: dry at 125°C for 20 s (only needed for standards), ash at 300°C for 20 s and volatilize at 2300°C for 5 s. Turn on all components of the flame atomic fluorescence unit. Adjust the nitrogen-sheathed air—acetylene flame to be slightly lean. Run the sample by initiating the furnace program. Standards are run in an identical fashion to the above except that 1-μl aliquots of appropriate concentrations of standard solutions are added to a blank filter disc before insertion into the furnace.

DEVELOPMENT OF METHODOLOGY

Light scatter

The combined furnace-flame approach was chosen to minimize errors caused by light scatter. Scatter of source radiation by particles in the atomizer is a potentially serious problem with atomic fluorescence spectrometry, particularly non-dispersive a.f.s.

Scatter was measured by using a mercury electrodeless discharge lamp as radiation source. Mercury was either not in the samples or was removed during ashing. A 10 mg ml^{-1} aluminium solution was aspirated, and the lamp intensity was adjusted to give a signal similar to that obtained on the analyte channels. Air filters were then analyzed. For atomization times of less than 10 s, light scatter was insignificant. This speaks well for the strategy of using the furnace as the volatilizer and the flame as the atomizer. Longer atomization times, however, resulted in the release of carbon particles into the flame causing appreciable light scatter. An atomization time of 5 s was found to be adequate.

Shot noise

A gated detector is employed to prevent emission from the atomizer from registering as signal, but shot noise can be a serious problem in non-dispersive atomic fluorescence. Use of the furnace as atomizer was avoided not only because of light scatter but because the intense furnace emission during atomization of most elements resulted in excessive noise levels.

Operating parameters

Of the elements analyzed, zinc was found to be lost at the lowest temperature from air filter samples. This limited the ashing temperature to less than 300°C. An ashing time of 20 s was adequate. Drying was not necessary for the exposed filters but filter papers treated with standard solutions were dried at 125°C for 20 s. The volatilization temperature must be high enough to release the least volatile element, in this case iron. A suitable volatilization temperature was 2300°C, for 5 s.

Argon was used as the carrier gas but nitrogen would also be satisfactory. The signal is affected by the carrier gas flow rate. Condensation occurs in the transfer tube which reduces the amount of analyte reaching the flame. A rapid flow rate minimizes condensation but causes the flame to burn unsteadily. In addition, high flow rates can cause the filter disc to be entrained in the carrier gas prior to vaporization. A carrier gas flow rate of 300 cm^3 min^{-1} was found to be best.

Standardization

It would be highly desirable to standardize by simply introducing a mixed metal standard solution directly into the furnace. However, since volatilization is matrix-dependent, release of the metals from the residue of exposed filters may occur quite differently than from the dried residue of a standard solution. Chemical interference in the flame might also be a problem.

To investigate potential trouble from these sources, atomization peaks for each element were traced with a recorder at a chart speed of 40 mm s^{-1}, from standard solutions, blank filters plus standard solutions, exposed air filters and exposed air filters plus standard solutions. Figure 2 is a typical set

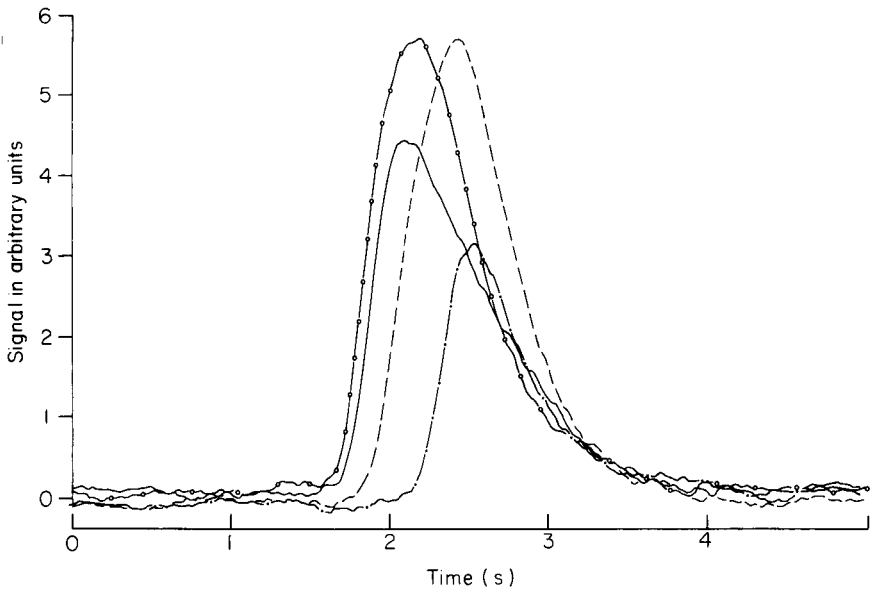

Fig. 2. Atomization tracings for lead: (···) standard solution alone; (-o-) standard solution on blank air filter; (—) exposed air filter; (———) standard solution on exposed air filter.

of tracings for lead. A significant difference in peak position and shape is noted for the various traces. The peak for the standard solution alone is sharpest and latest in time. The half-width of the peaks from the filter samples is approximately 20% greater than that from the standard solution alone. However, the standard solution on the filter paper gives peaks of very similar shape and time to the exposed air filter. Iron behaved in an identical manner to lead. For these two elements it is necessary to use filter papers spiked with standard solution for standardization.

Typical responses for cadmium are shown in Fig. 3. Although peak positions vary slightly, peak shapes are identical in this case. Zinc tracings showed that the peak shapes and positions are the same in all cases. For these two metals standard solutions alone would be satisfactory. However, a mixed metal standard solution on blank filter papers was used so that all four elements could be determined together.

RESULTS AND DISCUSSION

Lead, zinc, cadmium and iron were the metals chosen because they were present in easily detectable quantities in air filters from downtown Toronto. Air filters were cut in half; discs from one half were analyzed by the proposed procedure and the other half analyzed by a conventional wet chemical a.a.s. procedure for air filters [7]. The results are presented in Table 1. They are in good agreement.

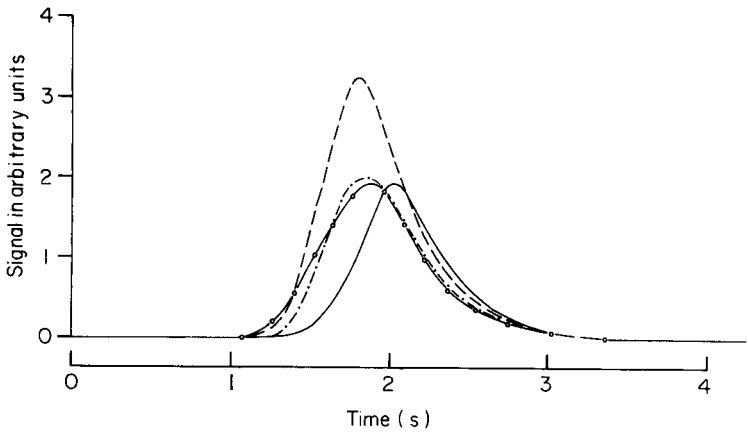

Fig. 3. Atomization tracings for cadmium; symbols as in Fig. 2.

It may seem risky to take 3-mm discs from air filters and use them as representative of the whole filter. This is in marked contrast to the large sample size used in the conventional a.a.s. method. Several 3-mm discs were taken from single air filters and analyzed by the proposed a.f.s. method. The data for lead were typical: the relative standard deviation obtained was 4% (n = 10) which is adequate for air filter analysis.

Since fluorescence intensity is directly proportional to source intensity, there is a theoretical advantage in using high-intensity radiation sources. These may not, however, result in better detection limits because of proportionally greater problems from light scatter. In this study hollow-cathode lamps were used for iron and zinc and electrodeless discharge lamps for lead and cadmium. The latter sources gave spectral output gains of up to 20× compared with hollow-cathode lamps. Electrodeless discharge lamps were not available for zinc and iron. The detection limits for Fe, Zn, Pb and Cd (defined as the amounts giving a signal equal to twice the standard deviation of the noise) were 4, 0.25, 5 and 0.01 ng, respectively.

Theoretically, the 405.9-nm direct fluorescence line gives the strongest lead fluorescence. In addition, if the wavelengths of the source radiation are filtered out, any residual light scatter will be eliminated. An R106 photomultiplier and UG-1 absorption filter were used to monitor this line. No significant improvement in detection limit was obtained.

Other sample types

The proposed method is potentially attractive for the analysis of particulates on water filters. Preliminary results are favourable, indicating that this application is well worth pursuing.

The proposed procedure was adapted for the analysis of organic samples such as NBS SRM Orchard Leaves and Bovine Liver. Few problems were encountered with the latter sample, but orchard leaves, because they contain

TABLE 1

Metals determined in air filters by combined furnace—flame a.f.s. and by conventional a.a.s.

Sample	Pb (μg m^{-3})		Cd (ng m^{-3})		Zn (ng m^{-3})		Fe (ng m^{-3})	
	A.f.s.	A.a.s.	A.f.s.	A.a.s.	A.f.s.	A.a.s.	A.f.s.	A.a.s.
1	0.52	0.52	1.4	1.5	10	9	35	42
2	0.85	0.80	0.2	0.2	16	15	47	50
3	0.46	0.47	1.3	1.2	10	9	33	36

appreciable amounts of refractory elements such as silicon gave problems because of light scatter. In many cases, adequate compensation for light scatter can be obtained by measuring the scatter signal with a radiation source of an element not present in the samples and subtracting this from the signal on the analyte channels.

Conclusions

The method presented for the direct simultaneous multi-element analysis of air filters is relatively simple. Standardization is readily accomplished by using blank air filters spiked with a mixed metal standard solution. Light scatter, a potentially serious problem with non-dispersive a.f.s., is negligible in this application. The results obtained by the proposed method are in good agreement with those obtained by a standard a.a.s. procedure. Replicate analysis of different discs from the same air filter show that the analytical results for a single disc satisfactorily describe the composition of the whole filter. The method shows promise for the multi-element analysis of other types of sample.

The authors gratefully acknowledge funding supplied by the Ontario Ministry of the Environment under the Research Grants Program of the Air Resources Branch and the National Research Council of Canada.

REFERENCES

1 J. B. Willis, Anal. Chem., 47 (1975) 1752.
2 J. E. O'Reilly and D. G. Hicks, Pittsburgh Conference on Analytical Chemistry and Applied Spectroscopy, Cleveland, Ohio, March, 1979.
3 B. V. L'vov, Inzh. Fiz. Zh., 2 (1959) 44.
4 B. V. L'vov, Atomic Absorption Spectral Analysis, 1st edn., Nauka, Moscow, 1966.
5 D. J. Koop, M. D. Silvester and J. C. Van Loon, Pittsburgh Conference on Analytical Chemistry and Applied Spectroscopy, Cleveland, Ohio, March, 1978.
6 P. L. Larkins, Spectrochim. Acta, Part B, 26 (1971) 477.
7 P. N. Vijan, J. A. Pimenta and A. C. Rayner, Ontario Ministry of the Environment, Air Quality Laboratory Procedure, 1977.

Analytica Chimica Acta, 110 (1979) 9—19

COMPARISON OF THREE ANALYTICAL METHODS FOR THE DETERMINATION OF TRACE ELEMENTS IN WHOLE BLOOD

NEIL I. WARD, ROGER STEPHENS and DOUGLAS E. RYAN*

Trace Analysis Research Centre, Chemistry Department, Dalhousie University, Halifax, N.S. B3H 4J1 (Canada)

(Received 2nd May 1979)

SUMMARY

Three different analytical techniques were compared in a study of the role of trace elements in multiple sclerosis. Data for eight elements (Cd, Co, Cr, Cu, Mg, Mn, Pb, Zn) from neutron activation, flame atomic absorption and electrothermal atomic absorption methods were compared and evaluated statistically. No difference (probability less than 0.001) was observed in the elemental values obtained. Comparison of data between suitably different analytical methods gives increased confidence in the results obtained and is of particular value when standard reference materials are not available.

There are a number of elements whose presence in trace amounts is considered essential to human health; the importance of these elements has come to be recognised in recent years [1—7]. The metabolism of a healthy individual maintains their concentrations within narrow limits. Within a group of normal individuals, the concentration spread is widened by the usual statistical fluctuations, but still lies within a statistically definable range. This observation implies that the detection of a trace element imbalance may reflect physiological changes or disorders [8—11]. Thus the subject of trace element determinations in human tissues forms a significant application of analytical chemistry, because of its diagnostic implications, and because the need for such data is fundamental to a better understanding of the role of trace element requirements in human health.

Current analytical methodology permits elements in the 0.1 $\mu g\ g^{-1}$ range or higher (e.g., Al, Cu, Fe, Se, Zn) to be determined with some degree of confidence. However, requirements for accurate analyses at the ng g^{-1} level and lower (e.g., Co, Cr, Mn, Mo, V) make great demands on existing techniques. The concentrations involved tend to lie close to, or below, detection limits. Such analyses therefore require either a time-consuming pre-concentration step, with its attendant risks of contamination or analyte loss during sample handling, or a sensitive method with a selectivity high enough to give reliable data down to its detection limit. In either case, the problem is compounded by a general lack of standard reference materials, availability of which would permit systematic errors caused by contamination, analyte loss or matrix interferences to be detected.

These difficulties were encountered during a study of the role of trace elements in multiple sclerosis [12, 13]. The problem was approached by using three distinctly different analytical methods to determine eight trace elements in whole blood. The methods used were neutron activation analysis (n.a.a.), electrothermal atomic absorption spectrometry (e.a.a.s.), and Zeeman-modulated atomic absorption spectrometry (z.m.a.a.s.). The approach comprized an initial comparison of the methods for NBS Bovine Liver to establish their reliability on a known sample. The trace elements were then determined in whole blood samples taken from 63 multiple sclerosis patients and from 61 controls. Because of the widespread interest in achieving reliable analyses for trace metals, the analytical aspects of this work are discussed in the present paper.

EXPERIMENTAL

Instrumentation

Neutron activation analysis was used as a multi-element method, after removal of sodium by hydrated antimony pentoxide [14] which enabled short-lived nuclides such as Cu, Mg and Mn to be determined. Samples were irradiated in the Dalhousie University SLOWPOKE-2 reactor at a flux of 5×10^{11} n cm^{-2} s^{-1}, and were counted with a 60 cm^3 Canberra Ge(Li) detector (full width at half maximum of 1.88 keV at the 1.332-MeV photopeak, Compton ratio of 35:1, and an efficiency of 9.5%) in conjunction with a Tracor Northern TN-11 4096-channel pulse-height analyzer.

For electrothermal atomic absorption, a standard Perkin-Elmer model 403 spectrometer with deuterium arc background correction was used with the HGA-2200 graphite furnace and control unit.

For Zeeman-modulated atomic absorption measurements, a laboratory-built instrument was used; its design and performance have been described elsewhere [15]. Lead samples were determined by using a laboratory-built electrothermal atomizer. All other elements were determined by flame atomization; the air-acetylene flame was supported on a standard Varian-Techtron burner assembly. The nebulizer was modified by addition of a pre-heater on the air inlet, which raised the air temperature to around 100°C. This overcame problems of low sensitivity and poor reproducibility caused by the high sample viscosity and surface tension at room temperature, and permitted the direct aspiration of whole blood samples after addition of Triton X-100 (see below).

Procedures

For all analyses, standard addition methods were employed to compensate for the physical and chemical matrix effects anticipated for the present samples. Replicate analyses ($n > 5$ in all cases) were used to establish the precision of individual calibration points. Neutron activation analysis was used to monitor and check for contamination of the reagents and materials

used throughout the work. All elemental standards were prepared from Fisher Atomic Absorption 1000 μg ml^{-1} standard solutions and analytical-grade reagents.

Analysis of Bovine Liver

Initial comparison of the three methods was obtained by analysis of NBS-SRM 1577 Bovine Liver. Samples were digested for 12 h with nitric acid in a Teflon bomb. For the determination of Cd, Co, Cr and Pb, 250—500 mg samples were used; for the remaining elements, the sample size was 100 mg. Neutron activation was done directly on the digest solution. The n.a.a. technique used with samples of this type has been reported elsewhere [14]; the essential parameters are summarized in Table 1. For e.a.a.s. and z.m.a.a.s. the digest solution was diluted with an equal volume of a 2% (v/v) solution of Triton X-100 (Fisher Scientific Co.). This procedure effectively prevents sample losses from sputtering, as well as interferences from the build-up of carbon aggregates, during the ashing cycle of e.a.a.s. It also reduces solution viscosity sufficiently to permit ready nebulization of the solution into a flame. The benefits of the technique have been fully discussed elsewhere [16—18], and the method will not be considered further here other than to say that it was found to provide an effective and most convenient way of introducing the bovine liver digest, and, subsequently, whole blood samples into the graphite furnace or the flame atomizer with a minimum of prior sample handling. Tables 2 and 3 show those elements measured by e.a.a.s. and z.m.a.a., respectively.

Blood

Whole blood samples were collected [13], by the standard venipuncture technique, into 10-ml evacuated blood collection tubes (Becton, Dickinson

TABLE 1

Elements measured by neutron activation analysis (n.a.a.)

	Element	Nuclide	γ-ray energy used (keV)	Nuclide half-life	Detection[c] limit (μg ml^{-1})
Short-lived nuclides[a]	Cu	^{66}Cu	1039	5.1 min	0.3
(irradiation time 180 s,	Mg	^{27}Mg	1014[b]	9.5 min	1
decay time 60 s, count	Mn	^{56}Mn	847	2.58 h	0.006
time 600 s)					
Long-lived nuclides	Co	^{60}Co	1173	5.26 y	0.008
(irradiation time 16 h,	Cr	^{51}Cr	320	27.8 d	0.01
decay time 6 d, count	Zn	^{65}Zn	1115	245 d	0.2
time 1800 s)					

[a]After HAP separation. [b]^{27}Mg measurement at 844 keV is affected by the ^{56}Mn photopeak at 847 keV. [c]Detection limits (μg ml^{-1}) based on the criterion reported by Currie [27].

TABLE 2

Elements measured by electrothermal atomic absorption spectrometry

Element	Sample volume (μl)	Wavelength (nm)	Operating parameters						Detection limit (μg ml^{-1})	Ref.
			Dry		Ash		Atomize			
			°C	s	°C	s	°C	s		
Cd	10	228.8	110	30	300	60	2000	8	0.0001	[28, 29]
Co	10	240.7	110	45	250[a]	15	2650	4	0.0008	[30]
					500	15				
					1100	30				
Cr	30	357.9	110	60	1300	60	2700	4.5	0.0008	[31, 32]
Cu[b]	10	324.7	120	35	530	60	2300	4.5	0.02	[33]
Mg[b]	10	285.2	105	45	500	60	2300	4	0.08	[34]
Mn	20	279.5	110	30	1100	50	2650	4	0.002	[35, 36]
Pb	10	283.3 (217.0)	100	25	525	40	2300	4	0.001	[16, 37]
Zn	10	213.9	150	30	400	60	1900	4.5	0.03	[38, 39]

[a]Ramp mode ashing. [b]Sample dilution required.

TABLE 3

Elements measured by Zeeman-modulated atomic absorption spectrometry

Element	Wavelength (nm)	Magnetic field (kG)	Term	Detection limit (μg ml^{-1})	Ref.
Cd	228.8	3.5	$^1S_0$—$^1P_1$	0.00009	[40—42]
Cu	324.7	3.5	$^2S_{1/2}$—$^2P_{3/2}$	0.02	[42, 43]
Pb[a]	283.3 (217.0)	4	$^3P_0$—$^3P_1$	0.006	[44]
Zn	213.9	5	$^1S_0$—$^1P_1$	0.04	[40]

[a]Electrothermal filament technique.

Vacutainers) containing 143 USP units of sodium heparin anti-coagulant. The sample population was from two groups: 63 multiple sclerosis patients (23 male, 40 female; median age 49 years) and 61 controls (22 male, 39 female; median age 36 years). Reported cases of possible contamination sources during sample collection, storage and preparation for analysis [19—24] were considered and controlled throughout the procedure. Analyses were done in the same way as for the bovine liver digest: n.a.a. on the whole blood, and dilution of the whole blood with Triton X-100 prior to e.a.a.s. and z.m.a.a.

RESULTS AND DISCUSSION

Table 4 shows the results obtained for bovine liver compared with existing

TABLE 4

Analysis of NBS Bovine Liver (NBS-SRM 1577)

Element	Amount found ($\mu g\ g^{-1}$, dry weight basis)			Cert.[a]/noncert.[b] values ($\mu g\ g^{-1}$ d.w.)
	E.a.a.s.	Z.m.a.a.	N.a.a.	
Cd[c]	0.29 ± 0.03[d]	0.27 ± 0.02	ND[e]	0.27 ± 0.04
Co[c]	0.21 ± 0.04	ND	0.18 ± 0.03	(0.18)
Cr[c]	0.19 ± 0.01	ND	0.21 ± 0.04	0.2
Cu	190 ± 3	195.0 ± 3	188 ± 10	193 ± 10
Mg	610 ± 15	ND	608 ± 6	604 ± 9
Mn	10.8 ± 0.8	ND	10.0 ± 0.7	10.3 ± 1.0
Pb[c]	0.32 ± 0.06	0.35 ± 0.04	ND	0.34 ± 0.08
Zn	126 ± 8	134 ± 3	129 ± 4	130 ± 13

[a]Certified NBS values [25]. [b]Noncertified values [26]. [c]250- and 500-mg portions of standard material analysed. All other values based on 100-mg portions. [d]Mean (n = 6), ± standard deviation. [e]ND, not determined.

certified and non-certified values [25, 26]. The agreements observed between the three present methods, as well as with the existing data, are felt to be satisfactory. Apart from cobalt (±16%), the other elements have a minimum relative deviation from the certified/non-certified value of ±7%.

Elemental content of whole blood

The means and ranges for concentrations ($\mu g\ ml^{-1}$) of Cd, Co, Cr, Cu, Mg, Mn, Pb and Zn in whole blood from multiple sclerosis patients and controls, determined by e.a.a.s., z.m.a.a.s. and n.a.a. are shown in Fig. 1. Range values are given after rejection of any outliers on the basis of Chauvenet's criterion method.

Overall there is good agreement between the elemental values in relation to the method of analysis. All eight elements are easily measured above their calculated detection limits, although Co, Cr and Mn at the lower range values can be determined only with a relatively lower precision by n.a.a.

The general trend shows higher elemental concentrations for multiple sclerosis individuals. A minimum overlap of the range between the multiple sclerosis and control groups is obtained for manganese and zinc. It can easily be seen from Fig. 1 that for the essential trace elements (Co, Cr, Cu, Mg, Mn and Zn) a very wide spectrum of concentration levels is present in whole blood (manganese at the nanogram level, and magnesium at the microgram level), although each element maintains a fairly narrow concentration range. Table 5 compares the elemental content (mean and range in $\mu g\ ml^{-1}$) of whole blood from the control group determined by e.a.a.s., z.m.a.a. and n.a.a., with reported literature values. All elements show a high degree of accordance with reported literature values. Under the experimental conditions (Table 1) used for the multi-element determination of whole blood by n.a.a., it was not

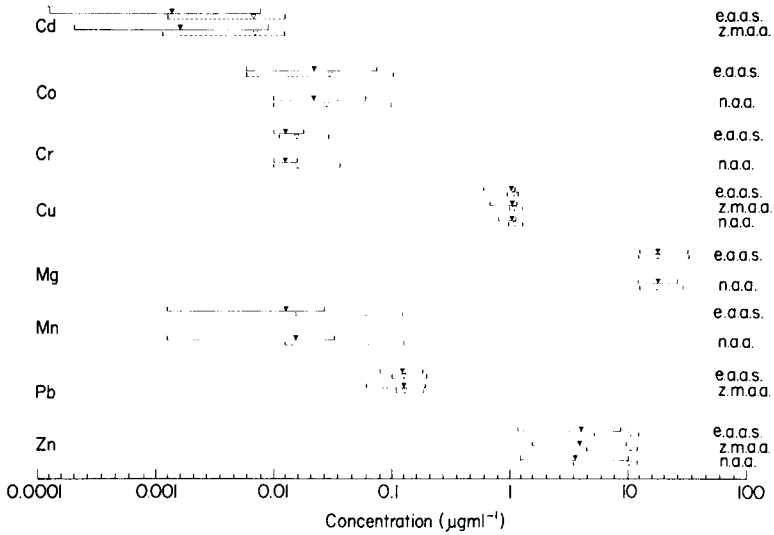

Fig. 1. Elemental means (▾ or ▽) and ranges of concentrations ($\mu g\ ml^{-1}$) of whole blood for control (solid line) and multiple sclerosis (broken line) individuals.

possible to measure Cd(^{111m}Cd, $t_{\frac{1}{2}}$ 49 min) as the elemental level is below the detection limit.

Statistical correlation between analytical methods

Table 6 shows the statistical correlation (in terms of the correlation coefficient r, for F degrees of freedom) between the elemental concentrations of whole blood measured by the three methods. For all eight elements, where such correlations are possible, there is a very highly significant (probability less than 0.001) level of confidence (99.9%) that there is no difference between the analytical methods used. Therefore, as in the example of zinc determined by e.a.a.s. and n.a.a. the marked increase in concentration range between controls (Fig. 2A) and multiple sclerosis (Fig. 2B) groups does not change the very highly significant level (r = 0.81 and 0.85, respectively) of confidence between the two methods.

CONCLUSIONS

In a matrix as complex as whole blood, particularly at the low analyte levels determined here, a number of potential interferences must be anticipated. These can be broadly categorized into the usual groups characteristic of each technique; e.g., spectral, physical interferences during sample introduction, chemical interferences during atomization in a.a.s. analysis, etc. In no instance, however, would identical interferences be expected for all three methods. For example, spectral interferences in n.a.a. clearly differ from the

TABLE 5

Elemental content of whole blood

Element		This work[a]			General reference		Reported values		
		E.a.a.s.	Z.m.a.a.	N.a.a.	Iyengar et al.[b]	Underwood[c]	E.a.a.s.[d]	Z.m.a.a.[e]	N.a.a.[f]
Cd	Mean	0.0023	0.0031	*[g]	0.0052	0.007	0.0034	*	0.002
	Range	(0.0002—0.0090)	(0.0004—0.0096)		(0.0011—0.0074)	(0.003—0.054)	(±0.0003)[h]		
Co	Mean	0.042	*	0.04	0.058	0.018	0.024	*	0.0046
	Range	(0.008—0.086)		(0.01—0.08)	(0.0003—0.099)	(0.007—0.036)	(±0.002)		(±0.0011)
Cr	Mean	0.020	*	0.02	0.054	*	0.012	*	0.053
	Range	(0.010—0.035)		(0.01—0.03)	(0.0065—0.1070)		(0.0009—0.040)		(±0.003)
Cu	Mean	1.15	1.22	1.2	1.01	0.98	1.10	*	1.1
	Range	(0.78—1.36)	(0.85—1.60)	(0.9—1.5)	(0.64—1.28)	(±0.13)	(±0.07)		(±0.1)
Mg	Mean	37.7	*	36	37.8	*	30.3	*	*
	Range	(21.0—57.0)		(19—50)	(27.1—45.5)		(26.0—34.0)		
Mn	Mean	0.020	*	0.028	0.031	0.008	0.0122	*	0.026
	Range	(0.002—0.052)		(0.002—0.057)	(0.0016—0.075)	(±0.002)	(±0.0039)		(±0.002)
Pb	Mean	0.180	0.194	*	0.214	0.18	0.27	0.15	*
	Range	(0.090—0.320)	(0.080—0.275)		(0.088—0.40)	(±0.04)	(0.15—0.29)		
Zn	Mean	6.60	6.59	6.2	7.0	8.8	5.74	*	6.3
	Range	(1.60—9.40)	(3.00—9.90)	(1.9—10.3)	(4.8—9.3)	(±0.2)	(3.62—7.94)		(±0.1)

[a]Elemental concentrations ($\mu g\ ml^{-1}$) for control samples after rejection of outliers by Chauvenet's criterion method. [b]Reference [45]; ($\mu g\ g^{-1}$). [c]Reference [7]. [d]References; Cd—Zn [29, 46, 31, 47—50, 39]. [e]Reference [40]. [f]References; Cd—Zn [51, 52]. [g]*, Not reported/or determined. [h]Standard deviation of mean.

TABLE 6

Statistical relationships between e.a.a.s., z.m.a.a. and n.a.a.

Element		E.a.a.s./z.m.a.a.		E.a.a.s./n.a.a.		Z.m.a.a./n.a.a.	
		Controls	MS	Controls	MS	Controls	MS
Cd	F[a]	56	58	ND[d]		ND	
	r[b]	0.97, VHS[c]	0.95, VHS				
Co	F	ND		59	59	ND	
	r			0.88, VHS	0.92, VHS		
Cr	F	ND		59	61	ND	
	r			0.90, VHS	0.93, VHS		
Cu	F	52	56	52	56	52	56
	r	0.74, VHS	0.58, VHS	0.76, VHS	0.61, VHS	0.61, VHS	0.61, VHS
Mg	F	ND		59	61	ND	
	r			0.78, VHS	0.80, VHS		
Mn	F	ND		59	61	ND	
	r			0.90, VHS	0.87, VHS		
Pb	F	ND		ND		59	61
	r					0.73, VHS	0.71, VHS
Zn	F	59	59	59	59	59	59
	r	0.91, VHS	0.91, VHS	0.81, VHS	0.85, VHS	0.72, VHS	0.76, VHS

[a]Degrees of freedom ($n - 2$), after rejection of outliers by Chauvenet's criterion method. [b]Correlation coefficient. [c]Very highly significant ($F < 60$, $r = 0.408$, probability less than 0.001 or 99.9% level). [d]Not determined.

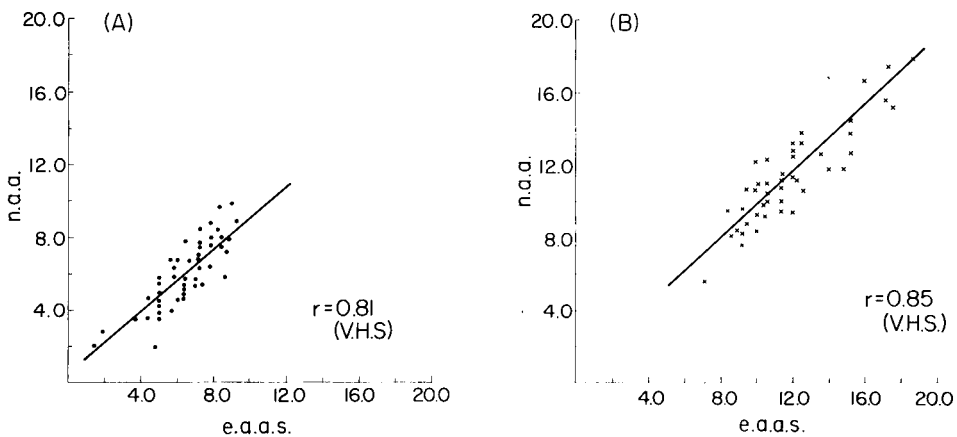

Fig. 2. Correlation of zinc concentration ($\mu g\ ml^{-1}$) determined by e.a.a.s. and n.a.a. in whole blood: (A) control individuals; (B) multiple sclerosis patients.

other two, while the different background correction techniques used with e.a.a.s. and z.m.a.a. make their identical response to a spectroscopic interference highly improbable. Similarly, the differences between methods of sample introduction, atomization, etc., make a common response to a physical

or chemical interference equally unlikely. It is therefore considered that the correlation observed between the three techniques argues that all three were, in fact, close to a true value for the analyte concentration in the sample as presented to the instrument; this is further supported by the agreement with reported literature values. This conclusion gives some confidence (a) in the ability of the methods individually to give valid analytical data, and (b) in the effectiveness of the standard addition approach in compensating for the physical and chemical interferences which undoubtedly exist in the present analyses. The fact that excellent correlation was obtained even at analyte concentrations down to the detection limit, where errors are most likely to appear, gives strong emphasis to these points. (The precision reported for values close to the detection limits arises because of the number of samples taken; a single sample measured under the same conditions would be subject to a correspondingly greater statistical error, although not, presumably, to any greater systematic error.)

It is therefore concluded that the technique of comparing data between suitably different analytical methods is a practical way of testing the validity of those methods under circumstances, such as were encountered here, where the problems of low analyte concentration and potential matrix interferences must be demonstrably overcome without resort to standard reference materials.

Estimating the reliability of a method in this way is useful. It enabled the present analyses to be performed directly on whole blood with some confidence that no untoward interferences arising from the increased matrix complexity were biasing results. The possibility of analyzing whole blood is advantageous, since it avoids the potential errors of serum separation or digestion steps, and the attendant simplicity of the procedure probably contributed in turn to the satisfactory nature of the results. In addition, it is considered that the procedure shows the data distinguishing the multiple sclerosis and normal populations to be reliable; the usefulness of this conclusion is self-evident. However, the comparison of different methods during a given analysis does not completely take the place of a standard reference material, because errors arising during sample collection, transportation, etc. will not necessarily become apparent. Therefore the procedure does not automatically verify the absolute accuracy of the data obtained, and their interpretation must be subject to this reservation.

This work was supported by a grant from the Natural Sciences and Engineering Research Council of Canada.

REFERENCES

1 R. E. Burch, H. K. J. Hahn and J. F. Sullivan, Clin. Chem., 21 (1975) 501.
2 I. J. T. Davies, The Clinical Significance of the Essential Biological Metals, Heinemann Medical Books, London, 1972.

3 D. H. K. Lee (Ed.), Metallic Contaminants and Human Health, Academic Press, New York, 1972.
4 T. H. Maugh, Science, 181 (1973) 253.
5 A. S. Prasad, Trace Elements and Iron in Human Metabolism, Plenum, New York, 1978.
6 J. G. Reinhold, Clin. Chem., 21 (1975) 476.
7 E. J. Underwood, Trace Elements in Human and Animal Nutrition, Academic Press, New York, 4th edn., 1977.
8 I. Lombeck and H. J. Bremer, Nutr. Metab., 21 (1977) 49.
9 J. T. McCall, N. P. Goldstein and L. H. Smith, Fed. Proc., Fed. Am. Soc. Exp. Biol., 30 (1971) 1011.
10 W. Mertz, Clin. Chem., 21 (1975) 468.
11 C. C. Pfeiffer, Psych. Bull., 14 (1978) 47.
12 D. E. Ryan, J. Holzbecher and D. C. Stuart, Clin. Chem., 24 (1978) 1996.
13 D. E. Ryan, J. Holzbecher and N. I. Ward, to be published.
14 N. I. Ward and D. E. Ryan, Anal. Chim. Acta, 105 (1979) 185.
15 R. Stephens, Talanta, 25 (1978) 435.
16 F. J. Fernandez, Clin. Chem., 21 (1975) 558.
17 F. D. Posma, J. Balke, R. F. M. Herber and E. J. Stuik, Anal. Chem., 47 (1975) 834.
18 N. I. Ward, Heavy Metal Pollution in the New Zealand Environment, Thesis, Massey University, Palmerston North, New Zealand, 1977, pp. 47—59.
19 V. D. Anand, J. M. White and H. V. Nino, Clin. Chem., 21 (1975) 595.
20 J. E. Gorsky and A. A. Dieta, Clin. Chem., 24 (1978) 169.
21 E. Z. Helman, D. K. Wallick and J. M Reingold, Clin. Chem., 17 (1971) 61.
22 B. Maziere, A. Gaudry, J. Gros and D. Comar, Radiochem. Radioanal. Lett., 28 (1977) 155.
23 S. B. Nackowski, R. D. Putnam, D. A. Robbins, M. O. Varner, L. D. White and K. W. Nelson, Am. Ind. Hyg. Assoc. J., 38 (1977) 503.
24 A. Taylor and V. Marks, Ann. Clin. Biochem., 10 (1973) 42.
25 National Bureau of Standards, Certificate of Analysis, Standard Reference Material 1577, Bovine Liver, Washington, D.C., (1977).
26 A. Chattopadhyay, K. M. Ellis and K. N. DeSilva, I.A.E.A., Int. Symp. Nucl. Activ. Tech. Life Sci., IAEA-SM-227/113, Vienna, Austria, 1978.
27 L. A. Currie, Anal. Chem., 40 (1968) 586.
28 E. F. Perry, S. R. Koirtyohann and H. M. Perry, Clin. Chem., 21 (1975) 626.
29 F. C. Wright and J. C. Riner, At. Absorpt. Newsl., 14 (1975) 103.
30 D. C. Manning, Am. Lab., 5 (1973) 37.
31 F. J. Feldman, E. C. Knoblock and W. C. Purdy, Anal. Chim. Acta, 38 (1967) 489.
32 R. S. Pekarck, E. D. Hauer, R. W. Wannemacher and W. R. Beisel, Anal. Biochem., 59 (1974) 283.
33 M. A. Evenson and B. L. Warren, Clin. Chem., 21 (1975) 619.
34 J. P. Matoušek and B. J. Stevens, Clin. Chem., 17 (1971) 363.
35 F. Bek, J. Janouskova and B. Moldan, At. Absorpt. Newsl., 13 (1974) 47.
36 R. T. Ross and J. G. Gonsalex, Bull. Environ. Contam. Toxicol., 12 (1974) 470.
37 G. Nise and O. Vesterberg, Clin. Chim. Acta, 84 (1978) 129.
38 M. D. Stevens, W. F. MacKenzie and V. D. Anand, Biochem. Med., 18 (1977) 158.
39 J. B. Dawson and B. E. Walker, Clin. Chim. Acta, 26 (1969) 465.
40 H. Koizumi and K. Yasuda, Anal. Chem., 48 (1976) 1178.
41 Y. Uchida and S. Hattori, Oyo Butsuri, 44 (1975) 852 (Jap.).
42 D. E. Veinot and R. Stephens, Talanta, 23 (1976) 849.
43 V. Otruba, J. Jambar, J. Komarek, J. Horak and L. Sommer, Anal. Chim. Acta, 101 (1978) 367.
44 T. Hadeishi and R. D. McLaughlin, Anal. Chem., 48 (1976) 1009.
45 G. V. Iyengar, W. E. Kollmer and H. J. M. Bowen in H. F. Ebal (Ed.), The Elemental Composition of Human Tissues and Body Fluids, Verlag Chemie, New York, 1978.

46 E. M. Butt, R. E. Nusbaum, T. C. Gilmour and S. L. Didio, Arch. Environ. Health, 8 (1964) 52.
47 P. Del Castilho and R. F. M. Herber, Anal. Chim. Acta, 94 (1977) 269.
48 H. E. Refsum, H. D. Meen and S. B. Strömme, Scand. J. Clin. Lab. Invest., 32 (1973) 123.
49 J. P. Buchet, R. Lauwerys, H. Roels and C. DeVos, Clin. Chim. Acta, 73 (1976) 481.
50 N. P. Kubasik, M. T. Volosin and M. H. Murray, Clin. Chem., 18 (1972) 410.
51 W. A. Haller, R. H. Filby and L. A. Rancitelli, Nucl. Appl., 6 (1969) 365.
52 P. S. Tjioe, J. J. M. DeGoeij and J. P. W. Houtman, J. Radioanal. Chem., 37 (1977) 511.

Analytica Chimica Acta, 110 (1979) 21—28

DITHIZONE EXTRACTION AND FLAME ATOMIC ABSORPTION SPECTROMETRY FOR THE DETERMINATION OF CADMIUM, ZINC, LEAD, COPPER, NICKEL, COBALT AND SILVER IN SEA WATER AND BIOLOGICAL TISSUES

HALLDÓR ÁRMANNSSON*

Department of Oceanography, The University, Southampton (Gt. Britain)

(Received 5th March 1979)

SUMMARY

The method previously described for the determination of Cd, Zn, Cu, Ni and Co in sediments has been adapted for the determination of these metals, and lead and silver in sea water and biological tissues. For sea water the only treatment preceding extraction is pH adjustment; biological tissues are digested in nitric and perchloric acids and the residue taken up in dilute hydrochloric acid prior to pH adjustment and extraction. The method is sufficiently sensitive to allow Cd, Zn, Cu and Ni to be determined in all sea waters, Co and Ag in coastal waters, but Pb only in polluted water.

A method for the determination of some trace metals in sediments [1] had the advantage that most of the interferences commonly associated with the determination of trace metals in complex matrices were avoided. It is useful in environmental studies to be able to apply the same basic analytical method to various components with advantages in economy of analytical effort and comparability of data. In this work the method developed for sediments was adapted for use with sea water and biological tissues.

The determination of lead in these materials did not prove as problematic as in the case of sediments since the concentrations of interfering aluminium and titanium are very low in sea water and most biological tissues. The concentration of lead in unpolluted open sea water is, however, too low to be determined by this method, although lead concentrations found in polluted sea water can be determined. Cobalt has been determined in coastal sea-water samples, but its concentration in open sea water may be below the detection limit for the method. The method had already been used for the determination of silver in sediments, and it was found that it could also be used to determine silver in sea water and biological tissues.

---

*Present address: Department of Natural Heat, Orkustofnun, The National Energy Authority, Laugavegi 116, 105 Reykjavík, Iceland.

Preliminary studies

Sea water. Dithizone in chloroform was used as extractant. Each sample was extracted twice with 0.2% dithizone solution and once with 0.02% dithizone solution. For sediments, three 5-ml volumes were used [1], but since the sea-water sample volumes are large, larger extractant volumes are preferred because of the solubility of chloroform in water. Extraction with two 10-ml volumes of 0.2% dithizone solution and one 5-ml volume of 0.02% dithizone gave good recoveries for sea-water volumes ranging from 400 to 2000 ml. A sample volume of 850 ml was chosen, because this could be extracted efficiently in a 1-l separating funnel, and provided adequate sensitivity.

It was found necessary to distil hydrochloric acid (constant boiling mixture) and to monitor the trace metal contents of perchloric acid batches prior to use. Satisfactory reagent blanks were then obtained. Glass fibre filters and membrane filters both contain significant amounts of trace metals. These could be leached from the membrane filters with 2 M hydrochloric acid. The glass fibre filters were deemed unsuitable because of their large zinc contents.

Attempts to use the method on sea water stored, acidified and frozen in plastic containers produced erratic results. The storage of unfrozen sea water in plastic containers resulted in decreasing trace metal concentrations, but storage in glass containers caused increases in copper and zinc concentrations. It is recommended that samples are extracted prior to storage if they cannot be determined immediately.

The extractable forms were examined. Two samples were irradiated with a 1000-W medium pressure mercury arc lamp. The results (Table 1) suggest that some zinc and probably a trace of copper are present in a form not extractable into dithizone/chloroform (probably organic complexes). The differences in cobalt values are not analytically significant.

Biological tissues. Several acid mixtures were tried but nitric acid followed by a small amount of perchloric acid proved most satisfactory with respect to both completeness of dissolution and to keeping blanks small. As for sea water, the trace metal contents of batches of perchloric acid were monitored. Glass flasks, PTFE beakers and silica flasks were used for the digestion. Silica flasks proved most satisfactory. Metals were leached from the glass flasks, and slightly low results were obtained with PTFE beakers. It was found advan-

TABLE 1

The effect of u.v. irradiation of sea water on dithizone-extractable trace metal concentrations

Sample	Treatment	Cd ($\mu g\ l^{-1}$)	Zn ($\mu g\ l^{-1}$)	Cu ($\mu g\ l^{-1}$)	Ni ($\mu g\ l^{-1}$)	Co ($\mu g\ l^{-1}$)
I	None	0.14	1.3	0.68	0.54	0.09
	Irradiation	0.14	1.9	0.76	0.59	0.13
II	None	0.10	1.9	0.69	0.73	0.06
	Irradiation	0.10	2.4	0.86	0.68	0.10

tageous to use hydrochloric rather than nitric acid to aid the dissolution of the digested residue because of possible interference of nitrate ions with the extraction of nickel and cobalt.

In some samples a white residue persisted when dissolution of the digested residue was attempted. This residue proved extremely insoluble, but satisfactory results were obtained for all the metals determined except cadmium if this residue was extracted along with the solution. Cadmium results were enhanced under these circumstances. A similar residue was observed for calcium-rich sediments, and was found to be a calcium compound. Some calcium was carried through to the determination stage and caused a positive interference in the determination of cadmium (scattering effects). The residue dissolved in a large quantity of hydrochloric acid. The present effect is probably similar. If the residue cannot be dissolved, it must be separated from the solution by centrifugation if cadmium is to be determined.

As iron was thought to interfere in the a.a.s. determination of cadmium [1], solutions of standard reference kale [2] were extracted with dithizone as described below, and iron was determined in the remaining solution. The concentration found was similar to that reported by Bowen [2] suggesting that no iron had been extracted. Accordingly, iron is not likely to interfere under the conditions described.

EXPERIMENTAL

Reagents and apparatus

Varian-Techtron Atomic Absorption Spectrometers (Models 1100 and AA5) were used in accordance with manufacturer's recommendations.

Analytical-grade reagents were used unless otherwise stated.

Dilute ammonia solution. Add enough ammonia (Aristar grade) to distilled water to make the pH 8—9.

Hydrochloric acid (constant boiling). Mix concentrated hydrochloric acid and distilled water (8.25 + 6.75), and distil. Prepare 2 M and 0.2 M solutions by dilution.

Nitric acid was distilled from a silica still; chloroform was also distilled before use.

Dithizone solutions. Recrystallize the dithizone by passing a current of filtered air into a nearly saturated solution of dithizone in chloroform at 40°C. Wash the precipitate with a small amount of carbon tetrachloride. Make a 0.2% (w/v) solution in chloroform and clean by first shaking with dilute ammonia and then with 0.2 M hydrochloric acid, using 100—200 ml of aqueous solution for each 100 ml of dithizone solution. Prepare 0.02% (w/v) dithizone solutions daily from the 0.2% solution.

Filters. Soak membrane filters (0.45 μm pores, 90 mm diameter) in 2 M hydrochloric acid overnight, rinse with distilled water, and pass ca. 1 l of distilled water through prior to use.

Procedure for sea water

Collect the sample in a plastic container. Filter and discard the first 500 ml of filtrate. If the total concentration of dissolved elements is to be measured, irradiate with a 1000-W mercury arc lamp for 5—15 h. Transfer 850 ml to a 1-l separating funnel, check that the pH is ca. 8, add 10 ml of 0.2% dithizone solution and shake vigorously for 5 min. Run the organic layer into a 100-ml separating funnel.

Raise the pH of the aqueous phase to ca. 9.5 with 0.2 ml of ammonia liquor, and repeat the extraction with 10 ml of 0.2% dithizone solution. Finally, extract with 5 ml of 0.02% dithizone. Wash the combined extracts with 50 ml of dilute ammonia, and wash this extract with 5 ml of chloroform. Run the organic phases into a second 100-ml separating funnel, add 50 ml of 0.2 M hydrochloric acid and shake vigorously for 2 min. Separate the phases and wash the aqueous portion with 5 ml of chloroform. Evaporate the aqueous portion to dryness. Wash the sides of the beaker with ca. 10 ml of distilled water, evaporate to dryness and dissolve the residue in 5 ml of 2 M hydrochloric acid (solution A). Add 3 ml of perchloric acid to the organic portion, evaporate to dryness, add a further 2 ml of 60% perchloric acid and ensure that all organic matter has been oxidized. Evaporate, wash down the sides of the beaker with ca. 10 ml of distilled water, evaporate to dryness and take up the residue in 5 ml of 2 M hydrochloric acid (solution B).

For blanks, add 20 ml of 0.2% dithizone and 5 ml of 0.02% dithizone solutions to a 100-ml separating funnel. Wash with 50 ml of dilute ammonia solution and proceed as for the samples. Add 0.2—0.3 ml of concentrated ammonia to each beaker before the last evaporation to dryness.

Determine cadmium at 228.8 nm, zinc at 213.8 nm and lead at 217.0 nm in solution A; and copper at 324.7 nm, nickel at 232.0 nm, cobalt at 240.7 nm and silver at 328.1 nm in solution B, using suitable scale expansion.

Procedure for biological tissues

Freeze-dry the sample to constant weight. Grind in a ball mill to obtain a homogeneous powder. Weigh 0.5—3 g accurately into a 100-ml conical silica flask. Add 10—20 ml of nitric acid and leave covered on a sandbath at ca. 100°C for 3 h. Remove the cover and evaporate to dryness. If the solution is still coloured when evaporated, repeat the treatment with 5—10 ml of nitric acid, digesting for 30 min. When the solution is nearly colourless, add 5 ml of (1 + 1) nitric—perchloric acid and evaporate to dryness. Add ca. 50 ml of water and 10 ml of hydrochloric acid (constant boiling), and heat on a hot plate. If a residue remains, add more hydrochloric acid until a clear solution results. If 50—100 ml are not enough to produce a clear solution, centrifuge and discard the residue only if cadmium is to be determined. Add 3 ml of 50% (w/v) citric acid solution and sufficient ammonia to bring the pH to 8 (indicator paper). Cool, run the solution into a 150-ml separating funnel and adjust the pH to 8 with ammonia and/or hydrochloric acid (constant boiling) using indicator papers. Add 5 ml of 0.2% dithizone, shake vigorously for 2 min

and run the organic layer into a 100-ml separating funnel. Raise the pH of the solution to 9.5 with ammonia and repeat the extraction. Extract once more, this time with 5 ml of 0.02% dithizone solution. If the dithizone still changes colour, repeat the extractions with 0.02% dithizone until it does not. Wash the combined dithizone extracts with dilute ammonia, run the dithizone layer into a second 100-ml separating funnel and proceed as for sea water. If zinc concentrations are high, turn the burner through 90° for the determination. Determine high copper concentrations at 327.4 nm, turning the burner through 90° if necessary.

RESULTS AND DISCUSSION

Sea water

Sea-water samples were spiked with cadmium, zinc, lead, copper, nickel and cobalt and satisfactory recoveries obtained (Table 2). Silver was not tested, but since sediment samples and biological tissue samples (see below) gave satisfactory recoveries by analogous methods, silver is probably adequately recovered from sea water.

The metals were determined in replicate in two sea-water samples and coefficients of variation calculated. These ranged from 4% to 29% (Table 3), and are considered satisfactory for the concentrations in question.

Reagent blanks, efficiency of nebulization and hollow-cathode lamp stability were all possible factors influencing detection limits. Those obtainable under the recommended conditions are listed in Table 3. There is considerable room for improvement by increasing the sample volume and reducing the final determination volume.

The results obtained by the proposed methods for zinc and copper in a sea-water sample (1.9 μg Zn l^{-1} and 0.76 μg Cu l^{-1}) were compared with results obtained independently by APDC extraction (1.9 μg Zn l^{-1} and 0.83 μg Cu l^{-1}) and by Chelex-100 ion-exchange (0.83 μg Cu l^{-1}); the comparability proved satisfactory (a.a.s. was used in all cases). A comparison of some other recent analyses of sea water for the metals studied here shows that the only method which appears significantly better than the present one is the Chelex-100/a.a.s.

TABLE 2

Recoveries of metal spikes from sea-water samples

Metal	Conc. in sample (μg l^{-1})	Spike added (μg/900 ml)	Mean spike recovery (%)
Cd	0.08	0.09; 0.45	100
Zn	3.8	2.0; 6.0	101
Pb	<0.04	0.50; 1.50	>95
Cu	0.50	1.16; 3.48	97
Ni	0.57	1.00; 3.00	95
Co	<0.05	0.10; 0.32	>98

TABLE 3

Coefficients of variation for six replicate analyses of two sea-water samples, and detection limits

Metal	Sample	Mean conc. ($\mu g\ l^{-1}$)	Coefficient of variation (%)	Detection limit ($\mu g\ l^{-1}$)
Cd	A	0.12	7	0.05
	B	0.30	10	
Zn	A	2.6	8	0.6
	B	10.1	5	
Pb	A	<0.04	—	0.04
	B	0.28	23	
Cu	A	0.48	7	0.06
	B	1.51	5	
Ni	A	0.76	6	0.3
	B	1.58	4	
Co	A	0.15	14	0.04
	B	0.16	11	
Ag	B	0.08	29	0.05

scheme described by Riley and Taylor [3]. This method has been used satisfactorily for copper in this laboratory (see above); the coefficient of variation was similar to that obtained by the present method [4].

Trace metal contents of sea water from Southampton Water and the Solent. Several sea-water samples were obtained from Southampton Water and the Solent during the period March 1975—February 1976. The approximate sampling times and the analytical results are given in Table 4. All the samples were collected during an inflowing tide and should represent Solent sea water. Variation in trace metal concentrations is expected to be due to either seasonal variation or local pollution. There is a seasonal variation observed for the zinc and cadmium concentrations (Fig. 1), with high values in spring and low values in autumn and winter. A similar trend is observed for the lead values, but the lead results are fewer and less reliable. These observations are similar to those of Fukai et al. [5, 6] who measured zinc concentrations over 16 months (January 1970—April 1971) off Monaco and found increases in March, July and November—December 1970 and minimum concentrations in May and October. These authors did not define the nature of the increase, but noted that a major portion arrived in the form of dithizone-extractable zinc which then is possibly transformed into unextractable forms.

Copper concentrations are significantly higher in samples taken near the Fawley oil refinery than in the rest of the samples. Similar high results have been reported for the same location by Matharu [7]. This is due to local pollution as is indicated by very high copper concentrations which have been recorded in sediments from the same area [8]. As some increases were recorded for zinc and cadmium in the sediments, some effects might have been expected in the sea water, but if there are any increases in these metals

TABLE 4

Trace metal concentrations ($\mu g\ l^{-1}$) in sea-water samples from Southampton Water and the Solent

Collection time	Sampling location[a]	Cd	Zn	Pb	Cu	Ni	Co	Ag
Mid-March 1975	1	0.35	9.3	0.6	2.5	0.50	ND[b]	ND
Mid-April 1975	2	ND	13.2	0.3	0.93	1.40	0.09	ND
Early Sept. 1975	1	0.16	2.9	0.4	2.6	0.72	0.16	ND
Mid-Sept. 1975	2	0.17	3.8	<0.1	0.78	0.82	0.09	ND
Early Oct. 1975	3	0.12	2.6	<0.1	0.48	0.76	0.15	ND
Mid-Oct. 1975	2	0.14	1.9	ND	0.76	0.59	0.13	ND
Mid-Nov. 1975	3	0.10	4.8	ND	0.76	1.09	0.16	ND
Early Jan. 1976	2	0.10	2.4	ND	0.86	0.68	0.10	ND
Late Feb. 1976	4	0.30	10.1	0.28	1.51	1.58	0.16	0.08

[a](1) Fawley, (2) Calshot, (3) Lymington, exit of River Beaulieu, (4) The Needles. [b]ND, not determined.

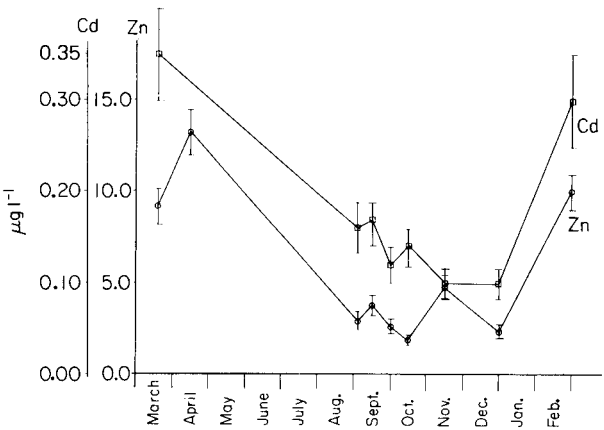

Fig. 1. Seasonal variation of zinc and cadmium concentrations in sea water from Southampton Water and the Solent.

from local pollution, they are probably smaller than those from seasonal changes.

Biological tissues

The standard reference kale [2] was analysed in replicate and with spikes. The mean concentrations, coefficients of variation and percentage recoveries are given in Table 5, along with previously reported values for the kale [2]. The agreement is satisfactory although the copper values are low. The present nickel value is probably the best available.

The method was also applied to various tissue samples. The details of the samples and the results are shown in Table 6.

TABLE 5

Previously reported values [2], mean concentrations, coefficients of variation (s_r), and spike recoveries for trace metals in reference kale

	Cd	Zn	Pb	Cu	Ni	Co	Ag
Reported values ($\mu g\ g^{-1}$)	0.84	31.8	3.2	4.9	11.0[a] 2.6	0.056	0.03[a]
Mean value found ($\mu g\ g^{-1}$)	0.90	29.9	2.6	4.2	0.81	0.05	0.03
s_r (%)[b]	7	3	13	4	11	15	100
Spike added (μg/1,0149 g)	0.60	60.0	3.0	3.0	2.0	0.90	0.12
Spike recovery (%)	101	101	103	95	104	101	86

[a]Values representing single determinations. [b]6 determinations.

TABLE 6

Trace metal concentrations ($\mu g\ g^{-1}$) in tissue samples

Sample	Origin	Cd	Zn	Pb	Cu	Ni	Co	Ag
Kelp	Woolston, Southampton Water	0.75	53.2	2.3	3.0	1.5	0.54	0.03
Whale heart	Off Iceland	ND[a]	103	0.62	7.6	0.31	0.07	0.04
Whale meat	Off Iceland	ND	42	0.45	2.9	0.17	0.07	0.02
Whale fat	Off Iceland	ND	26	1.37	1.2	0.60	0.38	0.02
Trout	Lake Mývatn, Iceland	ND	39	0.89	2.6	0.34	0.14	0.04

[a]ND, not determined.

This work was supported by the Icelandic Science Foundation and the Icelandic Students' Loan Fund. The author thanks Dr. J. D. Burton for his supervision and for critically reading the manuscript, and Dr. P. J. Ovenden for also critically reading the manuscript.

REFERENCES

1 H. Ármannsson, Anal. Chim. Acta, 88 (1977) 89.
2 H. J. M. Bowen, Adv. Act. Anal., 1 (1969) 101; Atomic Energy Rev., 13 (1975) 451.
3 J. P. Riley and D. Taylor, Anal. Chim. Acta, 40 (1968) 479.
4 R. M. Moore and J. D. Burton, Nature, 214 (1976) 241.
5 R. Fukai, L. Huynh-Ngoc and C. N. Murray, J. Oceanogr. Soc. Jpn., 29 (1973) 44.
6 R. Fukai and L. Huynh-Ngoc. J. Oceanogr. Soc. Jpn., 31 (1975) 179.
7 H. S. Matharu, Ph. D. thesis, University of Southampton, 1975.
8 H. Ármannsson, Ph.D. thesis, University of Southampton, 1979.

Analytica Chimica Acta, 110 (1979) 29—34

DETERMINATION OF PLATINUM IN ALUMINA-SUPPORTED AUTOMOTIVE CATALYST MATERIAL BY ELECTROTHERMAL ATOMIC ABSORPTION SPECTROMETRY

NOEL M. POTTER* and RICHARD A. WALDO

Analytical Chemistry Dept., General Motors Research Laboratories, Warren, Michigan 48090 (U.S.A.)

(Received 10th April 1979)

SUMMARY

Platinum (0.01—0.2%) is determined after dissolution in sulfuric and hydrochloric acids and addition of palladium and rhodium to compensate for interelement effects. At the 0.06% level, the relative standard deviation is 2%. The results agree within 4% with those obtained by chemical methods.

Previous methods of measuring the noble metal contents of automotive catalyst materials [1, 2] have given highly accurate and precise results, but they require considerable skill and operator time. Because platinum is a major active component of most automotive catalyst materials, rapid methods for its determination are especially desirable. Instrumental techniques such as x-ray fluorescence [3], neutron activation [4, 5], and emission spectrography [6] have been applied for the determination of platinum in a variety of materials including alumina-base reforming catalysts. Electrothermal atomic absorption spectrometry has also been successfully employed for the determination of platinum in geological materials [7] and reforming catalysts [8]. Because of the low levels of platinum (ca. 0.06%) and the successful experience gained in the determination of rhodium in automotive catalyst material [9], the heated graphite furnace coupled with atomic absorption spectrometry (a.a.s.) was selected for use.

EXPERIMENTAL

Apparatus and operating parameters

The instrumentation included a Perkin-Elmer Model 403 spectrometer with deuterium background correction, an HGA-2100 and a temperature ramp programmer [9]. A Leeds and Northrup recorder was operated in the low chart speed mode (2.5 cm min^{-1}) for peak-height measurements and in the high chart speed mode (15 cm min^{-1}) for peak-area measurements. Areas were measured with a planimeter. The Jarrell—Ash Model 45466

platinum hollow-cathode lamp was operated at 20 mA, and the resonance line at 265.9 nm was used; the slit width was set so that the spectral band-pass was 0.7 nm.

Injected samples (25 μl) were brought from ambient temperature to 240°C in 23 s, maintained at 240°C for 2 s, then heated to 1850°C over 20 s and held at 1850°C for another 15 s, prior to atomization at 2700°C for 9 s. A continuous flow of argon (40 ml min^{-1}) was maintained in the furnace at all times. Each new graphite furnace tube was pre-conditioned by cycling the system five times with any one of the calibration solutions; each tube was used about 50 times before being replaced.

Sample preparation

The catalyst materials and platinum-free γ-alumina (used to prepare calibration solutions) were ground to pass through a 150-μm sieve to facilitate sample dissolution and corrected for adsorbed water concentrations as described previously [9].

Standards and reagents

All chemicals were ACS reagent grade. A platinum standard solution (1 mg ml^{-1}) in ca. 1 M hydrochloric acid was prepared as described previously [9]. Calibration solutions containing 0—5.0 μg Pt ml^{-1} were prepared by adding appropriate amounts of standard solution to 1-g portions of γ-alumina contained in 100-ml volumetric flasks. These calibration solutions were processed like the sample solutions. The calibration curve was linear from 0 to 3 μg ml^{-1} with a slight curvature from 3 to 5 μg ml^{-1}.

A palladium stock solution (1 mg ml^{-1}) was prepared from palladium metal (Spex Industries, Inc.) in the same way as the platinum stock solution. A rhodium stock solution (0.76 mg ml^{-1}) was prepared by dissolving $RhCl_3$ (Spex Industries, Inc.) in 100 ml of (1 + 4) hydrochloric acid and diluting to 1 l. Portions of these two solutions were injected directly into the graphite furnace to verify the absence of measurable amounts of platinum. The stock solutions are stable for at least six months.

Determination of platinum

A weighed portion of ground sample material containing 100—400 μg of platinum was placed in a 100-ml volumetric flask, and ground platinum-free γ-alumina was added to bring the total weight to 1 g. Any alumina adhering to the wall of the flask was washed down with no more than 10 ml of deionized water. To flasks containing samples or calibration solutions, 5 ml of concentrated sulfuric acid and 10 ml of concentrated hydrochloric acid were added. Each flask was placed on a steam plate for 72 h. After dissolution of the alumina, 0.76 mg and 2.5 mg of rhodium and palladium, respectively, were added to each flask. The flasks were cooled, diluted to volume, and mixed. The platinum absorbance was measured after injecting 25 μl of solution into the graphite furnace. Each calibration solution was measured

four times and each sample solution twice. Peak heights were used to calculate concentrations.

Interference studies

A stock solution containing dissolved aluminum (25 g l^{-1}, equivalent to 51 g l^{-1} of Al_2O_3) and sulfuric acid (250 ml l^{-1}) was used to simulate dissolved catalyst material. Platinum, palladium and rhodium were added to 100-ml volumetric flasks containing 10 ml of concentrated hydrochloric acid and 20 ml of the synthetic catalyst solution. The appropriate contaminant was added to each flask; absorbances were measured and were compared to absorbances obtained from calibration solutions.

RESULTS AND DISCUSSION

The procedure described applies to γ-alumina-supported catalysts with platinum concentrations between 0.01% and 0.2%, but not to catalyst supports containing silica, organic binders, α-alumina, or other insoluble substances. It can be applied to catalysts containing palladium—platinum concentration ratios up to 12:1 and rhodium—platinum ratios of up to 3:1.

Platinum, because of its finely divided state, was usually soluble under the dissolution conditions. However, if a slight reddish skim, which could contain platinum, appeared on the sample solutions, it could be dissolved by adding 0.25 ml of concentrated nitric acid to the solutions and heating at 100°C for 15 min.

Calibration and sample solutions were always prepared in the same manner so that all matrices would be similar. Background correction was essential because of extraneous emission from the graphite tubes and absorption of the 265.9-nm radiation by the vaporized aluminum. The argon flow was not interrupted during atomization to achieve greater sensitivity, because the deuterium lamp would not compensate for the extraneous absorption caused by the volatilized residual alumina. Similarly, sample injections greater than 25 μl resulted in excessive extraneous absorption. In the atomization cycle, after the initial drying step, sulfuric acid and aluminum were vaporized by increasing the temperature to 1850°C in 20 s and holding at 1850°C for 15 s. This temperature was a compromise. At higher temperatures, more aluminum was volatilized, but platinum was also volatilized, causing a decreased platinum signal. At lower temperatures, insufficient aluminum was vaporized, causing extraneous absorption upon atomization. Finally, the platinum was atomized at 2700°C without use of the ramp programmer, to achieve a sharp peak. No memory effect from the furnace was observed when platinum concentrations were less than 3 μg ml^{-1}; for greater concentrations, the slight memory effect was eliminated by keeping the furnace at 2700°C for an additional 9 s.

A batch of 12 samples can be processed in 2—3 h after sample dissolution. Although approximately 72 h are required to dissolve the catalyst material, little operator time is involved.

TABLE 1

Effect of palladium, rhodium and nitric acid on platinum signals[a]

Pd ($\mu g\ ml^{-1}$)	Peak height (mm)	Rh ($\mu g\ ml^{-1}$)	Peak height (mm)	HNO_3 (ml)	Relative peak height (mm)
0	163	0	163	0	100
1	202	0.76	181	0.25	94
5	214	7.6	189	0.50	89
10	234	15.2	200	1.00	81
50	234				

[a]Solutions contained 5 ml of 18 M H_2SO_4, 10 ml of 11 M HCl, 1.0 g of Al_2O_3, and 400 μg Pt per 100 ml.

TABLE 2

Effect of palladium and rhodium on platinum peak heights and areas[a]

Pt ($\mu g\ ml^{-1}$)	Relative peak height		Relative peak area	
	No Pd, Rh	With Pd, Rh	No Pd, Rh	With Pd, Rh[b]
1	28	61	24	27
2	67	117	48	50
3	120	163	70	76

[a]Solutions contained 5 ml of 18 M H_2SO_4, 10 ml of 11 M HCl and 1.0 g of Al_2O_3 per 100 ml. [b]25 μg Pd ml^{-1}; 7.6 μg Rh ml^{-1}.

Effect of other components

Because automotive catalysts contain palladium and/or rhodium the effect of these elements on the platinum absorption signal was examined (Table 1). As the palladium and rhodium concentrations were increased, the height of the platinum signal increased. With palladium concentrations between 10 and at least 50 $\mu g\ ml^{-1}$, the platinum signal was constant. When both palladium and rhodium in the same solutions were varied from 25 to 50 $\mu g\ ml^{-1}$ and 7.6 to 15 $\mu g\ ml^{-1}$, respectively, the recorded peak heights for platinum were constant.

When peak areas were examined (Table 2) the effect of palladium and rhodium upon the platinum absorbance signal was minimal, indicating that palladium and rhodium increase the rate of volatilization. However, peak heights were preferred to facilitate data handling. To eliminate the problem of peak-height enhancement, 2.5 mg of palladium and 0.76 mg of rhodium were added to all samples and calibration solutions in 100-ml volumetric flasks. A 1-g portion of most automotive catalysts will contain less than 2.5 mg of palladium and 0.2 mg of rhodium. Thus, the contribution of palladium and rhodium from the sample will not further enhance the platinum

absorbance signal. If higher concentrations are encountered, the additions of palladium and rhodium must be reduced accordingly to avoid further enhancement of the platinum absorbance peaks.

Sulfuric and hydrochloric acids were used for sample dissolution. Sulfuric acid is not lost during heating, thus the final concentration can be controlled by adding known amounts to samples and calibration solutions. Since hydrochloric acid can be lost upon heating, synthetic catalyst solutions were prepared to study this effect; concentrations of hydrochloric acid from 1 to 15 ml per 100 ml of solution did not affect the platinum signal. Nitric acid decreased the platinum recorded peak height (Table 1). Therefore, when nitric acid was needed to dissolve any reddish skim, 0.25 ml of nitric acid was added to all samples and calibration solutions. The presence of 1 g of dissolved alumina enhanced the platinum signal by approximately 25%. Thus, all samples and calibration solutions were made to contain 1 g of dissolved alumina.

Used automotive catalysts contain, in addition to noble metals, several contaminants, primarily oil and gasoline additives, which could affect the platinum absorption signal. Spectrographic analysis of used catalysts showed that the concentration of several elements can approach 0.1%. Synthetic dissolved catalyst solutions containing the equivalent of 1% of these contaminants (phosphorus, zinc, magnesium, calcium, lead, iron, barium, and boron) did not affect the platinum signal. In addition, 2.5% cerium used as an additive in certain catalysts had no effect.

TABLE 3

Evaluation of accuracy of the method[c]

Sample	Concentration (%)			Pt found (%)
	Pt[a]	Rh[b]	Pd[a]	
1	0.044	0.019	—	0.044
2	0.023	0.012	—	0.024
3	0.043	0.020	—	0.041
4	0.022	0.011	—	0.021
5	0.0098	0.0055	—	0.0099
6	0.039	—	0.016	0.039
7	0.062	—	0.025	0.060
8	0.042	—	0.017	0.039
9	0.057	—	0.023	0.056
10	0.036	—	0.014	0.033
11	0.039	—	0.015	0.040
12	0.067	0.0050	0.034	0.068
13	0.202	0.013	0.097	0.22
14	0.077	0.0069	0.033	0.083

[a]Wet chemical analysis. [b]X-ray fluorescence and wet chemical analysis, average value. [c]R.s.d. = 2% (n = 8).

Precision and accuracy

A series of ground catalyst samples containing platinum, palladium, and rhodium were analyzed to evaluate this method. Platinum concentrations, determined by established chemical methods [1, 2], are compared to results obtained by the proposed method in Table 3. The calculated average relative deviation between the two sets of data is 4%. The relative standard deviation calculated from eight results on sample 9 was 2%.

REFERENCES

1 S. Kallmann, Talanta, 23 (1976) 579.
2 N. M. Potter, Anal. Chem., 48 (1976) 531.
3 P. N. Gerrard and N. Westwood, J. S. Afr. Chem. Inst., 25 (1972) 275.
4 R. A. Nadkarni and G. H. Morrison, Anal. Chem., 46 (1974) 232.
5 R. F. Hill and W. J. Mayer, IEEE Trans. Nucl. Sci., NS-24 (1977) 2549.
6 K. Dixon and T. W. Steele, J. S. Afr. Chem. Inst., 25 (1972) 275.
7 R. J. Combes and A. Chow, Talanta, 24 (1977) 421.
8 J. Janouskova, M. Nehasilova and V. Sychra, At. Absorpt. Newsl., 12 (1973) 161.
9 N. M. Potter, Anal. Chem., 50 (1978) 769.

Analytica Chimica Acta, 110 (1979) 35—47

THE DETERMINATION OF TOTAL GASEOUS MERCURY IN AIR AT BACKGROUND LEVELS

F. SLEMR*, W. SEILER, C. EBERLING and P. ROGGENDORF

Max-Planck Institute for Chemistry, Saarstrasse 23, 65 Mainz (Federal Republic of Germany)

(Received 7th February 1979)

SUMMARY

A method is described for the determination of the total gaseous mercury in air at concentrations ranging from ca. 0.1 ng m^{-3} to 1 μg m^{-3}. The method is based on the collection of mercury species on gold-coated quartz wool followed by detection with an atomic absorption detector. The collection efficiencies for mercury, dimethylmercury, methylmercury(II) chloride, and mercury(II) chloride are nearly quantitative at flow rates up to 10 l min^{-1} and at temperatures up to 50°C. The absolute detection limit of the method is 20 pg of mercury. Under field conditions the precision of the analytical procedure was 14.5% (n = 5) for 400-l samples of air and a mercury concentration of 1.5 ng m^{-3}. Measurements of the mercury distribution in the atmosphere show an ambient background level in clean air masses of 1.0—4.0 ng m^{-3}.

During the past decade, several methods for the determination of mercury in air, generally based on the collection of mercury on suitable materials followed by determination by atomic absorption (a.a.s.) or atomic emission (a.e.s.) spectrometry, have been developed. Most of these methods are suitable for determinations of mercury in polluted air but are not sufficiently sensitive for the determination of mercury in clean air in which the concentration (1 ng m^{-3}) is one or two orders of magnitude less. Furthermore, most methods available have been designed and tested for elemental mercury but not for dimethylmercury (DMM), methylmercury(II) chloride (MMC), and mercury(II) chloride (MC) which are present in the atmosphere [1—3].

The object of this work was to develop a technique for measurements of total mercury in air at levels of 1 ng m^{-3}. Gold was selected as the collecting material. The collection efficiencies were studied for mercury, DMM, MMC, and MC as a function of the sampling flow rates, concentration, temperature, type of collector material, etc. The collecting material has been improved and a method devised for determining background mercury concentrations in the short sampling times necessary in mercury distribution measurements made by mobile sampling units.

EXPERIMENTAL

Sampling device

Air samples are obtained with a sampling device working independently of the analytical system. In the sampling device (Fig. 1) the air is sucked in by a pump with metal bellows at flow rates up to 10 l min^{-1} and passed through an aerosol filter before it enters the mercury collector. The flow rate, measured by a mass flowmeter, is integrated electronically to give the total volume of sampled air. After reaching a preselected sampling volume, the solenoid valves at the inlet and outlet of the mercury collector are closed. The collector is then disconnected from the sampling device, closed with Parafilm and taken to the laboratory for analysis. For long-term measurements, 10 collectors can be attached to the airflow sequentially, after a preselected period ranging from 30 min to several hours; samples can be taken automatically over periods ranging from 5 to 48 h as necessary.

The aerosol filter consists of a glass tube (60 mm long, 20 mm diameter) tightly packed with 2 g of quartz wool. A filter of this type collects 80% of particles with radii larger than 0.8 μm [4]. It was found that mercury on aerosols contributed less than 5% to the total mercury concentration in remote areas. As this contribution was small relative to the standard deviation of the mercury determination in air, the aerosol filter was omitted in the majority of measurements.

Collectors and their packing

The collector is shown in Fig. 2. The quartz tube, filled with a suitable

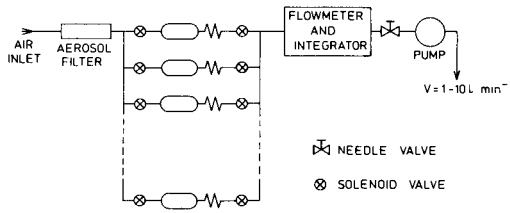

Fig. 1. Schematic diagram of the sampling device.

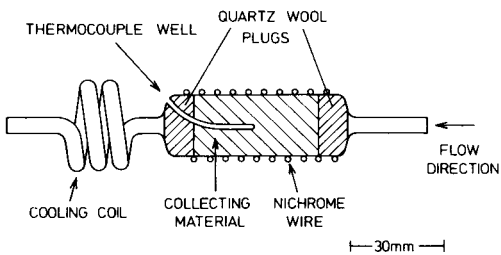

Fig. 2. Mercury collector.

collecting material held between two quartz wool plugs, is 50 mm long and 20 mm in diameter with a volume of 16 cm^3. The collector can be heated to a maximum temperature of 1000°C by a nichrome wire wrapped around the tube. The applied temperature is measured with a chromel—alumel thermocouple inserted into a well and recorded on a strip chart. The outlet of the collector is equipped with a cooling coil to prevent excessive heating of the connections to the analytical system.

Two collecting materials were employed: (A) 1.5 g of gold wool (99.995% purity) with an average filament diameter of 25 μm and a total gold surface area estimated at 405 cm^2 (this value includes a factor of 3 introduced to account for the roughness of the gold surface [4]); (B) 0.17 g of gold-coated quartz wool prepared by coating a thin mat of quartz wool on both sides in a conventional bell jar vacuum coater. The average filament diameter was 6.6 μm and the thickness of the gold layer was of the order of 0.1 μm. To estimate the gold surface area in the collectors two factors must be considered: the quartz wool surface is not completely coated because of the mutual screening of the filaments in the mat, and the roughness of the quartz wool surface is probably less than that of the gold wool. Assuming that ca. 75% of the quartz wool surface area is coated with gold and applying a roughness correction factor of 2, the gold surface area in the collector is estimated at ca. 510 cm^2.

Analytical device

Figure 3 shows the flow scheme used for the analytical device. Outdoor air, used as a carrier gas, is passed through a purification train (to remove mercury, water and other impurities) consisting of 5 glass columns filled with: granular $CaCl_2$, granular P_2O_5 (each 50 mm i.d., 200 mm long); molecular sieves 5A and 13X (2-mm diameter beads, each column 30 mm i.d. and 180 mm long); and a column (30 mm i.d., 180 mm long) packed with 1.5 g of gold-coated quartz wool. The purified mercury-free gas then passes through an injection port and the collector tube and finally enters the optical cell of the a.a.s. mercury detector. During changes of collectors, the injection port and the collector are bypassed to maintain a constant flow rate of about 1 l min^{-1} through the optical cell.

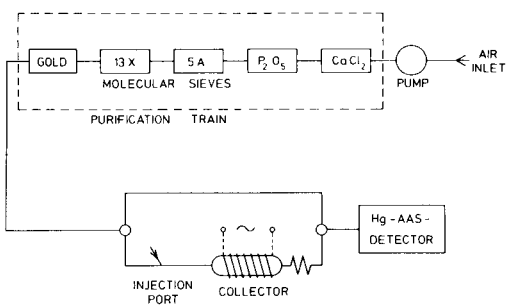

Fig. 3. Schematic diagram of the analytical device.

After insertion into the analytical system, the collector is purged with the carrier gas for ca. 1 min. Subsequently, the collector is again bypassed and heated to 700°C to release the collected mercury. After heating for 90 s the carrier gas is passed through the collector and the mercury released is swept into the optical cell of the detector. The collector is then cooled to room temperature and loaded with a known amount of elemental mercury, and the heating period is repeated. The mercury content of the air sample is calculated from the measurement and calibration signal. Finally, after cooling, the collector is heated for a third time, after which it is mercury-free and ready for further use.

Mercury a.a.s. detector

The mercury released from the collector is determined at 253.7 nm by an atomic absorption photometer designed in this laboratory. A schematic diagram of the detector is shown in Fig. 4. The radiation emitted by a low-pressure mercury germicidal lamp (General Electric G4T4) is split into a sample and a reference beam. The radiant power of each beam (measured by RCA 935 photocells) is adjusted by altering the slits mounted on the lamp housing. The optical cell (208 mm long, 19 mm diameter) is kept at 100°C to prevent condensation of water and other substances.

In contrast to the conventional design of atomic absorption photometers, the mercury lamp is pulsed at 750 Hz so that the signals of both photocells can be processed in a lock-in amplifier. This gives a substantial reduction in the electrical and mechanical noise and improves considerably the sensitivity of the mercury detector.

Several tests were performed with a mercury atomic emission detector which has the advantage of responding to all mercury species without the necessity for their decomposition to elemental mercury. The detector, with mercury excitation in a microwave-induced argon plasma, was essentially the same as described by Kaiser et al. [5].

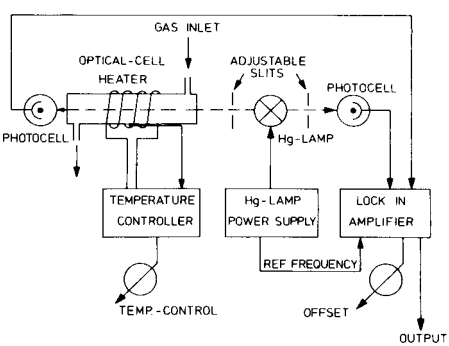

Fig. 4. Block diagram of the mercury a.a.s. detector.

Calibration

The injection of known amounts of air saturated with mercury onto a collector in the analytical device was used to calibrate the system. The air was saturated in a three-stage saturator filled with liquid mercury (Fig. 5). The vessel was kept at 0.0 ± 0.1°C and purged by mercury-free air at flow rates of ca. 5 cm^3 min^{-1}. The calibration gas samples were taken at the end of the saturator by gas-tight syringes and injected into the injection port of the analytical device. The collector was then heated and the amount of the revolatilized mercury determined by the a.a.s. detector. The performance of the saturator was checked by varying the number of the stages and the carrier gas flow rate. The mercury concentration in the calibration gas samples was compared with mercury-saturated air from a closed thermostated glass bulb filled with a few grams of mercury. Equivalent readings were obtained in all tests.

Preparation of test atmospheres

Test atmospheres for the determination of the collection efficiencies of mercury, DMM, MMC and MC on the collectors were prepared by static and dynamic methods. In the static method, a known volume of air saturated with mercury or DMM was injected into a 4-l glass bulb and mixed by an internal stirrer. The concentration of the test atmospheres prepared by this procedure could be varied between a few ng m^{-3} and a few μg m^{-3}. Gas mixtures with low mercury concentrations must be prepared freshly before use; they are unstable if stored for longer than 30 min.

The same method was also used to prepare test atmospheres containing the potentially interfering substances listed below. The concentrations of

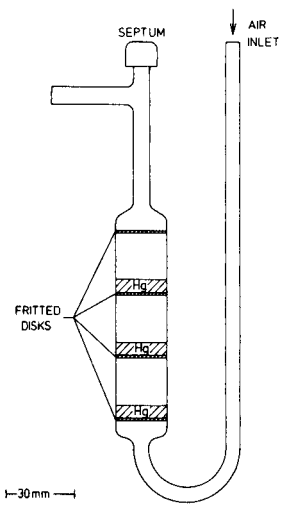

Fig. 5. Three-stage mercury saturator for the preparation of calibration gas mixtures.

these species, in the range of several ppm, were at least 10 times higher than the observed concentrations in clean air.

The dynamic method of generating gas mixtures of mercury and DMM employed three different permeation tubes: two polyethylene tubes (P_1, P_2) for mercury and one PTFE tube (P_3) for DMM. The dimensions of these tubes were: P_1, 50 mm long, 6 mm o.d., 4 mm i.d.; P_2, 50 mm long, 8 mm o.d., 3.2 mm i.d.; P_3, 57 mm long, 4 mm o.d., 3 mm i.d. The permeation rates of the first tube were 575 and 133 pg Hg min^{-1} at 25 and 12°C, respectively. The second tube delivered 6.7 pg Hg min^{-1} at 5.5°C, and the third provided 473 ng DMM min^{-1} at 30°C. With carrier gas flow rates of 0.5—10 l min^{-1} the concentrations of these test atmospheres covered the ranges 0.67—1150 ng Hg m^{-3} and 47.3—946 μg DMM m^{-3}.

Because of the rather low vapour pressures of MMC and MC, the test atmospheres for these species could be generated simply with a three-stage saturator, as described above, filled with crystalline MMC and MC. For MMC the concentrations obtained were 154 and 12 ng MMC cm^{-3} at 22 and 0°C, respectively [6] and the concentration of MC was 1.14 ng MC cm^{-3} at 20°C [7]. Difficulties were encountered with gas-tight syringes for the injection of gas mixtures of MMC and MC, probably because of adsorption on the surface of the syringes. The large scatter of the a.a.s. detector signals corresponding to MMC and MC injections could be reduced by careful, reproducible equilibration of the syringe used.

Collection efficiencies and capacities

The efficiencies of the collectors were determined with test atmospheres at mercury concentrations varying between 6.7 ng m^{-3} and 20 mg m^{-3}. For tests at high mercury concentrations the collector was inserted into the analytical system. The test samples were then injected upstream of the collectors and the amount of mercury, S_1, passing the collector was measured directly by the mercury detector. Subsequently, the amount of mercury, S_2, collected was determined. The collection efficiency, CE, was then calculated from $CE = 100\ S_2/(S_1 + S_2)\%$. The experiments were carried out at flow rates of 1 l min^{-1} with different volumes of test atmospheres corresponding to 200—1500 pg of mercury.

At lower mercury concentrations, a certain volume of the test atmosphere was passed through two collectors in series which were analyzed individually. The collection efficiency was calculated from the signals obtained as described above. These measurements were performed at concentrations of 6.7 ng m^{-3}, 144 ng m^{-3} and 292 μg m^{-3} and flow rates of 1 and 10 l min^{-1}. The same procedure was applied to determine the collector efficiencies for DMM, MMC, and MC.

To determine the collector capacity, the collector was incorporated in the analytical system which was flushed with a test atmosphere of mercury instead of the mercury-free carrier gas used in normal operation. A flow rate of 1 l min^{-1} was maintained until mercury was first observed in the detector.

The collector capacity was then calculated from the concentration of the test atmosphere and from the volume that passed the collector until the breakthrough of mercury. The measurements were carried out at different mercury concentrations ranging from 1 to 23 $\mu g\ m^{-3}$ and were then extended to MMC and DMM. The conversion of these compounds to elemental mercury, necessary for a.a.s. detection, was achieved by inserting a heated (700°C) gold-coated quartz wool collector between the collector and the mercury detector. Tests described below indicated that both DMM and MMC were quantitatively converted to elemental mercury at this temperature.

RESULTS AND DISCUSSION

Mercury—a.a.s. detector

Commonly the signal peak height is used as a measure of the mercury content but some authors, e.g. Long et al. [8] have found that the signal peak area is more precise. These two modes of evaluation were tested; no difference was found when a digital integrator (SpectraPhysics, Autolab Minigrator) was used to determine the peak area. Therefore, the easier evaluation from peak heights was preferred throughout.

The analytical curve of the detector was linear within the range 10—1616 pg of mercury, which was the maximum used. The relative standard deviation of the signal corresponding to 109 pg of mercury was 1.7% (n = 5). The definitions given by Parris et al. [9] give the lower detection limit of the detector as 10 pg for mercury. The detector worked satisfactorily under field conditions, even on board ships at times when strong vibrations, high temperature changes, and high relative humidities occurred.

Release temperature

The collectors were loaded with a certain amount of mercury and then heated to 700°C to release the collected mercury. After the determination of the mercury released the collector was heated again. Generally, the small signal observed during this second heating cycle amounted to ca. 6% of the signal obtained in the first heating cycle. This value could not be decreased by increasing the release temperature to 800°C or extending the heating period of the collector to several minutes. Adsorption of the released mercury on the walls of the flow system, downstream of the collector, is assumed to occur; to reduce the systematic error introduced by this memory effect, each collector can be heated twice and the signals can be added. The calibration should be performed in the same way. As 5 heating cycles would then be necessary for one determination (including the final cleaning of the collector) such a laborious procedure was used only when highly variable mercury concentrations had to be measured.

It was observed that the mercury recovery from the individual collector depended on the number of determinations performed with it. This behaviour was studied by injecting the same amount of mercury alternately into the

collector and directly into the mercury detector. Initially, the signal obtained from the freshly prepared gold-coated quartz wool collector represented, typically, 90% of the signal corresponding to the direct injection. This is a reasonable value in view of the memory effects described above and also the peak spreading in the connecting tubing. After 50 measurements, this value declined typically to 40%; the collector was then discarded. This decline was probably caused by condensation of minute amounts of gold vapour in the unheated parts of the collector. For this reason the collectors must be calibrated individually, immediately after the measurement of the mercury samples in them, as described above. No difference was observed between the simultaneous measurement of mercury in air collected by fresh and old collectors processed in this manner.

Capacity of the collectors

The collector capacities are listed in Table 1. In view of the uncertainties involved in their determination, the values given might be in error by ca. 30%. For elemental mercury, no breakthrough could be observed, even after experiments with a gas mixture containing 23 μg Hg m^{-3} flowing for 3 days through the collector at 1 l min^{-1}. Thus, the given capacities (99 μg Hg) for gold wool and gold-coated quartz wool collectors represent only the lower limit. For DMM and MMC the capacities amount to 32 and 36 μg Hg, respectively, for the gold wool collector and to 43 and 58 μg Hg, respectively, for the gold-coated quartz wool collector. Comparison of the data obtained for gold wool and for gold-coated quartz wool indicates that the collection capacity is directly proportional to the gold surface area.

The collector capacities given in Table 1 yield an indication of the character of bond between the mercury species and the gold surface. Assuming that the gold surface is covered by a monomolecular layer of DMM or MMC, the surface area occupied by one DMM or MMC molecule would be 0.43 nm^2 and 0.37 nm^2, respectively. Despite the uncertainties of this estimation, such values are comparable with the values reported for other small molecules [10]. So the collector capacity of the gold surface for DMM and MMC seems to be limited to that represented by a monomolecular layer. The considerably higher capacities for elemental mercury are assumed to result from the low steric hindrance and the diffusion of mercury atoms into the collector metal.

TABLE 1

Capacity of gold wool and gold-coated quartz wool collectors

	Capacity (μg Hg) for			Estimated gold surface area (cm^2)
	Hg	DMM	MMC	
Gold wool	99	32	36	405
Gold-coated quartz wool	99	43	58	510

For practical purposes, the actual amounts of mercury collected did not exceed 10 ng of mercury, i.e. more than 3 orders of magnitude lower than the capacity of the collectors.

Collection efficiency

The collection efficiencies of the gold wool and gold-coated quartz wool collectors are listed in Table 2, which includes data published by other authors. Mercury, DMM, MMC, and MC are collected nearly quantitatively at flow rates of 1 l min^{-1}. The collection efficiencies decrease to 91—96% if the sampling flow rate is increased to 10 l min^{-1}. Measurements at higher sampling flow rates were not carried out because of the difficulties of providing a mercury-free carrier gas at such high flow rates. The only data available for flow rates higher than 10 l min^{-1} were reported by Rawlings [2], who found a collection efficiency of 30% for elemental mercury at 113 l min^{-1} compared with 90% at 5 l min^{-1}.

The data indicate that the collection efficiencies depend on the residence time T of the air sample within the plug of collecting material, defined as $T = V/F$, where F is the sampling flow rate and V is the free volume of the plug of collecting material in the collector, i.e. the volume of the plug minus the volume of the collecting material. The data in Table 2 indicate that the collection efficiencies of the mercury species decrease markedly at residence times shorter than about 1×10^{-3} s. For the present collectors this value would correspond to a sampling flow rate of about 1×10^{4} l min^{-1}, which is three orders of magnitude higher than that used in the sampling device.

Most of the collector efficiencies reported were determined with test atmospheres involving rather high mercury concentrations [2, 12—14]. The validity of these collection efficiencies is then extended to mercury deter-

TABLE 2

Parameters and collection efficiencies of gold collectors

Ref.	F[a] (l min^{-1})	A[b] (cm^2)	V[c] (cm^3)	T[d] (s)	Collection efficiencies (%)			
					Hg	DMM	MMC	MC
This work[e]	1	405	12.6	8×10^{-1}	100	97	99	98
	10	405	12.6	8×10^{-2}	95	96	94	95
This work[f]	1	510	12.6	8×10^{-1}	100	98	104	102
	10	510	12.6	8×10^{-2}	91	94	91	95
[11]	100	359	1	6×10^{-4}	—	—	—	—
[12]	0.75—2.0	370	0.5	2×10^{-2}	100	100	100	100
[13]	0.3	39	0.5	1×10^{-1}	100	100	100	—
[2]	4.7	37	0.04	5×10^{-4}	90	64	0[g]	—
	113	37	0.04	2×10^{-5}	30	0[h]	0[g]	—

[a]Sampling flow rate. [b]Estimated gold surface area. [c]Free volume of the collecting plug (see text). [d]Residence time (see text). [e]Gold wool. [f]Gold-coated quartz wool. [g]Assumed. [h]Extrapolated.

minations at ambient concentrations several orders of magnitude lower than those used for the tests. Such an extension may be dangerous if the mercury collectors have a definite collection threshold as is encountered frequently in gas sampling [15]. The concentration dependence of the mercury collection efficiency of the collectors was therefore studied in the concentration range 20 $\mu g\ m^{-3}$—6.7 $ng\ m^{-3}$. In this range the efficiency was independent of mercury concentration. The collection efficiencies may also be influenced by deposition on the gold surface of atmospheric substances which then hinder the adsorption or absorption of mercury species or may even deactivate the surface of the collecting material chemically [13], so that the efficiency would decrease with increasing sampling volume. This possible effect was studied by means of two collectors in series; the first was "deactivated" by the passage of 500 l of urban or maritime air and the second collector was freshly cleaned by the procedure described above. The collection efficiencies were then measured indirectly as the amount of mercury compound passing the "deactivated" collector and collected on the second, clean collector. The results, summarized in Table 3, show that the efficiency of the "deactivated" collectors for DMM, MMC and MC is generally lower than that of a normal clean collector. The difference is most pronounced for the collector "deactivated" by urban air for which the collection efficiency of DMM is only 73%. Deactivation with maritime air gives collection efficiencies that are not significantly affected, with the exception of the collection efficiency of MMC.

Several experiments were also carried out to establish if desorption of the mercury species from the collector occurred. A collector loaded with a known amount of mercury, DMM, MMC, and MC was flushed with 300 l of mercury-free air and subsequently analyzed. Slight desorption was found for DMM, MMC, and MC (7, 3 and 3%, respectively) but mercury itself was not desorbed from the collector.

In the course of long-term measurements the collection efficiencies of the gold wool collectors gradually decreased to ca. 60% after ca. 50 measurements. This decrease arises mainly from sintering of the gold wool during the heating procedure and by mechanical settling during transport and handling

TABLE 3

"Deactivation" of gold-coated quartz wool collectors by traces of substances present in air

	Collection efficiency (%) at 10 l min^{-1}			
	Hg	DMM	MMC	MC
Clean collector	91	94	91	95
Collector "deactivated" by 500 l of urban air	94	73	82	85
Collector "deactivated" by 500 l of simulated maritime air[a]	95	89	80	91

[a]Air was sucked through a wash bottle filled with artificial sea water.

so that some of the air flow passes over rather than through the collecting material. In contrast to gold wool, the gold-coated quartz wool collectors did not show any decrease in collection efficiencies, even after 50 measurements, and are therefore preferred for field measurements.

Interferences and precision

Long et al. [8] have shown that other atmospheric constituents, e.g. H_2S and NO_2, interfere with measurements of mercury in air. Therefore, the method was tested for interferences by passing through the collector 4 l of mercury-free test atmospheres of air which contained: 1000 ppm of methane, ethane, ethene, propene, butane, butene, carbon dioxide; 500 ppm of water; 350 ppm of carbon monoxide; 100 ppm of methanol, propanol, heptanol, acetylene, trifluoromethane; 50 ppm of chloroform; 25 ppm of nitrous oxide; 15 ppm of H_2S, acetone; 2 ppm of nitrogen dioxide; 0.2 ppm of benzene, toluene and sulfur dioxide. The collector contents were then analyzed in the same manner as an air sample. The signals did not exceed the blank value of 20 pg typical for clean collectors and so interference by the species tested is improbable. Additional evidence for the absence of interferences was derived from simultaneous analyses of replicate air samples by the a.a.s. and a.e.s. mercury detectors. At a mercury concentration of 1.5 ng m^{-3}, no statistically significant difference ($P = 95\%, n = 6$) was found between the results obtained by these detectors, although it is rather improbable that they are subject to the same interferences. The concentrations of potential interferents used in these tests corresponded to those in moderately polluted air. In heavily polluted atmospheres, however, interferences may occur and the double amalgamation procedure described by Aubort et al. [16] should be used.

Another systematic error may arise from the ability of the mercury—a.a.s. detector to respond only to mercury and not to mercury compounds. Since the mercury—a.e.s. detector responds to all mercury-containing species [17], the results of the interference test described above imply that the mercury compounds are converted quantitatively to elemental mercury during the releasing procedure prior to detection by the mercury—a.a.s. detector, or the compounds are lost between the collector and the detector, or the atmospheric mercury occurs predominantly in the elemental form. The former two possibilities were studied together in detail. Collectors loaded with known amounts of DMM, MMC and MC were analyzed by the method described here. DMM and MMC were converted quantitatively to mercury but the signal for MC corresponded to 50 ± 10% of the signal expected for the amount of MC loaded. Consequently, the data obtained by this method do not represent the total mercury content of the air if it contains significant amounts of MC. Johnson and Braman [1] found that ca. 20% of the total mercury concentration in the air is due to MC and related compounds. The present measurements of mercury aerosols in remote areas indicate that the contribution of MC, which is adsorbed partially on the aerosol filter, to the total mercury is less than 20%. Therefore the systematic error introduced by non-quantitative detection of MC should not exceed 10%.

The mercury measurements may be influenced by contamination of the collectors during transport, storage and handling. The degree of contamination was determined by means of blank collectors treated in the same way as other collectors with the omission of the sampling step. Typical blank values were 20 pg for collectors stored for a period of one day so that ca. 200 pg of mercury must be collected to obtain an accuracy of ca. 10%. The blank value did not exceed 40 pg even when the collectors were stored for weeks in a laboratory atmosphere containing 100 ng Hg m^{-3}.

The precision of the complete analytical procedure including sampling, analysis and calibration under field conditions on board a research vessel was 14.5% (n = 5) for 400 l of sampled air with a mercury concentration of 1.5 ng Hg m^{-3}.

Conclusions

The method presented is suitable for the determination of total gaseous mercury in air at concentrations ranging from ng m^{-3} to $\mu g\ m^{-3}$, which covers the range expected for clean and urban air. The sampling device and the analytical device can be handled independently from each other. This arrangement has the advantages that air samples can be taken simultaneously at different locations, stored if necessary, and taken on carriers (e.g. balloons) where the analytical system cannot be installed. The complete mercury instrument is easy to handle, does not consume much electrical power, does not need a carrier gas supply, is insensitive to vibrations, temperature changes and high relative humidity, and can be operated in automobiles, ships and aircraft.

For a sampling flow rate of 10 l min^{-1} and a sampling volume of 200 l, ca. 20 min are needed to take a sample of background air. This sampling duration

TABLE 4

Typical measurements of total mercury concentration in air

Location	Date	Concentration (ng Hg m^{-3} (STP))
Mainz, University Campus	3/10/1977	9.9
France, height 11,300 m[a]	6/7/1977	3.2
France, height 9,800 m[a]	6/8/1977	3.3
Atlantic Ocean, west of Spanish coast[b]	10/8/1977	4.8 ± 2.5 (n = 13)[c]
Atlantic Ocean, north of Cabo Verde Islands[b]	10/12/1977	1.3 ± 0.2 (n = 7)[c]
Atlantic Ocean, east of Fern. de Norona Islands[b]	10/19/1977	1.8 ± 1.9 (n = 9)[c]

[a]Measured in aircraft. [b]Measured on board ship. [c]Mean value of mercury concentration measured between 8 a.m. and 11 p.m.

is suitable for most measurements in the field. In polluted air the sampling time can be reduced to ca. 5 min.

The instrument described has been used for measurements of the global distribution of mercury in the lower and upper troposphere and lower stratosphere. Background mercury concentrations of the order of 1—4 ng Hg m^{-3} [18] were found: typical results are shown in Table 4.

This work, performed within the program of the Sonderforschungsbereich 73 "Atmospheric Trace Components", received support from the Deutsche Forschungsgemeinschaft. Thanks are due to W. Geins and G. Schuster for their assistance in some measurements.

REFERENCES

1 D. L. Johnson and R. S. Braman, Environ. Sci. Technol., 8 (1974) 1003.
2 G. D. Rawlings, Dissertation, Texas A & M University, August 1974.
3 B. A. Soldano, P. Bien and P. Kwan, Atmos. Environ., 9 (1975) 941.
4 C. L. Eberling, Dissertation, University of Mainz, 1975.
5 G. Kaiser, D. Götz, P. Schoch and G. Tölg, Talanta, 22 (1975) 889.
6 Y. Talmi and R. E. Mesmer, Water Res., 9 (1975) 547.
7 Handbook of Chemistry and Physics, 52nd edn., The Chemical Rubber Co., Cleveland, Ohio, 1972.
8 S. I. Long, D. R. Scott and R. J. Thompson, Anal. Chem., 45 (1973) 2227.
9 G. E. Parris, W. R. Blair and F. E. Brinckman, Anal. Chem., 49 (1977) 378.
10 L. I. Osipow, Surface Chemistry, ACS Monograph Series No. 153, Reinhold, New York, 1964, p. 35.
11 S. H. Williston, J. Geophys. Res., 73 (1968) 7051.
12 R. S. Braman and D. L. Johnson, Environ. Sci. Technol., 8 (1974) 996.
13 Å. Henriques and I. Isberg, Chem. Scripta, 8 (1975) 173.
14 I. Scullman and G. Widmark, in R. W. Frey and O. Hutzinger (Eds.), Analytical Aspects of Mercury and Other Heavy Metals in the Environment, Gordon & Breach, London, 1975, p. 69.
15 J. P. Lodge, Jr., Proceedings of the 7th IMR Symposium, October 1974, Gaithersburg, NBS Publication No. 422, 1976, p. 311.
16 J.-D. Aubort, H. Rollier and A. Ramuz, Trav. Chim. Aliment. Hyg., 68 (1977) 155.
17 B. A. Soldano and P. W. O. Kwan, Appl. Spectrosc., 29 (1975) 271.
18 C. L. Eberling, W. Geins, F. Slemr and W. Seiler, Air Pollution Measurement Techniques, Special Environmental Report No. 10, World Meteorological Organization, Geneva, Switzerland, 1977, p. 118.

Analytica Chimica Acta, 110 (1979) 49—54

ATOMIC ABSORPTION SPECTROMETRY OF TELLURIUM WITH ELECTROTHERMAL ATOMIZATION IN A MOLYBDENUM MICROTUBE

KIYOHISA OHTA and MASAMI SUZUKI*

Department of Chemistry, Faculty of Engineering, Mie University, Kamihama-cho, Tsu-shi, Mie-ken 514 (Japan)

(Received 20th March 1979)

SUMMARY

Hydrogen, added to argon purge gas, is necessary to protect the molybdenum microtube atomizer from oxidation, but it increases the atomization temperature and decreases the maximum absorbance of tellurium. A mixture of thiourea and copper removes the interfering effects of diverse elements and counteracts the effect of hydrogen. Tellurium (20—200 ppm) in copper can be determined after extraction as a chloride complex.

Flame atomic absorption spectrometry (a.a.s) has been utilized in analysis for tellurium, especially coupled with the hydride generation technique [1]. Greenland and Campbell [2] developed a hydride generation—flameless a.a.s. method for rapid determination of nanogram amounts of tellurium in silicate rocks; tellurium hydride was passed through a resistance-heated quartz cell for atomization. A problem of this method is that copper suppresses the generation of tellurium hydride. There is little information concerning electrothermal atomization with carbon or metal atomizers. Hwang et. al. [3] obtained a sensitivity (1% absorption) of 6×10^{-10} g for tellurium at 214.3 nm using a tantalum ribbon atomizer. A sensitivity of 1×10^{-10} g was claimed for a graphite furnace atomizer [4].

In the present work, the electrothermal atomization of tellurium is investigated with a metal atomizer and a fast-response detection system to evaluate the atomization characteristics and interference phenomena for tellurium, and to develop a favourable atomization technique for real samples. The fast-response detection system allows the rapid atomization to be recorded without distortion. The molybdenum micro-tube has the advantages that it is readily made; brief heating suffices to provide a uniform temperature throughout the atomizer, giving the maximum atom cloud concentration very rapidly.

EXPERIMENTAL

Apparatus

Atomic absorption measurements were made with a Nippon Jarrell-Ash

0.5-m Ebert-type monochromator coupled to an R106 photomultiplier tube (Hamamatsu TV Co.) and a fast-response amplifier which was assembled in this laboratory. The output signal from the amplifier was monitored on a Memoriscope (Iwatsu MS-5021). A Hitachi chart recorder (056-1001) was also used.

The atomizer was a molybdenum micro-tube (25 mm long and 1.5 mm bore) [5] mounted in the absorption chamber (300 ml volume) which was purged with argon at 480 ml min^{-1} and hydrogen at 20 ml min^{-1} (unless otherwise stated). The tube temperature was measured as described previously [6].

The light source was a tellurium electrodeless discharge lamp (Hamamatsu TV Co.) operated by a 27-MHz microwave generator (Hamamatsu C977 power supply). The analytical wavelength used was 214.28 nm. Background absorption was checked with a deuterium lamp (Original Hanau D200F). All sample solutions were injected with a glass micropipette.

Reagents

A tellurium stock solution (1 mg Te ml^{-1}) was prepared by dissolving tellurium metal in the minimum volume of aqua regia. This was evaporated with concentrated hydrochloric acid on a water bath and diluted with 6 M hydrochloric acid. More dilute standard solutions were prepared by dilution with water immediately before use. All reagents were of analytical-reagent grade.

Procedures

The sample solution (1 μl) was placed in the micro-tube atomizer and dried at 50°C for 10 s, followed by ashing at 200°C for 3 s. Tellurium was atomized by heating to a final temperature of 2200°C. All atomic absorption signals were traced on the Memoriscope.

Determination of tellurium (20—200 ppm) in copper

Dissolve 0.1—0.5 g of the sample with 10 ml of aqua regia, and evaporate on a hot water bath. Repeat the evaporation after addition of 10 ml of 6 M hydrochloric acid. Dissolve the residue in 0.01 M hydrochloric acid and dilute to 25 (or 100) ml with the 0.01 M acid. Transfer 1 ml of the solution to a separatory funnel and add 1.7 ml of concentrated hydrochloric acid. Extract the tellurium complex into 3 ml of methyl isobutyl ketone (MIBK). Take an aliquot (e.g. 1 ml) of the organic phase and mix with the same volume of ethanolic thiourea solution (2%). Place 1 μl of this mixture into the microtube atomizer, atomize tellurium and measure the maximum absorbance. Prepare the calibration graph by extracting tellurium from standard solutions containing the same concentration of copper as the sample.

RESULTS AND DISCUSSION

Atomization characteristics of tellurium

It is necessary to mix hydrogen with the argon purge gas in order to protect the atomizer from oxidation by traces of oxygen in the argon. Therefore, the dependence of atomization profile for a sodium tellurite solution (0.125 ng of Te) on purge gas flow rates was examined. The results are shown in Fig. 1. The lowest atomization temperature of tellurium was achieved in a pure argon atmosphere. The peak temperature (the temperature at which maximum absorption is observed) increased and the peak broadened with increasing hydrogen flow. No absorbance was obtained in pure hydrogen. The highest peak was also achieved in pure argon. It seems reasonable to assume, therefore, that tellurium hydride can be formed in the atomizer and the presence of increasing concentrations of hydrogen shift the dissociation of the hydride in favour of the undissociated species. The higher specific heat and thermal conductivity of hydrogen than argon was also responsible for decreasing tellurium atomization at the higher flow rates. The delayed peak shows that greater heat is required for dissociating the hydride at greater hydrogen flows. A similar effect of hydrogen has been shown for selenium [7].

Thiourea reversed the effect of adding hydrogen. The atomization temperature of tellurium in the presence of thiourea in 480 ml Ar min^{-1} and 20 ml H_2 min^{-1} was similar to that of tellurium alone in pure argon, although the peak height was decreased (Fig. 2). Thiourea reduces tellurium(IV) to tellurium(II), followed by the formation of tellurium(II)—thiourea complex [8]. This may contribute to the tellurium atom production at comparatively low temperatures. A further increase in the flow rate of hydrogen again increases the peak temperature and reduces the sensitivity even in the presence of thiourea. Therefore, the limited flow rate of hydrogen (20 ml min^{-1}) was used in subsequent work.

The atomization of tellurium from its diethyldithiocarbamate (DDTC) and chloride complexes is also shown in Fig. 2. The complexes were extracted into MIBK as described previously [9, 10]. The chloride complex ($TeCl_6^{2-}$) gave a low absorbance at a relatively high temperature. The favourable effect of thiourea was also evident in the atomization of tellurium from these complexes. An equal volume of 2% thiourea solution in ethanol was mixed with the organic phase before atomization. Similar atomization profiles were observed for both complexes and were similar to that obtained for an aqueous telurite solution containing thiourea.

Sensitivity, reproducibility and interferences

The maximum absorbance was reproducible, and was measured to obtain the calibration graph. The absolute sensitivities (1% absorption) were 4.7×10^{-12} and 1.2×10^{-12} g of tellurium for pure tellurite solution and that containing thiourea, respectively. The coefficient of variation for the determination of 0.5 ng of tellurium was 3.7% (10 replicates).

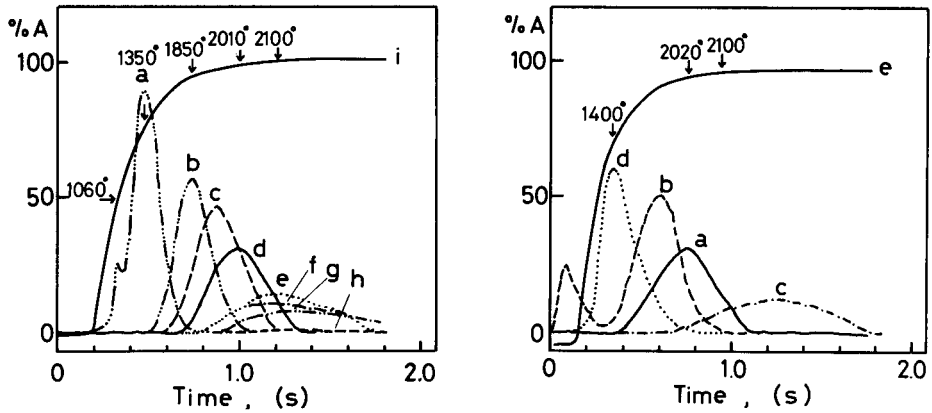

Fig. 1. Memoriscope traces of effect of hydrogen flow rate on atomization of tellurium (0.125 ng) from aqueous solution. (a) 500 ml Ar min^{-1} ; (b) 490 ml Ar min^{-1} and 10 ml H_2 min^{-1} ; (c) 485 ml Ar min^{-1} and 15 ml H_2 min^{-1} ; (d) 480 ml Ar min^{-1} and 20 ml H_2 min^{-1} ; (e) 400 ml Ar min^{-1} and 100 ml H_2 min^{-1} ; (f) 300 ml Ar min^{-1} and 200 ml H_2 min^{-1} ; (g) 200 ml Ar min^{-1} and 300 ml H_2 min^{-1} ; (h) 500 ml H_2 ; (i) temperature increase.

Fig. 2. Memoriscope traces for atomization of tellurium (0.125 ng). (a) Aqueous Te(IV) solution; (b) DDTC complex in MIBK; (c) chloride complex in MIBK; (d) aqueous Te solution containing 4 μg of thiourea; (e) temperature increase. Gas flows, 480 ml Ar min^{-1} and 20 ml H_2 min^{-1}.

The effects of various acids, (0.05 M hydrochloric, nitric, perchloric, phosphoric and sulphuric) on tellurium atomization were tested. Nitric, perchloric, phosphoric and sulphuric acids showed complex atomization profiles (Fig. 3). For nitric acid the absorption at lower temperatures was from NO. Molecular absorption was also observed at lower temperatures for other acids. Therefore, the absence of acids, except for a low concentration of hydrochloric acid, is advisable for atomization of tellurium.

The effects of 100-fold amounts of aluminium, antimony, arsenic, bismuth, chromium, copper, gallium, iron, lead, nickel, selenium, tin and zinc on the atomization of 0.125 ng of tellurium were also investigated. Antimony, arsenic and selenium were added as antimony potassium tartrate, sodium arsenite and selenious acid, respectively; other elements were added as their chlorides. All the samples were checked for background effects. Pronounced interferences were observed for aluminium and bismuth (Fig. 4). Arsenic, gallium and lead increased the peak atomization temperature. Other elements had little effect on atomization of tellurium, therefore the absorption profiles of tellurium in the presence of antimony, chromium, copper, iron, nickel and selenium are not shown. Thiourea did not affect the interferences of aluminium and bismuth. However, all interferences were eliminated by the addition of copper and thiourea (Fig. 4).

Antimony, arsenic, bismuth, lead, selenium and tin can be extracted with tellurium as DDTC complexes. The effects of 10-fold amounts of these elements co-extracted with tellurium were examined. As shown in Fig. 5,

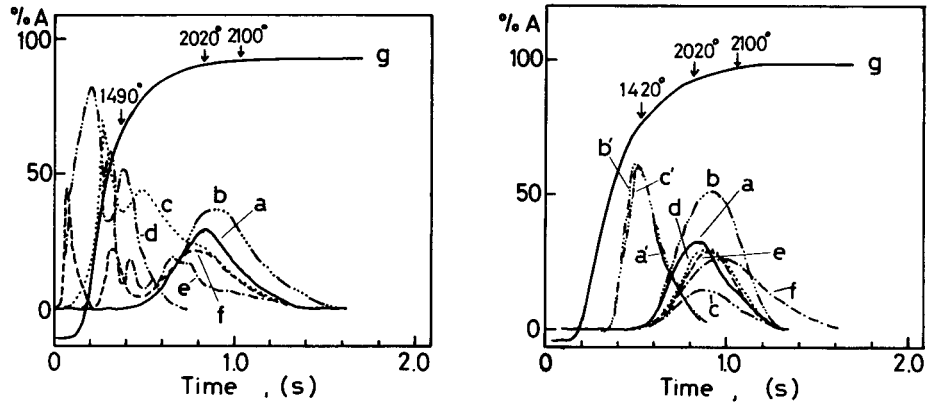

Fig. 3. Memoriscope traces for effect of acids on atomization of tellurium (0.125 ng). (a) 1×10^{-3} M HCl; (b) 0.05 M HCl; (c) 0.05 M HNO_3; (d) 0.05 M H_2SO_4; (e) 0.05 M H_3PO_4; (f) 0.05 M $HClO_4$; (g) temperature increase. Gas flows as in Fig. 2.

Fig. 4. Memoriscope traces of effects of 12.5 ng of various elements on tellurium atomization (0.125 ng Te). (a) Te alone; (b) Te and Al; (c) Te and Bi; (d) Te and Ga; (e) Te and As; (f) Te and Pb; (a'), (b') and (c') Cu (12.5 ng) and thiourea (4 μg) were added to (a), (b) and (c). (g) temperature increase. Gas flows as in Fig. 2.

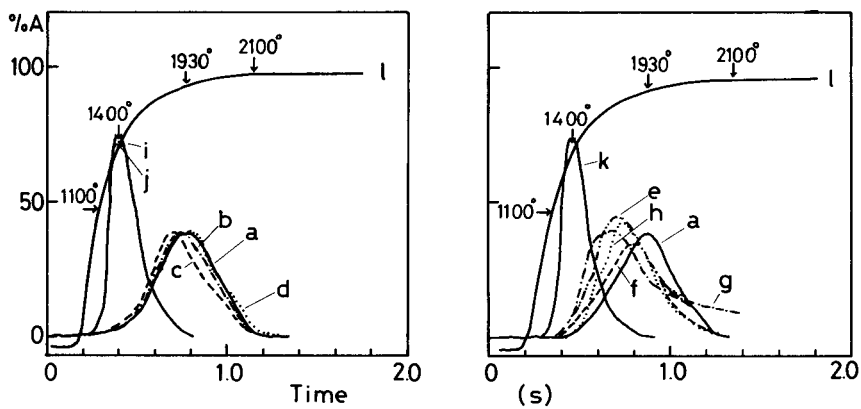

Fig. 5. Memoriscope traces of effects of 1.25 ng of various elements extracted with tellurium (0.125 ng) as DDTC complex in MIBK. (a) Te alone; (b) Te and Bi; (c) Te and As; (d) Te and Sb; (e) Te and Pb; (f) Te and Sn; (g) Te and Se; (h) Te and Cu; (i)Cu (12.5 ng) and thiourea (4 μg) added to (c), (d) or (h); (j) Cu (12.5 ng) and thiourea (4 μg) added to (b); (k) Cu (12.5 ng) and thiourea (4 μg) added to (e), (f), (g) or (h); (l) temperature increase. Gas flows as in Fig. 2.

these elements interfered with the atomization of tellurium, but not in the presence of copper and thiourea. The tellurium complex was extracted in the presence of a 100-fold amount of copper, and thiourea solution was mixed with the organic phase before atomization.

For the chloride complex no interferences were observed from antimony, iron and tin co-extracted with tellurium from 7.5 M hydrochloric acid if

TABLE 1

Determination of tellurium in copper

Sample	Tellurium found (ppm)	
	Proposed method	Gravimetric method
1	27, 33, 29	34
2	74, 70, 70	60
3	160, 160, 170	140

copper was also present, because 6% of the copper was also extracted. The absorption profiles are not shown because they are similar to those for DDTC complex.

Determination of tellurium in copper

The atomization in the molybdenum microtube was applied to the determination of tellurium in copper. Extraction of the chloride complex was used for preliminary separation of tellurium from most of the matrix. Copper (6%) was coextracted, which served to suppress the interferences from other elements co-extracted with tellurium.

The results of tellurium determinations in some copper samples by the recommended procedure are listed in Table 1, together with the values obtained by a gravimetric method [11]. The results demonstrate the usefulness of the electrothermal atomization with a molybdenum microtube. The values obtained by the present method were in somewhat poor agreement with those obtained by gravimetry, perhaps because of the small sample size in the present method, which could be influenced by sample segregation.

In conclusion, atomization of tellurium is favoured by the addition of copper and thiourea to the tellurium solution, and the interferences from diverse elements are suppressed in this way. However, a preliminary separation, such as solvent extraction, of tellurium from matrix material is advisable for complex samples.

REFERENCES

1 K. C. Thompson and D. R. Thomerson, Analyst, 99 (1974) 595.
2 L. P. Greenland and E. Y. Campbell, Anal. Chim. Acta, 87 (1976) 323.
3 J. Y. Hwang, C. J. Mokeler and P. A. Ullucci, Anal. Chem., 44 (1972) 2018.
4 C. W. Fuller, Electrothermal Atomization for Absorption Spectrometry, Chem. Soc., London 1977, p. 81.
5 K. Ohta and M. Suzuki, Anal. Chim. Acta, 77 (1975) 288.
6 K. Ohta and M. Suzuki, Anal. Chim. Acta, 83 (1976) 381.
7 K. Ohta and M. Suzuki, unpublished work.
8 K. W. Bagnall, in J. C. Bailar, Jr., H. J. Emeleus, R. Nyholm and A. F. Troutman-Dickenson, Comprehensive Inorganic Chemistry, Vol. 2, Pergamon Press, 1973. 935 pp.
9 I. Havezov and N. Jordanov, Talanta, 21 (1974) 1013.
10 O. Kammori, T. Takahari and S. Bando, Bunseki Kagaku, 16 (1967) 826.
11 E. Keller, J. Am. Chem. Soc., 22 (1900) 241.

Analytica Chimica Acta, 110 (1979) 55—60

DETERMINATION OF SUBMICROGRAM AMOUNTS OF TIN BY ATOMIC ABSORPTION SPECTROMETRY WITH ELECTROTHERMAL ATOMIZATION

MAMORU TOMINAGA* and YOSHIMI UMEZAKI

National Research Institute for Pollution and Resources 4-26, Ukima, Kita-ku, Tokyo (Japan)

(Received 14th March 1979)

SUMMARY

The determination of tin is described with particular reference to the addition of organic compounds to the graphite tube for the suppression of interferences of other ions. Most were suppressed by adding 20 μl of 10% ascorbic acid to 20 μl of sample in the furnace. The method was used for the determination of tin in waste-waters and sediments.

Atomic absorption spectrometry with flames is effective for the determination of tin owing to its selectivity and rapidity, but its sensitivity is poor even in a nitrous oxide—acetylene flame [1]. Several workers have had to apply concentration and isolation procedures before the determination [2—4]. Little has been published regarding the electrothermal atomization of tin. Del Monte Tamba and Luperi [5] and Trachman et al. [6] reported that far higher sensitivity was obtained using a graphite furnace than a flame in the analysis of steel and biological materials.

This report describes a direct determination of submicrogram amounts of tin in waste waters and sediments by atomic absorption spectrometry with a graphite furnace, and evaluates the effect of adding organic compounds to the sample solution in the graphite tube to suppress interferences [7].

EXPERIMENTAL

Apparatus and reagents

A Perkin-Elmer graphite furnace (HGA-2100) was used in conjunction with a Perkin-Elmer 403 atomic absorption spectrometer and a Hitachi 056 recorder. The light source was a Hamamatsu TV tin single-element hollow-cathode lamp. A deuterium lamp was used for background compensation. Sample solutions were injected into the graphite tube by micropipette (Rainin Co. P-20).

The instrumental parameters were as follows: lamp current, 12 mA; spectral bandwidth, 0.3 nm; wavelength, 224.6 nm. The atomization cycle was: dry at 100°C (60 s); char at 700°C (40 s); atomize at 2500°C (10 s).

Tin metal (1 g) was dissolved in 100 ml of concentrated hydrochloric acid and diluted to 1 l with distilled water. This solution was diluted as necessary with hydrochloric acid (10% v/v). All acids used were of super-special grade (Wako Pure Chemicals). Other reagents were of analytical-reagent grade.

General atomic absorption procedure

Sample solution (20 μl) was injected into the graphite tube. The argon gas flow rate was 80 ml min^{-1} and the gas flow was interrupted during the atomizing step. The measuring conditions are indicated above. Tin was measured by peak height. Background correction with a deuterium lamp was used when necessary.

In the procedure finally recommended, 20 μl of 10% (w/v) ascorbic acid solution was injected immediately after the sample solution.

RESULTS AND DISCUSSION

Atomizing conditions

Optimal conditions for drying were 100°C for 60 s for 20 μl of tin solution. The absorbance of tin decreased if the charring temperature exceeded 800°C. The optimal charring temperature was 700°C. The absorbance of tin did not decrease over 2 min at this temperature. The flow of argon sheath gas was interrupted during the atomizing step to give maximum sensitivity. As the atomizing temperature increased the sensitivity increased. The maximum temperature of the instrument, 2800°C, gave maximum sensitivity. But at this temperature the life of the graphite tube was much decreased. Thus an atomizing temperature of 2500°C was chosen as a reasonable compromise which ensured 100—150 measurements with the same tube.

A calibration graph obtained under these conditions was linear up to 150 $\mu g\ l^{-1}$ for 20-μl injections of standard tin solutions. The sensitivity (1% absorption) was 5×10^{-11} g and the coefficient of variation was 3% ($n = 10$) at 50 $\mu g\ l^{-1}$.

Effect of other species

Figure 1 shows the effect of acids on tin absorbance. Increasing concentrations of hydrochloric, nitric and phosphoric acids had no effect even at 2 N concentrations. However, the sensitivity in phosphoric acid was about half that in hydrochloric or nitric acid. The absorbance in sulfuric acid and perchloric acid decreased rapidly as the acid concentration increased. The depressive effects of phosphoric, sulfuric and perchloric acids could not be suppressed by the addition of 2 M hydrochloric or nitric acids. The determination of tin in samples containing these depressive acids will therefore involve sample pretreatment or the use of a standard addition method.

Table 1 shows the effects of foreign metal ions in 1000-fold weight excess over tin. Aluminium, cadmium, iron, zinc, potassium, magnesium and sodium seriously affected tin absorption. The effects were depressive except that of

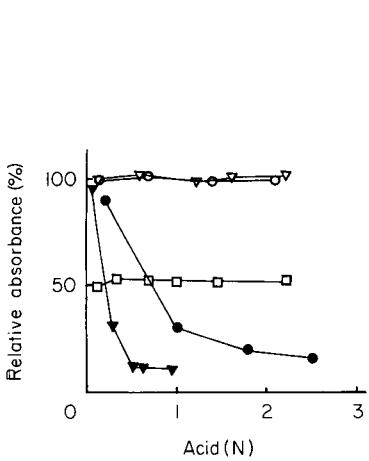

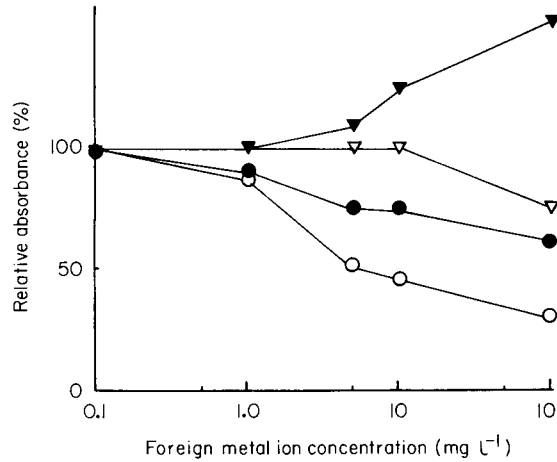

Fig. 1. Effect of acids on atomic absorption of tin (2 ng): (▽) HNO_3; (○) HCl; (□) H_3PO_4; (●) H_2SO_4; (▼) $HClO_4$.

Fig. 2. Effect of foreign metal ions on atomic absorption of tin (2 ng): (▼) $AlCl_3$; (▽) $Pb(NO_3)_2$; (●) $Fe(NO_3)_3$; (○) Na_2SO_4.

TABLE 1

Effect of foreign metal ions on the percentage recovery of tin[a]

Metal ion	Added as			Metal ion	Added as		
	Chloride	Nitrate	Sulfate		Chloride	Nitrate	Sulfate
Al^{3+}	158	175	62	K^+	100	55	38
Ca^{2+}	100	100		Mg^{2+}	100	74	66
Cd^{2+}	75	56		Mn^{2+}	100		
Co^{2+}	100	100		Na^+	72	78	31
Cr^{3+}		85		Ni^{2+}	100	100	
Cu^{2+}	100	100	100	Pb^{2+}	88	85	
Fe^{3+}	52	62		Zn^{2+}	48	34	100

[a]Tin (100 $\mu g\ l^{-1}$) and foreign metal ion (100 $mg\ l^{-1}$) in 10% HCl.

aluminium. Figure 2 shows the variation in the absorbance of 50 μg Sn l^{-1} as a function of some foreign metal ion concentrations. Many metals gave negative errors when present in 100-fold amounts, as typified by lead nitrate. The effect of iron (and zinc) was also present at 10-fold amounts. Sodium sulfate and many other sulfates (but not copper or zinc sulfate) also interfered in greater than 10-fold amounts. The interference of aluminium as nitrate or chloride was obtained for 50-fold amounts or more.

The addition of chemical compounds into the graphite tube has been recommended for the suppression of interferences [7]. Regan and Warren [8]

reported the addition of ascorbic acid as an interference-suppressing reagent in the determination of lead. Such an effect would also be expected for tin. Table 2 shows how several organic compounds suppress the interferences of zinc chloride, iron(III) nitrate and sodium sulfate. A 20-μl aliquot of 10% solution of the organic compound solution was injected into the graphite tube to mix with the 20 μl of sample solution, previously injected, before the dry, char and atomize steps. Tartaric acid, sucrose, L-ascorbic acid, D-glucose and D-fructose were effective suppressors for zinc and iron, but for sodium sulfate only ascorbic acid was effective. Carbon powder and the chelating reagents, triethanolamine and phenyl fluorone, were not effective.

Figure 3 shows the effect of ascorbic acid concentration on the interferences of several metal ions. All were suppressed by the addition of a $\geqslant$10% ascorbic acid solution. Table 3 shows the effect of ascorbic acid on the interferences of other metal ions present in 1000-fold amounts. The addition of ascorbic acid was effective in eliminating the interferences in nearly all instances, making it possible to determine tin directly. It is surmised that ascorbic acid produces a uniform mixture of carbon and sample during the charring step, and would promote the formation of an atomic vapor from oxides or inter-elemental compounds, thus reducing interference. However, little is known about the processes involved in such interferences or their removal.

Analysis of waste-waters and sediments

Table 4 shows the recovery of tin from several waste-waters to which tin was added to give a concentration of 50 μg l^{-1}. The ascorbic acid addition procedure gave good recoveries. This method was also applied to the determination of tin in several sediments. Samples were digested with a mix-

TABLE 2

Comparison of various organic compounds for the suppression of interferences on the percentage recovery of tin[a]

Organic material	Salt added		
	$ZnCl_2$	$Fe(NO_3)_3$	Na_2SO_4
None	48	62	31
Tartaric acid	100	100	61
Sucrose	100	100	33
L-Ascorbic acid	100	100	100
D-Glucose	100	100	46
D-Fructose	100	100	46
Citric acid	109	100	39
Carbon powder	37	78	10
Triethanolamine	71	54	30
Phenyl fluorone	78	69	32

[a]Tin (100 μg l^{-1}), foreign metal ion (100 mg l^{-1}), in 10% HCl and an aqueous 10% solution of the organic material. Carbon powder was suspended in distilled water.

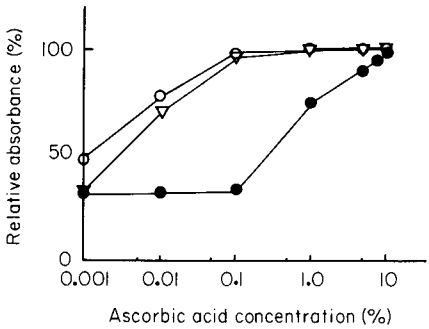

Fig. 3. Effect of concentration of ascorbic acid solution on interferences on atomic absorption of tin (2 ng): (○) $ZnCl_2$; (▽) $Zn(NO_3)_2$; (●) Na_2SO_4 (metal at 100 mg l^{-1}).

TABLE 3

Effect of ascorbic acid on interferences of foreign metal ions on the percentage recovery of tin[a]

Salt added	No ascorbic acid added	Ascorbic acid added	Salt added	No ascorbic acid added	Ascorbic acid added
$AlCl_3$	158	115	$Mg(NO_3)_2$	74	92
$Al(NO_3)_3$	175	116	$MgSO_4$	64	100
$Al_2(SO_4)_3$	62	100	NaCl	72	100
$CdCl_2$	75	100	$NaNO_3$	78	100
$Cd(NO_3)_2$	56	100	Na_2SO_4	31	100
$FeCl_3$	52	100	$ZnCl_2$	48	100
$Fe(NO_3)_3$	62	100	$Zn(NO_3)_2$	34	100
KNO_3	55	100			
K_2SO_4	38	108			

[a]Tin (100 μg l^{-1}) and foreign metal ion (100 mg l^{-1}) in 10% HCl.

ture of nitric, perchloric and hydrofluoric acids. The solutions obtained were diluted with 10% hydrochloric acid and tin was determined with and without ascorbic acid addition, as well as by a standard addition method also not involving ascorbic acid addition. Table 4 shows also the results obtained. In all samples, the results obtained by direct measurement in the absence of ascorbic acid were lower than those obtained by the other two methods. The standard addition and ascorbic acid addition methods were in good agreement. The coefficients of variation calculated from five measurements on samples a, b and c with ascorbic acid addition were 8.2, 7.2 and 3.1%, respectively.

The direct determination of tin with the addition of ascorbic acid is therefore a simple and rapid method not requiring any special pretreatment. The addition of an appropriate compound such as ascorbic acid may also be effective in removing interferences in the determination of other elements with the graphite furnace.

TABLE 4

Recovery of tin added to waste-waters in 50 $\mu g\ l^{-1}$ quantities, and the results obtained for tin in sediments after acid digestion

Sample	Tin found[a] ($\mu g\ l^{-1}$)		Standard addition
	Ascorbic acid not added[a]	Ascorbic acid added[a]	
Waste-waters			
A	0	48	—
B	0	51	—
C	4	51	—
D	15	53	—
Sediments			
a	15	75	73
b	5	28	33
c	125	268	261

[a]Tin values were found by reference to the appropriate calibration graph.

REFERENCES

1 B. Moldan, I. Rubeska, M. Miksovsky and M. Huka, Anal. Chim. Acta, 52 (1970) 91.
2 T. Kono, Jpn. Anal., 20 (1971) 552.
3 J. D. Mensik and H. J. Seidemann, At. Absorpt. Newsl., 13 (1974) 8.
4 E. P. Welsch and T. T. Chao, Anal. Chim. Acta, 82 (1976) 337.
5 M. G. Del Monte Tamba and N. Luperi, Analyst, 102 (1977) 489.
6 H. L. Trachman, A. J. Tyberg and P. D. Branigan, Anal. Chem., 49 (1977) 1090.
7 R. D. Ediger, At. Absorpt. Newsl., 14 (1975) 127.
8 J. G. T. Regan and J. Warren, Analyst, 101 (1976) 220; 103 (1978) 447.

Analytica Chimica Acta, 110 (1979) 61—66

THE DETERMINATION OF METALS AT PPB LEVELS BY THIN-FILM X-RAY FLUORESCENCE SPECTROMETRY AFTER COPRECIPITATION WITH A MOLYBDENUM CARRIER COMPLEX

A. J. PIK, A. J. CAMERON, J. M. ECKERT*, E. R. SHOLKOVITZ and K. L. WILLIAMS

Department of Inorganic Chemistry, University of Sydney, Sydney, N.S.W. 2006 (Australia)

(Received 8th March 1979)

SUMMARY

A method is described for the determination of iron, cobalt, nickel, copper, zinc, cadmium and lead in water at $\mu g\ l^{-1}$ levels, in which the metals are coprecipitated with a molybdenum—pyrrolidinedithiocarbamate carrier complex. The precipitate is collected as a thin film on a membrane filter (0.4-μm pore-size) and analysed directly by x-ray fluorescence spectrometry. Detection limits, for 100-ml water samples and counting times of 200 s per element, are 1 μg metal l^{-1} or lower. Total dissolved metal concentrations are obtained without boiling or u.v. irradiation of the water sample. The method is applicable to river and estuarine waters and is not affected by dissolved organic matter.

The determination of metals in natural waters requires a preliminary concentration step if the metals are present at $\mu g\ l^{-1}$ levels or lower. In this paper, a method is described for the determination of dissolved Fe, Co, Ni, Cu, Zn, Cd and Pb in which preconcentration is done by coprecipitation with a molybdenum—pyrrolidinedithiocarbamate complex. The precipitate is collected as a thin film which is analysed by x.r.f. spectrometry. Optimum x.r.f. operating conditions are defined and the performance of the method in the presence of sea salt and dissolved organic matter is assessed.

The proposed method combines high sensitivity with a simple, rapid analytical finish. Detection limits of 1 $\mu g\ l^{-1}$ or lower are obtained for the specified metals by direct multi-element analysis of the precipitate; acid digestion, a requirement of procedures coupling coprecipitation with analysis by a.a.s. or a.s.v., is unnecessary. A 4*d* metal, molybdenum, is used as the carrier, instead of the 3*d* metals of published metal—complex coprecipitation methods [1—7], for two reasons. The carrier metal, present in gross amounts, cannot itself be determined after coprecipitation; molybdenum is therefore a convenient carrier when a water sample is to be analysed for 3*d* metals. Further, the characteristic x-ray spectral emissions of molybdenum do not interfere with the most sensitive lines of the specified analyte metals.

Molybdenum has been used previously, by Ulrich and Hopke [8], to check the efficiency of coprecipitation of trace metals with organic complexing

agents. The water samples tested in that study contained relatively high metal concentrations and the addition of a carrier metal was shown to be unnecessary. The method described in this paper, however, was developed for the 1—100 μg metal l^{-1} range and the inclusion of the carrier was found to be essential.

EXPERIMENTAL

Reagents

Distilled-deionized water was used for all solution preparations and dilutions.

Molybdate solution. Dissolve 0.322 g of ammonium heptamolybdate tetrahydrate in water and dilute to 500 ml.

APDC solution. Dissolve 1 g of ammonium pyrrolidinedithiocarbamate (APDC) in water and dilute to 100 ml. Filter through a membrane filter (0.4-μm pore-size) and remove trace metal impurities from the filtrate by extraction with 5-ml quantities of carbon tetrachloride. The APDC solution should be used within 24 h, but it may be kept for up to a week if refrigerated.

Acetate solution. Dissolve 108.3 g of anhydrous sodium acetate in water and dilute to 500 ml. Filter through a 0.4-μm membrane filter, add 1 ml of APDC solution and extract with 5-ml quantities of carbon tetrachloride.

Coprecipitation procedure

Filter the water sample through a membrane filter (0.4-μm pore-size) and reduce the pH of the filtrate to below 2 by addition of 15 M nitric acid (5 ml per litre of filtrate should be sufficient). Transfer 100 ml of the acidified filtrate to a 250-ml polythene bottle fitted with a screw cap and adjust the pH to 4.4 (±0.1) with the acetate solution (5 ml per 100 ml of acidified filtrate should be enough).

Add 1 ml of the molybdate solution, followed by 5 ml of the APDC solution. Cap the bottle, shake it for 30 s and allow to stand for 30 min. Filter the suspension under suction through a polycarbonate filter (0.4-μm pore-size), which is used without prior washing. Place the loaded filter in a plastic box and dry, first in an air oven at 50°C for 12 h and then in a vacuum desiccator for a further 12 h. In the present investigation, precipitates were collected on Nuclepore polycarbonate membrane filters (37 mm diameter) with a Sartorius vacuum filtration unit (3.1-cm^2 filtration area).

Prepare a set of thin-film standards, including a blank, by treatment of standard solutions of the analyte metals in water. The precipitates are stable and standards prepared on polycarbonate filters can be used repeatedly.

X.r.f. analysis

The precipitates were analysed with a Philips PW1450 sequential x-ray spectrometer, with a computer-controlled system for automatic data collection and reduction. The loaded filters were mounted, with the sample side towards the x-ray beam, in standard sample holders (Philips type PW1527), fitted with

adaptor rings to suit the PW1450 sample changer. Teflon backing discs to support the filters were discarded because they produced excessive background levels by scattering of the primary x-ray beam. However, it was found necessary to fit Teflon sleeves, 2 mm thick, inside the sample holders, to eliminate interference by several of the analyte metals which may be present in the sample holders in trace amounts.

An initial series of experiments was performed to determine optimum instrumental conditions for the determination of each element. Optimum operating conditions were determined for tubes with Cr, Mo and Au anodes and the effects of the choice of analytical emission line, dispersion crystal, collimation and detector were explored. Sensitivities, determined with each of the three tubes and expressed as net counts s^{-1} μg^{-1} per kW of tube power, are shown in Table 1. It is concluded that cadmium is determined most sensitively with the chromium tube, lead with the molybdenum tube and the remaining metals with the gold tube. For routine analysis, however, the PW1450 system does not provide for convenient interchange of tube anode. Since the instrument employed in this study is used normally for the determination of light elements in silicate rocks, the chromium tube was most readily available and was used to obtain the results discussed in the rest of this paper. Analytical conditions with the chromium tube are summarized in Table 2.

RESULTS AND DISCUSSION

The carrier complex itself precipitates quantitatively in the pH range 4.0—

TABLE 1

Optimum sensitivities (net counts s^{-1} μg^{-1} kW^{-1})[a] for various x-ray tube anodes

Metal	Fe	Co	Ni	Cu	Zn	Cd	Pb
Cr anode	51	50	52	48	39	45	12
Mo anode	137	141	151	168	128	7	63
Au anode	352	379	434	420	370	15	40

[a]Determined on a single standard with 40-s counting times per element.

TABLE 2

X.r.f. analytical conditions with the chromium anode tube
(Collimator on setting C and PHS on Auto.)

Element	Line	Crystal	Detector[a]	kV	mA
Fe, Co, Ni, Cu, Zn, Mo	K_α	LiF 200	FS	60	45
Cd	L_α	PET	F	40	60
Pb	L_α	LiF 200	FS	50	45

[a]FS = flow + scintillation detectors in tandem.

4.5 but precipitation efficiency falls off rapidly outside this range, e.g., to 26% at pH 2.2 and to 4% at pH 5.2. For the seven analyte metals, coprecipitation efficiencies were determined at the 200 $\mu g\ l^{-1}$ level and pH 4.4, by a.a.s. analysis of the acid-digested precipitates; the results are shown in Table 3. The efficiencies were not affected either by the use of single-metal standards instead of a composite standard (containing all 7 metals) or by variations in sample volume from 100 to 400 ml.

Under the conditions of the proposed method, the precipitate formed when the molybdate and APDC solutions are mixed is initially yellow but may turn mauve on standing. The colour change is attributed to a reduction reaction, Mo(VI) to Mo(V) [9, 10], caused here by the excess of APDC. The analysis is not affected by this reaction.

Calibration, precision and limits of detection

All calibration graphs were linear in the concentration range 1—100 $\mu g\ l^{-1}$, indicating that the precipitates approximate thin films sufficiently well to make the calculation of correction factors for interelement effects unnecessary. In the equation of the regression line, $y = mx + b$ (where y is the count rate and x the amount of metal in the precipitate), m measures the sensitivity of the method and b is the background. Values of m and b obtained for each of the analyte metals in a typical calibration run are given in Table 4 which also includes estimates of precision at 1, 10 and 50 $\mu g\ l^{-1}$ levels and limits of detection, calculated as $(3/m)\ (b/T)^{\frac{1}{2}}$, where T is the counting time (200 s for the data of Table 4). Lower limits of detection can be obtained, if necessary, for all of the metals except cadmium by the use of Mo or Au tubes.

The effects of day-to-day variations in instrumental conditions were considerably reduced by using the molybdenum in the carrier complex as an internal standard; x-ray intensity measurements made on each element were automatically compared with the intensity of Mo K_α emission from standard or sample and normalized prior to calibration or analysis. This eliminated the need for frequent re-runs of the standards, except when checks were desired or when major adjustments to the instrument (such as tube change) necessitated re-calibration. The use of 3-kW x-ray tubes in conjunction with the very stable 100-kV power supply of the Philips PW1450 system proved markedly superior to that of older equipment on which some preliminary studies were made. Computer-controlled automation of the system greatly simplified the collection and calculation of the x-ray data, so that the total analysis time

TABLE 3

Coprecipitation efficiencies determined on a composite standard containing each metal at the 200 $\mu g\ l^{-1}$ level

Metal	Fe	Co	Ni	Cu	Zn	Cd	Pb
Coprecipitation (%)	90	85	93	89	83	91	81

TABLE 4

Sensitivity, background, precision and limits of detection with the chromium anode tube

Metal	Fe	Co	Ni	Cu	Zn	Cd	Pb
Sensitivity and background[a]							
m(c s^{-1} μg^{-1})	137	134	139	128	97	112	24
b(c s^{-1})	204	150	225	321	284	52	335
Precision[b]							
s_r(%) for 1 μg l^{-1}	10	4	8	40	30	20	110
s_r(%) for 10 μg l^{-1}	2	2	2	3	10	3	20
s_r(%) for 50 μg l^{-1}	1	0.4	0.6	0.5	3	2	2
Limits of detection (μg l^{-1})	0.2	0.2	0.2	0.3	0.4	0.1	1.6

[a]Slope and intercept of regression line in a typical calibration run; 20 composite standards, in the range 1—100 μg l^{-1}, were determined with 40-s counting times per element.
[b]5 precipitates were determined, with 100 s counting times per element, at each concentration.

for each precipitate was only about 5 min (simultaneous, multispectrometer x.r.f. systems would be even faster).

Interferences

No interferences were observed with metal ions at levels likely to be encountered in river and estuarine waters. Iron, however, causes spectral interference and flaking of the precipitate when present in concentrations above 1000 μg l^{-1}.

The effects of dissolved organic matter (DOM) and salinity were studied by the analysis of water samples collected from the Hawkesbury River, N.S.W. To decompose DOM, filtered and acidified samples were treated with hydrogen peroxide (0.2 ml of 30% w/v solution per 400 ml of water sample) and irradiated with a 35-W U-tube immersion lamp for 5 h [11]. Excess of hydrogen peroxide was eliminated by allowing the irradiated samples to stand for 48 h before analysis. The metal concentrations determined by the proposed method with and without this prior treatment were not significantly different for any of the analyte metals.

The proposed method also proved to be effective, without modification, for estuarine water samples. The effect of salinity was tested by adding the metals, in 5, 20 and 100 μg l^{-1} concentrations, to Hawkesbury River water samples varying in salinity from 0 to 28 parts per thousand. Comparison with standards prepared from solutions in distilled-deionized water indicated recoveries in the range 80—120% at each concentration and over the whole salinity range. The results for a high salinity water sample are shown in Table 5.

TABLE 5

Recovery of metals from estuarine water (salinity = 28‰)[a]

Metal added ($\mu g\ l^{-1}$)	Recovery (%)						
	Fe	Co	Ni	Cu	Zn	Cd	Pb
5	82	92	90	108	120	110	108
20	100	100	100	105	100	105	95
100	102	101	102	102	118	102	106

[a]Concentrations in the water, before additions, were: Fe 7, Co 0.3, Ni 1, Cu 1, Zn 4 and Cd 1.5 (all as $\mu g\ l^{-1}$); Pb not detected.

The work described in this paper was supported by a grant from the Australian Research Grants Committee, and the x.r.f. equipment was made available by the Department of Geology and Geophysics of the University of Sydney. We also acknowledge the help of Mr. J. Bogi of the N.S.W. Institute of Technology, Dr. G. E. Batley, A.A.E.C., Lucas Heights, N.S.W. and Dr. E. A. Boyle, M.I.T., Cambridge, Massachusetts.

REFERENCES

1 C. L. Luke, Anal. Chim. Acta, 41 (1968) 237.
2 R. Püschel, Talanta, 16 (1969) 351.
3 H. Watanabe, S. Berman and D. S. Russell, Talanta, 19 (1972) 1363.
4 K. V. Krishnamurty and M. M. Reddy, Anal. Chem., 49 (1977) 222.
5 E. A. Boyle and J. M. Edmond, Anal. Chim. Acta, 91 (1977) 189.
6 V. Hudnik, S. Gomiscek and B. Gorenc, Anal. Chim. Acta, 98 (1978) 39.
7 H. Hellmann, Fresenius Z. Anal. Chem., 289 (1978) 24.
8 M. M. Ulrich and P. K. Hopke, Res. Dev., 28 (1977) 34.
9 F. W. Moore and M. L. Larson, Inorg. Chem., 6 (1967) 998.
10 L. Ricard, J. Estienne, P. Karagiannidis, P. Toledano, J. Fischer, A. Mitschler and R. Weiss, J. Coord. Chem., 3 (1974) 277.
11 T. M. Florence and G. E. Batley, Talanta, 23 (1976) 179.

Analytica Chimica Acta, 100 (1979) 67—74

DETERMINATION OF MICROGRAM AMOUNTS OF PALLADIUM IN TITANIUM ALLOYS BY X-RAY FLUORESCENCE SPECTROMETRY AFTER SOLVENT EXTRACTION AND COLLECTION ON A FILTER PAPER

KIYOSHI IWASAKI

Industrial Research Institute of Kanagawa Prefecture, Kanazawa-ku, Yokohama 236 (Japan)

(Received 7th March 1979)

SUMMARY

Palladium is separated from large amounts of titanium matrix and other elements by solvent extraction with diethyldithiocarbamate, and is collected into the small central area on a filter paper for subsequent x-ray fluorescence measurement. The palladium diethyldithiocarbamate chelate is extracted quantitatively into chloroform at pH 9.5 in the presence of large amounts of tartrate and EDTA. Palladium in the range 30—100 μg can be determined with coefficients of variation of 0.6—1.4%. The detection limit is 0.3 μg of palladium; up to 500 μg of copper does not interfere.

For the determination of small or trace amounts of palladium in titanium alloys, Sawada and Kato [1] have reported a spectrophotometric method based on 1-(2-pyridylazo)-2-naphthol. Direct x-ray fluorescence (x.r.f.) measurements have been recommended by Matsumura et al. [2] for rapid, non-destructive analyses of disks of the bulk alloys. This x.r.f. method, however, is unsatisfactory when standard samples are not available or when the amount of palladium present is very low. Wires and chips which do not have the planar surface required for x.r.f. measurement are also classified as unsuitable samples.

To overcome such limitations, preliminary separation and concentration techniques have been applied successfully. For example, Klima and Scholes [3] proposed separation by precipitation with phenylarsonic acid and the subsequent collection of the precipitate on an organic membrane for small amounts of niobium, zirconium and tantalum in carbon steel. Trace quantities of eight elements (cobalt, copper, iron, etc.) can be separated by ion exchange from molybdenum, and were collected on a paper disk loaded with ion-exchange resin [4]. Recently a new technique has been developed with the aim of utilizing solvent extraction in x.r.f. analysis for trace elements, and has been applied to the determination of microgram amounts of indium in aluminum alloys [5—7]. The method consists of extracting the elements to be determined and collecting this extract on a filter paper.

The object of the work described here was to develop a rapid, simple and highly sensitive x.r.f. method for the determination of microgram amounts of palladium in titanium alloys. Optimum conditions of extracting palladium as its diethyldithiocarbamate chelate into chloroform followed by collection of the extract on a filter paper are reported. The effects of coexisting elements and the results for some artificial mixtures of alloys are also discussed.

EXPERIMENTAL

Reagents

A standard palladium(II) solution (1.00 mg Pd ml^{-1} in ca. 1 M hydrochloric acid) was prepared by dissolving the pure metal (> 99.9%) in aqua regia, evaporating the solution to dryness and taking up the residue with hydrochloric acid. The solution was diluted to 10.0 μg ml^{-1} with water before use. Sodium diethyldithiocarbamate (NaDDTC) solution (1% w/v) was prepared by dissolving the analytical-grade reagent in water just before use. The reagents were all of analytical-reagent grade, and distilled water was used.

Toyo filter papers No. 5A, 15 cm diameter (Toyo Roshi, Co., Ltd.) were used.

Apparatus

The equipment [5] used for the collection of $Pd(DDTC)_2$ on a filter paper can be prepared very easily with three glass Petri dishes and cotton cloth as shown in Fig. 1. The cotton cloth is wound round the outside of the central dish, which is then placed in the large dish. The top dish is used bottom up to hold the paper in position and press it against the cloth. Chloroform in the large dish permeates to the paper through the cloth.

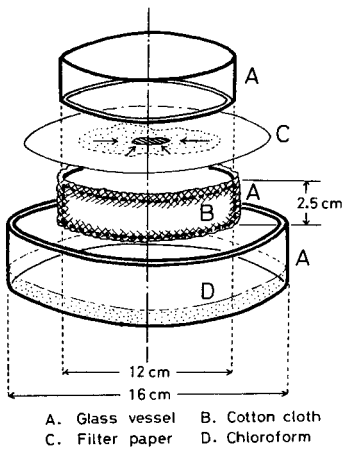

Fig. 1. Equipment for the collection of $Pd(DDTC)_2$. (A) Petri dish; (B) cotton cloth; (C) filter paper; (D) chloroform.

X.r.f. measurements were made with a Rigaku-denki KG-X type spectrometer equipped with a 2-kW tungsten target tube (Philips), a primary (0.45 mm × 10 cm) and a secondary (0.15 mm × 10 cm) collimator, a lithium fluoride (200) analyzing crystal, a scintillation counter and a pulse-height analyzer. A specimen can be rotated at 25 rpm for uniform exposure to the primary x-ray beam.

General procedure

To an aliquot of a palladium(II) solution (3—200 μg Pd) in a 100-ml beaker, add 5 ml of 5% (w/v) sodium tartrate solution and 5 ml of 5% (w/v) EDTA solution and adjust to pH 9.5 with 5 ml of 10% (w/v) ammonium chloride and ammonia solution. Transfer the solution to a 100-ml separatory funnel and dilute with water to the 50-ml mark. To this, add 2 ml of 1% (w/v) NaDDTC solution, mix and allow to stand for 5 min. Then, shake the solution vigorously for 3 min with about 5 ml of chloroform to extract the $Pd(DDTC)_2$ formed. After the chloroform layer has separated, transfer most of it dropwise into the central area (7—8 cm diameter) of a filter paper (15 cm diameter). Concurrently, blow a gentle stream of warm air over the surface of the paper to speed up evaporation. Shake the aqueous layer lightly with 1—2 ml of chloroform, and combine this chloroform layer on the same filter paper.

Then, concentrate the palladium chelate into a small central area (2 cm diameter) of the paper with chloroform as indicated in Fig. 1, to allow effective and quantitative exposure to the primary x-ray beam from the tube. Repeat this procedure 3 times, evaporating the chloroform from the paper between treatments. Finally, support the paper (specimen) on a sample holder and measure the intensities of the Pd K_α line (16.76° 2θ) and background (16.2° 2θ), with the tube operated at 50 kV and 30 mA and counting times of 100 s.

RESULTS AND DISCUSSION

Quantitative extraction of palladium

Bode [8] showed, in his systematic investigation of the solvent extraction of metal diethyldithiocarbamates, that palladium(II) is extracted quantitatively with NaDDTC into carbon tetrachloride over the pH range 4—11. Chloroform [9] and methyl isobutyl ketone [10] can also be used as the solvent. Chloroform was the most favorable for the present work because its low boiling point was advantageous for the subsequent drying of the extract. Extractions were done at pH 9.5 in the presence of large amounts of tartrate and EDTA, which were required to prevent the precipitation of hydroxides of titanium and interferences from other metals in applications to practical samples. Under such conditions, palladium(II) could be extracted quantitatively and separated from large amounts of tin(IV) and molybdenum(VI). Molybdenum, having a relatively large mass absorption coefficient for the

Pd K_α line, may cause low results by matrix interference if it is not removed, as has been observed in the direct x.r.f. measurement of solid samples of Ti—15Mo—0.2Pd alloy [2].

Palladium(II) also reacts with dithizone [11] and dimethylglyoxime [12] to form complexes which are extracted quantitatively into chloroform. In preliminary experiments, however, these complexes could not be collected quantitatively on filter papers.

Quantitative collection of $Pd(DDTC)_2$ on a filter paper

After transference to a filter paper, $Pd(DDTC)_2$ present as a dispersion was concentrated as a spot in a small central area by allowing chloroform to permeate from the edge towards the center of the paper. This procedure was repeated alternately with drying of the paper. Figure 2 shows the relation between the number of repetitions of this procedure and the intensity of the Pd K_α line for 30 μg and 100 μg of palladium. It can be seen that three treatments are sufficient to obtain constant and reproducible intensities of the Pd K_α line.

In order to confirm whether this collection was quantitative, the intensity of the Pd K_α line was measured by placing an aluminum mask with a circular window on the specimen paper, and compared with the intensity obtained from the same paper without the mask. Only that part of the $Pd(DDTC)_2$ spot within the window was thus available to the primary x-ray beam. If collection of $Pd(DDTC)_2$ within the spot is quantitative, windows with dia-

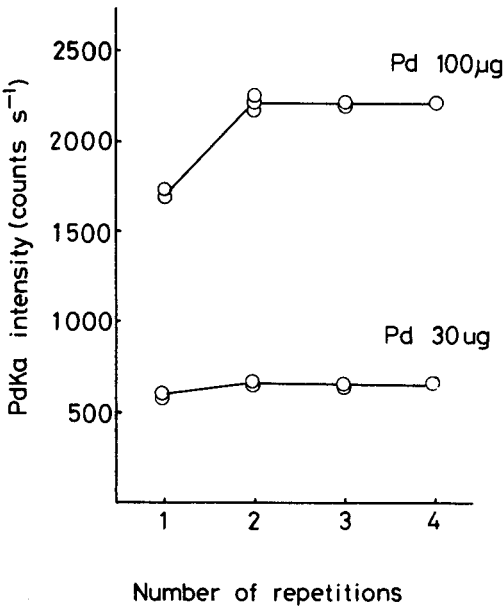

Fig. 2. Relation between the number of repetitions of the concentration process and the intensity of Pd K_α line.

TABLE 1

Relative intensity of the Pd K_α line measured after placing aluminum masks with windows of different diameters on specimen papers prepared from increasing amounts of palladium

Window diameter (mm)	Relative intensity			
	30 μg Pd	50 μg Pd	100 μg Pd	200 μg Pd
Without mask	1.00	1.00	1.000	1.000
20	1.00	1.00	1.012	1.000
15	0.99	0.99	0.992	0.938
10	0.99	0.93	0.853	0.595

TABLE 2

Relation between the area occupied by $Pd(DDTC)_2$ on the filter paper before collection and the intensity of Pd K_α line measured after collection

Pd (μg)	Area (cm^2)	Line intensity (counts s^{-1})	Pd (μg)	Area (cm^2)	Line intensity (counts s^{-1})
50	6	1127	100	7	2212
50	9	1132	100	9	2237
50	71	1110	100	84	2216
50	75	1119	100	87	2250

meters larger than the size of the spot will not cause variations in the line intensity. The results are indicated as relative values in Table 1 for 30—200 μg of palladium. It was concluded that $Pd(DDTC)_2$ (up to 200 μg of Pd) could be collected quantitatively into a 2-cm diameter spot by three treatments with chloroform.

The size of the area occupied by the palladium chelate on the filter paper before collection, i.e., the extent of dispersion of the chelate, had little effect on the intensity of the Pd K_α line measured after collection (Table 2). This supports the conclusions drawn from Table 1.

Calibration line, sensitivity and reproducibility

The standard specimens for calibration were prepared from the standard solution of palladium(II). The intensities (count rates) of the Pd K_α line (counts s^{-1}) were linearly related to the amounts of palladium over the range 3—200 μg. For standards taken through the entire procedure, the coefficients of variation (n = 5) were 1.4% and 0.6% for 30 μg and 100 μg of palladium, respectively. The slope of the calibration line gave the sensitivity as 22.2 counts s^{-1} μg^{-1}. The detection limit was ca. 0.3 μg for a counting time of 100 s; this limit is defined as the amount of palladium required to give a count equivalent to three times the square root of the background count. The background count rate was about 310 counts s^{-1}.

TABLE 3

Effect of co-existing elements on the determination of 30 μg of palladium

Element	Added (μg)	Extracted (μg)[a]	Mean Pd found (μg)	Relative error (%)	No. of detns.
Cu(II)	50	50	29.9	−0.3	3
	150	150	30.2	0.7	3
	300	300	30.3	1.0	3
	500	500	29.7	−1.0	2
Co(II)	50	46—48	30.0	0.0	3
	150	115—135	30.0	0.0	3
	300	190—250	29.9	−0.3	3
	500	350—430	29.6	−1.3	3
	10×10^3	0[b]	30.0	0.0	3
Fe(III)	300	30—35	30.2	0.7	3
	1×10^3	80—100	29.6	−1.3	3
	10×10^3	0[b]	30.3	1.0	2
Mn(II)	300	100—110	30.2	0.7	3
	1×10^3	—	30.0	0.0	2
	10×10^3	0[b]	30.0	0.0	2
Mo(VI)	10×10^3	0	30.0	0.0	3
Sn(IV)	10×10^3	0	29.8	−0.7	3
H_3BO_3	1×10^5	—	29.8	−0.7	1
$NaBF_4$	1×10^5	—	29.9	−0.3	1
NaF	1×10^5	—	30.0	0.0	1

[a]Extraction was carried out at pH 9.5 in the presence of tartrate. [b]5 ml of 5% EDTA was added before extraction.

Effect of co-existing elements

Several metals which may be present in titanium alloys were examined for their effect on the determination of palladium. Each metal ion was added to a standard solution containing 30 μg of palladium(II) before extraction. Some typical results are listed in Table 3. Copper(II) and cobalt(II), added as nitrate, did not interfere in amounts up to 500 μg, although their chelates were extracted (80% Co, 100% Cu) and collected together with $Pd(DDTC)_2$. Iron(III) and manganese(II), added as nitrate, were extracted partially (10% Fe, 30% Mn); 1 mg of these ions was tolerated. The results suggest that the diethyldithiocarbamates of these ions did not interfere in the collection of $Pd(DDTC)_2$ on the filter paper unless extracted in large amounts, and that absorption of the Pd K_α line by these elements was negligible. Extraction of large amounts of foreign ions should be avoided because their chelates would form large spots and, consequently, cause incomplete collection of $Pd(DDTC)_2$ within the specified area. In the presence of EDTA, palladium(II) could be extracted selectively and separated from large amounts of cobalt(II), iron(III) and manganese(II). Tin(IV) (added as sulfuric acid solution) and molybdenum(VI) (as ammonium molybdate) were tested up to 10 mg. Both were practically not extracted above pH 9. Detailed tests were not done for

aluminum(III), vanadium(V), chromium(III), zirconium(IV), niobium(V), tantalum(V) and tungsten(VI), which were not extracted above pH 7. Large amounts of fluoride, borate and fluoroborate did not interfere with the extraction of palladium(II). Accordingly, during sample preparation, hydrofluoric acid could be used for dissolving titanium alloy, and boric acid for masking hydrofluoric acid.

Application to practical samples

In order to demonstrate the usefulness of this technique for practical samples, palladium was determined for some artificial mixtures. The mixtures were prepared as follows: exactly weighed 0.5-g samples of titanium metal, a known amount of palladium(II), 2 g of solid tartaric acid and, if necessary, other metals or metal ions were treated with 25 ml of acid mixture (6 ml of 12 M HCl, 3 ml of 47% HF and 16 ml of water) in a 200-ml polyethylene beaker on a steam bath. After complete dissolution, 3 ml of concentrated nitric acid was added to oxidize the metal ions to their higher valency states, and 1 g of boric acid was added to mask residual hydrofluoric

TABLE 4

Determination of palladium in artificial mixtures and in a Ti—Pd alloy

Sample		No. of detns.	Pd found (μg)	Relative error (%)
Artificial mixture				
A Ti(IV)	100 mg	4	40.2 ± 0.1[a]	+0.5
Sn(IV)	5 mg			
Pd(II)	40.0 μg (0.038%)			
B Ti(IV)	100 mg	4	39.6 ± 0.3[a]	−1.0
Mo(VI)[b]	30 mg			
Pd(II)	40.0 μg (0.031%)			
C Ti(IV)	100 mg	3	39.3 ± 0.2[a]	−1.8
Zr(IV)[b]	10 mg			
Al(III)	20 mg			
Pd(II)	40.0 μg (0.031%)			
D Ti(IV)	50 mg	5	19.8 ± 0.1	−1.0
Al(III)	5 mg			
Co(II)	5 mg			
Pd(II)	20.0 μg (0.033%)			
E Ti(IV)	250 mg	3	2.5 ± 0.2[a]	0.0
Pd(II)	2.5 μg (0.001%)			
Ti—Pd alloy	50.0 mg	4	90.1 ± 0.5	
Ti—Pd alloy + Pd(II)	50.0 mg 30.0 μg	4	121.2 ± 0.7	

[a]EDTA was not added before extraction. [b]Pure metal was added and treated.

acid. This procedure of dissolution is of course recommended for a practical Ti—Pd alloy. The specimen paper was prepared from an aliquot of this solution under the conditions described in the general procedure. The results, including those for a Ti—Pd (0.1% level) alloy, were satisfactorily accurate (Table 4).

The proposed technique has several advantages. Very sensitive determinations are possible with the chelate collection on a paper; for example, even 0.001% of palladium can be determined within 8% error. Standard papers can be prepared easily from solutions containing known amounts of palladium(II). The direct collection of the extract on a filter paper is simple and very rapid compared with other typical techniques such as the ring-oven method described by Armitage and Zeitlin [13], or the back-extraction and successive collection of the extract on an ion-exchange resin-loaded paper disk reported by Hubbard and Green [14].

The author wishes to thank Dr. Katsu Tanaka for helpful discussions.

REFERENCES

1 T. Sawada and S. Kato, Jpn. Anal. (Bunseki Kagaku), 11 (1962) 544.
2 T. Matsumura, N. Kotani and T. Goto, Jpn. Anal. (Bunseki Kagaku), 19 (1970) 1393.
3 Z. Klima and P. H. Scholes, Analyst, 98 (1973) 351.
4 E. F. Spano and T. E. Green, Anal. Chem., 38 (1966) 1341.
5 K. Iwasaki, K. Tanaka and N. Takagi, Jpn. Anal. (Bunseki Kagaku), 23 (1974) 1179.
6 K. Iwasaki and K. Tanaka, Bunseki Kagaku, 24 (1975) 619.
7 K. Iwasaki, Bunseki Kagaku, 26 (1977) 724.
8 H. Bode, Fresenius Z. Anal. Chem., 143 (1954) 182.
9 H. Malissa and S. Gomišček, Anal. Chim. Acta, 27 (1962) 402.
10 P. Hannaker and T. C. Hughes, Anal. Chem., 49 (1977) 1485.
11 J. Stary, The Solvent Extraction of Metal Chelates, Pergamon, Oxford, 1964, p. 148.
12 R. S. Young, Analyst, 76 (1951) 49.
13 B. Armitage and H. Zeitlin, Anal. Chim. Acta, 53 (1971) 47.
14 G. L. Hubbard and T. E. Green, Anal. Chem., 38 (1966) 428.

Analytica Chimica Acta, 110 (1979) 75—79

MULTI-ELEMENT ANALYSIS OF JAPANESE TEA LEAVES BY NEUTRON ACTIVATION ANALYSIS AND THE SINGLE COMPARATOR METHOD

KIYOHISA FUJINAGA*† and KIYOSHI KUDO

Ibaraki Electrical Communication Laboratory, Nippon Telegraph and Telephone Public Corporation, Tokai, Ibaraki (Japan)

(Received 12th February 1979)

SUMMARY

The reliability of the single comparator method in neutron activation analysis has been studied by comparing the calculated and experimental k values and by determining the concentration of trace elements in iron. The method has been applied to the analysis of tea leaves for thirteen elements; their concentrations varied over five orders of magnitude.

The single comparator method in neutron activation analysis (n.a.a.) is useful for the determination of many elements in one sample and for the analysis of many samples. The method is based on the simultaneous irradiation of samples and a single standard (comparator) for all other elements under investigation. In the first critical evaluation of the method [1] a constant, k, was derived from all the nuclear constants involved in activation and counting. The k values of the elements to be determined do not remain constant for a change of irradiation position or reactor neutron spectrum as the ratio of the thermal to epithermal neutron fluxes is changed.

De Corte et al. [2] extended the method to a three-comparator technique; the flux monitors cobalt, indium and gold are irradiated with the samples, the flux ratios are calculated from the absolute activities of the three comparators, and the k values are corrected for each new ratio.

In the work described here, the reliability of the single comparator method was first studied by comparing the calculated and experimental k values of some elements. When a sample is irradiated together with a single comparator the results are calculated from the equation [1, 2]: $W = k\ W^* A_{sp}/A^*_{sp}$ where W is the weight of the element; k is a constant derived from all nuclear constants involved in activation and counting; $A_{sp} = A_p/SDC$ where A_p is the photopeak counting rate of the radioisotope formed by the (n,γ) reaction, $S = 1 - \exp(-\lambda t_i)$ (saturation factor dependent on decay con-

†Present address: Musashino Electrical Communication Laboratory, Nippon Telegraph and Telephone Public Corporation, Musashino, Tokyo 180, Japan.

stant λ and irradiation time t_i), $D = \exp(-\lambda t_d)$ (decay factor where t_d is decay time), and $C = [1 - \exp(-\lambda t_m)]/\lambda t_m$ (measurement factor correcting for decay during measuring period t_m). The asterisks indicate the quantities for the single comparator, ^{60}Co, used in this work.

The k values of the elements to be determined are evaluated from the ratio of the thermal to epithermal neutron fluxes, which can be determined by irradiation and absolute counting of three comparators ^{60}Co, ^{114m}In and ^{198}Au. The determination of the k values in this manner is useful when cadmium irradiation is not allowed.

The single comparator method introduces additional sources of error related to the measurement of SDC, $S^*D^*C^*$ and k. The first two of these factors depend only on irradiation, decay and measurement times, which are generally easily determined with good precision. Table 1 compares the calculated k values of eight elements with the experimental k values obtained from the above equation by irradiating known amounts of the elements and of the cobalt comparator. The calculated k values, computed from the individual nuclear constants [1], agree well (Table 1) with the experimental k values. Determinations of some of the elements in iron by the single comparator method were in good agreement (Table 2) with those by the relative method. Thus the reliability of the single comparator method and that of the relative method are about the same.

TABLE 1

Comparison of the calculated and experimental k values

Radioisotope	γ-energy (keV)	k values	
		Calculated	Experimental
^{64}Cu	511	13.0	14.1
^{69m}Zn	439	999	940
^{24}Na	1368	34.8	33.0
^{198}Au	412	0.292	0.283
^{122}Sb	564	11.4	10.1
^{59}Fe	1099	15600	15600
^{114m}In	190	101	94.3
^{60}Co	1173	1.0	1.0

TABLE 2

Determination of elements (expressed as $\mu g\ g^{-1}$) in iron by the single comparator method (SCM) and the relative method (RM)

Element	Cu	Na	Ir	Au	Co
SCM	4.6	19	0.8	2.00	35
RM	5.0	20	—	1.94	35

EXPERIMENTAL

Sample preparation

The tea leaves supplied by the University of Tokyo were "Sen-cha", a middle grade green tea (TL-B) and old tea leaves (TL-C). They were prepared by pulverizing with an agate ball mill, sieving with a Saran fiber sieve [3], and drying to constant weight at 90°C for 24 h in an oven. The dried samples (350—450 mg) were packed in small polyethylene capsules and sealed in polyethylene bags.

Cobalt and indium wires (0.25 mm and 0.15 mm diameter, respectively) were cut into lengths weighing ca. 1 mg for use as comparators. The purity of these wires was 99.99%. The gold comparator was prepared by evaporating 10 μl of aqua regia containing 1000 μg ml^{-1} of gold in a quartz tube. The self-shielding effect of these materials was negligible [4]. The three comparators were sealed in a polyethylene bag.

Irradiation

The samples and comparators were irradiated together in a polyethylene irradiation capsule, in the pneumatic tube of the reactor JRR-2 at the Japan Atomic Energy Research Institute for 2 and 20 min at a thermal neutron flux of 5×10^{13} n cm^{-2} s^{-1}.

Activity measurement

Irradiated samples and comparators were counted on a coaxial Ge(Li) detector (25 cm^3) coupled with a 4096-channel pulse-height analyzer. The system resolution was 2.0 keV (FWHM) for the 1332-keV γ-ray of ^{60}Co, and the relative detection efficiency was determined with a number of calibrated standard radioisotopes.

The samples were measured after decay for at least 7 h because of the strong activities of ^{56}Mn, ^{42}K and ^{24}Na. The elemental concentrations were calculated from the relationship given above. In the determination of the elements, several peaks with high intensity from each nuclide, not overlapped by foreign peaks, were chosen for evaluation when multiple peaks were detected.

RESULTS AND DISCUSSION

Typical γ-ray spectra of the TL-C leaf samples are shown in Fig. 1: after irradiation for 20 min, spectrum A was recorded by counting for 1×10^3 s after 2 d decay, spectrum B was obtained by counting the same sample for 1.4×10^4 s after 12 d decay, and spectrum C was obtained by counting for 1×10^5 s (27.8 h) after 38 d decay.

The photopeaks of ^{64}Cu, ^{82}Br, ^{24}Na, ^{42}K and ^{140}La were detected in spectrum A. In spectrum B, seven more nuclides (^{46}Sc, ^{86}Rb, ^{65}Zn, ^{60}Co, ^{59}Fe, ^{40}K and ^{47}Sc) were detected but ^{64}Cu, ^{24}Na and ^{42}K had decayed below their detection limits; ^{40}K was a natural radioisotope and ^{47}Sc was

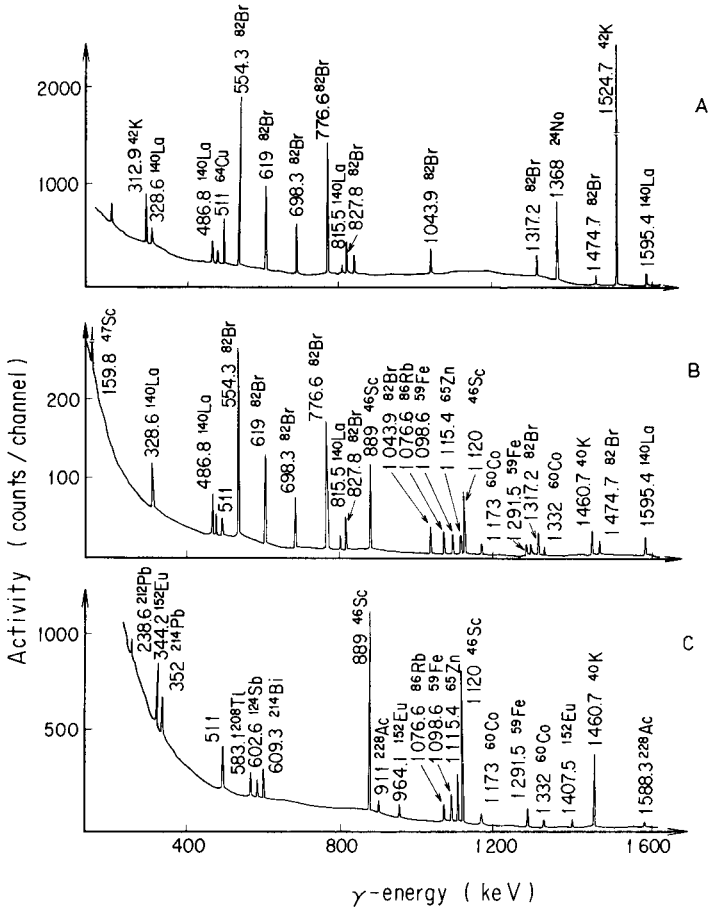

Fig. 1. Gamma-ray spectra of Japanese tea leaves TL-C measured after irradiation for 20 min.

produced by the $^{46}Ca(n, \gamma)^{47}Ca \xrightarrow{\beta^-} {}^{47}Sc$ reaction. The photopeaks of ^{152}Eu and ^{124}Sb were detected in spectrum C in which ^{212}Pb, ^{214}Pb, ^{208}Tl, ^{214}Bi and ^{228}Ac were the photopeaks of natural radioisotopes.

Table 3 shows the analytical results obtained by the single comparator method; thirteen elements were determined in TL-C and eleven elements in TL-B. In the determination of sodium, the activity of ^{24}Na produced by the $^{27}Al(n,\alpha)^{24}Na$ reaction was negligible compared with that produced by the $^{23}Na(n,\gamma)^{24}Na$ reaction, because the concentrations of aluminium were 420 ppm in TL-B and 2000 ppm in TL-C [3]. The activities of iron, cobalt and antimony were very low, and their determinations were made near the detection limits.

The results for manganese, zinc, potassium and rubidium are in good agreement with the reported values [3]. The results for bromine are in reasonable agreement with reported values whereas the lanthanum and

TABLE 3

Determination of elements in Japanese tea leaves

Element	Found ($\mu g\ g^{-1}$)		Element	Found ($\mu g\ g^{-1}$)	
	TL-B	TL-C		TL-B	TL-C
Mn	520	2580	Na	51	39
Fe	120	210	K	2.25%	1.06%
Co	0.10	0.08	Rb	22	11
Cu	14	8[a]	Sc	0.02	0.13
Zn	58	12	La		1.27[c]
Sb	0.03	0.04	Eu		0.29
Br[b]	10.2	19.2			

[a]Reported value 59 ± 37 $\mu g\ g^{-1}$ [3]. [b]Reported values are 13.0 ± 0.2 and 25.0 ± 0.3 $\mu g\ g^{-1}$, respectively [3]. [c]Reported value 1.60 ± 0.03 $\mu g\ g^{-1}$ [3].

TABLE 4

Concentration of trace elements in tea leaves from different sources

Sample	Br ($\mu g\ g^{-1}$)	Na ($\mu g\ g^{-1}$)	K (%)	Mn ($\mu g\ g^{-1}$)
Argentina	1.8	33.5	1.69	509
Ceylon	0.6	39.6	1.71	298
Japan	0.7	120.8	1.92	250
Ceylonta	9.8	—	1.60	298
Iran	4.4	146	1.95	481
Lipton	8.8	27	1.18	1327
TL-B (Sen-cha)	10.2	51	2.25	520
TL-C (old tea leaves)	19.2	39	1.06	2580

copper values for TL-C are lower than the reported values [3].

Table 4 compares the concentrations of some elements in tea leaves from different sources [5–7] with the present results; the values of bromine and manganese in TL-C are higher than those in leaves from other sources.

The authors thank Dr. N. Niizeki and Prof. K. Fuwa for their encouragement throughout this work.

REFERENCES

1 F. Girardi, G. Guzzi and J. Pauly, Anal. Chem., 37 (1965) 1085.
2 F. De Corte, A. Speecke and J. Hoste, J. Radioanal. Chem., 3 (1969) 205.
3 K. Fuwa, K. Notsu, K. Tsunoda, H. Kato, Y. Yamamoto, K. Okamoto, Y. Dokiya and S. Toda, Bull. Chem. Soc. Jpn., 51 (1978) 1078.
4 Y. Kamemoto and S. Yamagishi, Bull. Chem. Soc. Jpn., 37 (1964) 664.
5 M. Kasrai, M. J. Shoushtarian and M. H. Bozorgzadeh, J. Radioanal. Chem., 41 (1977) 73.
6 T. Takeo and M. Shibuya, Radioisotopes, 20 (1971) 45.
7 M. Shimkova and F. Kukula, Isotopenpraxis, 10 (1974) 219.

Analytica Chimica Acta, 110 (1979) 81—86

DETERMINATION OF SILVER FISSION PRODUCT IN HIGH-TEMPERATURE NUCLEAR REACTOR FUELS BY ION-EXCHANGE SEPARATION AND γ-COUNTING

W. AMIAN, R. HECKER and D. STÖVER*

Institut für Reaktorentwicklung, Kernforschungsanlage Jülich, Postfach 1913, 517 Jülich, (Federal Republic of Germany)

(Received 22nd December 1978)

SUMMARY

The content of silver fission product and its radial distribution in spherical coated fuel particles can be measured by stepwise chemical removal of pyrolytic carbon layers coupled with an anion-exchange separation procedure and subsequent γ-counting. An adsorption efficiency better than 98% ranging over five orders of magnitude in silver concentration was found for a bromide-containing medium. Silver to carbon ratios down to 10^{-12} are measurable so that this method is useful for studying the diffusion of silver in pyrolytic carbon.

Coated-particle fuels have been chosen for use in all existing and planned high-temperature gas-cooled nuclear reactors (HTRs) [1]. The particles consist of small spherical ceramic fuel kernels, usually about 200—600 μm in diameter, surrounded by two or more layers of coating material which is intended to retain most of the fission products. Current designs call for an inner "buffer" layer of low-density pyrolytic carbon, which can accommodate volatile fission products and also absorb fission recoils from the fuel kernel. The outer layer is a very dense relatively impervious material which is normally pyrolytic carbon or silicon carbide. The so-called BISO particles consist of a (U, Th)O_2 fuel kernel of 400—600 μm diameter, depending on the type of fuel used, surrounded by two layers (each 80—100-μm thick) of the different types of pyrolytic carbon. The TRISO particles are of similar overall size and construction but have an additional silicon carbide layer (20—30-μm thick) between the two pyrolytic carbon layers.

The coated-particle fuel provides very good retention of fission products in fuel consumption greater than 100 000 MWd/to and at temperatures around 1000°C. The excellent behavior of such fuels has been demonstrated in several HTRs during the past decade [2]. However, in advanced reactor designs such as helium turbines in a direct coolant cycle [3] and process heating plants [4], the gas outlet temperatures are higher. This may cause enhanced diffusivity of special fission products such as the silver isotopes when the long-lived silver-110 m is used to monitor the release of silver.

^{110m}Ag is produced from the stable fission product ^{109}Ag, thus the resulting activity per fuel particle is very low compared to that of other fission products, and its determination in these irradiated fuels together with other fission products is difficult.

Chemical removal

To determine the transport behavior of silver in the coated particle layers, its radial distribution within a single particle has to be measured after different times of annealing at different temperatures [5]. Typical handling procedures are as follows. First, the diameter of the particle — typically less than 800 μm — is determined by a shadow microscope, and the mass of the particle (usually less than 1 mg) is measured on a microbalance. The particle is then placed in an etching retort for stepwise removal of the pyrolytic carbon layer; the etching solution consists of chromium(VI) oxide in nitric acid. Three particles are processed in parallel at 120°C for periods of 10 min to 1 h, depending on the layer material. For the given reaction times, about 10 to 20 μm of the carbon layer is removed. The procedure of visual inspection, determination of mass and diameter, and etching is repeated until the total layer has been removed. However, if definite parts of the removed layers, as dissolved in the etching solution, are analyzed for γ-rays with high-resolution Ge(Li) detectors, this simple procedure becomes inadequate because of the very low activity of ^{110m}Ag. It is therefore necessary to resort to radiochemical separation.

The main problem then arises from the composition of the carbon etching solution. The ratio between the chromium (VI) ions in the etching solution and the dissolved ^{110m}Ag ions to be detected is 4×10^{13} to 4×10^{16}. This high ratio puts severe limitations on the radiochemical separation scheme.

Ion-exchange separation

To overcome these difficulties and to simplify the chemistry involved, an ion-exchange separation was used. It is known [6] that silver forms a stable bromide complex in sulphuric acid solution, so that it can be separated on anion-exchange resins. Chromium(VI) would also be adsorbed, but chromium(III) is not adsorbed. The same is true for all other metallic fission products which do not form anionic complexes.

The predominant fission products show good decontamination factors as indicated by the γ-spectra measured before and after separation (Fig. 1). The detail of interest is inset at the upper right part of each spectrum; the arrows indicate where silver is expected to show its dominant peak (885 keV). The upper spectrum was obtained from the original solution: ^{144}Ce, ^{137}Cs, ^{95}Zr and ^{95}Nb predominate and their intensities are such that the sample must be measured at a relatively large distance from a small-volume detector in order to maintain the energy resolution of the detector. Silver is not detected and the background count in this region of the spectrum is very low, even for acquisition times exceeding 1 h, because the detector

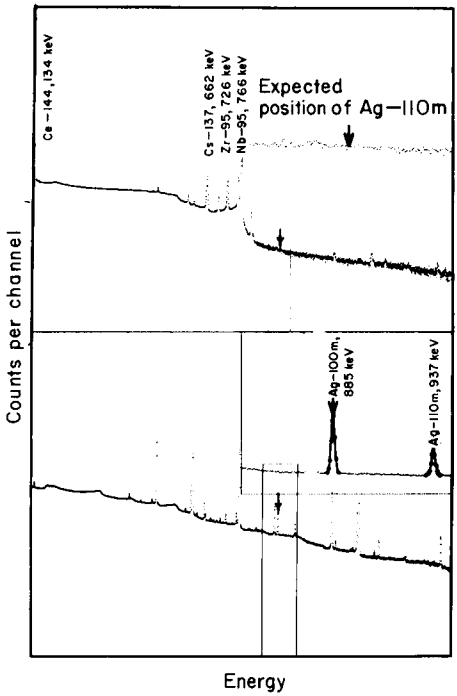

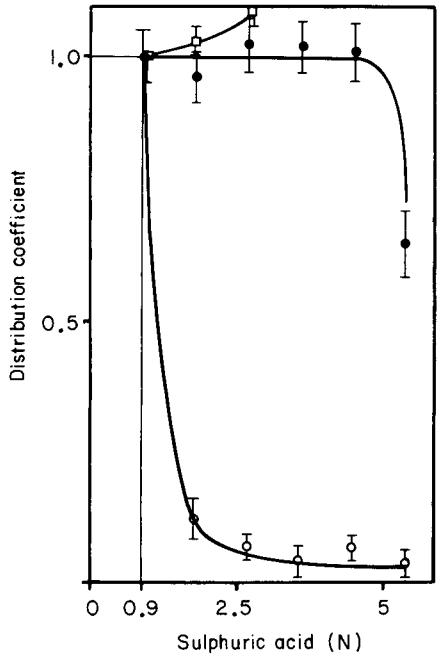

Fig. 1. Influence of ion-exchange separation on γ-spectra. Upper spectrum pertains to the original etching solution and lower spectrum to the resin after exchange separation.

Fig. 2. Distribution coefficients (normalized to 1 for 0.9 M H_2SO_4) for different isotopes versus sulphuric acid molarity. (•) Ag; (○) Zr; (□) Ce.

efficiency in this geometry is very small. The lower part of Fig. 1 shows the γ-ray spectrum of the ion exchanger itself. Silver can be seen very clearly; the highly active components are lost, and in addition to the silver peaks, other fission products, notably ^{106}Ru—^{106}Rh (511, 622, 873 keV) become visible.

Variation in the molarity of the sulphuric acid solution changes the distribution coefficients of the species in the sample. Figure 2 shows a plot of the distribution coefficients vs. the sulphuric acid molarity for ^{110m}Ag, ^{95}Zr and ^{144}Ce. The coefficient for silver is constant over a wide range of acidity, whereas that for ^{95}Zr decreases by more than an order of magnitude, and that for ^{144}Ce increases with increasing acidity. All others remain constant within experimental errors. Since the lower γ-energy line of ^{144}Ce at 133 keV has the highest detection efficiency in the Ge(Li) detector and therefore contributes most to the count rate and dead time, the optimum acidity is 2.5—3 M. The decontamination factors summarized in Table 1 were obtained for this acid range. These values sufficed for the determination of silver as indicated in Fig. 1.

TABLE 1

Decontamination factors of the most important fission products

Product	^{137}Cs, ^{134}Cs	^{144}Pr—Ce	^{95}Zr—Nb	^{106}Ru—Rh
Factor	10^{-6} 10^{-6}	1.6×10^{-4}	1.9×10^{-2}	2.9×10^{-1}

Solutions with known amounts of silver were prepared, to determine the efficiency of adsorption of the ion-exchange resin. After γ-spectrometric measurement of the silver content of the solution, other fission products were added. These solutions were processed and the silver activity adsorbed on the resin was measured. The results are plotted in Fig. 3. These experiments showed that the efficiency of adsorption exceeded 98%, ranging linearly over more than five orders of magnitude down to the detection limit of the equipment, i.e. ca. 5 pCi.

EXPERIMENTAL

Ion-exchange columns

The peristaltic pump used (Ismatec MP25) had 25 tygon tubes, so that 25 separations could be done simultaneously. The polyethylene columns (10-mm diameter) were filled with anion-exchange resin (Bio-Rad AG2-X8, chloride form, 200—400 mesh) to a height of 65 mm. Before operation, the columns were treated with 25 ml of 3 M sulfuric acid.

Sample preparation

The etching solution was 10 M in nitric acid and 4 M in chromium(VI) oxide. Approximately 10 μg of pyrolytic carbon was peeled off in each

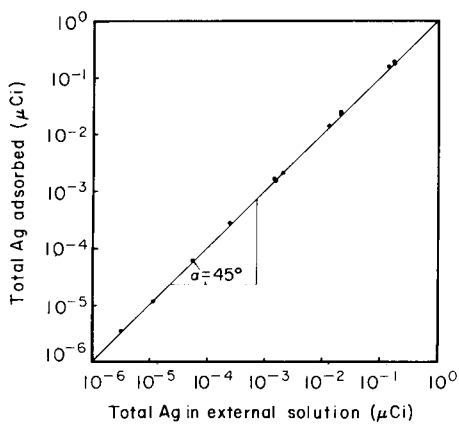

Fig. 3. Effectiveness of the ion-exchange resin for ^{110m}Ag.

etching step on heating with 20 ml of etching solution. To prevent too strongly exothermic a reaction of hydrazine with chromium(VI), the solution was then diluted with water to 70 ml. Hydrazine hydrate (25 M) had to be added dropwise very carefully; a total of 4 ml was used, 2.5 ml of which was needed for complete reaction.

Any precipitate of the hydrous chromium(III) oxide was dissolved by adding 10 ml of 3 M sulfuric acid and heating. The solution was then evaporated to about 5 ml, with constant stirring, These steps required great care, because the chromium oxide became inert towards both acid and base, if ignited too strongly. Oxides of nitrogen were also expelled by this treatment. The residual 5 ml of solution was adjusted to about 3 M in sulfuric acid and 400 μl of 9 M hydrobromic acid was added.

This solution (ca. 40 ml) was pumped onto the top of the anion-exchange column at a flow rate of about 0.4 ml min^{-1}. Before and after separation the columns were washed with 25 ml of 3 M sulfuric acid.

After washing, the resin was drained and compressed to a height of 30 mm manually, within the original polyethylene column. These columns were placed upside down on a Ge(Li) detector for counting. The efficiency of the detector relative to a 3 × 3-in. NaI detector was 26%. The detector was calibrated for the column geometry by using columns containing known amounts of silver added before processing under the same conditions as etching solutions.

RESULTS AND CONCLUSIONS

Figure 4 shows an example of the silver distribution measured in pyrolytic carbon layers. The fuel tested consisted of (U, Th)O_2 microspheres with radii

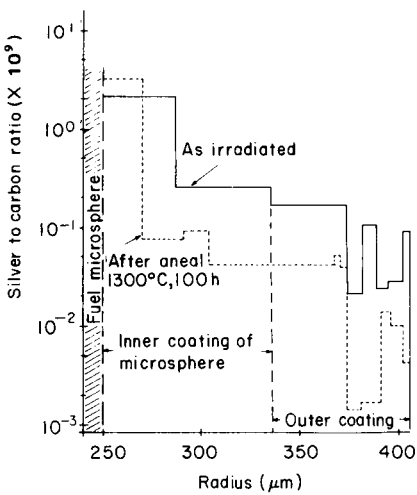

Fig. 4. Radial distribution of measured silver concentrations in pyrolytic carbon layers, of BISO particles and behaviour under the annealing treatment. The Ag:C ratio is plotted against the radius of the sphere.

up to 250 μm; the first coating, i.e. the buffer layer, extended from 250 μm to 340 μm, and the second coating, i.e. the very dense pyrolytic carbon layer, from 340 μm to 405 μm. The upper histogram in Fig. 4 shows the distribution of silver after irradiation with decreasing concentration towards the circumference. Some scatter is visible in the outer part of the layer. The lower histogram shows the same distribution after annealing at 1300°C for 100 h.

In general, the amount of silver within the layers decreases because of diffusion; silver is finally released from the particle. Silver to carbon ratios down to 10^{-12} could be measured in single specimens with masses of about 10^{-5} g which is the mass of the layer removed by an etching step.

It can be concluded that silver fission product can be determined as ^{110m}Ag by a combination of well known chemical reactions, ion-exchange separation and γ-counting techniques. The main problem was the isolation of the silver isotopes from the mixture of highly active metallic fission products in the etching solution described. By stepwise chemical removal of spherical particles, it was possible to measure radial concentration profiles of silver in the pyrolytic carbon layers.

The limit of detection is sufficiently low to allow these measurements to be made with standard coated particles irradiated to realistic fuel burn-up values.

The comparison of concentration profiles as irradiated and after annealing in single particles allows the diffusion coefficients of silver in pyrolytic carbon layers to be derived. Because silver is a "key" isotope for HTR fuels, low-level contaminations of natural silver have to be detected. The method described may have further applications in this field.

REFERENCES

1 E. Balthesen, K. Ehlers, H. Huschka and H. Nickel, Trans. Am. Nucl. Soc., 20 (1975) 268.
2 V. S. Boyer, G. M. Insch, J. W. Landis, H. Hennies, H. W. Müller, L. R. Shepherd and J. D. Thorn, in High Temperature Reactors, Nuclear Energy Maturity, Proceedings of the Paris Conference, Progress in Nuclear Energy Series 1976, Pergamon Press, Oxford, 1976.
3 D. Haferkamp, K.-U. Schneider, A. Hodzic and H. Schwarz, Reaktortagung Mannheim, 1977.
4 R. Fischer, H. Reutler, W. Jäger, E. Arndt, A. Hodzic, K.-M. Schneider and V. Evers, Reaktortagung Hannover, 1978; J. Weisbrodt, Alternativen der Energiepolitik, Rech-Verlag, München, 1978.
5 H. D. Röhrig, D. Stöver, N. Neef and R. Hecker, J. Am. Ceram. Soc., 59 (1976) 185.
6 K. Samsahl, P. O. Wester and O. Landstroem, Anal. Chem., 40 (1968) 181.

Analytica Chimica Acta, 110 (1979) 87—94

DETERMINATION OF SELENIUM AND TELLURIUM IN ELECTROLYTIC COPPER BY ANODIC STRIPPING VOLTAMMETRY AT A GOLD FILM ELECTRODE

T. W. HAMILTON and J. ELLIS*

Chemistry Department, University of Wollongong, P.O. Box 1144, Wollongong, N.S.W. 2500 (Australia)

T. M. FLORENCE

Analytical Chemistry Section, Australian Atomic Energy Commission Research Establishment, Lucas Heights, N.S.W. 2234 (Australia)

(Received 23rd March 1979)

SUMMARY

A simple procedure for the determination of selenium and tellurium in electrolytic copper is described. These two elements are first separated from copper by passing an ammoniacal solution of the sample through Chelex-100 resin. Voltammetric interferences from nitrite liberated during the dissolution of the metal sample in nitric acid and from arsenic and antimony present in the metal are eliminated by addition of hydrogen peroxide. Excess of peroxide is quickly decomposed by the copper(II) ions present. As little as 0.01 μg Se g^{-1} and 0.02 μg Te g^{-1} can be determined; relative standard deviations (n = 5) are in the ranges 1.4—3.7% for selenium concentrations of 7.3—0.6 ppm in copper and 1.6—3.1% for tellurium concentrations of 4.6—0.5 ppm.

Trace amounts of selenium and tellurium markedly affect the conductivity, softening temperature, and mechanical working properties of electrolytic copper [1—3] and several methods have been developed for trace analysis of these elements in copper. The copper metal is dissolved in nitric acid and the selenite separated from the large excess of copper(II) ions, most commonly by co-precipitation from ammoniacal solution with iron(III) hydroxide [4] or lanthanum hydroxide [5]. Two or three such precipitations are normally required to achieve quantitative separation of the selenium and tellurium from copper; the procedure is therefore rather lengthy. Moreover, the presence of iron(III) or lanthanum ions and as much as 100 ppm of co-precipitated copper in the final solution interferes to some extent with most methods of analysis. Stringent control of pH is essential when iron(III) hydroxide is used as the co-precipitating agent, and a minimum sample size of 20 g of copper is common for these co-precipitation methods.

Various solvent extraction procedures [6—8] have been used for the separation of selenium and tellurium, including extraction into toluene with 3,3′-diaminobenzidine [9] and extraction into chloroform as selenium

xanthate [10] which gives incomplete separation from copper and may be affected by volatilization of selenium during the prior digestion with sulphuric acid [11]. Procedures based on electrolytic separation [12] are subject to selenium losses from the same cause. Because of these difficulties, a chelating ion-exchange resin (Chelex-100) which gave a rapid and complete separation of copper from the selenite and tellurite was used in the proposed method.

Selenium and tellurium in a variety of materials have been determined spectrophotometrically [13, 14] and, after conversion to their hydrides, by atomic absorption [15] or by inductively-coupled plasma emission spectrometry [16]. Other techniques which have been used include fluorescence [17], x-ray fluorescence [18], gas chromatography [19] and neutron activation analysis [20]. Selenium and tellurium have been determined separately by a variety of electrochemical methods [21—23] but no reference to their simultaneous determination was found. The successful determination of selenite by anodic stripping voltammetry (a.s.v.) at a tubular gold electrode [24] suggested the use of a gold film/glassy carbon electrode (GCE) for determination of selenite and tellurite.

EXPERIMENTAL

Apparatus

Voltage ramps were generated by a PAR-175 Universal Programmer linked to a PAR-174 potentiostat and current-to-voltage converter. Output voltage was recorded on a Houston 2000 X—Y recorder. A PAR-173 Potentiostat/Galvanostat and PAR-179 Digital Coulometer were used for coulometric measurements. PAR cells and glassy carbon electrodes were used, in conjunction with a saturated calomel electrode (SCE) and a platinum auxiliary electrode. The SCE was isolated from the sample solution by a salt bridge containing 0.5 M sodium nitrate. Flow of moist high-purity nitrogen into the cell was directed through one of two valves: the first allowed the gas to bubble through the solution for purging while the second directed the gas over the top of the solution during an analysis. These valves were operated by an automatic controller as were all stages of the a.s.v. analysis. Details of this controller will be described elsewhere.

Reagents

Aristar (B.D.H.) nitric acid, hydrochloric acid and ammonia solutions were used without further purification. Standard solutions of selenium or tellurium (5×10^{-2} M) were made by dissolving sodium selenite (B.D.H., >99%) or potassium tellurite (Merck, >99%) in water and diluting each day to give the working solutions (1—7.5 ppm). The gold(III) stock solution was made by dissolving gold sponge (Fluka, 99.9995%) in a minimum of aqua regia and diluting with 1 M nitric acid. Sodium perchlorate was Merck Suprapur. Water was distilled and redistilled twice from quartz. Chelex-100

resin (Bio-Rad Laboratories) was 100—200 mesh and was regenerated by washing with 2 M nitric acid (analytical reagent), water, 0.5 M ammonia solution (analytical reagent) and finally with 0.1 M ammonia solution (Aristar grade).

Electrode preparation

Before each deposition of a gold film, polish the electrode with alumina powder (0.5 μm) and then wash successively with methanol, nitric acid and distilled water. Submerge the electrode in 15 ml of 0.1 M sodium perchlorate and leave on open circuit during a 20-min purge with nitrogen. Add an aliquot of gold(III) solution (to give [Au] = 50 ppm) and purge the solution for a further 5 min. After ensuring that gas bubbles are not lodged on the surface of the GCE, apply —0.2 V to the electrode and deposit the equivalent of 2×10^{-2} coulombs of gold on the surface (28 mm^2). For optimum performance, keep the electrode in purged 0.1 M nitric acid for 24 h before use and store under these conditions between analyses.

Procedure

Dissolve 0.5 g of copper sample in 2 ml of 15 M nitric acid. Warm the solution to 80—90°C to drive off most of the nitrous fumes and add 0.625 ml of hydrogen peroxide (500 ppm). After 10 min, cool the solution and add 3 ml of 15 M ammonia solution. Add the ammoniacal solution to a column of Chelex-100 resin (1.5 × 12 cm) and wash onto the column with a minimum (5 ml) of 0.1 M ammonia solution. Elute the column with 0.1 M ammonia solution and collect the eluate in a 50-ml volumetric flask containing 2 ml of 15 M nitric acid until the flask is full to the mark.

Pipette 10 ml of the eluate into the cell and purge the solution with nitrogen for 15 min before immersing the gold film electrode. With the auxiliary electrode on open circuit and the working electrode earthed, purge for a further 5 min. Commence stirring, condition the working electrode for 30 s at +1.2 V, and then deposit selenium and tellurium on the working electrode at —0.1 V for 20—200 s, depending on the selenite concentration. Cease stirring and, after 20 s, scan the working electrode from —0.1 V to +1.2 V at 40 mV s^{-1}. Repeat from the conditioning step until a stripping peak of constant height is obtained for tellurium (usually 2 cycles). Add a tellurium spike such that the tellurium concentration is increased by about 80% and repeat the a.s.v. determination. The determination may be repeated with a second spike to verify linearity of electrode response. Verify that a constant selenium stripping peak height has been attained, and then make one or two standard additions of selenium to the same solution in the cell.

RESULTS AND DISCUSSION

When solutions prepared from copper nitrate (analytical grade) were spiked with selenium and tellurium and passed down the Chelex resin, sub-

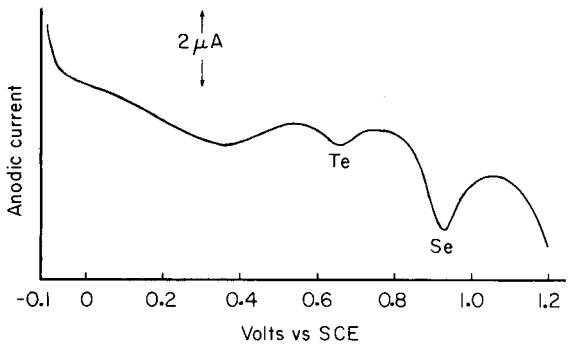

Fig. 1. Anodic stripping current—voltage curve for 10 ppb Se(IV) and 10 ppb Te(IV); 35-s deposition at −0.1 V in 0.1 M HNO_3; prior deposition of 2×10^{-3} coulombs of gold on the GCE.

sequent a.s.v. analysis indicated complete recovery of both elements, whose anodic oxidation peaks occur at +0.90 V and +0.64 V respectively (Fig. 1). Neither element interfered with the determination of the other up to a concentration ratio of at least 1:5.

However, when a sample of copper metal was dissolved in nitric acid, serious interferences arose from two sources. First, nitrite ion produced as a reduction product during dissolution of the metal gave an oxidation wave within 20 mV of the selenium peak. It was found that the nitrite concentration had to be reduced to 10 ppb to eliminate this peak. Secondly, the arsenic and antimony in the copper produced stripping peaks which interfered with the selenium determination. Because antimony(V) and arsenic(V) are electrochemically inactive under the conditions of the a.s.v. analysis, both of these interferences could be eliminated by adding a controlled excess of hydrogen peroxide to the nitric acid digest. Nitrite was oxidized to nitrate; arsenic and antimony to the pentavalent state. There was negligible oxidation of selenium and tellurium to electrochemically inactive Se(VI) or Te(VI). Excess of hydrogen peroxide was rapidly destroyed by the catalytic activity of copper ion in solution. After only 10 min at 80—90°C the solution could be treated with 15 M ammonia solution ready for copper removal with the chelating resin.

This procedure was used to analyse two certified samples of electrolytic copper (certified by Spectroscopic Society of Canada and designated SSC-1 and SSC-3) for selenium and tellurium (Table 1). The determination of lower concentrations of selenium and tellurium was examined by spiking solutions of duplicate samples of high-purity copper metal, for which the selenium and tellurium concentrations were <0.1 ppm.

Anodic stripping voltammetry with the gold film electrode gives a detection limit of 0.1 (1.3×10^{-9} M) selenium and 0.2 $\mu g\ l^{-1}$ (1.6×10^{-9} M) tellurium in solution. The detection limits were calculated as $2 \times 2\frac{1}{2}$ the standard deviation of the blank. They correspond respectively to 0.01 and 0.02 ppm in

TABLE 1

Determination of selenium and tellurium in copper ($\mu g\ g^{-1}$)

Element	Sample	Se/Te content (μg)	Weight added (μg)	Weight found (μg)	Weight recovered (%)	R.s.d. ($n=5$) (%)
Se	SSC-1[a]	7.28	—	7.80	107.2	1.6
	SSC-3[a]	3.87	—	4.24	109.6	1.5
	Copper	0.07	2.25	2.34	100.8	1.4
	Copper	0.07	1.20	1.28	100.8	3.6
	Copper	0.07	0.50	0.58	101.7	3.7
	Blank	—	—	0.06	—	5.8
Te	SSC-1	4.57	—	4.55	99.5	2.3
	SSC-3	2.53	—	2.65	104.8	1.8
	Copper	<0.02	1.50	1.48	98.7	2.6
	Copper	<0.02	2.25	2.28	101.4	1.6
	Copper	<0.02	0.50	0.50	100.0	3.1
	Blank	—	—	<0.02	—	—
	Blank + added Te	—	0.10	0.10	100.0	7.3[b]

[a]Certified values are 7.28 ppm Se and 4.57 ppm Te for SSC-1 and 3.87 ppm Se and 2.53 ppm Te for SSC-3.
[b]$n=10$.

copper because 0.5 g of copper gives 50 ml of solution. Relative standard deviations (n = 5) ranged from 1.4 to 3.7% for selenium concentrations of 7.3—0.6 ppm in copper and from 1.6 to 3.1% for tellurium concentrations of 4.6—0.5 ppm. The time required for the dissolution and separation was 30 min, with a further 20—120 min for the subsequent electrochemical analysis, depending on the deposition time required.

No interference effects were found from 20 ppm of the following elements in copper: silver, cadmium, nickel, lead, tin, zinc, sulphur, iron, bismuth, manganese. These concentrations exceed those normally found in electrolytic copper. Compared with other methods of analysis, the ion exchange—a.s.v. procedure for determination of selenium and tellurium offers advantages in terms of simplicity, sensitivity, specificity and cost effectiveness. It requires no special apparatus beyond basic a.s.v. equipment. The use of the gold film avoids the cost of a solid gold electrode, enabling the facile preparation of a fresh surface by polishing and electrodeposition of gold should there be contamination of the working electrode.

Characteristics of the gold film electrode

The performance of the gold film—glassy carbon electrode was markedly affected by the condition of the GCE surface prior to deposition of gold

and by the amount of gold plated onto the electrode. It has been shown [25] that mercury plates onto numerous active sites of the GCE in the form of discrete particles, leaving less active portions of the electrode uncovered. It would appear that gold is deposited in a similar manner: the rate of deposition of gold showed no change at the point where an amount of gold equivalent to an atomic monolayer (1.2×10^{-4} coulombs) had been deposited. Moreover, when the electrode was wiped free of gold with a tissue and not re-polished before re-plating with gold, the sensitivity of the electrode towards selenium fell successively with each cycle of this operation (Table 2). In the case of a solid gold electrode, Andrews and Johnson [26] found a single stripping peak for selenium when the selenium was deposited as a monolayer on the gold surface. Progressive oxidation of the GCE surface would thus decrease the number of active sites on the GCE and the fixed mass of gold would tend to deposit increasingly in larger particles at fewer sites and so the specific surface available for selenium deposition would fall.

The variation of selenium peak height (for 100-s deposition from a 50-ppb selenium concentration) with the amount of gold plated onto the electrode is shown in Fig. 2. The scatter reflects the difficulty in obtaining a reproducible GCE surface prior to each gold plating step. The gold reduction peak at +0.85 V behaved similarly; because only the very surface layer of the gold film is oxidized during the oxidation period prior to the cathodic scan [27], the increase in gold reduction peak with an amount of gold far beyond that necessary to form a uniform monolayer on the GCE indicates that the effective surface area of the gold film is increasing. A single gold film can be used for at least 150 determinations before decline in sensitivity requires re-polishing of GCE and deposition of a new gold film.

In addition to the role of the gold film, the sensitivity of the analysis for selenium and tellurium was affected by deposition potential, deposition time, conditioning potential, conditioning time and scan rate. The selenium peak height increased with increasingly negative deposition potential up to a limiting value at −0.2 V. A deposition potential of −0.1 V was used for optimum reproducibility. The selenium peak height also increased with deposition time (Fig. 3) until the surface of the gold film was saturated, beyond which the proportionality of peak height to selenium concentration was lost.

TABLE 2

Passivation of the GCE measured as a decrease in the electrode response to selenium as successive gold films (2×10^{-3} coulombs) are plated onto the GCE

Generation of gold film	1	2	3	4	5
Se stripping peak height (μA)	12.2	4.9	2.0	1.1	0.7

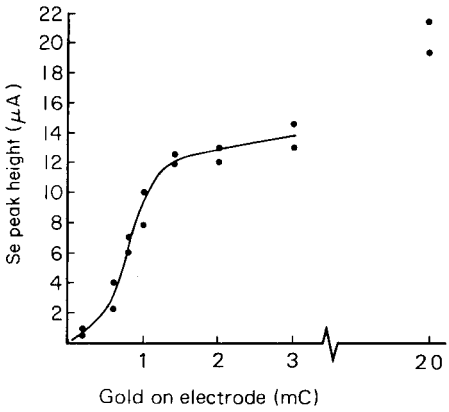

Fig. 2. Variation of selenium peak height with amount of gold deposited. [Se(IV)] = 50 ppb; deposition time 100 s.

Prior to deposition of selenium/tellurium the electrode was conditioned at a potential more positive than the oxidation potential of selenium to ensure that oxidation of selenium/tellurium (and of any impurities from the electrode surface) was complete. A conditioning potential of +1.2 V gave the highest selenium and tellurium anodic stripping peaks while the optimum conditioning time was 10—30 s. Times outside this range led to reduced reproducibility for successive scans. A scan rate of 40 mV s^{-1} gave good peak height and rapid analysis. The peak height for 5 ppb of selenium with a deposition time of 150 s varied linearly from 1 to 3 μA for scan rates of

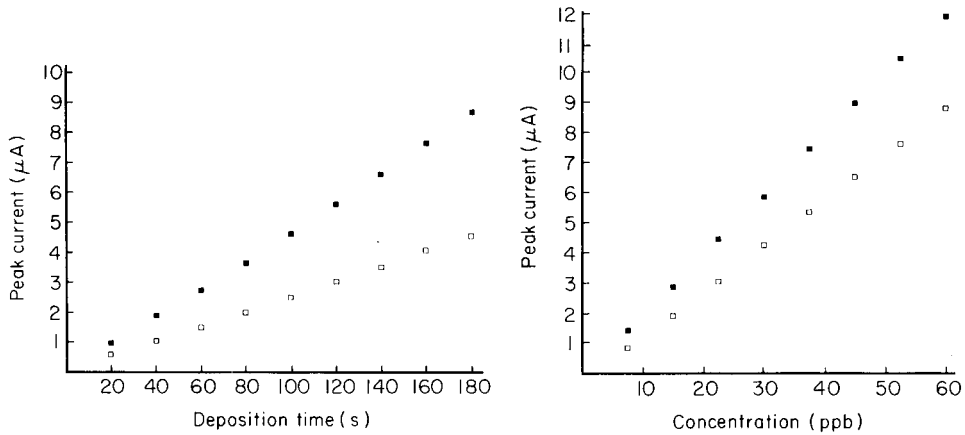

Fig. 3. Variation of Se and Te peak heights with deposition time. (▪) 12 ppb Se; (□) 30 ppb Te; 2 × 10^{-2} coulombs of Au.

Fig. 4. Calibration graphs for Se and Te. 2 × 10^{-2} coulombs of gold; deposition at —0.1 V in 0.1 M HNO_3; (▪) 50 s for Se; (□) 160 s for Te.

10—40 mV s^{-1}. When the established optimum conditions were used, the absolute responses (peak height vs. concentration) for selenium and tellurium were as shown in Fig. 4. These results were calculated from both peak height and peak area: no significant differences were found and peak height was used for convenience.

REFERENCES

1 K. E. Mackay and G. Armstrong Smith, Trans. Inst. Mining Met., Sect. C., 75 (1966) C269.
2 D. A. Reese and L. W. Condra, Wire Ind., Oct. (1969) 883.
3 L. K. Bigelow and J. H. Chen, Met. Trans. B., 7 (1967) 661.
4 J. D. Mullen, Talanta, 23 (1976) 846.
5 W. Reichel and B. G. Bleakley, Anal. Chem., 46 (1974) 59.
6 P. Stanfscheff, Fresenius Z. Anal. Chem., 220 (1966) 33.
7 S. Landsberger and G. G. J. Boswell, Anal. Chim. Acta, 89 (1977) 281.
8 M. Bedrossian, Anal. Chem., 50 (1978) 1898.
9 K. L. Cheng, Chem. Anal., 45 (1956) 67.
10 E. M. Donaldson, Talanta, 24 (1977) 441.
11 G. Tolg, Talanta, 19 (1972) 1489.
12 G. Norwitz, Anal. Chim. Acta, 5 (1951) 109.
13 T. Kawashima, S. Kai and S. Takashima, Anal. Chim. Acta, 89 (1977) 65.
14 E. M. Donaldson, Talanta, 23 (1976) 823.
15 J. A. Fiorino, J. W. Jones and S. G. Capar, Anal. Chem., 48 (1976) 120.
16 M. Thompson, B. Pahlavanpour, S. J. Walton and G. F. Kirkbright, Analyst, 103 (1978) 568.
17 O. E. Olson, J. Assoc. Off. Anal. Chem., 52 (1969) 627.
18 J. A. Corbett and W. C. Godbeer, Anal. Chim. Acta, 91 (1977) 211.
19 Y. Shimoishi and K. Tôei, Anal. Chim. Acta, 100 (1978) 65.
20 O. J. Kronborg and E. Steinnes, Analyst, 100 (1975) 835.
21 M. Volaire, O. Vittori and M. Porthault, Anal. Chim. Acta, 71 (1974) 185.
22 T. A. Krapivkina, E. M. Roizenblat and G. A. Kalambet, Ind. Lab., 41 (1975) 317.
23 A. M. Shafiqul, O. Vittori and M. Porthault, Anal. Chim. Acta, 87 (1976) 437.
24 R. W. Andrews and D. C. Johnson, Anal. Chem., 48 (1976) 1056.
25 M. Stulikova, J. Electroanal. Chem. 48 (1973) 33.
26 R. W. Andrews and D. C. Johnson. Anal. Chem., 47 (1975) 294.
27 S. B. Brummer and A. C. Makrides, J. Electrochem. Soc., 111 (1964) 1122.

Analytica Chimica Acta, 110 (1979) 95—106

A RELIABLE SOURCE OF VERY SMALL AMOUNTS OF HYDROGEN CHLORIDE FOR ANALYTICAL PURPOSES

ELIO SCARANO*

Istituto di Chimica Analitica, Università di Roma, Città Universitaria, 00185 Roma (Italy)

CLAUDIO CALCAGNO and LAURA CIGNOLI

Istituto di Chimica Analitica, Facoltà di Farmacia, Università di Genova, 16132 Genova (Italy)

(Received 19th January 1979)

SUMMARY

Sources of small quantities of hydrogen chloride (nmol s^{-1} and pmol s^{-1}), based on molecular diffusion through a membrane from a reservoir of strong hydrochloric acid, are described. Accurate procedures of standardizing and checking the sources are reported. Extension to other reagents is possible. This standardized source provides a reliable means for the preparation of gaseous reference mixtures as well as standard solutions of hydrochloric acid.

Sources of very small known amounts of chemical species in the purest possible state are of great importance in modern analytical chemistry [1]. The preparation of dilute standard solutions of chemicals and their delivery in small volumes entails numerous drawbacks [1]. An alternative way is to use gaseous mixtures of the chemical and an inert carrier gas; at least a hundred such mixtures have been prepared and many are commercially available but only about ten, classifiable on the basis of their reliability and employment, have been described in the literature. Some are called reference materials [2], others are concerned with atmospheric pollution [3—14], and a few have been described for general analytical purposes [15—17]. Common gaseous standards include sulfur dioxide, nitrogen dioxide, carbon dioxide, carbon monoxide, propane, butane, ammonia and hydrogen chloride. The generation rates of the sources range from 10^{-2} to 10^{-13} mol s^{-1}, and the concentrations of the gaseous standards range from a few per cent to ppm and ppb levels.

The problems of concern in gaseous standard mixtures involve preparation, standardization, stability and delivery. Preparation was the principal problem initially, the methods involving static and dynamic mixing [14, 15, 18], coulometry [19], and saturation [13, 16, 17, 20, 21]. In 1966, O'Keeffe and Ortman [3] developed the permeation tube method for easily liquefiable gases; this method rapidly became popular and McKinley extended the prin-

ciple to all types of gases [22]. Later, the main problems concerned standardization and stability [9—12].

In this paper, a reliable source for the delivery of very small amounts of gases and the preparation of dilute gaseous reference mixtures (GRM) are described. The source, based on the permeation principle, has been modified and improved to give easy and inexpensive laboratory preparation and a source geometry suitable for mathematical treatment [23]. Efforts have also been made to refine standardization methods. Hydrogen chloride was chosen for this study, because of its widespread use as a donor of hydrogen and chloride ions in the form of hydrochloric acid.

The source was a gas-tight glass flask (the generating cell) containing a Teflon tube (the tubular membrane). The cell was filled with a concentrated (above 8 M) aqueous solution of hydrochloric acid, possessing a gaseous pressure of hydrogen chloride, P_{HCl}. An inert carrier gas (nitrogen) was allowed to flow inside the tubular membrane. Because of the difference in P_{HCl} between the inside and outside of the membrane, hydrogen chloride passed through into the carrier gas, giving a gaseous mixture (HCl—GM). Under constant temperature and flow-dynamic conditions on both sides of the membrane, the generating cell was characterized by a generating constant, K_c (mol s^{-1}). Following a variation in the temperature or flow conditions, a new steady state and K_c value were reversibly reached in ca. 30 min. K_c was accurately reproducible even after months of disuse, during which room temperature was maintained but both the agitation inside the cell and the carrier gas flow were stopped. Because of the very large reservoir of hydrochloric acid, K_c was practically uninfluenced by use of the source over very long periods.

To find K_c, careful titrimetric, potentiometric and coulometric determinations were carried out. The range of K_c investigated was 10^{-9}—3×10^{-12} mol s^{-1}, corresponding to the concentration range 10^{-6}—3×10^{-9} M (i.e. 24.5 ppm—73 ppb, v/v) with a nitrogen flow rate of 10^{-3} l s^{-1} at 25°C and 760 mm Hg total pressure.

A generating cell with a known, stable, and reproducible value of K_c constituted a secondary standard or reference source of both hydrogen chloride (the delivery of known amounts being only time-dependent), and of gaseous reference mixtures (HCl—GRM), provided that a stable nitrogen flow-rate was used.

EXPERIMENTAL

Materials and apparatus

Reagent-grade chemicals, high-purity nitrogen and twice-distilled water were used. Pyrex glass, Teflon, and stainless steel were used to construct the apparatus; short Teflon tubes overlapped with Tygon tubes were used as connections.

The generating cell was a modified 1-l Erlenmeyer flask. The tubular membrane was 1 m long and 1.6 mm wide with a 0.15-mm wall thickness. The cell,

made completely gas-tight by means of carefully machined Teflon gaskets and screw caps, was almost completely filled with the generating solution, and was immersed to the level of the screw caps in a well-insulated bath (Fig. 1), which gave constant temperature within ±0.01°C. Temperature varations greater than 5°C may cause the cell to break because of the liquid volume variation. To avoid breakage, either of the two screw caps was temporarily unscrewed when the temperature was varied. When in use, vigorous, constant and reproducible stirring was maintained in the cell.

Figure 2 shows the conventional, cylindrical analysis cell with ground-glass cones for: a glass electrode; Ag/AgCl (0.1 M KCl) reference electrode; a platinum cathode; a counterflow shield tube with silver anode (as shown in Fig. 2); and an opening (normally closed with a glass plug) for adding reference sol-

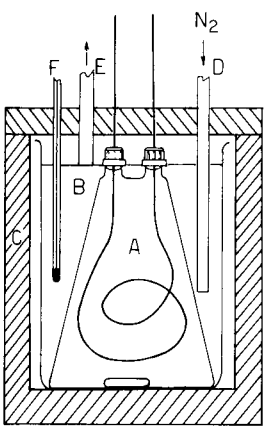

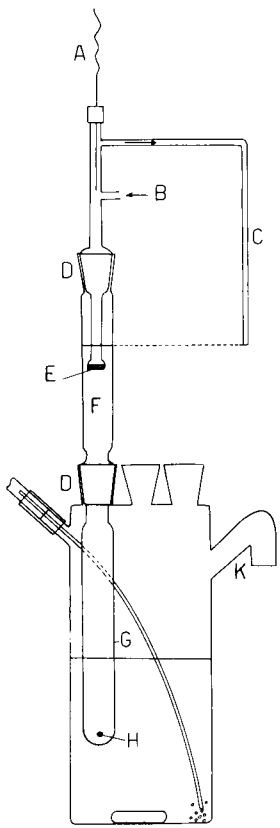

Fig. 1. Generating cell compartment. (A) Generating cell; (B) glass vessel; (C) polyurethane box; (D) water inlet; (E) water outlet; (F) thermometer.

Fig. 2. Analysis cell and anode compartment. (A) Silver wire anode; (B) 0.1 M KCl solution inlet; (C) 0.1 M KCl solution outlet; (D) ground-glass joint; (E) low-porosity sintered glass frit; (F) 0.1 M KCl solution; (G) jacket; (H) ceramic frit; (K) gas vent.

utions. The cathode was made of 1-mm thick platinum wire, covered with a glass jacket, leaving exposed 2 cm of wire. The cell contained 100 ml of 0.1 M KCl solution (pH 4—5) into which the HCl—GM bubbled through a Teflon tube, 0.5—1 mm i.d.

Effective, constant agitation was maintained during experiments and the temperature was maintained at 28 ± 0.1°C. The anode compartment was connected to a reservoir of 0.1 M KCl solution which was allowed to pass during experiments at 2 ml min^{-1}. The nitrogen flow-rate was fixed at 2 l h^{-1} (±5%). A three-way stopcock between the generating and analysis cells allowed the HCl—GM to pass into the analysis cell or to the vent.

Reference solutions were 10^{-2}—10^{-3} m borax, Na_2CO_3, or hydrochloric acid solutions in 0.1 m KCl or in water. An analytical balance (sensitivity 10^{-5} g) was used to prepare the reference solutions. Polyethylene washbottles (50 ml) with a Teflon tube (i.d. 0.5—1 mm) fitted (gas-tight) through the screw cap, were used as dispensers for the solutions and were weighed immediately before and after delivery.

A null-point research pH-meter (Amel, Milan) with a readability of 10^{-3} pH unit was used for measurements. A chart recorder permitted a resolving power of 10^{-4} pH and made it easy to check the pH for noise and drift. Coulometric sources were a Yew d.c. voltage-current standard (Type 2853) and an Amel 831 coulometer with incorporated timer. Glass tubes with ceramic frit (303/95 NS jacket ceramic junction, Ingold, Switzerland) were used for the reference electrode and the anode compartment.

Preliminary experiments

Some preliminary investigations of the experimental conditions and procedures were made.

In the range pH 4—5, the analysis cell solution was generally stable to within 10^{-3} pH unit. The pH began to decrease linearly, immediately after the HCl—GM was passed through the solution, for small pH variations. When the HCl—GM flow was diverted to the vent, the pH variation stopped immediately. This behaviour did not take place if the tubing contained water, even in small amounts. The flow of HCl—GM gradually dried the membrane inside, and when the water had been completely eliminated, the dissolved hydrogen chloride was released, a sudden change of pH occurred, and a regular pH variation followed.

The absorption efficiency was complete [20] and was not influenced by temperature, bubble size or stirring efficiency.

There was no evidence that the mixing efficiency of the hydrogen chloride released from the walls of the tubular membrane by the flow of nitrogen was not complete when the gaseous mixture reached the analysis cell. It was experimentally verified [23] that there was complete mixing of the carbon dioxide, released by the tubular membrane, with a slowly flowing aqueous solution in a cell similar to that used here.

The pH increased immediately (under stirring) when the coulometric current

was generated, and stopped increasing as soon as the current was interrupted. In contrast, the pH increased slowly for 5—15 min after interruption if a naked platinum wire was used as cathode, or if the glass cover of the cathode was defective.

Above pH 5, residual quantities of carbon dioxide caused trouble. Only in coulometric experiments (when the analysis cell was never opened), was it possible to work up to pH 6.

For a short time after assembly of the analysis cell, or after a long period of disuse, drifts and sudden changes of pH occurred; these were attributed to cell impurities, the alkalinity of the glass, and to the return of "dirty" liquid droplets into the solution from the top and the walls of the cell. A stabilization period was therefore necessary; this was dependent on the history of the cell and varied from 2—4 h for the above-mentioned effects, and from 10—30 min after short interruptions. The stabilization period was also dependent on the care taken in preparing the 0.1 M KCl solution and in handling the analysis cell and its components. The process of stabilization was regularized and shortened by keeping the solution temperature at 28°C, i.e., well above room temperature so that the condensed water returning into the solution gave effective washing.

The absence of leaks in the generating cell was very important if irregularities in the pH and poor precision in the determination of K_c were to be avoided. Accurate manufacture and assembly of the cell were essential. The geometry of the generating cell was also important. If the length of the tubular membrane and, to a lesser extent, its position in the generating cell varied, K_c was subject to change. Traces of reducible matter, which interfered strongly in coulometric determinations were present in the cell solution but could be eliminated electrolytically. The anode compartment was designed to avoid enrichment of silver ion in the analysis cell solution as this could nullify the effectiveness of the coulometric determinations. Nevertheless, trace amounts of reducible matter (e.g. of Ag^+ from the reference solution compartment) accumulated through time, and made the pre-electrolysis procedure necessary.

Experimental procedures

Before experiments, checks were made for pH stability and for regular responses to the HCl—GM flow and coulometric current. The determinations of K_c were made with the generating cell at 25 ± 0.01°C, with the exception of those devoted to ascertain the temperature dependence. Several similar generating cells were used.

pH standardization. The glass—Ag/AgCl (0.1 M KCl) electrode couple was standardized with buffer solution (pH 4.01), thoroughly washed with 0.1 M KCl solution, and then placed in the analysis cell. Such standardization was adequate for a long period; it must be emphasized that the pH measurements are not absolute, but only relative.

Pre-electrolysis of the analysis cell solution. To eliminate trace amounts of reducible impurities in the analysis cell solution, pre-electrolysis was carried

out, after adjusting to pH 3—3.5 with hydrochloric acid, for a period of hours or days, depending on the circumstances. In the continuous coulometric determinations of K_c (see later), the pre-electrolysis was performed automatically with currents in the range $(0.5—100) \times 10^{-6}$ A.

Titrimetric determinations of K_c. A stable (within 10^{-3} pH units) pH_1 value was initially reached in the range pH 4—5. An accurately weighed amount, p_b (g), of a solution of borax or sodium carbonate of concentration C_b m, containing an amount q_b (mol) of base, was added to the analysis cell solution. The HCl—GM was allowed to pass for time t_b (s), until pH_1 was again reached. Thus $K_c = (2q_b + q_d)/t_b$, where q_d (mol) $\cong (p_b\ 10^{-pH_1})/(0.83 \times 10^{-3})$, i.e., the equivalent amount of strong base corresponding to the dilution effect (0.83 being the activity coefficient of the hydrogen ion at 0.1 ionic strength).

Checking of coulometric sources and procedures. A stable pH_1 value was reached in the range pH 4—5. An amount p_a (g) of HCl solution of concentration C_a m, containing q_a mol of hydrochloric acid was added. The starting pH_1 was restored by means of coulometric currents, i_i (A) (in the range $3 \times 10^{-5}—10^{-3}$ A), for time intervals t_i (s) (in the range $10—2 \times 10^3$ s). From $q_i = \Sigma i_i t_i/96{,}486$ was calculated C_a (found) $= (q_i + q_d)/p_a$, where q_d (mol) $\cong (p_a\ 10^{-pH_1})/(0.83 \times 10^{-3})$ was used as the correction for the dilution effect.

Coulometric determinations of K_c *(continuous mode).* The HCl—GM was allowed to pass through the analysis cell solution in the range pH 4—6. The coulometric compensation current, i_c (A) necessary to maintain the solution pH constant to within 10^{-3} pH for a long time was found. Hence $K_c = i_c/96{,}486$.

Coulometric determinations of K_c *(discontinuous mode).* A stable value of pH_1 in the range 4.5—6 was established. The stirring of the solution was stopped and, 60 s later, with the solution quite still, an electric current i_d (A) was delivered for a period t_1 (s). The stirring of the solution was resumed, the HCl—GM was allowed to enter, and the time t_2 (s) necessary to reach pH_1 was measured. Hence $K_c = (i_d\ t_1)/(96{,}486\ t_2)$.

K_c *as a function of the temperature.* The dependence of K_c on the temperature was obtained by determining values for K_c at different generating cell temperatures 1 h after stabilization, with the continuous coulometric procedure.

RESULTS

Representative results are reported in Tables 1—6. Table 1 shows the precision in the titrimetric determinations of K_c (the amounts of reference base ranged from 3 to 1 μmol for borax and from 0.3 to 0.01 μmol for sodium carbonate).

Data for the reliability of coulometric sources, for the evidence of the presence of reducible impurities, and for the effectiveness of the pre-electrolysis procedure are reported in Table 2 (the amounts of hydrochloric acid ranged from 4.5 to 0.03 μmol).

The results for K_c by the coulometric procedures (Tables 3 and 4) show

TABLE 1

Titrimetric determinations of K_c

Reference solution	C_b (10^{-3} m)	No. of detns.[a] (n)	K_c (10^{-10} mol s^{-1})
Borax in 0.1 M KCl	1.033	4	7.833 ± 0.022 (0.28%)
Na_2CO_3 in water	10.538	7[b]	6.179 ± 0.070 (1.13%)
Na_2CO_3 in water	10.538	9[b]	6.028 ± 0.137 (2.28%)
Na_2CO_3 in water	10.538	9[b,c]	6.163 ± 0.061 (0.98%)
Na_2CO_3 in water	10.538	5[b]	6.128 ± 0.085 (1.38%)

[a]Two different generating cells. [b]The same generating cell, different days (respectively days 6, 7, 7, 10 of the month). [c]Fresh amount of Na_2CO_3 solution in the dispenser.

TABLE 2

Checking of coulometric sources and procedures

C_{HCl} taken (10^{-3} m)	No. of detns. (n)	t[a] (h)	C_{HCl} found (10^{-3} m)	Difference (%)
10.240	10	0	10.304 ± 0.019 (0.18%)	+0.63
10.240	11	5	10.249 ± 0.083 (0.81%)	+0.09
9.925	8	3	9.898 ± 0.030 (0.30%)	−0.27
1.053	18	2	1.089 ± 0.011 (1.04%)	+3.42

[a]Pre-electrolysis time.

the following features: evidence for the presence and the elimination of reducible matter; the greater reliability of the discontinuous mode, because of its higher sensitivity and minor dependence on reducible impurities, especially at the lowest K_c values; the very low level of K_c attainable (the minimum value investigated was 3×10^{-12} mol s^{-1}, with results analogous to those in Table 4).

Table 5 shows that titrimetric and coulometric procedures give closely similar values for K_c, at least down to 5×10^{-10} mol s^{-1}. The reported data are part of a series of experiments carried out for a month, with some days of total interruption.

Small errors were attributed to the increased concentration of the aqueous reference solutions, caused by solvent water loss by evaporation when many deliveries were made with the same batch of reference solution (see, for example, Table 1). No error was attributed to consumption of the hydrogen chloride in the generating solutions, because of their very high reserve capacity (see later).

The dependence of K_c on the temperature of the generating cell (Table 6) is in accordance with the formula

$$\ln (K_c)_T/(K_c)_{298.2} = -(E/R)(T^{-1} - 1/298.2)$$

where T (K) is the temperature of measurement, 298.2 (K) is the reference

TABLE 3

Coulometric determinations of K_c (generating solution, 12 M HCl)

Time[a] (h)	i_c (10^{-6} A)	K_c, continuous mode (10^{-10} mol s^{-1})	K_c, discontinuous mode (10^{-10} mol s^{-1})	No. of detns.[b] (n)
0	62.0	6.43		
1	60.0	6.22		
			6.178 ± 0.020 (0.33%)	5
2	59.5	6.17		
3			6.231 ± 0.036 (0.57%)	4
4	59.5	6.17		
21	59.5	6.17		
22	58.5	6.06		
			6.069 ± 0.031 (0.51%)	5
24	58.5	6.06		
			6.103 ± 0.031 (0.51%)	5
26	58.5	6.06		
94	62.0	6.43		
			6.404 ± 0.095 (1.48%)	4
96	61.5	6.37		
100	60.0	6.22		
			6.198 ± 0.034 (0.54%)	5
116	61.0	6.32		
117	60.0	6.22		
119	58.5	6.06		
			6.087 ± 0.020 (0.33%)	6

[a]During the intervals room temperature was maintained; a coulometric current of 30—40 × 10^{-6} A was allowed to flow; the HCl—GM was passed through the analysis cell solution. [b]In most cases, the first discontinuous determination of a series gave an anomalous result which was not used in the computation of the mean values of K_c.

temperature, R is the gas constant (1.986 kcal mol^{-1}), and E is the activation energy (kcal mol^{-1}). Experimental values of E were in accordance with those expected [7], as well as the variation of K_c with T, i.e., ca. 10% per degree [10]. After a temperature change, the new value of K_c was reached within 30 min. The temperature dependence was reversible in every case.

Variations of flow dynamic conditions on either side of the tubular membrane caused effects that lasted for 30 min; experiments with no agitation inside the generating cell showed poor precision and irregular variations in pH. The values of K_c depended slightly on the nitrogen flow, as expected [23]; this dependence was not studied in detail.

DISCUSSION

Permeation devices have unique advantages and also some disadvantages. Some improvements, realized through the new generating cell design and

TABLE 4

Coulometric determinations of K_c (generating solution, 8 M HCl)

Time[a] (h)	i_c (10^{-6} A)	K_c, continuous mode (10^{-12} mol s^{-1})	K_c, discontinuous mode (10^{-12} mol s^{-1})	No. of detns.[b] (n)
0	3.0	31.1		
			12.10 ± 0.46 (3.8%)	4
4	1.5	15.5		
23	1.3	13.5		
			18.27 ± 3.65 (20%)	5
25	1.3	13.5		
			8.90 ± 0.83 (9.3%)	4
			8.64 ± 0.30 (3.5%)	4
28	1.2	12.4		
			8.14 ± 0.24 (3.0%)	4
68	2.0	20.7		
70	1.5	13.8		
			9.22 ± 0.54 (5.9%)	5
73	1.2	12.4		
			8.86 ± 0.62 (7.0%)	6
75	1.2	12.4		
77	1.2	12.4		
			8.99 ± 0.27 (3%)	5
96	1.2	12.4		
			8.92 ± 0.22 (2.5%)	6

[a,b] As in Table 3. The coulometric current in the intervals was 0.5×10^{-6} A.

TABLE 5

Comparison between titrimetric and coulometric (discontinuous mode) determinations of K_c for a given generating cell on different days

Day	No. of detns. (n)	K_c (10^{-10} mol s^{-1})	
		Titrimetric	Coulometric
18	7		6.014 ± 0.041 (0.68%)
19	5		5.954 ± 0.039 (0.68%)
20	5		5.942 ± 0.048 (0.80%)
20	9	5.983 ± 0.049 (0.82%)	
21	5		5.945 ± 0.016 (0.27%)
21	9	5.981 ± 0.105 (1.75%)	
25	4		5.934 ± 0.024 (0.41%)
25	9	5.953 ± 0.043 (0.73%)	

working features are as follows. Low pressure on the reservoir side of the membrane is obtained through the adoption of liquid solutions of gaseous reagents, instead of liquefied or pressurized gaseous reagents which involve

TABLE 6

Dependence of K_c on the generating cell temperature

$(T - 273.2)$ (K)	i_c (10^{-6} A)	K_c (10^{-10} mol s^{-1})	Activation energy (kcal mol^{-1})
20.00	47.7	4.94	15.500
22.98	62.5	6.48	15.334
24.42	70.5	7.31	16.579
25.00	74.5	7.72	—
28.00	97.0	10.05	15.679

relatively high pressures and can cause swelling and rupture of the membrane, e.g., with carbon dioxide [3], or slow deformations in time, especially if large temperature variations occur, thus affecting the values of K_c [10, 11]. Uniform, controlled and reproducible conditions have also been arranged on the reservoir side of the membrane. With liquefied gases, as a consequence of the consumption, the membrane is partly in contact with both the liquid and gaseous phases, in a ratio variable with time; in such cases, mass transport is diffusion-controlled and, consequently, dependent on shocks, vibrations and temperature unevenness. In the cell described here, the tubular membrane is always almost completely surrounded by the generating solution, whose volume is unchanged; stirring inside the cell thus secures reproducible flow-dynamic and thermal conditions and regular mass transport which contribute to the stability and reproducibility of the values of K_c. The flow dynamic conditions on the other side of the membrane are also greatly improved, making rigorous theoretical treatment possible [23]. Protection against atmospheric agents has also been improved. Because of the inward diffusion of atmospheric components, the chemical and physical structure of the membrane may change [3, 8, 9, 11]. In the cell described here, the inside of the membrane can be easily isolated from the environment all the time, and moisture is rapidly eliminated. For the direct gravimetric determination of K_c, absorbent weighing tubes can be used without dismounting and exposing the apparatus to the atmosphere.

Consumption of the reagent has been decreased. Permeation tubes have a high reserve of the reagent, but consumption occurs even in periods of disuse. Consumption of the reagent is very limited in periods of disuse because of the automatic limitation of the diffusion process when the gaseous reagent pressure in the tubular membrane equals that in the generating cell. Yet the reserve can be equally high. For hydrogen chloride, calculations show that a generating cell, filled with 1 l of 12 M HCl, with $K_c = 10^{-9}$ mol s^{-1}, will consume only 0.26% of the total amount of available hydrogen chloride in a year of uninterrupted use; if $K_c = 10^{-11}$ mol s^{-1}, and the cell is filled with 8 M HCl, the consumption will be 40 ppm after 1 year.

Other advantages of the proposed modification are: inexpensive apparatus;

ease of assembly; the generating cell can be refilled and re-used indefinitely; the value of K_c can be varied widely by altering the nature, length, and wall thickness of the tubular membrane, the composition of the generating solution, quite apart from the temperature and flow rate of the carrier gas; more than one reagent gas can be mixed with the carrier gas; the principle can be extended to many other reagent gases, provided that a solvent in which the reagent gas is highly soluble exists and the solution shows a gaseous pressure of few mm Hg.

It is essential for K_c and the composition of the gas mixture to be accurately known. The standardization procedures must rely on absolute methods of analysis, e.g., gravimetry, volumetry, titrimetry, coulometry and differential pressure measurements, effected under the same conditions of use as the gas mixture. Therefore methods based on accumulation, in static conditions, of the gaseous reagent on the carrier gas side of the membrane, in amounts such that the volume or pressure variations can be measured, are not suitable for giving reliable values of K_c, which are dependent on the difference in gaseous reagent pressure on the two sides of the membrane and also on the flow dynamic conditions [23]. For very low values of K_c, standardization procedures may be too slow for amounts of gaseous reagent sufficiently large for their analysis to the high accuracy required, to be collected. Rapid and accurate procedures are therefore essential because slow standardization procedures cannot reveal variations in K_c and cannot give reliable values for the composition of the gas mixture [12, 24]. In refining titrimetric, potentiometric and coulometric procedures, their present limitations for very low K_c values have been exposed, but these can be overcome [1].

The stability of a source is the fundamental requirement for reliability and its suitability for standardization. Stability arises from a number of factors of which the most important (physical and chemical characteristics of the membrane, flow dynamics and thermal conditions, high reserve of the reagent) have been considered. With the apparatus described, nano- and subnanomolar amounts of the reagent can be obtained easily with the aid of a stopcock and a time-measuring device, and reliable gas mixtures can be obtained if a stable and known carrier gas flow-rate is available.

This work was supported by a grant from the Consiglio Nazionale delle Ricerche, Roma, Italy.

REFERENCES

1 J. W. Mitchell, Anal. Chem., 45 (1973) 492A.
2 J. P. Cali, Anal. Chem., 48 (1976) 802A.
3 A. E. O'Keeffe and G. C. Ortman, Anal. Chem., 38 (1966) 760.
4 A. E. O'Keeffe and G. C. Ortman, Anal. Chem., 39 (1967) 1047.
5 F. P. Scaringelli, S. A. Frey and B. E. Saltzman, Am. Ind. Hyg. Assoc. J., 28 (1967) 260.
6 L. A. Elfers and C. E. Decker, Anal. Chem., 40 (1968) 1658.

7 B. E. Saltzman, C. R. Feldman and A. E. O'Keeffe, Environ. Sci. Technol., 3 (1969) 1275.
8 F. P. Scaringelli, A. E.O'Keeffe, E. Rosenberg and J. P. Bell, Anal. Chem., 42 (1970) 871.
9 R. N. Dietz, E. A. Cote and J. D. Smith, Anal. Chem., 46 (1974) 315.
10 A. Cedergren, A. Wikby and K. Bergner, Anal. Chem., 47 (1975) 100.
11 E. E. Hughes, H. L. Rook, E. R. Deardorff, J. H. Margeson and R. G. Fuerst, Anal. Chem., 49 (1977) 1823.
12 H. J. Purdue and R. J. Thompson, Anal. Chem., 44 (1972) 1034.
13 E. Erdös and J. Bares, Collect. Czech. Chem. Commun., 29 (1964) 2718.
14 R. C. Paule, Anal. Chem., 44 (1972) 1537.
15 D. N. Hume and B. J. Duffield, 3rd Analytical Conference, 24—29 August 1970, Budapest, Hungary.
16 E. Scarano, M. Forina and C. Calcagno, Anal. Chem., 45 (1973) 557.
17 E. Scarano, M. Forina and G. Gay, Anal. Chem., 43 (1971) 1310.
18 B. E. Saltzman, Anal. Chem., 33 (1961) 1100.
19 P. Hersch, C. J. Sambucetti and R. Deuringer, Chim. Anal., 46 (1964) 31.
20 E. Scarano, G. Gay and M. Forina, Anal. Chem., 43 (1971) 206.
21 M. Forina, Ann. Chim. (Rome), 65 (1975) 491.
22 J. J. McKinley, 16th National Symposium, Analysis Instrumentation Division, Instrument Society of America, May 25—27, 1970, Pittsburg, Pa.
23 E. Scarano and C. Calcagno, Anal. Chem., 47 (1975) 1055.
24 D. P. Lucero, Anal. Chem., 43 (1971) 1744.

Analytica Chimica Acta, 110 (1979) 107—115

DIFFERENTIAL PULSE POLAROGRAPHIC STUDY OF THE DEGRADATION OF CEPHALEXIN
Determination of Hydrogen Sulphide and other Degradation Products

A. G. FOGG* and N. M. FAYAD

Department of Chemistry, Loughborough University of Technology, Loughborough, Leics. (Gt. Britain)

C. BURGESS

Glaxo Operations (U.K.) Ltd., Barnard Castle, Co. Durham, (Gt. Britain)

(Received 9th April 1979)

SUMMARY

Differential pulse polarography (d.p.p.) is used to study the degradation of cephalexin. Hydrogen sulphide, evolved during the degradation of cephalexin solutions, was removed continuously in a stream of nitrogen and determined periodically. Other electroactive degradation products were observed by d.p.p. of the degraded sample solutions. The degradation mechanism is highly dependent on pH, the initial concentration of cephalexin, temperature, the particular buffer used, and the presence of dissolved oxygen. The formation and degradation of the diketopiperazine derivative formed by intramolecular aminolysis, particularly at neutral pH, can be followed by means of its polarographic peak at —0.9 V (pH 7.4). Approximately half the total sulphur originally present in cephalexin is liberated as hydrogen sulphide at pH 7.4 at 37°C. Increasing the degradation temperature to 80°C and sweeping out the hydrogen sulphide with nitrogen increases the yield of a major product which gives a peak at —1.26 V. At pH 8.5 (80°C, 100 μg cephalexin ml^{-1}) the percentage of the sulphur evolved as hydrogen sulphide increases with time, and a peak appears at —0.96 V (probably 2-hydroxy-3-phenyl-6-methylpyrazine) which increases as the peak at —1.26 V becomes smaller. Other products formed under different conditions (concentration, pH, temperature) are reported. At pH 3 (80°C) only 8% conversion via intramolecular aminolysis and 5% evolution of total sulphur is indicated after four hours.

Elegant studies have been made of the degradation of cephalexin (I) solutions by Yamana et al. [1, 2], Bundgaard [3, 4] and Dinner [5]. During degradation at pH 7 and 35°C, a 98% loss of the primary amine group occurs indicating essentially complete degradation of cephalexin via the diketopiperazine derivative (II) formed by intramolecular aminolysis [3]. Primary amine analysis indicates that above pH 10 only 32% of the cephalexin degrades by intramolecular aminolysis, the remainder degrading by hydrolysis of the β-lactam ring. After degradation at pH 3, Dinner [5] isolated the thiolactone (III) and the diketopiperazine derivative (V), and Bundgaard [4] showed that IV is a precursor of V. Degradation is very rapid at high pH owing to specific base catalysis by hydroxyl ion, but is slow and independent of pH below pH 5.

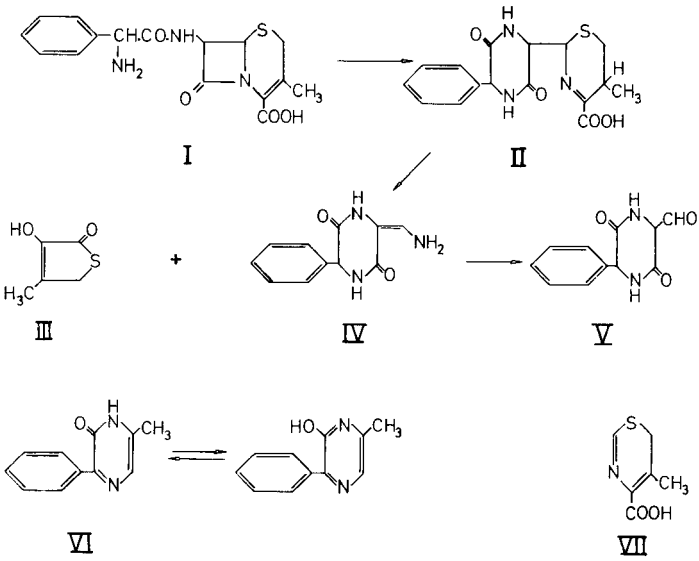

Barbhaiya et al. [6] showed that the fluorescent product formed by treating cephalexin first in sodium hydroxide solution at room temperature and then in pH5 buffer at 100°C is VI. Hughes et al. [7] had shown previously that in the degradation of ampicillin and aminobenzylpenicilloic acid the main fluorescent degradation product is 2-hydroxy-3-phenylpyrazine. Bontchev and Papazova [8] indicated that VII is formed when cephalexin is hydrolysed in 12.5% sulphuric acid solution.

The differential pulse polarography (d.p.p.) of several cephalosporines was reported previously [9] and the possibility of using d.p.p. to study their degradation indicated. Cephalosporins with a substituted 3-methyl group give a d.p.p. peak at about −1 V (pH 2–4). These peaks are close to the cathodic limit but can be used quantitatively and to follow their degradation in solution. Several cephalosporins, e.g. cephaloridine, cephalonium and cefuroxime, contain other reducible groups and give other polarographic peaks at less negative potentials.

Cephalexin, which has an unsubstituted 3-methyl group and no other reducible group, does not give a peak at the dropping mercury electrode, but some of its degradation products act as depolarizers. In particular, a major degradation product (in pH 7.4 buffer at 37°C), the diketopiperazine derivative (II), gives a distinct peak at −0.9 V (pH 7.4). The formation and degradation of this diketopiperazine derivative was followed polarographically [9]. A distinct smell of hydrogen sulphide was observed and a polarographic peak at −0.56 V was associated with the presence of hydrogen sulphide. The degradation products responsible for the peaks at −0.78 V and −1.26 V were not identified. The purpose of the present work was to extend this study of cephalexin degradation, and in particular to determine the hydrogen sulphide formed.

EXPERIMENTAL

Polarographic measurements were made with a PAR 174 polarographic analyser (Princeton Applied Research Corp.). For differential pulse operation a forced drop time of 0.5 s, a scan rate of 5 mV s^{-1} and a pulse height of 50 mV were used with a dropping mercury electrode, a platinum counter electrode and a saturated calomel reference electrode. The water-jacketed polarographic cell was kept at 25°C. Solutions for polarography were deoxygenated with nitrogen gas which had previously been passed through a vanadium(II) scrubber. Polarography of degraded solutions was always carried out at pH 7.4 in phosphate buffer regardless of the pH at which degradation was effected.

For comparative purposes, degradation studies were carried out with and without the removal of hydrogen sulphide. In the former case, cephalexin solutions were degraded in a gas wash bottle whilst a slow stream of nitrogen (or air when the effect of dissolved oxygen was being studied) was passed through the solution. The nitrogen or air was presaturated with water in a second wash bottle; both bottles were placed in a water bath at the required degradation temperature. The hydrogen sulphide was then stripped from the nitrogen by absorption in a suitable solution. Small amounts of hydrogen sulphide ($<2 \times 10^{-5}$ mol) were collected in 10.0 ml of a standard 10^{-3} M cadmium nitrate solution, which was then transferred completely to a polarographic cell containing 10 ml of deoxygenated supporting electrolyte (52.2 g of citric acid and 28.1 g of potassium hydroxide in 500 ml of distilled water) for determination of the excess of cadmium by its d.p. peak at −0.61 V. Infrequently, larger amounts of hydrogen sulphide were absorbed in 1 M sodium hydroxide solution and titrated potentiometrically with standard 0.1 M silver nitrate solution (sulphide-selective electrode).

Cephalexin was provided by Glaxo Ltd., and 2-hydroxy-3-phenyl-6-methylpyrazine was kindly provided by Dr. D. W. Payling, Fisons Pharmaceuticals Ltd. The diketopiperazine derivative (II) was prepared as described by Bundgaard [3]: this sample (m.p. 146—148°C) was used as a polarographic standard for determining the amount of II in degraded solutions. The melting point given is lower than that reported by Bundgaard (m.p. 160—162°C), but the sample gave only one polarographic peak.

RESULTS

The initial degradation studies were made as described previously [9] on buffered solutions (pH 7.4) containing cephalexin (100 μg ml^{-1}) without removal of the hydrogen sulphide formed. At 60°C the compound responsible for the peak at −1.26 V was formed in high yield (see Fig. 1a): the yield was about double that obtained at 37°C [9]. Smaller peaks were also evident at −0.16 V and −0.78 V later in the degradation. After degradation at 80°C for 2 h, the peak at −1.26 V was about five times larger than any

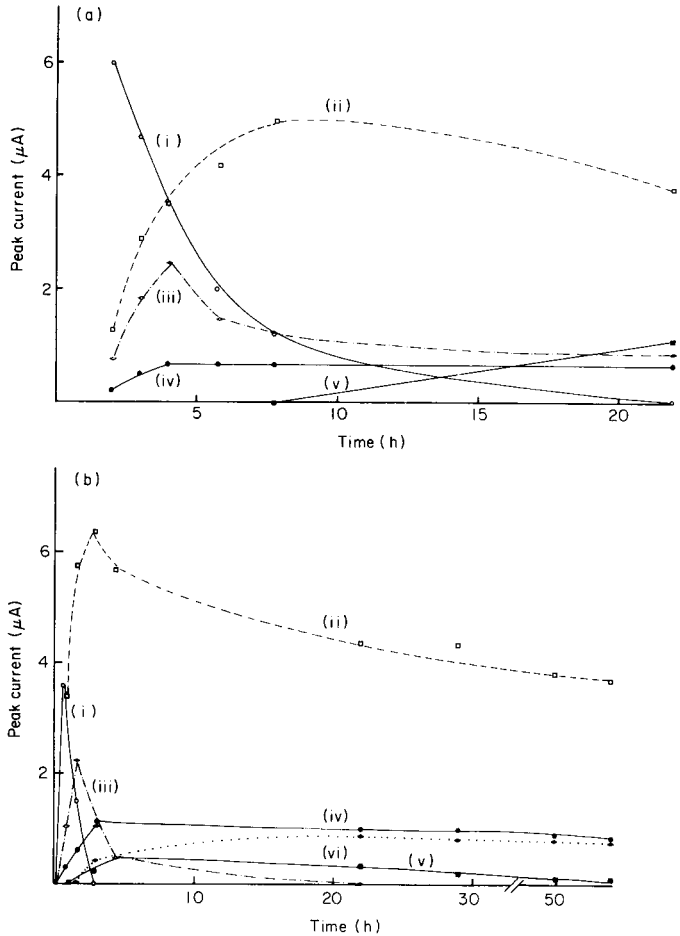

Fig. 1. Degradation of cephalexin in 0.5 M phosphate buffer at pH 7.4. Initial cephalexin concentration, 100 μg ml^{-1}. Temperature: (a) 60°C, (b) 80°C. Peak potentials: (i) −0.9 V (diketopiperazine compound II), (ii) −1.26 V, (iii) −0.56 V (hydrogen sulphide), (iv) −0.16 V, (v) −0.78 V and (vi) −0.96 V (VI).

other peak present (see Fig. 1b). The peak at −0.78 V disappeared after degradation for 54 h; in addition to the peak at −0.16 V another peak appeared at −0.96 V later in the degradation after II had degraded. This latter peak was identified by t.l.c. and by comparison with polarograms obtained with a sample of the pure compound as being due to 2-hydroxy-3-phenyl-6-methylpyrazine (VI); this compound had been isolated from degraded cephalexin solutions by Barbhaiya et al. [6] and identified by unambiguous synthesis. The hydrogen sulphide peak at −0.56 V was evident in all these polarograms.

The effect of the initial cephalexin concentration on the degradation was studied next, again without removal of hydrogen sulphide. Polarograms obtained for 5-μg ml^{-1} solutions degraded at 37°C were of a similar pattern to those for 100-μg ml^{-1} solutions degraded at 37°C or 80°C. When 5-mg ml^{-1} solutions were degraded at 80°C, however, the peak at —1.26 V disappeared and a peak appeared at —1.44 V (irrespective of the concentration at which the polarography was done). Another difference was the presence of a peak at —1.06 V which decayed after about 2 h; the peak at —0.96 V then appeared and in turn decayed with time. A peak also appeared at —0.36 V early in the degradation of the 5-mg ml^{-1} solutions: the compound responsible for this peak degraded more slowly than II. It disappeared completely after 22 h, and two small new peaks appeared at —0.22 V and —0.84 V after 54 h.

When nitrogen was passed through the degrading solution to remove the hydrogen sulphide for determination, the polarograms obtained were modified. Not only the hydrogen sulphide peak at —0.56 V, but also the peaks at —0.78 V (37°C and 80°C) and —0.16 V (80°C) disappeared. When, however, the hydrogen sulphide was removed with air instead of nitrogen, the peaks at —0.78 V and —0.16 V were present; these peaks are probably due to oxidation products of other degradation products with molecular oxygen.

A further effect of passing nitrogen was that the maximum transient yield of II and the compound responsible for the peak at —1.26 V increased by about 35% and 25%, respectively. The results of degradation studies at 37°C (phosphate buffer pH 7.4, 100 μg ml^{-1}) in which hydrogen sulphide was removed with nitrogen and determined, are summarized in Fig. 2. Figure 2a shows the fate of the sulphur during the degradation; after 240 h, II had degraded completely and about 50% of the total sulphur had been evolved as hydrogen sulphide. The remaining sulphur remains in solution in an electroinactive form, possibly as the thiolactone (III) identified by Dinner [5]; supporting evidence for this thiolactone was provided by t.l.c. results which showed the same R_F values are those obtained by Bundgaard [4]. A small peak appeared at —0.96 V after about 140 h indicating the formation of some 2-hydroxy-3-phenyl-6-methylpyrazine. In Fig. 2b, the heights of the peaks at —0.9 V and —1.26 V are compared throughout the degradation. The first-order rate constant for the degradation of II based on the height of its polarographic peak changes abruptly after 80 h from 0.021 h^{-1} to 0.012 h^{-1}. These values may be compared with the slightly larger rate constant obtained when hydrogen sulphide was not removed (0.025 h^{-1}).

The effect of flushing with nitrogen on the degradation at 80°C was similar. Only three main peaks were observed (—0.9 V, —0.96 V and —1.26 V). Production and degradation of II was rapid (Fig. 3). Hydrogen sulphide production was rapid initially (25% recovery of total sulphur after 3 h), but then slowed down considerably.

The effect of raising the pH of the degradation solution slightly was marked. Results obtained for a 100-μg ml^{-1} cephalexin solution at pH 8.5

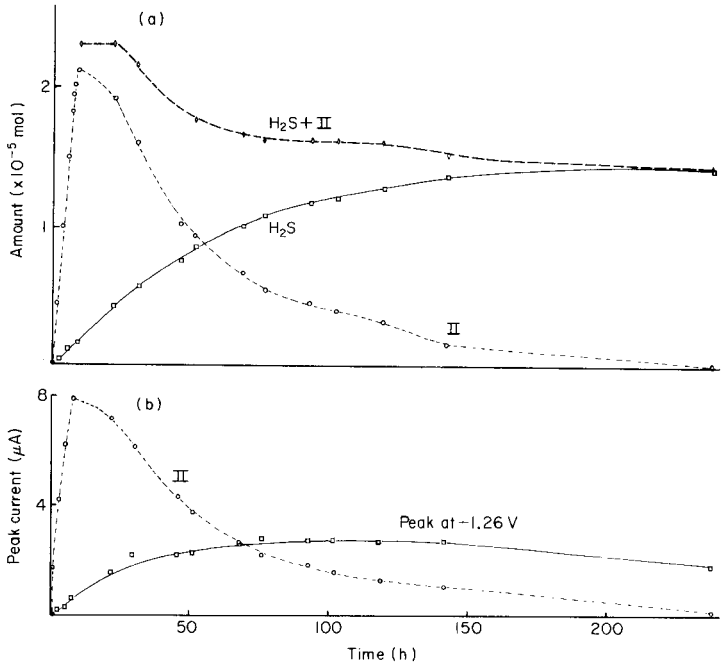

Fig. 2. Degradation of cephalexin in 0.5 M phosphate buffer (pH 7.4) at 37°C. Initial cephalexin concentration, 100 μg ml^{-1}. Initial amount of cephalexin, 2.73 × 10^{-5} mol. Hydrogen sulphide removed with nitrogen and determined with cadmium nitrate. (a) Amount of sulphur compounds formed; (b) Comparison of peak currents.

(phosphate buffer) and 80°C are shown in Fig. 4. A high proportion of the total sulphur (56%) was eliminated as hydrogen sulphide within 6 h. Another significant change in the degradation pattern was the large increase in the yield of 2-hydroxy-3-phenyl-6-methylpyrazine. A small new peak (at −1.08 V) appeared early in the degradation but the compound responsible had degraded completely after 21 h.

The hydrogen sulphide was more difficult to purge when the degradation was carried out at pH 10 in borate or phosphate buffer. After 45 min at 80°C, large peaks appeared at −1.08 V (in phosphate or borate), −1.26 V (in phosphate only) and −1.33 V (in borate only), in addition to small peaks at −0.56 V (sulphide), −0.62 V and −0.96 V (2-hydroxy-3-phenyl-6-methylpyrazine). With increased heating time the peak at −1.08 V became smaller, whereas those at −0.62 V, −0.96 V, −1.26 V and −1.33 V increased. The amount of the total sulphur evolved as hydrogen sulphide within the first 5 h was 10%, although some sulphide remained in the solution.

Degradation was also studied in distilled water without buffering. The pH of the 100 μg ml^{-1} cephalexin solution was 5.7. Hydrogen sulphide was obtained in relatively low yield at 80°C (about 24% of the total sulphur after

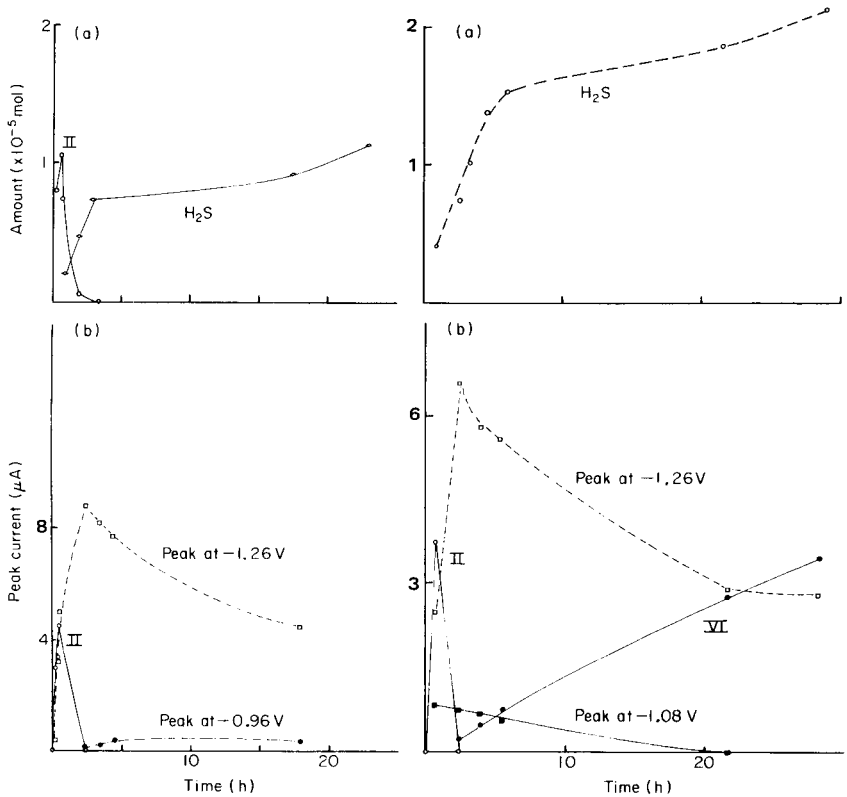

Fig. 3. Degradation of cephalexin in 0.5 M phosphate buffer (pH 7.4) at 80°C. Initial cephalexin concentration, 100 μg ml^{-1}. Initial amount of cephalexin, 2.73 × 10^{-5} mol. Hydrogen sulphide removed with nitrogen and determined with cadmium nitrate. (a) Amount of sulphur compounds formed; (b) comparison of peak currents.

Fig. 4. Degradation of cephalexin in 0.5 M phosphate buffer (pH 8.5) at 80°C. Initial cephalexin concentration, 100 μg ml^{-1}. Initial amount of cephalexin, 2.73 × 10^{-5} mol. Hydrogen sulphide removed with nitrogen and determined with cadmium nitrate. (a) Amount of sulphur compounds formed; (b) comparison of peak currents.

30 h). In addition to the peak at −0.9 V (compound II), peaks at −0.36 V, −0.98 V, −1.08 V and −1.44 V observed under other conditions were again observed. The compounds responsible for the peaks at −0.36 V and −1.08 V degraded, and the compounds responsible for the peaks at −0.36 V and −1.44 V were major products in degradations at high concentrations (10 mg ml^{-1}).

Degradation at 80°C in buffered solution at pH 3 showed a similar pattern to that in unbuffered solution at pH 5.7, but the rate of degradation was slower. The yields of II and hydrogen sulphide after 4 h were only 8% and 5%, respectively.

An attempt was made to prepare a sample of the compound responsible for the peak at −1.26 V by degrading a concentrated cephalexin solution in buffer pH 7.4 at 80°C for 6 h whilst flushing with nitrogen. After filtering off and weighing the grey-white precipitate that formed, however, the resulting solution showed polarographic peaks at −0.36 V (0.25 μA), −0.56 V (0.20 μA), −0.96 V (0.70 μA) and −1.26 V (2.6 μA). From 1 g of cephalexin (2.7×10^{-3} mol), the yield of the grey-white precipitate (IV) was 57%, and of hydrogen sulphide 58%. The precipitation of IV would prevent the formation of high concentrations of later degradation products. Polarographic peaks were not observed for IV or V (the latter compound should form from IV by degradation at pH 3 [5]); this could be due to the extremely low solubility of IV.

Cephradine, which has a very similar structure to cephalexin, was shown to give hydrogen sulphide on degradation, but no hydrogen sulphide was observed during the degradation of cephaloridine and cephalothin at pH 2.

DISCUSSION

The occurrence of d.p.p. peaks in this study is summarized in Table 1. Three peaks were identified: those of hydrogen sulphide, the diketopiperazine derivative (II) and 2-hydroxy-3-phenyl-6-methylpyrazine (VI). In an attempt to identify hydrogen sulphide positively, a mass spectrum was taken on a sample of the gas evolved. The m/z peak at 34 (H_2S) was present but the highest peak was at 74. That no mercaptan was present, however, was shown by the analytical results. Mercaptans do not react with cadmium nitrate solutions and that method determines only hydrogen sulphide. The initial potential of the 1 M sodium hydroxide solution after trapping the gas evolved from cephalexin and before adding the silver(I) was −800 mV which is consistent with the gas being hydrogen sulphide. Any mercaptan present would have given a second end-point at about −500 mV and this was not observed. There appears to be no previous reference to hydrogen sulphide being evolved during the degradation of cephalexin, although Abraham and Newton [10] postulated its formation in the degradation of cephalosporin C.

The peaks at −0.9 V and −0.96 V can be used to determine the amounts of the diketopiperazine derivative (II) and 2-hydroxy-3-phenyl-6-methylpyrazine in samples of cephalexin and in its solutions. Further work is in progress to identify the compounds which give the other peaks. The participation of dissolved oxygen in the degradation process has been demonstrated. In a similar study, Butler et al. [11] reported that different degradation products are produced in the presence and absence of molecular oxygen in the degradation of solutions of benzylpenicillin in tetramethylammonium phosphate buffer.

The present study illustrates the advantages of differential pulse polarography as a complementary technique for following degradation processes. The changes in concentration of several products can be followed concurrently. In this respect it is similar to h.p.l.c. but in the case of h.p.l.c.

TABLE 1

Differential pulse polarographic peaks (pH 7.4) appearing during the degradation of cephalexin

Peak potential (V)	Remarks about compound responsible
−0.16	Formed in low yield at 37°C and in relatively higher yield at 80°C in pH 7.4 buffer; oxidation product, not formed in absence of oxygen.
−0.22	Relatively minor product formed late in the degradation at high cephalexin level.
−0.36	Major product formed early in distilled water at 80°C (pH 5.7). Formed also in high yield at high cephalexin concentration in distilled water at 75°C.
−0.56	Hydrogen sulphide.
−0.78	Oxidation product, not formed in absence of oxygen.
−0.84	As for peak at −0.22 V.
−0.90	Diketopiperazine derivative (II): first major degradation product formed.
−0.96	2-Hydroxy-3-phenyl-6-methylpyrazine (VI). Forms late in degradation usually but good yields obtained fairly early at pH 8.5.
−1.08	High yield at pH 10 (80°C): degrades later.
−1.26	High yield at 80°C (pH 7.4 and 8.5).
−1.33	Associated with appearance of peak at −1.08 V in borate buffer only at pH 10: seems to appear when peak at −1.26 V is absent.
−1.44	High yield at 80°C (pH 7.4), also at high cephalexin concentration (37°C) as the −1.26 V peak is absent, and in unbuffered solution (pH 5.7).

there is the possibility of further hydrolysis and degradation during the separation.

REFERENCES

1 T. Yamana, A. Tsuji, K. Kanayama and O. Nakano, J. Antibiot., 27 (1974) 1000.
2 T. Yamana and A. Tsuji, J. Pharm. Sci., 65 (1976) 1563.
3 H. Bundgaard, Arch. Pharm. Chem. Sci. Ed., 4 (1976) 25.
4 H. Bundgaard, Arch. Pharm. Chem. Sci. Ed., 5 (1977) 149.
5 A. Dinner, J. Med. Chem., 20 (1977) 963.
6 R. H. Barbhaiya, R. C. Brown, D. W. Payling and P. Turner, J. Pharm. Pharmacol, F., 30 (1978) 224.
7 D. W. Hughes, A. Vilim and W. L. Wilson, Can. J. Pharm. Sci., 11 (1976) 97.
8 P. R. Bontchev and P. Papazova, Pharmazie, 33 (1978) 346.
9 A. G. Fogg, N. M. Fayad, C. Burgess and A. McGlynn, Anal. Chim. Acta, 108 (1979) 205.
10 E. P. Abraham and G. G. F. Newton, Biochem. J., 79 (1961) 377.
11 T. C. Butler, K. H. Dudley and D. Johnson, J. Pharmacol. Exp. Ther., 181 (1972) 201.

Analytica Chimica Acta, 110 (1979) 117—122

DETERMINATION OF NITRATE IN SUSPENDED PARTICULATE MATTER BY HIGH-PERFORMANCE LIQUID CHROMATOGRAPHY WITH U.V. DETECTION

TOSHIKAZU KAMIURA* and MASANOBU TANAKA

Department of Environmental Medicine, Osaka City Institute of Public Health and Environmental Sciences, 21, Tojo-cho, Tennoji-ku, Osaka 543 (Japan)

(Received 21st March 1979)

SUMMARY

For the determination of nitrate in suspended particulate matter (s.p.m.), high-performance liquid chromatography (h.p.l.c.) with a u.v. detector at 210 mm gives precise and accurate results. Chloride, bromate, iodide, nitrite, thiocyanate and various cations do not interfere. Calibration graphs are linear over the range 0—20 ppm of nitrate-nitrogen, and the limit of detection is 0.25 ng of nitrate-nitrogen. The coefficients of variation at 5.0- and 10.0-ppm levels are 3.4 and 2.9%, respectively. Results obtained by the h.p.l.c. method and by two 2,4-xylenol spectrophotometric methods for aqueous extracts of s.p.m. are compared. Agreement is generally good, particularly when choride is removed in the 2,4-xylenol method, but the spectrophotometric methods are much more prone to interference.

Nitrate in suspended particulate matter (s.p.m.) is assumed to be one product from photochemical reactions involving nitrogen oxides emitted from automobiles and other sources, and is also one of the important indicators used to estimate the degree of air pollution. Previous studies [1—4] have indicated that the chemical components of s.p.m. are complex and interfere in the 2,4-xylenol method used widely for the determination of nitrate.

Norwitz et al. [5, 6] have shown that the existing spectrophotometric methods for nitrate are not entirely satisfactory in the presence of strong interferences and have suggested methods for eliminating most of the inorganic interferences in the 2,4-xylenol spectrophotometric method. Although the improved 2,4-xylenol method can be applied to the determination of nitrate in s.p.m., it is time-consuming and the problem of the interaction between chlorides and some organic compounds in strong sulfuric acid remains.

Ultraviolet absorption methods have been used to determine nitrate in low-salinity soil solutions, water, and alkaline earth carbonates [7—10]. Recently a method involving the absorption by nitrate ion at or near 210 nm has been reported [7]. Although this method offered a sensitive, precise, and extremely rapid procedure, it is affected by other elements in the matrices.

This paper reports the application of the u.v. method to the determination of nitrate in s.p.m. by high-performance liquid chromatography (h.p.l.c.). The results obtained are compared with those from two 2,4-xylenol methods.

EXPERIMENTAL

Apparatus and reagent

A Shimadzu-Dupont LC-1 chromatograph (1.5-m Permaphase AAX column) with a u.v. detector was used to separate nitrate from the matrix in aqueous extracts of s.p.m. The u.v. detector was operated at 210 nm. A solution containing 4.5 ppm of copper(II) ion was used as the mobile phase. Air pressures of 80, 100, and 120 kg cm^{-2} were used as shown in the results section. The column temperature was 25°C.

The 2,4-xylenol spectrophotometric measurements were made with a Shimadzu double-beam spectrophotometer model UV-210.

All chemicals were of analytical-reagent grade.

Nitrate solutions. For the stock solution (1000 ppm nitrate-nitrogen), 7.2200 g of potassium nitrate was dissolved in 1 l of water. Working standards were prepared by suitable dilution immediately before use.

Procedures

The suspended particulate matter (collected on a glass fibre filter during a 24-h period with a high-volume air sampler) was extracted with hot water. After the aqueous extract had cooled, it was filtered through Toyo filter paper No. 5C.

H.p.l.c. method. A 5- or 10-μl aliquot was injected directly into the h.p.l.c. column by microsyringe without pretreatment. Peak heights were related to those of known amounts of nitrate.

2,4-Xylenol method A. Pipet 10-ml aliquots into 100-ml beakers, cover with a watch glass, cool in cracked ice and add 17.0 ml of sulfuric acid very slowly. Adjust the solutions to room temperature. Add 1.0 ml of 2,4-xylenol solution (2.5% w/v in acetone), swirl to mix thoroughly, and allow to stand for 10 min. Steam-distil into a mixture of 20 ml of water, 35 ml of propan-2-ol, and 5 ml of (0.88) ammonia liquor until the volume of liquid in the 100-ml volumetric flask is ca. 95 ml. Dilute the solutions to the mark and mix. Measure the absorbance at 455 nm against a reagent blank.

2,4-Xylenol method B. Transfer 25 ml of filtered sample solution to a 100-ml beaker. Add 5 ml of dilute sulfuric acid (5%) and heat almost to boiling. Add sufficient aqueous silver sulfate solution (0.44% w/v), while stirring, to precipitate the halide and provide a moderate excess of silver(I). Proceed as described for method A.

RESULTS AND DISCUSSION

Separation and determination of a mixture of nitrite and nitrate

Both nitrite and nitrate have significant u.v. absorptions at 210 nm and

their determination is possible after separation. Mixtures of nitrite and nitrate were first separated by employing a solution containing a trace of copper sulfate. Figure 1 shows a typical separation, which is probably due to the difference in the affinity of these anions for copper(II) and is affected by the pH and ionic strength of the mobile phase, column temperature, etc. When the pH of the mobile phase containing a trace of copper sulfate was adjusted to pH 3.3. with sulfuric acid, the separation was more satisfactory, with shorter retention times. However, the Permaphase AAX column can only be used between pH 3 and pH 8; because of the desirability of employing the column for a long time, a dilute solution containing a trace of copper sulfate was selected as the mobile phase.

Effect of other elements

Many anions and cations give significant u.v. absorption in the same region as that of nitrate [9—11]. The separation of nitrate from matrices containing other ions is therefore necessary for nitrate determinations. The elution profile obtained for a mixture of bromate, nitrite, bromide, and nitrate is shown in Fig. 2 and for a mixture of nitrite, nitrate, iodide and thiocyanate in Fig. 3. The concentrations of bromate, nitrite, bromide, iodide and thiocyanate in s.p.m. are usually less than that of nitrate except in the cases of unusual pollution, but direct application of the u.v. method to the determination of nitrate in s.p.m. would give unacceptable errors. In the h.p.l.c. method, anions giving u.v. absorption do not interfere in the determination of nitrate.

Chloride is a common component of s.p.m., normally at the same level as nitrate. In the methods, based on nitration reactions, e.g., the 2,4-xylenol

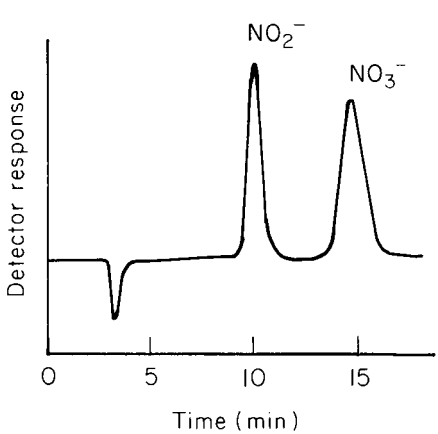

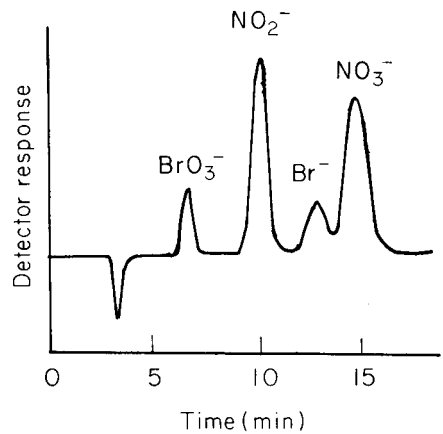

Fig. 1. Separation of a mixture of NO_2^- and NO_3^-. Amounts injected: 87 ng nitrite (NO_2^--N), 100 ng nitrate (NO_3^--N). Air pressure: 80 kg cm^{-2}.

Fig. 2. Chromatogram of a mixture of BrO_3^-, NO_2^-, Br^-, and NO_3^-. Amounts injected: 87 ng nitrite (NO_2^--N), 100 ng nitrate (NO_3^--N), 1023 ng bromate, 1000 ng bromide. Air pressure: 80 kg cm^{-2}.

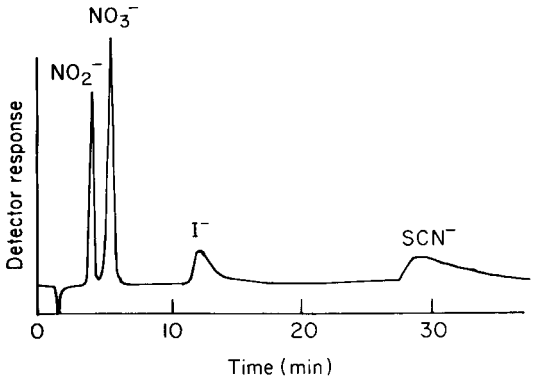

Fig. 3. Chromatogram of a mixture of NO_2^-, NO_3^-, I^-, and SCN^-. Amounts injected: 104 ng nitrite (NO_2^--N), 120 ng nitrate (NO_3^--N), 1200 ng iodide, 1200 ng thiocyanate. Temperature: 50°C. Air pressure: 120 kg cm^{-2}.

and the phenoldisulfonic acid methods, chloride causes serious losses of nitrate [5, 6, 12]. In contrast, chloride does not interfere in the determination of nitrate by the h.p.l.c. method as it has no u.v. absorption at or near 210 nm. This is one of the advantages of this method.

Elution data for some cations having significant absorption near 210 nm are shown in Table 1; ions such as Fe^{3+} and Cr^{6+} give a strong absorption [9—11], but the cations tested elute earlier than nitrate and therefore do not interfere in the determination of nitrate. Other cations were not tested.

Effect of organic compounds

The identification and determination of more than 100 organic compounds in s.p.m. has been reported [4]. Of these, polar oxygenated compounds and aromatic acids may possibly show slight interference in the determination of nitrate by the h.p.l.c. method, but they generally elute earlier than nitrate, and do not appear to interfere with the determination of nitrate and nitrite by the h.p.l.c. method.

TABLE 1

Elution data for some cations

Cation	Added as	Peak max. elution time (min)[a]
Fe^{3+}	$FeCl_3$	5.8
Cr^{6+}	$K_2Cr_2O_7$	6.0
Pb^{2+}	$Pb(CH_3CO_2)_2$	3.8
Cd^{2+}	$CdCl_2$	6.0

[a]Nitrite, ca. 10 min; nitrate, ca. 15 min.

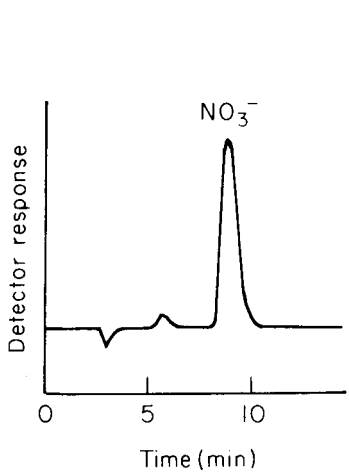

Fig. 4. Analysis of nitrate in aqueous extract of s.p.m. Air Pressure: 100 kg cm^{-2}.

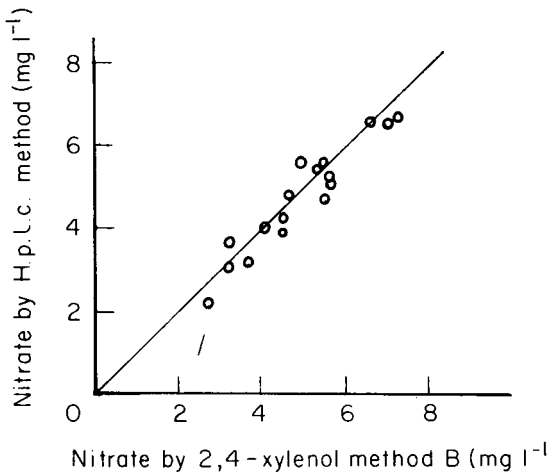

Fig. 5. Correlation between values for nitrate in aqueous extracts of s.p.m. measured in aqueous extracts of s.p.m. measured by 2,4-xylenol method B and the h.p.l.c. method.

Calibration curve for nitrate by the h.p.l.c. method

A linear relationship is obtained for 0—20 ppm of nitrate-nitrogen. The limit of detection is 0.25 ng of nitrate-nitrogen (the quantity required to give a response that is twice the noise level). Coefficients of variation ($n = 10$) of 3.4 and 2.9% were obtained for 5.0 and 10.0 ppm of nitrate-nitrogen, respectively.

Application to the determination of nitrate in s.p.m.

The proposed method was applied to determinations of nitrate in aqueous extracts of the s.p.m. collected on the filter. Figure 4 shows the chromatogram. The first small peak is due to the cations. As measurable amounts of bromide and nitrite are usually not present, the chromatographic conditions were changed, as shown in Fig. 4, to shorten the time of analysis.

As an over-all check on accuracy, results from the h.p.l.c. method and from the two 2,4-xylenol methods were compared for the same aqueous extracts (Table 2). Good agreement between the h.p.l.c. method and 2,4-xylenol method B was obtained (Fig. 5). These results confirm that chloride ion is an important negative interferent in the 2,4-xylenol method.

For some aqueous extracts, satisfactory agreement could not be obtained; the nitrate values given by 2,4-xylenol method B were much lower than those obtained by the h.p.l.c. method. The concentrations of water-soluble halide, lead, and peroxide are insufficient to account for the negative interference [13]. There is one possible explanation for organic compounds giving negative interferences with 2,4-xylenol method B; toluene [14] gave a negative interference by forming nitrotoluene, which is not volatile in

TABLE 2

Determination of nitrate by different methods

Sample	Nitrate-nitrogen (mg l^{-1})		
	H.p.l.c. method	2,4-Xylenol method A	2,4-Xylenol method B
1	3.03	0.55	3.18
2	5.56	0.78	5.43
3	3.97	1.10	4.06
4	6.57	1.46	6.52
5	4.82	0.55	4.61
6	2.15	0.27	2.70
7	6.67	1.10	7.20
8	5.31	0.60	5.49
9	5.24	1.92	5.67
10	3.14	3.14	3.60

steam. In addition, methanol in the presence of chloride led to further reduction of the nitrate recovery in the 2,4-xylenol method; other unidentified organic materials in s.p.m. may also give negative interferences with the 2,4-xylenol method.

Conclusion

The proposed method gives precise and accurate results for the determination of nitrate in suspended particulate matter, with freedom from interferences. The method may be useful for studying reaction mechanisms in the collection of nitrogen dioxide by Saltzman reagents and aqueous triethanolamine solutions.

The authors are grateful to Mr T. Nakadoi, Mr M. Oka and Dr. H. Hase who have given assistance in various ways.

REFERENCES

1 G. M. Hidy, J. Air Pollut. Control Assoc., 25 (1975) 1106.
2 R. H. Hamerle and W. R. Pierson, Environ. Sci. Technol., 9 (1975) 1058.
3 R. G. Flocchini, T. A. Cahill, D. J. Shadoan, S. J. Lange, R. A. Eldred, P. J. Feeney, G. W. Wolfe, D. C. Simmeroth and J. K. Suder, Environ. Sci. Technol., 10 (1976) 76.
4 W. Cautrefls and K. Van Cauwenberghe, Atmos. Environ., 10 (1976) 447.
5 G. Norwitz and H. Gordon, Anal. Chim. Acta, 89 (1977) 177.
6 G. Norwitz and P. N. Keliher, Anal. Chim. Acta, 98 (1978) 323.
7 D. L. Miles and C. Espejo, Analyst, 102 (1977) 104.
8 P. A. Cawse, Analyst, 92 (1967) 311.
9 F. A. J. Armstrong, Anal. Chem., 35 (1963) 1214.
10 R. Bastian, R. Weberling and F. Palilla, Anal. Chem., 29 (1957) 1795.
11 R. Bastian, R. Weberling and F. Palilla, Anal. Chem., 28 (1956) 459.
12 M. J. Taras, Anal. Chem., 22 (1950) 1020.
13 B. R. Appel, E. M. Hoffer, E. L. Kothny and S. M. Wall, Environ. Sci. Technol., 11 (1977) 189.
14 D. G. Lewis, Anal. Chem., 33 (1961) 1127.

Analytica Chimica Acta, 110 (1979) 123—128

SIMULTANEOUS SPECTROPHOTOMETRIC DETERMINATION OF NITRITE AND NITRATE BY FLOW INJECTION ANALYSIS

LEIF ANDERSON

Department of Analytical Chemistry, Chalmers University of Technology and University of Gothenburg, S-412 96 Göteborg (Sweden)

(Received 27th February 1979)

SUMMARY

The flow injection principle is used in the photometric determination of nitrite and nitrate with sulfanilamide and *N*-(1-naphthyl)ethylenediamine as reagents. An on-line copper-coated cadmium reductor reduces nitrate to nitrite. The detection limit is 0.05 μM for nitrite and 0.1 μM for nitrate at a total sample volume of 200 μl. Up to 30 samples can be analyzed per hour with a relative precision of ca. 1%.

Two of the most frequently required determinations in environmental investigations are those of nitrite and nitrate. Numerous analytical methods, all based on reduction of nitrate to nitrite with subsequent colorimetric determination of the nitrite formed, have been presented [1—8]. Many of these methods have been adapted to automatic air-segmented continuous flow systems, e.g. the Technicon AutoAnalyzer system. Several reducing agents, such as zinc [2], cadmium [3], amalgamated [4, 5] or copperized cadmium [6, 7], have been investigated. Reductor columns are, however, difficult to operate in an air-segmented stream. This problem can be avoided by using the continuous flow injection technique developed by Růžička and Hansen [9, 10].

The flow injection technique is based on three main principles: sample injection, reproducible timing and controlled dispersion [10]. The dispersion can be described as limited, medium or large; in a colorimetric system based on a reaction between the sample and a suitable reagent, a medium dispersion is preferred. Thus in the flow injection determination of nitrate, the reductor column should not excessively increase the dispersion. In a copperized cadmium reductor, more than 90% of the total nitrate is reduced within 1—2 s with minimum risk of further reduction of nitrite [13]. Consequently, the reductor can be made very small which results in a minimal increase of dispersion. The Shinn method [11] for the determination of nitrite was chosen for this work because of its high sensitivity and relative freedom from interferences.

EXPERIMENTAL

Apparatus

A schematic diagram of the flow injection system is shown in Fig. 1. An Ismatec model MP13 peristaltic pump was used. Different flow rates were obtained by changing the pump tube diameters as indicated in the legend to Fig. 1. The injection port was a rotary valve similar in construction to those described previously [10, 12], the main difference being that the sample volume could be varied between 10 and 1000 μl simply by changing the length of the sample loop (see Fig. 2). A Glenco model 57V dual absorbance monitor, with cuvette volumes of 25 μl (light paths, 10 mm) was used as detector, and was connected to a Kipp and Zonen BD41 dual-channel recorder.

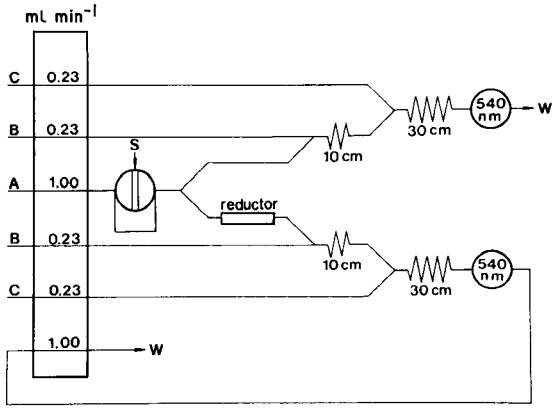

Fig. 1. Flow diagram for the colorimetric determination of nitrite and nitrate. The internal diameter of the tygon tubing was 0.64 mm for the 0.23 ml min^{-1} flow rates and 1.30 mm for the 1.00 ml min^{-1} flow rates; all other tubing was of 0.7 mm i.d. The reagents were: (A) carrier stream; (B) sulfanilamide solution and (C) diamine solution. S denotes the point of injection and W waste.

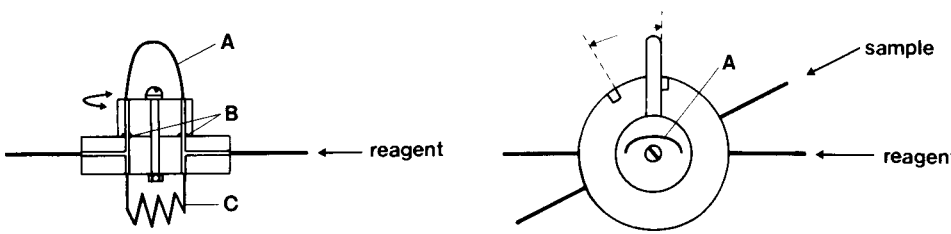

Fig. 2. Rotary-valve injection port. (A) Sample loop; (B) O-rings; (C) by-pass of higher hydrodynamic flow resistance than the sample loop (100 cm length and 0.5 mm i.d.).

Reagents

All reagents were of analytical-reagent grade. The cadmium granules (particle diameter <0.3 mm) were coated batch-wise with copper in a 1% (w/v) copper sulphate solution. The reductor tube (60 mm long with an inner diameter of 1 mm) was filled with copperized cadmium held in position with glass wool plugs. The copperized cadmium stock was stored under deaerated water.

The reaction medium (carrier stream) contained 0.4 M ammonium chloride and 0.3 M sodium chloride. The sulfanilamide reagent was prepared by dissolving 2.5 g of sulfanilamide and 13 ml of concentrated hydrochloric acid in 250 ml of the reaction medium. The diamine solution was prepared by dissolving 0.25 g of *N*-(1-naphthyl)ethylenediamine dihydrochloride and 10 g of sodium chloride in 250 ml of the reaction medium. The standard stock solutions of sodium nitrite and sodium nitrate were 0.001 M in 0.7 M sodium chloride. Working standard solutions were obtained by diluting with 0.7 M sodium chloride.

Procedure

The standards and samples were sucked into the sample loop of the injection valve by means of the peristaltic pump (see Fig. 2). After an injection, the valve was not returned to the reload position until the maximum absorbance value (540 nm) for the previous sample had been reached, because sample loading creates pressure variations which slightly affect the baseline.

The concentrations of nitrite and nitrate were evaluated from the peak heights by using calibration curves prepared from standards (see Fig. 3).

RESULTS

Optimum experimental conditions

Peaks obtained by injecting different sample volumes of a 1 μM nitrite standard are shown in Fig. 4. The optimum sample volume is of the order of 100 μl. Peak broadening is due to mixing in the manifold.

The coil lengths were optimized to give ample reaction times and minimum dispersion. Optimal conditions were obtained with coil lengths of 100 and 300 mm, respectively, at the flow rates chosen for the reagents (Fig. 1). The short reductor column produced only negligible dispersion with minimum loss in efficiency and reproducibility. The lifetime of the reductor column naturally depends on the amount of oxidizing material which passes through it; in continuous analysis, the lifetime was found to be not less than 8 h. Reactivation of the column in situ is not satisfactory. The column should therefore be repacked and replaced in the system on a daily basis.

Precision, detection limit and rate of analysis

Twenty consecutive analyses were made of a sample having nitrite and

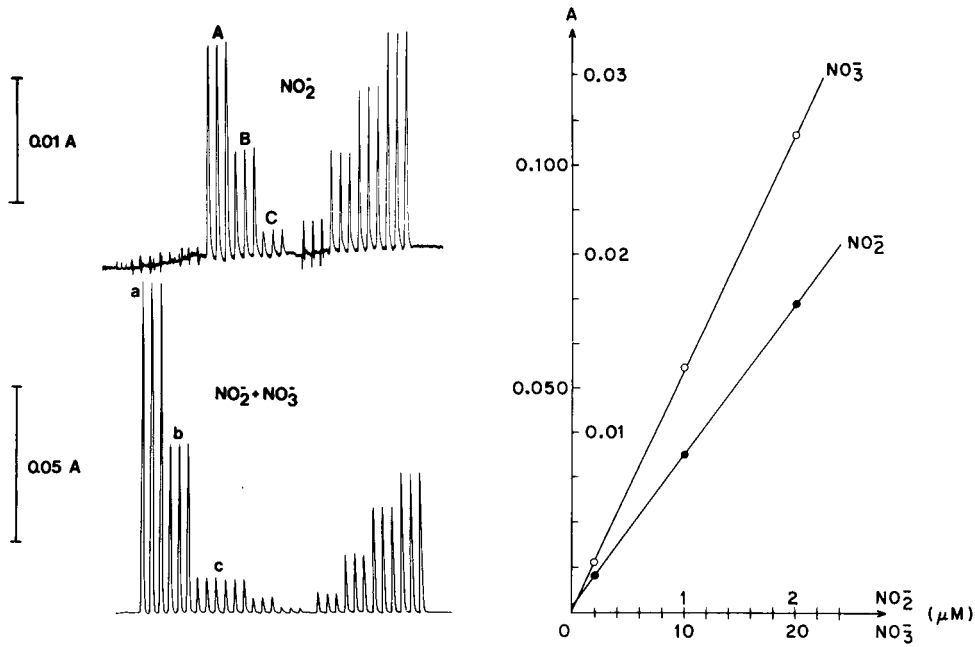

Fig. 3. Determination of nitrite and nitrate at a rate of 30 samples per h. For the outputs shown on the left, the concentrations of nitrite are 2, 1, 0.2 μM for A, B, C, and those of nitrate are 20, 10, 2 μM for a, b, c, respectively. The calibration curves prepared from these data are shown on the right.

nitrate concentrations of 0.4 and 4.0 μM, respectively. The relative standard deviations were better than 1% in both cases.

The spectrophotometric signal is due not only to the absorbance but also to the refraction of the sample. Refraction is of no practical importance at absorbance values above 0.05. The detection limit is determined by the difference in refraction between the reagent stream and the sample. Thus, in order to achieve low detection limits — 0.05 μM for nitrite and 0.1 μM for nitrate — it was necessary to adjust the refractive index of the reagents to a value as close as possible to those of the samples. For sea-water analysis, this was achieved by adding sodium chloride to the reagents. This also improved the reproducibility of dispersion because density differences were found to cause turbulence.

With a sample volume of 200 μl (100 μl for nitrite and 100 μl for nitrate), 30 samples could be analyzed per hour (Fig. 3).

Interferences

In the analysis of sea water, the only significant interference arises from turbidity caused by particles in the sample. Prior filtration of the sample is therefore necessary. For anoxic waters, however, sulfide concentrations over

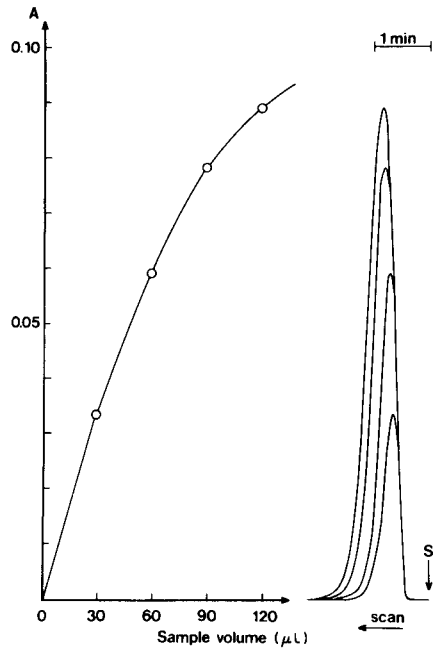

Fig. 4. Response curves obtained by injecting different sample volumes of a 1 μM nitrite standard.

2 μM were found to decrease the absorbance. This was overcome by adding an excess of either Cd^{2+} or Hg^{2+} to the sample [15].

DISCUSSION

The results reported above show that the dispersion pattern of a flow injection system is not significantly affected by a small reductor column (see Fig. 3). Consequently, the flow injection principle is suitable for the simultaneous determination of nitrite and nitrate in samples such as sea, tap or waste water. The optimum concentration range is 1—25 μM for each of these ions. These concentration ranges lie within the probable ranges for any sort of pulluted waters, although the lowest values reported fall near the detection limits of the flow injection method. Higher concentrations can be determined by decreasing the sample volume or by dilution.

The author is indebted to Professor David Dyrssen, Dr. Daniel Jagner and Dr. Anders Granéli for general discussions.

REFERENCES

1 J. B. Mullin and J. P. Riley, Anal. Chim. Acta, 12 (1955) 464.
2 T. J. Chow and M. S. Johnstone, Anal. Chim. Acta, 27 (1962) 441.

3 M. Bernard and G. Macchi, Automation in Analytical Chemistry, Technicon Symposia, 1965, Mediad, N.Y. 1966, 252.
4 A. W. Morris and J. P. Riley, Anal. Chim. Acta, 29 (1963) 272.
5 K. Grasshoff, Kieler Meeresforsch., 20 (1964) 5.
6 E. D. Wood, F. A. Armstrong and F. A. Richards, J. Mar. Biol. Ass. U.K., 47 (1967) 23.
7 A. Henriksen and A. R. Selmer-Olsen, Analyst, 95 (1970) 514.
8 F. A. J. Armstrong, C. R. Stearus and J. D. H. Strickland, Deep-Sea Res., 14 (1967) 381.
9 J. Růžička and E. H. Hansen, Anal. Chim. Acta, 78 (1975) 145.
10 J. Růžička and E. H. Hansen, Anal. Chim. Acta, 99 (1978) 37.
11 M. B. Shinn, Ind. Eng. Chem., Anal. Ed., 13 (1941) 33.
12 E. H. Hansen and J. Růžička, Anal. Chim. Acta, 87 (1976) 353.
13 F. Nydahe, Talanta, 23 (1976) 349.
14 J. D. H. Strickland and T. R. Parsons, A Practical Handbook of Seawater Analysis, Fisheries Research Board of Canada, Bulletin 167, 1968.
15 A. Timmer and T. Hoor, Mar. Chem., 2 (1974) 149.

Analytica Chimica Acta, 110 (1979) 129—137

HIGH-VOLUME SAMPLING OF AIRBORNE POLYCHLOROBIPHENYLS WITH AMBERLITE XAD-2 RESIN

PAUL V. DOSKEY and ANDERS W. ANDREN*

Water Chemistry Program, University of Wisconsin, Madison, Wisconsin 53706 (U.S.A.)

(Received 26th April 1979)

SUMMARY

Polyurethane foam, polyurethane foam coated with DC-200, Florisil, and Amberlite XAD-2 resin have been evaluated in a small-scale comparative study of their ability to sample airborne polychlorobiphenyls. XAD-2 resin has an excellent collection efficiency for tetrachlorobiphenyl at 1 l min^{-1} flow rates and is also suitable for high-volume air sampling. A high-volume air sampler was modified to sample both particulate and vapor-phase polychlorobiphenyls by incorporating the XAD-2 resin behind a glass fiber filter. When the sampling system was operated at a flow rate of 0.7 m^3 min^{-1} for 24 h, the collection efficiencies for tetrachlorobiphenyl and Aroclor 1221 were 96.5% and 83.0%, respectively.

Polychlorobiphenyls (PCBs) have been discovered in the North Atlantic atmosphere [1—3] and in Antarctic snow samples [4]. These findings suggest that the atmosphere is a major transport route. Murphy and Rzeszutko [5] found that precipitation is at present the major source of PCBs to Lake Michigan. These discoveries indicate the necessity to collect and quantify airborne PCBs. However, at present no collection method is uniformly accepted.

Polyurethane foam, which has been used extensively for high-volume sampling of airborne PCBs [2, 3], has been submitted to rigorous collection efficiency tests [6, 7]; collection efficiencies range from ca. 75 to 100% for different PCB isomers and mixtures. Murphy and Rzeszutko [5] reported a collection efficiency of 88% for polyurethane foam coated with DC-200 silicone oil. Giam et al. [8] used Florisil to sample laboratory air and reported a collection efficiency of 100%.

The number of methods available and the range of collection efficiencies reported make it necessary for a quantitative sampling methodology, which could easily be applied and which would simplify the intercomparison of data, to be found. This paper presents results from a comparison and evaluation of different collection methods for airborne PCBs.

A small-scale comparative study was initiated to evaluate the retention and collection efficiencies of polyurethane foam, polyurethane foam coated with DC-200, Florisil, and XAD-2 resin, a porous styrene—divinylbenzene copolymer, which has not been used to sample PCBs in air but has been

applied to collect chlorinated hydrocarbons and PCBs from water [9, 10].

The criteria which a collection method for atmospheric PCBs must meet are: the sampler must have a high collection efficiency for all PCB isomers, even the most volatile species; as the concentrations in air are usually in the low ng m^{-3} range, a substantial flow rate through the collection medium is essential to avoid extremely long sampling periods; it must be relatively easy to recover PCBs from the collection medium as only a small quantity is collected and lengthy procedures would allow more opportunity for loss of sample; interfering substances from the blank medium must be few to minimize difficulties in the quantification and interpretation of gas chromatograms.

Rather than try to adapt a high-volume air sampler to accommodate each of the adsorbent materials, the collection and retention efficiencies were evaluated under similar experimental conditions on a small scale at flow rates orders of magnitude lower than those experienced during high-volume air sampling; the results indicated trends which were used to determine the methods best suited for high-volume air sampling. A high-volume air sampler adapted to accommodate the medium was subsequently tested to determine its PCB collection efficiency.

EXPERIMENTAL

In the small-scale experiments the PCB adsorbent materials were held within glass tubing (0.95 cm i.d.) by a glass wool plug. The columns also contained 1 g of sodium sulfate. The Florisil column contained 0.3 g of 100—200 mesh Florisil (3% H_2O, w/w). The Amberlite XAD-2 resin column consisted of 0.4 g of dry XAD-2 resin (20—50 mesh). The polyurethane column contained a plug (1.3 cm diam.) cut from 3.8-cm thick polyurethane foam. Polyurethane foam coated with a solution of 1% DC-200 in hexane was also used.

Glass wool, Na_2SO_4, XAD-2 resin, and Florisil were cleaned by Soxhlet extraction (24 h) with petroleum ether. The polyurethane foam was rinsed with distilled water and Soxhlet-extracted for 12 h with petroleum ether and 12 h with acetone, then air-dried. Sodium sulfate and Florisil were activated at 320°C for 24 h. XAD-2 resin was dried at 60°C for 24 h. All solvents were of pesticide quality or double-distilled in glass.

A small-scale sampling apparatus was developed to test each adsorbent. The prefilter consisted of a Millipore holder containing a glass fiber filter for particulate matter and two XAD-2 resin columns for organic vapors. Two (three in certain experiments) air sampling columns were connected to both a vacuum pump and the prefilter. Flow rates were determined by a tri-flat variable-area flowmeter (Fischer and Porter Co.). All experiments were performed in the laboratory.

In the comparative study, ^{14}C-labelled 2,5,2′,5′-tetrachlorobiphenyl (1 μCi/0.03 mg) was used as the spiking material. Three different small-scale

experiments were performed: (1) elution efficiencies were determined by directly spiking the adsorbent, letting the spike air-dry, then eluting with petroleum ether; (2) retention efficiencies were determined by directly spiking the adsorbent, letting the spike air-dry, then drawing air through the column; (3) collection efficiencies were determined by sampling PCB vapor then drawing air through the columns for various lengths of time.

The collection efficiency experiments consisted of vaporizing PCBs in the injection port of a gas chromatograph. The spike was injected into a glass "T" joint joined to both the prefilter and sampling columns. The injection port was heated to 200—210°C before injection of the spike.

^{14}C-labelled 2,5,2′,5′-tetrachlorobiphenyl (TCB) was eluted from the adsorbent materials by allowing petroleum ether to equilibrate with the column for 30 min after which time the eluate was collected in a graduated receiving vessel. The column was then eluted with additional petroleum ether. The eluate was made up to 5 ml and transferred to a scintillation vial containing 10 ml of scintillation cocktail which contained toluene as the solvent and PPO and dimethyl-POPOP as fluors. The final concentration of fluors in the 15-ml counting solution was 0.5% PPO and 0.03% dimethyl-POPOP. ^{14}C was determined by the method of quench correction [11].

After completing the comparative study, a high-volume air sampler (GCA Precision Scientific, equipped with a Sierra model 310 flow controller) was modified to incorporate XAD-2 resin behind the filter holder assembly (Fig. 1). Particulates were sampled with a glass fiber filter (General Metal Works) and organic vapors with XAD-2 resin located in a screen-enclosed metal chamber (21-cm long). The chamber fits within a 30-cm long metal cylinder (9 cm i.d), threaded to accommodate both the filter holder assembly and the motor. The XAD-2 resin capsule fits tightly within the cylinder and is flanged at the top to prevent air flow around the chamber. The chamber parts are removable. The top and bottom are enclosed with 60-mesh screens to prevent the XAD-2 resin from entering the motor.

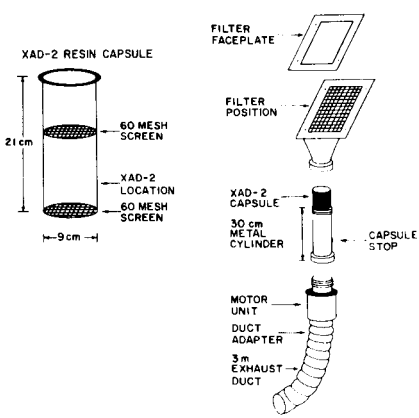

Fig. 1. Exploded view of high-volume PCB sampler and XAD-2 resin capsule.

The collection efficiency of the modified sampler was tested with a PCB vapor sampling technique. A g.c. injection port, into which a curved glass tube was inserted, was used to generate PCB vapor. The experimental procedure consisted of positioning the injection port above the filter, heating it to 200—210°C, and then injecting the spike into a 5 ml min^{-1} nitrogen carrier gas stream which subsequently flowed into the air stream of the sampler. After the sampling period had been completed, the tube, filter, and XAD-2 resin were analyzed for the PCB spike.

Retention and collection efficiency experiments were performed with TCB as the spiking material. Retention efficiency experiments consisted of spiking two 70-g portions of XAD-2 resin with TCB; one portion was placed in the sampler and the other was used as the analytical control. After the sampling period had been completed, the resin was Soxhlet-extracted for 24 h with 500 ml of petroleum ether. The extract was then concentrated (Kuderna—Danish concentrator) and prepared for scintillation counting. The collection efficiency experiments incorporated the vapor-generating device. Both retention and collection efficiency experiments were performed without a prefilter.

A second set of experiments tested the ability of the sampler to retain the most volatile PCB isomers. Aroclor 1221, which is composed predominantly of monochloro- and dichloro-biphenyl, was used as the spiking material. Two samplers were interconnected, one being used as a prefilter. A 70-g quantity of XAD-2 resin, spiked with Aroclor 1221, was placed in the second sampler. Each experiment included an analytical recovery control. In the analytical scheme, a 4-g alumina (6% H_2O, w/w) column (1 cm i.d.) was employed to remove interfering substances.

An experiment was also performed to obtain the collection efficiency of XAD-2 resin for Aroclor 1221 vapor. The vapor was generated in the g.c. injection port and subsequently collected by the XAD-2 resin. Air was sampled for a shortened period of 30 min to avoid collection of an excessive amount of interfering organic vapors. An air blank was subtracted from the actual sample.

Cleaning XAD-2 resin to obtain low blanks has been reported to be a problem [12]. For air sampling purposes, the XAD-2 resin is dried at 60°C for 24 h, Soxhlet-extracted with petroleum ether for 72 h (changing the solvent every 24 h), and dried overnight at 60°C. Quantities of clean resin (70 g) are stored in glass jars with foil-lined caps. Figure 2 presents chromatograms of an XAD-2 resin extract containing Aroclor 1242 before and after alumina cleanup which removes many of the early eluting resin contaminants from the extract.

After extraction of a collected air sample, the resin can be dried, stored, and reused. Some problems have been experienced with yellowing of the resin and permanent contamination upon collection of samples in heavily polluted areas. A more extensive cleanup of the resin, possibly with a polar solvent, may be necessary but has not been investigated.

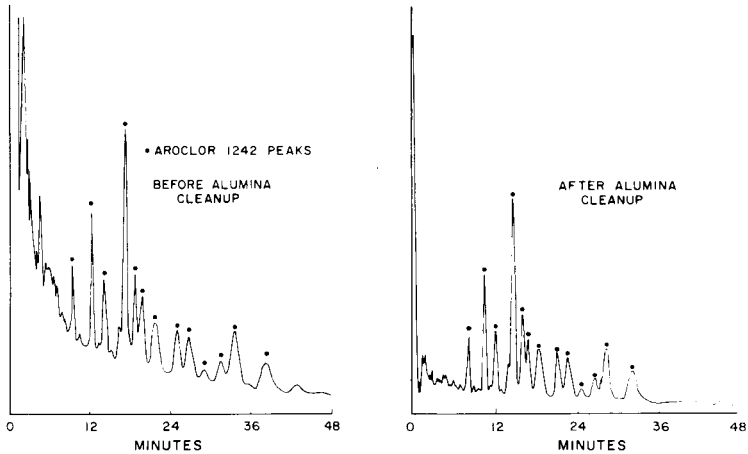

Fig. 2. XAD-2 resin extract containing Aroclor 1242 before and after alumina cleanup.

Analyses for carbon-14 were performed on a Packard model 3320 scintillation counter. Gas chromatographic analyses were performed on a Varian Aerograph Series 1700 chromatograph equipped with two scandium (^3H) foils. A 3.3-m column (2 mm i.d.) packed with 1.5% OV-17/1.95% QF-1 on 80—100 mesh GasChrom W(AW), and a 3.3-m column (2 mm i.d.) packed with 4% SE-30/6% OV-210 on 80—100 mesh GasChrom W(AW) were used for quantification. Nitrogen was used as the carrier gas at 12 ml min^{-1}. Aroclor 1221 was chromatographed isothermally at 165°C.

RESULTS AND DISCUSSION

The small-scale experiments were designed to compare the four adsorbent materials under similar experimental conditions. The retention and collection efficiencies were calculated by dividing the amount of TCB recovered from the first column by the total amount of TCB recovered. This method of calculation was considered to be necessary because of minor difficulties experienced in accurately reproducing the exact amount of PCB spike. XAD-2 resin, Florisil, polyurethane foam, and coated polyurethane foam had average retention efficiencies of 100%, 97%, 80% and 58%, respectively (Table 1). The collection efficiencies of XAD-2 resin, Florisil, and polyurethane foam were 99%, 100%, and 50%, respectively (Table 2); the collection efficiency of coated polyurethane foam was not determined because of its poor performance in the retention efficiency experiments.

Florisil and XAD-2 were efficient retainers and adsorbers of PCB, even in very small amounts. Difficulties were experienced with the mesh size of Florisil. The fine mesh adsorbent creates a large pressure drop across the column; this subsequently produces extremely low flow rates which make it difficult to include Florisil in a high-volume air sampling system in its present form.

TABLE 1

TCB retention efficiencies

Adsorbent	Flow rate (cm^3 min^{-1})	Volume of air sampled (m^3)	Recovery (%)[a]	1st column (ng)	2nd column (ng)	Retention efficiency (%
XAD-2	7000	10.1	100	301	0	100
	6200	8.6	77	223	0	100
	6400	8.8	72	215	0	100
			Av. 83 (92)[b]			Av. 100
Florisil	6000	8.0	91	272	0	100
	5600	7.4	94	282	0	100
	4200	11.3	94	272	0	97
	3800	18.5	104	300	12	96
	3400	16.5	90	255	15	94
			Av. 95 (99)			Av. 97
Polyurethane	7200	8.2	81	202	41	83
	7300	9.2	77	161	71	69
	7000	8.8	80	213	26	89
			Av. 79 (79)			Av. 80
Coated polyurethane	7300	9.2	84	182	70	72
	6500	8.9	71	96	116	45
	6800	9.3	81	140	103	58
			Av. 79 (79)			Av. 58

[a]TCB spike = 300 ng = 2.22×10^4 dpm.
[b]Average elution efficiencies from separate recovery experiment run in triplicate.

TABLE 2

TCB vapor collection efficiencies

Adsorbent	Flow rate (cm^3 min^{-1})	Volume of air sampled (m^3)	Recovery[a] (%)	1st column (ng)	2nd column (ng)	3rd column (ng)	Collectio efficienc (%)
XAD-2	8500	9.6	95	141	1	0	99
	5700	5.5	113	168	1	0	99
	9400	10.6	71	106	0	0	100
	8500	17.1	113	163	4	2	97
			Av. 98 (92)[b]				Av. 99
Florisil	4900	16.5	100 (99)	149	0	0	100
Polyurethane	15800	15.9	75 (79)	57	45	11	50

[a]TCB spike = 150 ng= 1.11×10^4 dpm.
[b]Average elution efficiencies from separate recovery experiment run in triplicate.

Based on the same criteria for all experiments, the retention efficiency of polyurethane foam was much lower than that of either XAD-2 resin or Florisil. As similar flow rates were used, differences in retention efficiencies from differences in flow rates were not a factor. The flow rate for the

polyurethane collection efficiency experiment was increased to ca. double that in the direct spiking experiment. The collection efficiency was reduced significantly. A rather small plug was used; the first plug in the sampling train may therefore have become saturated with PCBs. The actual depth of adsorbent (3.8 cm) was similar to the 5-cm plugs employed by Bidelman and Olney [2]. However, the volume of polyurethane used in this study (5.0 cm^3) was much less than the 393 cm^3 used by Bidelman and Olney [2] or the 181-cm^3 employed by Lewis et al. [7]. Using the first two plugs (total depth 7.6 cm) in the sampling train as a basis for the calculation resulted in a collection efficiency of 90%, which is in the same range as the collection efficiencies reported for polyurethane foam [2, 7].

The small-scale TCB experiments were used only as a preliminary test. Flow rates were in the 1 min^{-1} range and the amount of air sampled ranged from 7 to 19 m^3. The results cannot be used to indicate the performance characteristics of the adsorbent media under the m^3 min^{-1} flow rate conditions of high-volume air sampling. However, certain trends were evident. The TCB breakthrough for polyurethane was greater than that of XAD-2 resin or Florisil. This would seem to indicate that XAD-2 resin and Florisil are more efficient adsorbers. However, the use of a larger amount of polyurethane foam might produce greater collection efficiencies. The results indicated that XAD-2 resin had an excellent retention and collection efficiency for TCB. Its mesh size was also coarse enough, unlike Florisil, for incorporation into a high-volume air sampling system. Also unlike polyurethane, which must be cut into plugs from sheets of the material, XAD-2 resin can be used without further alteration.

The XAD-2 resin incorporated into the high-volume sampling system described in the experimental section was tested as discussed. The amount of XAD-2 resin used was determined from the small-scale experiments which indicated that a total depth of 2.8 cm of XAD-2 resin produced a sufficient collection efficiency. The thickness of the XAD-2 resin was the most important parameter. A depth of 2.8 cm in the capsule required 70 g of XAD-2 resin. The results from the TCB retention and collection efficiency experiments are presented in Table 3. In all experiments the tube and filter contained undetectable levels of the spike. Average recoveries of the sampling experiments (96.5%) were greater than those of analytical controls (93.4%) in all cases. Correcting the recoveries from the collection or retention efficiency experiments for analytical recovery would result in an efficiency of over 100%, and the retention or collection efficiencies were therefore reported as the analytical recoveries of the sampling experiments. Combining the results from the retention and collection efficiency experiments, the average efficiency for TCB was 96.5%. The resin retained both large (2283 ng) and small (218 ng) amounts of TCB; only a negligible amount was lost even after collection for 3 days.

In the Aroclor 1221 experiments (Table 4) the average recovery was 64.9% and recoveries for direct spikes on the resin with TCB and Aroclor

TABLE 3

TCB retention and collection efficiencies for PCB sampler

Sample[a]	ng/spike	Flow rate (m^3 min^{-1})	Volume of air sampled (m^3)	Analytical recovery (%)	Retention or collection efficiency (%)[b]
TCB DS1	257	0.7	1153	91.5	92.3
TCB DS2	257	0.7	1019		98.9
TCB DS3	242	0.7	3127		Av. 92.2
TCB VS6	218	0.7	719	94.2	101.2
TCB VS7	2283	0.7	1037	94.6	98.0
				Av. 93.4	Av. 96.5

[a]DS, direct spike applied to resin before putting it in air sampler. VS, spike was vaporized in g.c. injection port before collection.
[b]Recovery from collection efficiency experiment (not corrected for analytical recovery).

TABLE 4

Aroclor 1221 retention and collection efficiencies for PCB sampler

Sample[a]	ng/spike	Flow rate (m^3 min^{-1})	Volume of air sampled (m^3)	Analytical recovery (%)	Retention or collection efficiency (%)[b]
1221 DS1	4848	0.5	1344	60.3	75.6
1221 DS2	4848	0.5	1430	62.1	82.8
1221 DS3	4848	0.5	1492	72.3	90.6
				Av. 64.9	Av. 83.0
1221 VS1	4040	0.6	18	64.9	91.0

[a]DS, direct spike applied to resin before putting it in air sampler. VS, spike was vaporized in g.c. injection port before collection.
[b]Corrected for analytical recovery.

1242, with subsequent elution of the extract through alumina, were 85.5% and 80.1%, respectively. The low recoveries for Aroclor 1221 are probably a result of the high volatility of the mixture. For comparison with the TCB experiments, the retention efficiences were corrected for analytical recovery. The retention efficiency varied, the more volatile components being retained less efficiently. The monochloro- and dichloro-biphenyl components were collected with average efficiences of 72% and 86%, respectively. When three major peaks from Aroclor 1221 were employed for quantification, the average retention efficiency for the mixture was 83.0%.

In the Aroclor 1221 collection efficiency experiment (Table 4) the collection efficiencies for the mixture and and its monochloro- and dichloro-biphenyl components were 91%, 91% and 90%, respectively. Comparison

with the results of the direct spike experiments indicates that the resin initially collected Aroclor 1221 with a high efficiency. The components were stripped from the resin to a small extent during a 24-h sampling period, the amount retained being directly proportional to the volatility of the component. All of the present sampling techniques appear to underestimate the amount of mono- and dichloro-biphenyl in the atmosphere.

Conclusions

A modified PCB sampling technique with XAD-2 resin meets the criteria which a collection method for atmospheric PCBs must possess. The sampler has a high collection efficiency for TCB (96.5%) and a lower efficiency for Aroclor 1221 (83.0%). The low retention efficiencies for monochloro- (72%) and dichloro-biphenyl (86%) show that the system is not equally efficient for all PCB isomers. The maximum flow rate of the modified sampler (0.7 m^3 min^{-1}) makes extremely long sampling periods unnecessary. Recovery of PCBs from XAD-2 resin is relatively easy by Soxhlet extraction with subsequent elution of the concentrated petroleum ether extract through alumina. Analytical recoveries for TCB, Aroclor 1242, and Aroclor 1221 are 85.5%, 80.1% and 64.9%, respectively. For XAD-2 resin, blanks which are free of PCB-interfering substances can easily be obtained.

REFERENCES

1 G. E. Harvey and W. G. Steinhauer, Atmos. Environ., 8 (1974) 777.
2 T. F. Bidelman and C. E. Olney, Bull. Environ. Contam. Toxicol., 11 (1974) 444.
3 T. F. Bidelman and C. E. Olney, Science, 182 (1974) 516.
4 D. A. Peel, Nature, 254 (1975) 325.
5 T. J. Murphy and C. P. Rzeszutko, J. Great Lakes Res., 3 (1977) 305.
6 Environmental Science and Engineering, Inc., EPA-600/4-78-048 (1978), p. 103.
7 R. G. Lewis, A. R. Brown and M. D. Jackson, Anal. Chem., 49 (1977) 1671.
8 C. S. Giam, H. S. Chan and G. S. Neff, Anal. Chem., 47 (1975) 2320.
9 B. Ahling and S. Jensen, Anal. Chem., 42 (1970) 1485.
10 G. R. Harvey, W. G. Steinhauer and J. M. Teal, Science, 180 (1972) 643.
11 C. H. Wang, D. L. Willis and W. D. Loveland, Radiotracer Methodology in the Biological, Environmental, and Physical Sciences, Prentice-Hall, New York, (1975) 217.
12 C. A. Junk, J. J. Richard, M. D. Greiser, D. Witiak, J. L. Witiak, M. D. Arguello, R. Viek, H. J. Svec, J. S. Fritz and G. V. Valder, J. Chromatogr., 99 (1974) 752.

Analytica Chimica Acta, 110 (1979) 139—144

THE DETERMINATION OF SELENIUM(IV) BY THERMOMETRIC ENTHALPY TITRATION WITH THIOSULPHATE

J. K. GRIME*

Department of Chemistry, University of Denver, University Park, Denver, Colorado 80208 (U.S.A.)

A. D. CAMPBELL and A. H. YAHAYA

Department of Chemistry, University of Otago, P.O. Box 56, Dunedin (New Zealand)

(Received 20th April 1979)

SUMMARY

Selenium(IV) can be titrated in the range 0.2—6 mg with thiosulphate; relative standard deviations are 1.2—0.54%. Experimental conditions were manipulated to use the endothermic enthalpy of dilution and disproportionation of thiosulphate to advantage in improving end-point precision. Common anions do not interfere; interferences from copper(II), iron(III), lead(II) and mercury(II) can be minimized by masking.

There have only beerr two reports of an enthalpimetric approach to the determination of selenium(IV), both of which have limitations [1]. Dastoor and Haldar [2] reported a manual incremental thermometric enthalpy titration with potassium permanganate. The point-by-point enthalpograms, monitored by a Beckman thermometer, showed two breaks; the first occurred at an Se(IV):$KMnO_4$ ratio of 5:2, predicted by the relevant half-reactions, while the stoichiometry at the second (unexplained) break varied with the concentrations of selenium(IV) and permanganate used. By using the first break in the enthalpogram as the end-point, ca. 20 mg of selenium(IV) in a 30-cm^3 sample was determined with an accuracy better than 1%. Several interfering oxidizable species were removed by prior oxidation with potassium dichromate.

The determination of selenium(IV) by direct injection enthalpimetry has been reported with a 1 mol dm^{-3} solution of the sodium salt of quinoxaline-2,3-dithiol as reagent [3]. The precision is better than 0.6% for concentrations of selenium(IV) down to 2×10^{-3} mol dm^{-3}. The experimental conditions necessary to ensure precipitation of only the selenium—quinoxaline dithiol complex (and not the excess of dithiol reagent) resulted in a large exothermic contribution from the neutralization of the alkaline titrant by the acid present in the sample solution. Indeed, this temperature change represented 60—70% of the total temperature pulse. Interferences were reported from the partial precipitation of Cu(II) and Co(II) complexes; the soluble complexes of Ni(II) and Zn(II) did not interfere. Although the extraneous heat

effects can be corrected by blank injections, the measurement of a small analytical signal over a large "background" signal inevitably reduces the precision of such a method.

The volumetric titration of selenium(IV) with thiosulphate has been documented since 1886 [4] and a coulometric procedure has also been reported [5]. Selenium(IV) and thiosulphate react to form selenopentathionate and tetrathionate:

$$H_2SeO_3 + 4S_2O_3^{2-} + 4H_3O^+ \rightarrow Se(S_2O_3)_2^{2-} + S_4O_6^{2-} + 7H_2O$$

The reaction takes place rapidly and quantitatively [6] and although thiosulphate is known to catalyse the decomposition of selenopentathionate [7], this reaction cannot occur to any appreciable extent until the thiosulphate is in excess beyond the equivalence point.

The use of sodium thiosulphate as an enthalpimetric titrant has been limited by its endothermic heat of dilution, reported to be ca. 8.8 kJ mol^{-1} [8]. This effect is particularly important since heat capacity considerations demand a concentrated titrant in enthalpimetric techniques. The enthalpimetric determination of iodine with thiosulphate has however been reported with good precision [9, 10]. In the present report, the determination of submilligram amounts of selenium(IV) by thermometric enthalpy titration with sodium thiosulphate is discussed.

EXPERIMENTAL

Apparatus

Enthalpies were measured with a Tronac 450 calorimeter (Tronac, Inc., Orem, Utah). Details of slight modifications to the instrument have been discussed elsewhere [11]. Temperature changes, monitored as the imbalance potential of a d.c. Wheatstone bridge circuit, were amplified by a variable gain, null-detector microvoltmeter (Model 155, Keithley Instrument Co., Cleveland, Ohio) and recorded on a strip-chart potentiometer. Voltage measurements taken for caloric calibration of the titration enthalpograms were made with a Dana Instruments Model 3500 digital multimeter.

The 50-cm^3 quasi-adiabatic reaction cell (Tronac) used was immersed in a thermostatted water bath at 25.0°C (short-term stability ±0.0002°C). The titrant was added to the reaction cell from a 2-cm^3 micrometer syringe burette and the reactants were mixed by a glass paddle stirrer rotating at 60 rpm.

Reagents

All solutions were prepared from analytical-reagent grade chemicals unless otherwise stated. Deionized, distilled water was used throughout.

Selenium(IV) stock solution (0.0253 mol dm^{-3}) was prepared by dissolution of 1.999 g of elemental selenium (microanalytical-reagent grade) in the minimum amount of concentrated nitric acid with gentle heating and

subsequent dilution to exactly 1 dm^3 with water. More dilute solutions were prepared as required by dilution of the stock reagent. The purity of the selenium metal was confirmed by a permanganate—iron(II) back-titration method [12].

Sodium thiosulphate solutions, 0.983, 0.197 and 0.0944 mol dm^{-3}, were prepared by dissolution of the appropriate amount of sodium thiosulphate pentahydrate in water and standardization versus potassium iodate solutions prepared from Volucon concentrates.

Procedure

The micrometer syringe burette was filled with sodium thiosulphate solution of appropriate concentration and air bubbles were expelled. The solution was withdrawn from the tip of the delivery tubing leaving an air gap of ca. 20 cm, thus avoiding mixing of the reagents by capillary movement of the analytical solution up the delivery tube, prior to titration. An aliquot of selenium(IV) solution was introduced into the reaction cell followed by 2.0 cm^3 of a 10 mol dm^{-3} solution of hydrochloric acid. The total cell solution volume was then made up to ca. 30 cm^3 with water, and the cell and burette assemblies were immersed in the thermostatted water bath. Once thermal equilibrium had been obtained (as evidenced by an isothermal baseline), the burette motor was activated and the temperature change engendered by the reaction was monitored simultaneously as an imbalance potential on the strip-chart recorder. The titration was continued to a point corresponding to ca. 40% excess of thiosulphate. The instrumental parameters were as follows; titrant delivery rate (determined gravimetrically), 0.162 cm^3 min^{-1}, chart speed 4.0 cm min^{-1}, amplifier sensitivity ranges 0—300 μV, 0—3 and 0—10 mV as appropriate.

RESULTS AND DISCUSSION

Analytical results and precision data at three different concentrations of selenium(IV) (and thiosulphate) are shown in Table 1. Precision is good (1.2%) for titration of 0.2 mg of selenium(IV), but attempts to titrate 0.1 mg gave analytically unacceptable results (10% r.s.d.).

Shape of the enthalpogram

A typical enthalpogram is shown in Fig. 1. The experimental conditions were manipulated (see later) to maximize the gradient differential between the titration slope (AB) and the post-reaction slope (BC), resulting in an enhancement of the end-point (B) [13]. In practice, the end-point was located by the intersection of the extrapolated lines (AB) and (BC).

Observations made during the course of titrations suggest that the disproportionation of thiosulphate in acidic solution [14], to give sulphur dioxide and elemental sulphur, $HS_2O_3^- + H_3O^+ \rightleftharpoons SO_2(g) + 2H_2O + S(s)$, makes a significant contribution to the post-reaction slope. A blank titration of

TABLE 1

Titration of selenium(IV) with sodium thiosulphate

Se(IV) added (mg)	Range of Se(IV) found (mg)	No. of detns.	R.s.d. (%)	Voltage range (f.s.d.) (mV)
5.996[a]	5.97 —6.05	6	0.54	0—10
0.9994[b]	0.994—1.009	6	0.54	0—1
0.1999[c]	0.198—0.204	6	1.21	0—0.3

[a]3.00 cm^3 of 0.0253 mol dm^{-3} Se(IV) with 0.983 mol dm^{-3} thiosulphate. [b]5.00 cm^3 of 0.00253 mol dm^{-3} Se(IV) with 0.197 mol dm^{-3} thiosulphate. [c]1.00 cm^3 of 0.00253 mol dm^{-3} Se(IV) with 0.0944 mol dm^{-3} thiosulphate.

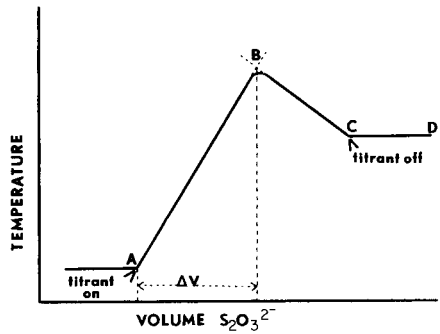

Fig. 1. Typical enthalpogram.

thiosulphate into the appropriate concentration of hydrochloric acid produced an identical endothermic gradient. The resultant solution exhibited considerable cloudiness, a phenomenon not observed in the titration of selenium(IV). Similar observations were made during a conventional volumetric titration; in this case, although the blank titrated solution became cloudy as before, yellow sulphur particles appeared in the titrated selenium(IV) solution. Apparently, the visual titration reaction products promote coagulation of colloidal sulphur particles.

The sharpness of the end-point depended on the concentration of acid and the titrant. The gradient of the post-reaction line (and therefore the end-point sharpness) was attenuated by reducing both these variables. This effect was particularly significant above pH 1.3 (i.e. less than 0.5 cm^3 of 10 mol dm^{-3} hydrochloric acid in the total reaction volume of 30 cm^3). Preliminary experiments showed that an acid concentration of 0.7 mol dm^{-3} in the cell (2.0 cm^3 of 10 mol dm^{-3} hydrochloric acid) gave a sharp end-point. Accordingly, this amount of acid was added in all subsequent determinations, except during the interference studies reported later.

Enthalpy of reaction

The complex thermal events occurring during (dilution of thiosulphate and acid) and after (disproportionation) the titration preclude an accurate assignment of the reaction enthalpy. An approximate figure of 173 kJ mol^{-1} (3.0% r.s.d.) was obtained by addition of the endothermic response obtained for a blank titration volume, to the selenium(IV)—thiosulphate enthalpogram. Joule heating calibration experiments were done before and after the titration and the results were weighted to determine the heat capacity at the end-point in the usual manner.

Clearly, the attendant (overall) endothermic heat effects associated with the addition of sodium thiosulphate to an acid solution represent only 5% of the total heat effect and do not significantly reduce the sensitivity of the analysis.

Interference studies

The effect of diverse ions was studied for the enthalpimetric titration of 0.999 mg of selenium(IV) with 0.197 mol dm^{-3} thiosulphate. The following ions, when present in an amount corresponding to at least 100 times the molar quantity of selenium(IV), caused no interference: SO_4^{2-}, PO_4^{3-}, NO_3^-, I^-, Ca(II), Mg(II), Ba(II), Zn(II) and Fe(II). Interference from iron(III) was minimized by increasing the hydrochloric acid concentration to 2 mol dm^{-3}. Positive interferences were given by Cu(II), Pb(II) and Hg(II) as shown in Table 2.

Interference from lead(II) was eliminated by masking with molybdate, but high concentrations of molybdate tended to obscure the end-point. Addition of high concentrations of chloride ion (NaCl) to the acid reaction mixture will also mask lead(II) interference. The results for molybdate masking are presented in Table 2. Mercury(II) interference was minimized by complexation with phosphorous acid prior to the inclusion of hydrochloric acid. Halogen complexation alone did not provide adequate masking. Copper(II)

TABLE 2

Effects of diverse ions on the determination of 0.999 mg of selenium by the recommended procedure

Ion added	Amount (mg)	Se(IV) found by normal procedure (mg)	Se(IV) found after masking[a] (mg)
Fe(III) as $FeCl_3$	35.5	1.14	1.00
Pb(II) as $Pb(NO_3)_2$	1.3	1.08	0.999
	2.6	1.15	0.999
Cu(II) as $CuCl_2$	4.0	1.10	0.993
	8.0	1.18	1.009
Hg(II) as $Hg(NO_3)_2$	2.5	1.52	1.004

[a]For masking agents, see text.

was effectively masked by the addition of CDTA (cyclohexanediaminetetraacetic acid) which apparently formed a very stable complex at pH 1; EDTA was ineffective at this pH.

In conclusion, the method reported represents a significant improvement on the existing enthalpimetric techniques for the determination of selenium (IV). The end-point enhancement provided by the use of sodium thiosulphate as a titrant gives analytical results with good precision down to a selenium(IV) concentration (in the cell) of 8.4×10^{-5} mol dm^{-3}.

REFERENCES

1 L. S. Bark, P. Bate and J. K. Grime, Selected Annual Reviews of the Analytical Sciences, 2 (1972) 143.
2 M. J. Dastoor and B. C. Haldar, Indian J. Chem., 5 (1967) 335.
3 A. E. Beezer and A. K. Slawinski, Talanta, 18 (1971) 837.
4 J. F. Norris and H. Fay, Am. Chem. J., 18 (1886) 703.
5 K. Rowley and E. H. Swift, Anal. Chem., 27 (1955) 818.
6 R. C. Brasted, in Comprehensive Inorganic Chemistry, Vol. 8, Van Nostrand, New York, 1961, p. 177.
7 M. Schmidt, W. Siebert and K. W. Bagnall, The Chemistry of Sulphur, Selenium, Tellurium and Polonium, Pergamon, Oxford, 1975, p. 281.
8 L. S. Bark and S. M. Bark, Thermometric Titrimetry, Pergamon, Oxford, 1969, p. 55.
9 P. T. Priestley, Analyst, 88 (1963) 194.
10 P. T. Priestley, W. S. Sebborn and R. F. W. Selman, Analyst, 88 (1963) 797.
11 J. K. Grime and K. R. Lockhart, Anal. Chim. Acta, 106 (1979) 251.
12 S. Barabas and W. C. Cooper, Anal. Chem., 28 (1956) 129.
13 G. A. Vaughan and J. J. Swithenbank, Analyst, 92 (1967) 364.
14 G. Charlot, Qualitative Inorganic Analysis, Methuen, London, 1954, p. 283.

Analytica Chimica Acta, 110 (1979) 145—151

APPLICATION OF TWO-DIMENSIONAL VARIANCE ANALYSIS FOR THE INVESTIGATION OF HOMOGENEITY OF SOLIDS

K. DANZER and G. MARX*

Technische Hochschule Karl-Marx-Stadt, Sektion Chemie und Werkstofftechnik, PSF 964, DDR-9010 Karl-Marx-Stadt (G.D.R.)

(Received 2nd January 1979)

SUMMARY

Homogeneity of solids can be examined by two-dimensional variance analysis. The particular advantages are that trends in inhomogeneity and concentration gradients can be detected, and that the total error and procedural error are obtained from the same experimental data. The distribution of boron in an iron surface is described as an example. The procedural error always contains an interaction (correlation) contribution which cannot be eliminated by general rules. This contribution is negligibly small for measuring concentration gradients but can be large for stochastical distributions. In the latter case, conventional stochastical selection of measuring points and simple variance analysis is preferred to two-dimensional variance analysis.

Solids are defined as being analytically homogeneous if fluctuations in the chemical composition determined in different areas of the sample are not significantly larger (in statistical terms) than the error of the analytical procedure [1]. Testing of homogeneity is based on the mathematical statement $x_i = \bar{x} + \alpha_i + \epsilon$, in which every measured value, x_i, comprises the sum of the mean, $\bar{x}$, the error contribution resulting from local fluctuations of the composition, α_i, and the error of the measurement, ϵ. In this model, the null hypothesis (for homogeneity) $H_0 : \alpha_i = 0$ corresponding to $H_0 : \sigma_t^2 = \sigma_p^2$ (where σ_t is the total error, and σ_p is the error of the analytical procedure) is compared to an alternative hypothesis (for inhomogeneity) $H_1 : \alpha_i > 0$ corresponding to $H_1 : \sigma_t^2 > \sigma_p^2$. The hypotheses are compared by the Fisher F-test, with a simple analysis of variances s_t^2 and s_p^2 [2].

Two prerequisites for the investigation of homogeneity must then be accomplished. Because of the statistical component distribution, the points of measurement on the sample have to be selected stochastically, and the error of the analytical method must be determined independently of the total error; in the case of destructive analytical methods, this is only possible by approximate methods.

The two-dimensional variance analysis should be tested above all with regard to the determination of the error of the analytical procedure independent of the total error. If the measurement areas are arranged in r rows

and c columns, the following improved mathematical model permitting simultaneous, independent evaluation of the total and procedural errors can be used [3]:

$$x_{ij} = \bar{\bar{x}} + \alpha_i + \beta_j + \gamma_{ij} + \epsilon \qquad (1)$$

According to this model, the measured value x_{ij} is composed of the total mean, $\bar{\bar{x}}$, a row deviation α_i, a column deviation β_j, the procedural error ϵ, and possibly an interaction contribution γ_{ij}.

The two-dimensional variance analysis is carried out according to the evaluation scheme in Table 1, where the measuring points are arranged in an $r \cdot c$ matrix. The computation of the different error contributions is given in Table 2.

Multiple dispersion decomposition allows the formulation of several F-tests to the testing of homogeneity within rows

$$\hat{F}_r = \bar{Q}_r / \bar{Q}_p = Q_r(c-1)/Q_p$$

and within columns

$$\hat{F}_c = \bar{Q}_c / \bar{Q}_p = Q_c\,(r-1)/Q_p$$

and of the total homogeneity

$$\hat{F} = \bar{Q}_t / \bar{Q}_p = Q_t(r-1)\,(c-1)/Q_p(r \cdot c - 1)$$

The quotients must always be established in the stated form.

APPLICATION TO SPECTROGRAPHIC ANALYSIS OF SURFACES

The improved model and the two-dimensional variance analysis were applied to surface investigations by spectrographic analysis. The excitation parameters and exposure conditions are given in Table 3. Several Fe_2B coatings on iron were investigated with respect to homogeneous distribution of boron within the surface layers. To this end, 16 spots, arranged regularly in 4 rows and 4 columns on the surfaces of the samples, were sparked. Some results are given in Table 4. The measured values x_{ij} are the differences between the plate blackening at the boron and iron lines.

Table 4(a) shows a situation where boron is evenly distributed over the surface. The dispersions within the rows and columns as well as the total error are not significantly greater than the error of the analytical procedure. The $\hat{F}$-values are smaller than the tabulated $F(0.95)$ quantities for the corresponding degrees of freedom. Table 4(b) shows a situation where boron is unevenly distributed. The presence of a considerable concentration gradient is proved by the highly significant row and column effects; the measured values increase from the right top corner to the left bottom corner of the matrix. Such a layer with a concentration gradient was obtained by oblique grinding of a boron coating.

The additivity of the single effects is the decisive assumption for the

TABLE 1

Two-dimensional variance analysis scheme

i \ j		1	2	... c	Sums of the rows $\sum_{j=1}^{c} x_{ij} = S_{..}$	Means of the rows $\bar{x}_i = x_{i.}$	Row deviations $\alpha_i = x_{i.} - \bar{\bar{x}}$
Measured values in the rows	1	x_{11}	x_{12}	... x_{1c}	$S_{1.}$	$x_{1.}$	α_1
	2	x_{21}	x_{22}	... x_{2c}	$S_{2.}$	$x_{2.}$	α_2
	⋮	⋮	⋮	⋮	⋮	⋮	⋮
	r	x_{r1}	x_{r2}	... x_{rc}	$S_{r.}$	$x_{r.}$	α_r
Sums of the columns $\sum_{i=1}^{r} x_{ij} = S_{.j}$		$S_{.1}$	$S_{.2}$	... $S_{.c}$	$S = S_{..}$		
Means of the columns $\bar{x}_j = x_{.j}$		$x_{.1}$	$x_{.2}$	... $x_{.c}$		$\bar{\bar{x}} = x_{..}$	
Column deviations $\beta_j = x_{.j} - \bar{\bar{x}}$		β_1	β_2	... β_c			

TABLE 2

Computation of the different error contributions

Error	Sum of the squares of the deviations (Q)	Variance $\bar{Q} = Q \cdot f^{-1}$ (f = degrees of freedom)
Total error	$Q_t = \sum_{i=1}^{r} \sum_{j=1}^{c} x_{ij}^2 - \frac{S^2}{r \cdot c}$	$\bar{Q}_t = Q_t \, (r \cdot c - 1)^{-1}$
Error between the r rows	$Q_r = \sum_{i=1}^{r} \frac{S_{i.}^2}{c} - \frac{S^2}{r \cdot c} = c \cdot \sum_{i=1}^{r} \alpha_i^2$	$\bar{Q}_r = Q_r \, (r - 1)^{-1}$
Error between the c columns	$Q_c = \sum_{j=1}^{c} \frac{S_{.j}^2}{r} - \frac{S^2}{r \cdot c} = r \cdot \sum_{j=1}^{c} \beta_j^2$	$\bar{Q}_c = Q_c \, (c - 1)^{-1}$
Error of the experiment (procedural error)	$Q_p = Q_t - Q_r - Q_c$	$\bar{Q}_p = Q_p \, [(r-1)(c-1)]^{-1}$

application of such two-dimensional variance analysis. This assumption is sometimes not completely justified. Non-additive effects are present, designated as interactions γ_{ij} (see eqn. 1), which must be added to the random

TABLE 3

Spectrographic operating conditions

Spectrograph	PGS-2, VEB Carl Zeiss Jena
Grating	651 lines mm^{-1}; blaze 300 nm; 1st order; dispersion 0.737 nm mm^{-1}; resolving power 45600
Slit width	20 μm
Slit illumination	Intermediate imaging Zeiss; intermediate diaphragm: 2 mm
Electrode arrangement	Point-to-plane; counter-electrode, pencil-shaped Cu, outside diam. 3 mm, diam. of apex of cone, 0.5 mm
Electrode gap	1.5 mm
Sample area excited	1 mm diam.
Excitation	High-voltage spark generator FF 20 (VEB Carl Zeiss Jena); controlled discharge, 12000 V, 1.0 A; accessory capacitance, 6 nF
Exposure time	60 s
Photographic material	ORWO WU 3
Development	Metol-hydroquinone (1 + 4), 4 min, 18°C
Blackening measurement	Rapid photometer II (VEB Carl Zeiss Jena)
Spectral lines measured	B I 249.7 nm/Fe I 249.6 nm

procedural error ϵ. This leads to false results in the application of two -dimensional variance analysis, when such interactions are not negligible with respect to the row and column effects and to the procedural error. Table 5 gives an example where such interactions considerably exceed all other error contributions. The data in Table 5 are derived from investigations of homogeneity by Maul and Quillfeld [4]. They estimated both the total error and the procedural error for the distribution of chromium and manganese in steels by the method of Skogerboe [5]; they found homogeneous distribution of chromium but inhomogeneous distribution for manganese in the steel sample investigated. Their statements appear plausible and are confirmed by the concentration ranges measured (1.60—2.00% Cr; 1.07—2.25% Mn). The two-dimensional variance analysis, however, provides in both cases the assertion that the elements are homogeneously distributed. This statement is correct for chromium but wrong for manganese because of the neglected interaction (or correlation) contribution.

Such correlation contributions appear frequently if the measured values are arranged alternately high and low, i.e. to give a chequered matrix. Table 6 shows an extreme model, which is a synthetic example (therefore the procedural error $Q_p = 0$). The total error in this example is identical with the interaction contributions Q_i. In this example the ostensible statement "homogeneous" results from complete correlation of the data.

The interaction contributions can be calculated by the methods of Tukey [6], Mandel [7] and Weiling [8] by complicated mathematical equations based on different assumptions, e.g. that the interaction contributions are proportional to α_i or β_j. The interaction contributions in Table 6 were

TABLE 4

Emission spectrographic results showing (a) a homogeneous and (b) an inhomogeneous distribution of boron (arbitrary units)

(a) Measured values x_{ij}

					$S_{i.}$
	0.617	0.570	0.574	0.560	2.321
	0.568	0.588	0.600	0.600	2.356
	0.662	0.594	0.592	0.554	2.402
	0.698	0.662	0.680	0.520	2.560
$S_{.j}$	2.545	2.414	2.446	2.234	9.639

$\bar{\bar{x}} = 0.602$

$\sum_i \sum_j x_{ij}^2 = 5.844$

$\frac{S^2}{r \cdot c} = 5.807$

$\sum_i \frac{S_{i.}^2}{c} = 5.815$

$\sum_j \frac{S_{.j}^2}{r} = 5.820$

Q		f	$\bar{Q}$	$\hat{F}$	$F(0.95)$
Q_t	= 0.037	15	0.0025	1.39	3.01
Q_r	= 0.008	3	0.0027	1.57	3.86
Q_c	= 0.013	3	0.0043	2.39	3.86
Q_p	= 0.016	9	0.0018	—	—

= −0.212

= 1.950

= 0.716

= 1.309

= 1.141

(b) Measured values x_{ij}

					$S_{i.}$
	+0.120	−0.469	−0.614	−0.821	−1.784
	−0.115	−0.290	−0.358	−0.555	−1.318
	−0.010	−0.080	−0.187	−0.135	−0.512
	+0.140	+0.120	−0.010	−0.020	+0.230
	+0.135	−0.719	−1.169	−1.631	−3.384

Q		f	$\bar{Q}$	$\hat{F}$	$F(0.95)$
Q_t	= 1.234	15	0.082	3.42	3.01
Q_r	= 0.593	3	0.198	8.25	3.86
Q_c	= 0.425	3	0.142	5.92	3.86
Q_p	= 0.217	9	0.024	—	—

TABLE 5

Investigation of the homogeneity of chromium and manganese in alloy steel [4]

(a) Measured values x_{ij} (% Cr)					S_i
1.60	2.00	1.95	1.70	1.95	9.20
1.90	1.75	2.00	1.95	1.60	9.20
1.83	2.00	1.83	1.65	1.60	8.91
1.60	2.00	1.75	1.85	1.75	8.95
1.60	1.95	2.00	1.95	2.00	9.50
S_j 8.53	9.70	9.53	9.10	8.90	45.76

(b) Measured values x_{ij} (% Mn)					S_i
1.30	1.70	1.30	1.65	1.45	7.40
1.30	1.50	1.25	2.25	1.70	8.00
1.50	1.65	2.25	1.07	2.20	8.67
1.85	2.05	1.33	1.50	1.70	8.43
2.10	1.55	1.93	2.25	1.85	9.68
8.05	8.45	8.06	8.72	8.90	42.18

	Q[a]			f	$\overline{Q}$	$\hat{F}$	$F(0.95)$
(1)	Q_t	=	0.584	24	0.024	1.04	2.24
	Q_r	=	0.045	4	0.011	0.49	3.01
	Q_c	=	0.179	4	0.045	1.96	3.01
	$Q_{p(1)}$	=	0.359	16	0.023	—	—
(2)	Q_t	=	0.584	24	0.024	1.41	2.40
	Q_r	=	0.045	4	0.011	0.65	2.81
	Q_c	=	0.179	4	0.045	2.65	2.81
	$Q_{i,r}$	=	0.061	4	0.015	0.89	2.81
	$Q_{i,c}$	=	0.161	4	0.040	2.34	2.81
	$Q_{p(2)}$	=	0.138	8	0.017	—	—

	Q[a]			f	$\overline{Q}$	$\hat{F}$	$F(0.95)$
(1)	Q_t	=	2.960	24	0.123	0.87	2.24
	Q_r	=	0.573	4	0.143	1.01	3.01
	Q_c	=	0.117	4	0.029	0.21	3.01
	$Q_{p(1)}$	=	2.270	16	0.142	—	—
(2)	Q_t	=	2.960	24	0.123	3.02	2.40
	Q_r	=	0.573	4	0.143	3.50	2.81
	Q_c	=	0.117	4	0.029	0.72	2.81
	$Q_{i,r}$	=	1.518	4	0.380	9.28	2.81
	$Q_{i,c}$	=	0.424	4	0.106	2.59	2.81
	$Q_{p(2)}$	=	0.328	8	0.041	—	—

[a](1) Neglecting and (2) incorporating the interaction contribution γ_{ij}.

TABLE 6

Synthetic example, with values arranged alternately high and low

Values				$S_{i.}$	
4	1	4	1	10	Q_t = 136—100 = 36
1	4	1	4	10	Q_r = 100—100 = 0
4	1	4	1	10	Q_c = 100—100 = 0
1	4	1	4	10	Q_p = 0
$S_{.j}$ 10	10	10	10	10	Q_i = 36

calculated as described by Mandel [7]. The Table shows that after elimination of the large interaction contributions, the distribution of manganese is indeed inhomogeneous, whereas that of chromium is homogeneous, as concluded previously, because they are very extensive and difficult to handle.

When implausible results are obtained for testing homogeneity, the two-dimensional variance analysis should not be applied. Better results are obtained by repeating each measurement for estimation of the procedural error.

We are grateful to Doz. Dr. Heckendorff from the Wissenschaftsbereich Wahrscheinlichkeitstheorie und Statistik of the Technische Hochschule Karl-Marx-Stadt for helpful discussions of statistical problems.

REFERENCES

1 K. Danzer, K. Doerffel, H. Ehrhardt, G. Ehrlich, P. Gadow and M. Geissler, Anal. Chim. Acta, in print.
2 K. Doerffel, Statistik in der analytischen Chemie, VEB Verlag für Grundstoffindustrie, Leipzig, 1966.
3 K. Danzer and G. Marx, 2. Tagung Feskörperanalytik, Tagungsber. Techn. Hochsch. Karl-Marx-Stadt, 1978, p. 24.
4 W. Maul and W. Quillfeld, Jenaer Rundsch., 22 (1977) 234.
5 R. K. Skogerboe, Appl. Spectrosc., 25 (1971) 259.
6 J. W. Tukey, Biometrics, 5 (1949) 232.
7 J. Mandel, J. Am. Stat. Assoc., 56 (1961) 878.
8 F. Weiling, Der Züchter, 33 (1963) 74.
9 L. Sachs, Angewandte Statistik, Springer Verlag, Berlin, 1974.

Analytica Chimica Acta, 110 (1979) 153—156

Short Communication

DETERMINATION OF SELENIUM IN PYRITE BY AN ION EXCHANGE—ELECTROTHERMAL ATOMIC ABSORPTION SPECTROMETRIC METHOD

C. M. ELSON*

Department of Chemistry, Saint Mary's University, Halifax, Nova Scotia B3H 3C3 (Canada)

and A. S. MACDONALD

Nova Scotia Department of Mines, Halifax, Nova Scotia B3J 2X1 (Canada)

(Received 29th March 1979)

Summary. After acid digestion of the pyrite, the solution is passed through a Dowex 50W-X8 column, primarily to remove interference from iron, and an aliquot of the effluent is injected into the graphite furnace. The response is linear up to 200 μg Se g^{-1} and the detection limit is 5 μg g^{-1}. After digestion, an analysis can be completed in 10 min.

Selenium, because of its strong chalcophilic tendencies, is concentrated in metal sulphide ores, mainly within sulphide minerals such as pyrite [1]. The concentration of selenium in pyrite is thought to reflect the composition of ore fluids and the physical and chemical conditions of ore deposition [2—4]; also of interest is the influence of post-depositional metamorphism on the selenium content of pyrite ores [1, 5].

The determination of selenium in geological materials is complicated by low natural abundance, inorganic interferences and matrix effects. Methods such as solvent extraction, hydride generation and precipitation have been developed, therefore, to minimize these problems by isolating selenium prior to analysis by various instrumental techniques [6—12]. Most of these procedures, however, involve a considerable amount of sample manipulation.

The method described here is based on cation-exchange pretreatment prior to analysis by electrothermal a.a.s. This method eliminates certain interferences, takes advantage of the increased sensitivity of the graphite furnace atomizer, and is quick and simple. The method is applied to two pyrites from Tasmania which were previously analyzed in a small, international interlaboratory study [13] and a series of 17 pyrites from British Columbia. The former samples come from the Mount Lyell pyrite—chalcopyrite deposit and the latter come from three zinc—lead sulphide deposits (Reeves MacDonald, H.B. and Jersey mines) occurring within a limestone formation of Early Cambrian age [14—16].

Experimental

Reagents. All chemicals were of reagent grade except the acids, which were

ultra-pure (J. T. Baker Chemical Co.). Water was distilled from an all-glass apparatus and glassware was cleaned with warm (1 + 1) nitric acid. Standard solutions were prepared by dissolving selenium dioxide in 0.05 M nitric acid.

The ion-exchange resin was Dowex 50W-X8 which had been treated with 2 M hydrochloric acid and packed into a column 1 cm in diameter and 8 cm long. The hold-up volume of the column was about 3.5 ml.

Sample preparation. Preparation of the Tasmanian pyrites has been described [13]. Pyrite concentrates from the British Columbia ore samples were prepared by crushing, sieving (−80 to +200 mesh) and then panning. The concentrates were passed through a Frantz Isodynamic magnetic separator to remove sphalerite and pyrrhotite, and then leached with hot 6 M hydrochloric acid to remove any galena and remaining carbonate minerals. Several samples containing small amounts of silicate minerals required further purification by physical separation in bromoform, by utilizing differences in density. The purity of the final concentrates was estimated, by inspection with a binocular microscope, to be better than 97%. Galena, sphalerite and graphite formed the main impurities and occurred mainly as inclusions within the pyrite grains.

Equipment. Absorbance measurements were made on a Perkin-Elmer atomic absorption spectrometer (Model 403) which was equipped with a heated graphite cell and controller (Perkin-Elmer HGA74 and HGA 2100), a deuterium arc background corrector and a selenium electrodeless discharge lamp (λ = 196.0 nm). The temperature program was: dry for 30 s at 150°C, char for 30 s at 400°C and atomize for 6 s at 2550°C. During atomization, the flow of nitrogen through the graphite furnace was interrupted.

Procedure. Weigh approximately 0.5 g of pyrite into a 50-ml beaker. Add 5 ml of concentrated nitric acid and 2 ml of 60% perchloric acid and cover. Heat gently on a sand bath for 2 h and then slowly evaporate to near dryness. Dissolve the residue in warm water plus 1 ml of concentrated nitric acid and dilute to 500 ml. Transfer a 10-ml aliquot to the ion-exchange column and adjust the flow rate to 3 ml min^{-1}; discard the first 6 ml of effluent and collect the next 5 ml. Inject 10 μl of this solution plus 20 μl of nickel(II) solution (1 mg Ni ml^{-1}) into the graphite furnace; nickel(II) prevents premature volatilization of selenium. Analyze effluent by the method of standard additions; also, add a known volume of selenium standard solution to a second 10-ml aliquot of sample, transfer to a second ion-exchange column, and collect and analyze the effluent as above.

Results and discussion

Analysis of untreated samples produced small and irreproducible selenium signals presumably caused by the iron suppressing the signals [17]. Furthermore, samples that had been extracted by published procedures [7, 9, 10] failed to exhibit significant, reproducible signals, again because of the interference from iron which is also extracted in these procedures [18]. By comparison, the cation-exchange pretreatment decreased the iron content of the

effluent to less than 0.5 $\mu g\ ml^{-1}$ (as determined colorimetrically). This represented an approximate thousand-fold reduction in iron to a level which did not affect the determination of selenium by electrothermal a.a.s. [17]. In fact, the absorbance signal of a selenium standard addition to a sample was only 15% smaller than the signal of a comparable standard solution. The ion-exchange procedure was also quick and simple: a digested sample was usually analyzed in less than 10 min.

Spiking the samples before and after the ion-exchange treatment produced two results per digest. These results usually agreed to within 4%; the worst case had a difference of 11%. Reagent blanks exhibited very small signals corresponding to a concentration of 1—2 $\mu g\ Se\ g^{-1}$ in the original ore. The calibration curve was linear over the range 0—200 $\mu g\ Se\ g^{-1}$ and the detection limit of the method was 5 $\mu g\ Se\ g^{-1}$ based on a signal equal to twice the background noise and the recommended dilution. This limit could be lowered if the final sample volume were reduced. Pierce and Brown [17] have reported a detection limit for the graphite furnace of 1 $\mu g\ l^{-1}$ which corresponds to 1 $\mu g\ g^{-1}$ in the present case.

The selenium contents of the pyrites examined are listed in Table 1; the errors represent the 95% confidence limits based on a minimum of four analyses. The Tasmanian pyrites have been analyzed previously [13] with the results: pyrite 1, 82 ± 9 $\mu g\ Se\ g^{-1}$ and pyrite 2, 64 ± 12 $\mu g\ Se\ g^{-1}$ (the errors represent one standard deviation). The results of the present study are in good agreement with those reported, and, incidentally, are close to the average value of 70 $\mu g\ Se\ g^{-1}$ reported for pyrites from pyrite—chalcopyrite deposits of this particular type [4].

The selenium values for the samples from the three British Columbian deposits lie within the range 10—31 $\mu g\ g^{-1}$, except for one value of 50 $\mu g\ g^{-1}$. Such generally low values appear to characterize pyrites from many zinc—lead sulphide deposits formed in carbonate rocks [4]. Although the three

TABLE 1

Selenium content of pyrites ($\mu g\ g^{-1}$)

Tasmania		British Columbia					
Mt. Lyell mine		Reeves MacDonald mine		H.B. mine		Jersey mine	
Pyrite 1	82 ± 5	RM-18	14 ± 1	HB-1	12 ± 2	CX-20	11 ± 2
Pyrite 2	64 ± 5	RM-20	16 ± 1	HB-4	19 ± 2	CX-23	11 ± 1
		RM-21	22 ± 2	HB-10	23 ± 1	CX-26	31 ± 1
		RM-26	25 ± 2	HB-12	22 ± 3	CX-44	13 ± 1
		RM-36	50 ± 1	HB-17	21 ± 3	CX-75	10 ± 1
		RM-52	26 ± 2				
		RM-77	15 ± 1				
	Mean values ± 1 s.d.	RM = 24 ± 12		HB = 19 ± 4		CX = 15 ± 9	

deposits were apparently formed under essentially similar conditions, they were later affected to different degrees by thermal metamorphism. The least affected was the Reeves MacDonald deposit; the H.B. deposit was moderately affected, and the Jersey deposit moderately to highly affected [16, 19]. The effects of this later thermal metamorphism on the selenium values of the pyrites can be gauged by comparing the mean values for the three deposits. These show an apparent trend toward lower values at increased metamorphic grade, but the means are not significantly different at the 95% confidence level. It must, therefore, be concluded that metamorphism has not significantly altered the original selenium values in the pyrites. This conclusion is in agreement with those from other studies of metamorphosed ore deposits [1, 5] and suggests that pyrite behaves as a relatively refractory material under conditions of low- to medium-grade metamorphism.

The authors are indebted to Dr. J. L. Walshe (University of Tasmania) for his generosity in supplying samples and to Ms. D. Hynes for her technical assistance. A grant to C. M. E. from the Natural Sciences and Engineering Research Council of Canada is gratefully acknowledged.

REFERENCES

1 F. Leutwein, in K. H. Wedepohl (Ed.), Handbook of Geochemistry, Vol. 2, Springer-Verlag, 1972, Chapter 34.
2 G. Loftus-Hill and M. Solomon, Miner. Deposita, 2 (1967) 228.
3 G. Loftus-Hill, D. I. Groves and M. Solomon, Aust. Inst. Min. Metall. Proc., 232 (1969) 55.
4 V. V. Ivanov and O. E. Yushko-Zakharova, in V. I. Smirnov (Ed.), Ore Deposits of the U.S.S.R., Vol. 3, English translation by D. A. Brown, Pitman, 1977, p. 453.
5 R. H. Mitchell, Norsk. Geol. Tiddskr., 48 (1968) 65.
6 J. C. Chambers and B. E. McClellan, Anal. Chem., 48 (1976) 2061.
7 A. Wyttenbach and S. Bajo, Anal. Chem., 47 (1975) 1813.
8 T. Stijve and E. Cardinale, J. Chromatogr., 109 (1975) 239.
9 M. W. Blades, J. A. Dalziel and C. M. Elson, J. Assoc. Off. Anal. Chem., 59 (1976) 1234.
10 G. L. Crenshaw and H. W. Lakin, J. Rev. U.S. Geol. Surv., 2 (1974) 483.
11 G. A. Cutter, Anal. Chim. Acta, 98 (1978) 59.
12 J. H. Howard III, Geochim. Cosmochim. Acta, 41 (1977) 1665.
13 P. Robinson and J. L. Walshe, Trans. Inst. Min. Metall. (Sect. B: Appl. Earth Sci.), 86 (1977) 216.
14 J. T. Fyles and G. Hewlett, B. C. Dep. Mines Bull., 41 (1959) 162.
15 D. F. Sangster, Proc. Geol. Assoc. Can., 22 (1970) 27.
16 A. S. Macdonald, Doctoral Thesis, University of British Columbia, 1973, p. 224.
17 F. D. Pierce and H. R. Brown, Anal. Chem., 49 (1977) 1417.
18 W. E. Clarke, Analyst, 95 (1970) 65.
19 T. W. Muraro, Tectonic History and Mineral Deposits of the Western Cordillera, Vol. 8, Can. Inst. Min. Metall., 1966, p. 239.

Analytica Chimica Acta, 110 (1979) 157—160

Short Communication

A NEW CATALYTIC ELECTRODE FOR THE AMPEROMETRIC DETERMINATION OF HYDROGEN PEROXIDE

A. IWASE*, S. KUDO and N. TANAKA

Department of Chemistry, Faculty of Science, Yamagata University, Yamagata 990 (Japan)

(Received 29th January, 1979)

Summary. The electrode is based on the decomposition of H_2O_2 by an inorganic polymer catalyst. The steady-state decomposition currents of H_2O_2 obtained with the catalyst electrode are independent of ionic strength (0.1—1.5) and pH (2.5—10.5). A linear relationship is obtained from 0.02 to 2 mM H_2O_2 in 0.1 M KCl at 25°C.

Several polarographic determinations of hydrogen peroxide based on anodic oxidation have been reported [1—3], and various electrodes for hydrogen peroxide have been constructed [4—6]. Aizawa et al. [4] reported a selective determination of hydrogen peroxide with a bio-catalyst electrode containing immobilized catalase. However, the response of the catalase electrode is sensitive to variation in pH. Oxygen electrode methods based on catalyzed reactions with a metal oxide as catalyst have been described by Schick et al. [5] and Updike et al. [6]. In the present communication, it is shown that a new electrode system involving a polymeric cobalt material as a catalyst for the conversion of peroxide to oxygen is useful for amperometric measurements of hydrogen peroxide. The polymeric catalyst is obtained by reaction of cobalt(II) acetylacetonate with hyperoxide ion and is very stable in acidic or alkaline solutions.

Experimental

Reagents. Hydrogen peroxide (30%; JIS, K-8230; Mitsubishi Gas Chemical Co.) was diluted with distilled water to give 0.01 and 0.1 M solutions, which were standardized by iodometric titration. All electrolyte solutions were prepared with distilled water. The buffer solution was 0.06 M Na_2HPO_4—KH_2PO_4 (pH 6.8). Unless otherwise specified, all materials were of analytical-reagent grade.

Preparation of the catalyst. A 50-ml portion of a solution containing 5mM cobalt acetylacetonate and 0.05 M tetramethylammonium perchlorate in dimethyl sulfoxide was placed in an electrolytic cell [7] and electrolyzed for 3 days at −1.1 V vs. SCE, at room temperature (ca. 20°C) in an open system. The brown product which separated out was filtered off and dried in a vacuum desiccator at room temperature. Analytical results for this material

were 13.4% C; 3.7% H; 60.1% ash. Although direct evidence for polymer formation was not obtained, the reproducibility of the analytical results for different batches of material supports the suggestion of compound formation.

Apparatus. An oxygen electrode of the Clark type (Yellow Springs Instruments Co., No. 5331) was used to detect the oxygen liberated. The catalytic electrode was prepared by the sandwich method described by Schick et al. [5] (Fig. 1). Cellophane dialysis membrane and the hydrophobic oxygen membrane supplied with the electrode were used as indicated. The brown product (20 mg) from the electrolysis was placed between the membranes. The probe was employed in conjunction with a Yanagimoto PA 101 polarograph and a cell assembly which provided constant temperature and stirring rate; Teflon-coated magnetic bars were used.

Procedures. A 50-ml aliquot of sample solution in a suitable buffer or electrolyte was added to the cell and deaerated with nitrogen. A potential of —0.6 V (where the current is proportional to the dissolved oxygen) was then applied. About 1 min later, the current—time curve of the oxygen liberated by decomposition of hydrogen peroxide was recorded. All amperometric measurements were conducted at 25°C except for the study on the temperature effect. The catalytic electrode was washed with distilled water three times before each use. Normally the electrode was stored in distilled water at room temperature.

Results and discussion

Typical decomposition current—time (i—t) curves obtained with the

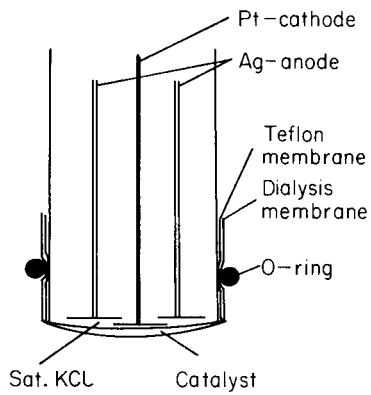

Fig. 1. Construction of catalytic electrode.

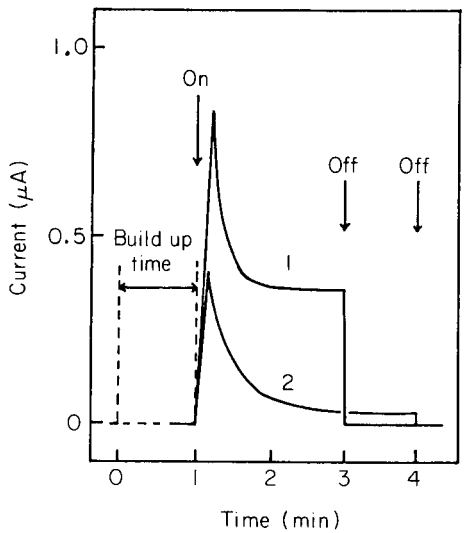

Fig. 2. Decomposition current—time curves for two concentrations of H_2O_2 in 0.1 M KCl: (1) 2 mM; (2) 0.2 mM.

catalytic electrode are shown in Fig. 2. Under the conditions used, a steady-state decomposition current was normally observed after 2—3 min, but longer times were required for peroxide concentrations below 0.1 mM. The initial peak in the *i—t* curve is probably caused by reduction of the oxide film on the platinum electrode and by charging current in the electrical double layer.

Table 1 shows the effect of pH on the steady-state current for 0.2 mM H_2O_2 in 1.0 M KNO_3; the pH of the solution was adjusted from about 2.5 to 10.5 by adding 0.1 M nitric acid, potassium hydroxide, and 0.06 M phosphate buffer. As can be seen, the results were almost constant over the pH range 2.4—10.5, the mean current being 38 ± 1 nA. The steady-state currents obtained for solutions containing 0.2 mM H_2O_2 and phosphate buffer (pH 6.8) with varying concentrations of KNO_3 were not affected by changes in ionic strength in the range 0.1—1.5; again the mean current was 38 ± 1 nA (4 measurements). In contrast, Schick et al. [5] reported that the steady-state current obtained with PbO_2 catalytic electrode is affected by ionic strength below 1.0. The activity of the polymeric cobalt catalyst is higher than that of the lead oxide catalyst, which is of particular interest, because it allows hydrogen peroxide to be determined over wide ranges of pH and ionic strength.

The temperature dependence of the steady-state current is shown in Fig. 3; the current was almost constant over the range 20—28°C, but increased above 30°C and decreased below 18°C.

A typical hydrogen peroxide calibration curve at constant temperature is shown in Fig. 4. In this experiment, the *i—t* curves for 0.01—60 mM hydrogen peroxide were measured under the same conditions as for Fig. 2. A linear plot with a slope of 0.87 was obtained in the range 0.02—2 mM. Above 3 mM, the steady-state current deviated from the linear relationship, probably because the oxygen liberated was lost by back-diffusion.

The stability of the electrode was confirmed. For 0.2 mM hydrogen peroxide solutions, the same reading was obtained for about 80 assays, but it was then necessary to change the catalyst. The precision obtained was ±3% for six assays. The lower limit of detection was 0.01 mM. Hence, this electrode is a useful tool for the assay of hydrogen peroxide, provided that dissolved oxygen can be removed.

TABLE 1

Effect of pH on the steady-state current of 0.2 mM H_2O_2 in 1.0 M KNO_3

pH	2.4	4.3	5.5	6.8	8.8	10.5
Current (nA)	37	39	39	38	38	37

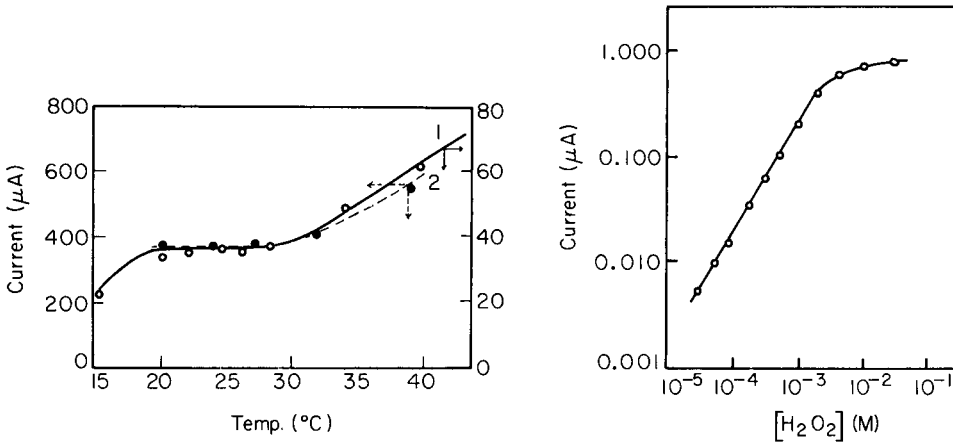

Fig. 3. Temperature-dependence of the steady-state current of H_2O_2 in 0.1 M KCl: (1) 0.2 mM H_2O_2; (2) 2 mM H_2O_2.

Fig. 4. Calibration curve for H_2O_2 in 0.1 M KCl at 25°C.

REFERENCES

1 L. C. Clark, Jr., Biotechnol. Bioeng. Symp., 3 (1972) 377.
2 S. Polous and R. Buvet, Bull. Chim. Soc. Fr., (1963) 2490.
3 J. Koryta, Collect. Czech. Chem. Commun., 18 (1953) 206.
4 M. Aizawa, I. Karube and S. Suzuki, Anal. Chim. Acta, 69 (1974) 431.
5 K. G. Schick, V. G. Magearu, N. L. Field and C. O. Huber, Anal. Chem., 48 (1976) 2186.
6 S. J. Updike, M. C. Shults, J. K. Kosovich, I. Treichel and M. Treichel, Anal. Chem., 48 (1975) 1457.
7 A. Iwase and S. Tada, Nippon Kagaku Kaishi, (1972) 1828.

Analytica Chimica Acta, 110 (1979) 161—166

Short Communication

CURRENT SAMPLING IN POLAROGRAPHY WITHOUT SYNCHRONIZATION WITH THE DROP TIME

ANTONÍN TROJÁNEK and IGOR HOLUB*

J. Heyrovský Institute of Physical Chemistry and Electrochemistry, Czechoslovak Academy of Sciences, Jilská 16, 110 00 Prague 1 (Czechoslovakia)

(Received 2nd March 1979)

Summary. The circuit proposed for sampling of polarographic currents enables oscillations on the recorded curves to be eliminated without distortion of the curve. The apparatus, based on a peak detector, can be used regardless of the shape and character of the curves, and does not require indication of drop disconnection. When the necessary conditions are fulfilled, the output signal is identical with the signal from a Tast polarograph.

The dropping mercury electrode is unique among electroanalytical sensors; as each drop falls, perfect surface renewal is ensured in a manner unattainable with other electrodes. However, the growth and fall of the drop cause periodic oscillations in the recorded polarographic current and thus complicate the evaluation of polarograms and possible further handling of the signal, especially with low concentrations of depolarizer. For these reasons, attempts have been made to eliminate the oscillations by using RC filters. Unfortunately, these filters lead to distortion of the curves in a manner depending on the time constant, and in flow-through analyzers there is a substantial decrease in the detector response rate [1].

In a polarograph described in 1959 [2], a peak detector was employed to record peak current values; this was possible only when a test polarogram recorded without use of the peak detector showed that the polarographic current increased or was constant with increasing potential [3]. Another simpler version of the peak detector can also be used when the polarographic current decreases with increasing potential [4]. Operation of the detector is based on the filtering properties of a circuit containing two diodes and two capacitors connected to the input of the recorder amplifier.

The most generally useful method of eliminating oscillations involves current sampling at the start of drop growth. Sampling again at the end of drop growth (Tast polarography) permits partial suppression of the unwanted charging current, which has a time dependence different from that of the faradaic current [5, 6]. The sampling rhythm is commonly determined by a mechanical drop-timer. The impulse that controls its operation yields a

reference time value, from which time is measured up to the recording of the current value and its transfer to a memory.

To attain maximum reliability, it is desirable to avoid the use of a mechanical drop-timer; moreover, timers are difficult to construct for flow-through analyzers. This problem can generally be solved by indicating natural disconnection of drops, e.g. by suitable handling of the polarographic signal itself [7] or by using the sudden change in the electrolytic cell impedance at the instant of drop disconnection [8].

The method of sampling of the polarographic current proposed below assumes the use of a dropping electrode with a natural drop time and does not require indication of drop times.

Experimental

Polarographic equipment. A block diagram of the polarograph is given in Fig. 1. The current signal between the auxiliary and working electrode connected potentiostatically is converted to a voltage signal by a current follower. A capacitor connected in parallel to the feedback resistor of the current follower suppresses sharp charging current peaks at the instant of drop disconnection. A peak detector and an analog memory (Fig. 2) are controlled by pulses *P*1 and *P*2 through electronic FET switches. Switch S1 opens the analog memory for storage of the detector output signal. As switch S2 is closed, a voltage appears on the detector output which is identical

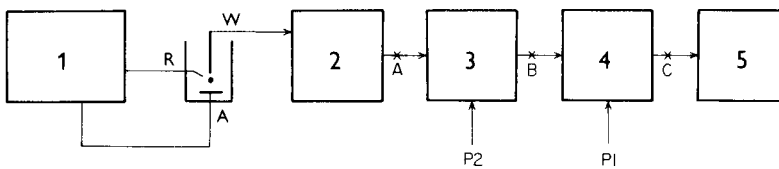

Fig. 1. Block diagram of the polarograph. (1) Potentiostat; (2) current follower; (3) peak detector; (4) analog memory; (5) recorder.

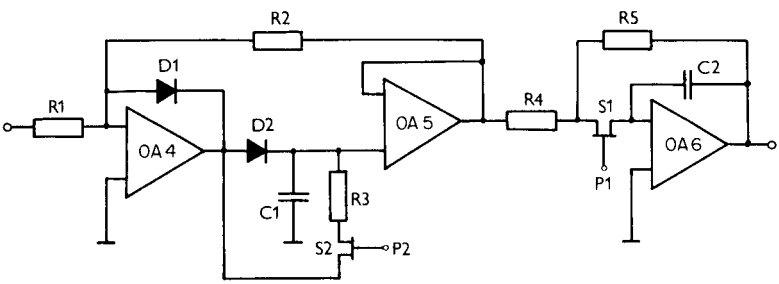

Fig. 2. The peak detector and analog memory circuits. The operational amplifiers used were: OA4, MAA-741, OA5 and OA6, WSH-220 (amplifiers with FET input). S1 and S2 were MH-2009 switches controlled from a pulse generator [9] through a WTA-029 transducer. D1 and D2 are silicon diodes (KA 502). $R1 = R2 = 1$ Mohm; $R3 = 500$ kohm; $R4 = R5 = 10$ kohm; $C1 = 1\ \mu F$; $C2 = 0.16\ \mu F$.

with the input voltage and thus the detector is ready for monitoring the new maximum value that appears during the period of pulse *P*2.

Figure 2 shows the peak detector (OA 4 and 5) and the analog memory (OA 6). The diode D2 is conducting (and the capacitor C1 is charged) only when the negative voltage applied to *R*1 from the output of the current follower rises. The feedback loop of amplifier 4 is then closed through amplifier 5, which is connected as a voltage follower, and the resistance *R*2. The output voltage of amplifier 5 is then equal to the inverse output voltage of the current follower. When the output voltage of the current follower starts to decrease, diode D2 closes, so that the voltages on the capacitor C1 and output of the voltage follower remain constant. The feedback element then receives the output of diode D1, which is now conducting.

Measuring principle. The principle of the current sampling is evident from Fig. 3, which depicts the time course of the voltage signal at points A, B and C of the polarographic circuit shown in Fig. 1. The peak detector (B) records the maximum value of the voltage signal (A) which appears between two pulses P2. Immediately before pulse *P*2 the value measured is stored in the memory (C). To obtain as many experimental values as possible, the period *T* of pulses *P*1 and *P*2 should be only a little longer than drop time t_1. The duration of pulse *P*1 must suffice for transfer of the signal to the analog memory and thus depends on the time constant of the memory. With the time constant $RC = 1.6 \times 10^{-3}$ s used here, a pulse length of 10 ms proved suitable. To suppress the "dead time" during which the current is not measured, the interval of time between pulses *P*1 and *P*2 must be as short as possible; values from 0.1 to 10 ms were tested without a perceptible effect on the shape and quality of the curves recorded. The length of pulse *P*2 is selected on criteria similar to those for pulse *P*1; in this work pulses of 1—10 ms long were satisfactory.

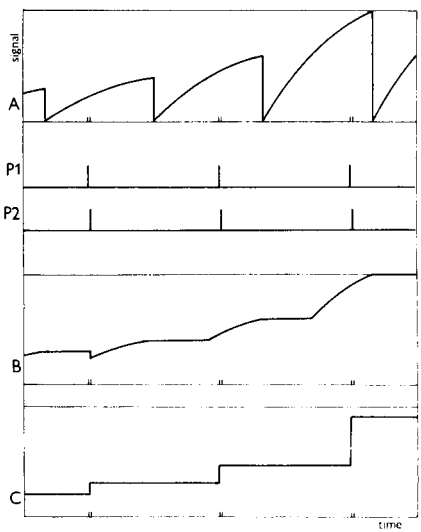

Fig. 3. Time dependence of the voltage signal at points A, B and C marked in Fig. 1.

Discussion

As can be seen from the schematic representation of the time dependence of the controlling pulses and the i—t curves (A) in Fig. 3, switch S2 closes at various stages of the drop growth because of non-synchronous sampling. The current value transferred to the analog memory thus depends not only on the shape of the i—t curve sampled, but also on the shape of the previous curve. This fact becomes clear on comparison of the recorded polarographic curve with the curve obtained by Tast polarography. When the value of the peak current decreases monotonously with time, the current values immediately before disconnection of the drop are stored in the memory. This occurs, for example, when cathodic processes are monitored with electrode polarization from negative to positive potentials. The apparatus then operates as a perfect Tast polarograph, but the number of sampling points is of course slightly less than in Tast polarography, because the period T of the pulses must in general be longer than t_1. In contrast, when the electrode is polarized in the opposite direction, the stored current values do not correspond to the values at the end of the drop.

The largest possible deviation Δt of the sampling time from the end of the drop obviously corresponds to the interval of time within which the i—t curve attains a current value larger than the maximum current on the preceding curve. The magnitude of this deviation can be assessed by using the relationship for the dependence of the instantaneous polarographic current on the electrode potential [10]. From the Ilkovič equation, when only the oxidized form is present in the solution, and if it is assumed that the square root of the ratio of the diffusion coefficient of the oxidized and reduced forms equals unity, then

$$i = Kt^{1/6} \{\exp [-(nF/RT)(E - E_F)]\}/\{1 + \exp [-(nF/RT)(E - E_F)]\} \quad (1)$$

where constant K is a function of the number of electrons exchanged, the mercury flow rate, the concentration and the diffusion coefficient of the electroactive substance; E is the electrode potential and E_F is the formal potential of the given electrochemical system.

If the potential changes by ΔE, the instantaneous current changes by

$$i = Kt^{1/6} (nF/RT) \Delta E \frac{\{\exp [-(nF/RT)(E - E_F)]\}}{\{1 + \exp [-(nF/RT)(E - E_f)]\}^2} \quad (2)$$

If the formal potential E_F is identified with half-wave potential $E_{1/2}$, then at a potential separated by $\bar{E}$ from $E_{1/2}$, the i—t curve attains a maximum value i^M equal to

$$i^M = Kt_1^{1/6} \{\exp [-(nF/RT)\bar{E}]\}/\{1 + \exp [-(nF/RT)\bar{E}]\} \quad (3)$$

at time t_1 (drop time). The subsequent curve at potential $\bar{E} + \Delta E$ attains the same value at time t given by the equation

$$i^M = Kt^{-1/6} \frac{\exp\left[-(nF/RT)\bar{E}\right]}{1 + \exp\left[-(nF/RT)\bar{E}\right]} + \Delta E\, Kt^{1/6} \frac{nF}{RT} \frac{\exp\left[-(nF/RT)\bar{E}\right]}{\{1 + \exp\left[-(nF/RT)\bar{E}\right]\}^2} \quad (4)$$

On substitution for i^M from eqn. (3)

$$(t/t_1) = \left(1 + (nF/RT) \frac{\Delta E}{1 + \exp\left[-(nF/RT)\bar{E}\right]}\right)^{-6} \quad (5)$$

Ratio t/t_1 is the time interval from the beginning of the drop growth within which sampling can occur, related to the drop time. Figure 4 shows the dependence of the calculated t/t_1 values on the potential $\bar{E}$ for four selected values of ΔE and four 1-e reductions. It can be seen that the relative deviation from the Tast mode is greatest at the foot of the polarographic wave.

Figure 5 shows a cyclic polarogram for a mixture of nickel, cadmium and copper ions. There is no perceptible difference in the branches corresponding to the opposite directions of polarization — the left branch is identical with Tast recording — because the large time deviation Δt occurs in potential regions within which it cannot cause a large deviation from the signal obtained by the Tast technique. At potentials sufficiently negative to the half-wave potential, the absolute error is relatively small because of the small time deviation. It also follows from the dependence of the faradaic current on $t^{1/6}$ that the current attains a value of almost 90% of the peak value at $t = 1/2\, t_1$.

Conclusion. The proposed method of polarographic current sampling does not require synchronization of drop disconnection with the start of current sampling and seems to be especially well suited for continuous flow-through monitoring. The recording obtained is analogous to that obtained by Tast polarography and is suitable for further handling. The curves obtained are

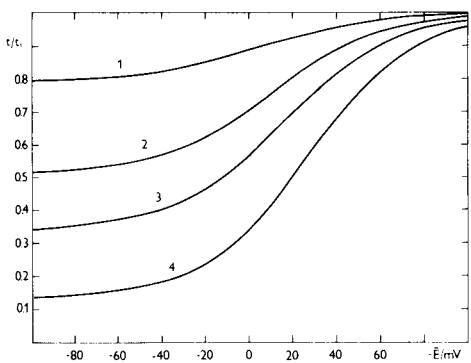

Fig. 4. The calculated dependence of the t/t_1 ratio on the electrode potential related to the half-wave potential for four selected values of ΔE: (1) 10^{-3} V; (2) 3×10^{-3} V; (3) 5×10^{-3} V; (4) 10^{-2} V.

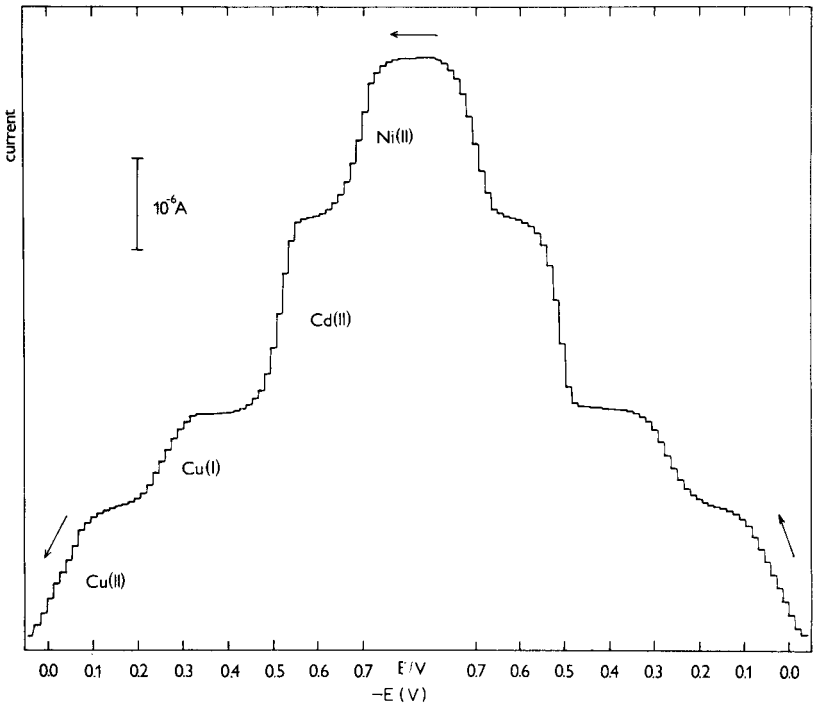

Fig. 5. Cyclic polarogram of 2×10^{-4} M Cu^{2+}, Cd^{2+}, Ni^{2+} in 0.1 M NH_4Cl + 0.1 M NH_4OH; $v = 5 \times 10^{-3}$ V s^{-1}; direction of polarization as indicated. The shortest drop time in the given potential region was t_1 = 2.6 s. The selected period of controlling pulses was T = 3 s. $P1$ = 10 ms and $P2$ = 1 ms, with an interval of 1 ms.

identical with the Tast curves for sufficiently low potential scan rates or for suitable direction of polarization.

REFERENCES

1 W. Lund and L.-N. Opheim, Anal. Chim. Acta, 82 (1976) 245.
2 M. T. Kelley, D. J. Fisher, W. D. Cooke and M. C. Jones, Proc. Int. Polarogr., 2nd, Cambridge, England, Aug. 24—29, 1959, in I. S. Longmuir (Ed.),Advances in Polarography, Pergamon Press, London, 1960, pp. 158—182.
3 M. T. Kelley, M. C. Jones and D. J. Fisher, Anal. Chem., 31 (1959) 1475.
4 A. Borello, M. De Carolis and G. R. Guidotti, J. Electroanal. Chem., 30 (1971) 231.
5 E. Wahlin and A. Brestle, Acta Chem. Scand., 10 (1956) 935.
6 K. Kronenberger, H. Strehlow and A. W. Elbel, Polarogr. Ber., 5 (1957) 62.
7 L. Pospíšil, Chem. Listy, 67 (1973) 1101.
8 R. G. Clem and W. W. Goldsworthy, Anal. Chem., 43 (1971) 918.
9 I. Holub and A. Trojánek, Chem. Listy, in press.
10 J. Heyrovský and J. Kůta, Principles of Polarography, Academic Press, New York, 1966.

Analytica Chimica Acta, 110 (1979) 167—170

Short Communication

MICROCOULOMETRIC DETERMINATION OF TOTAL INORGANIC AND ORGANIC SULFUR IN TRACE AMOUNTS IN WATERS

E. E. BRULL* and G. S. GOLDEN

United Technologies Research Center, Silver Lane, East Hartford, Connecticut 06108 (U.S.A.)

(Received 21st March 1979)

Summary. Sulfur and its compounds are converted to sulfur dioxide which is titrated microcoulometrically. Complete volatilization of inorganic sulfur is effected by adding a little phosphoric acid to the samples; metals are thus converted to their stable phosphate salts. The limit of detection is about 0.1 ppm based on a 25-μl sample. An analysis requires 4—5 min. The only interference arises from > 100 ppm halogen contents.

Although the determination of traces of total organic and inorganic sulfur compounds in aqueous solutions is often required in establishing sulfur material balances, few universal methods have been reported. If all the sulfur species can be converted to sulfate, i.e., by oxidation or combustion, the barium sulfate turbidimetric method can be used [1] but this method is time-consuming and inadequate for small samples. Van Grondelle et al. [2] give a very good alternative approach based on reduction of all sulfur to hydrogen sulfide followed by oxidation to sulfur dioxide which is then determined accurately by microcoulometry. However, the reduction apparatus is cumbersome and requires careful monitoring.

A simpler approach would be direct sample injection into a microcoulometric analyzer without prior complex sample treatment. Wallace et al. [3] and de Groot et al. [4] use this approach to determine trace sulfur in organic compounds. The method described below extends these methods to include both organic and inorganic sulfur in aqueous media. The aqueous sample is transferred to a small quartz boat which is then introduced into a combustion furnace where pyrolysis, volatilization, and conversion of sulfur compounds to sulfur dioxide takes place. Volatilization of the sulfur compounds is aided by adding a little concentrated phosphoric acid to the sample prior to pyrolysis and oxidation in an oxygen atmosphere at 800°C. On pyrolysis, phosphoric acid forms involatile phosphorus oxides and/or stable metal phosphates. If the sulfur salts do not decompose at 800°C, the phosphate will react metathetically with all sulfates, sulfides, and sulfites at this temperature.

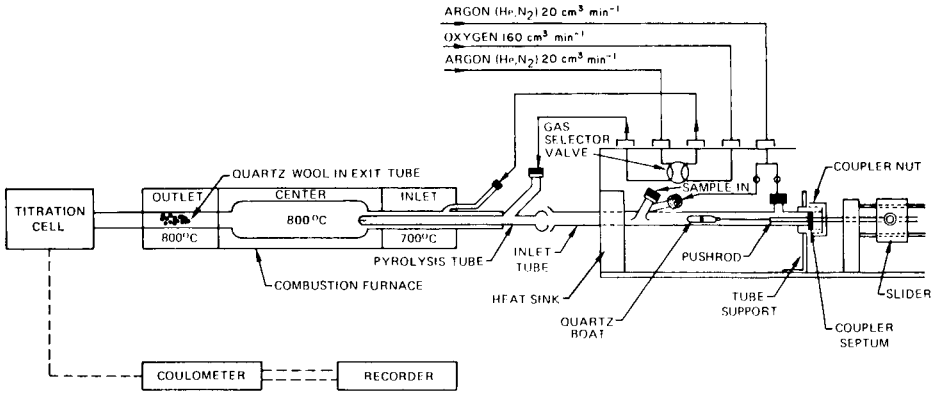

Fig. 1. Block diagram of instrument.

Experimental

Apparatus. The apparatus (Fig. 1) consists of the following standard Dohrmann microcoulometric components: (a) SBI single boat inlet; (b) S-300 pyrolysis furnace; (c) COT pyrolysis tube; (d) T-300 titration cell; (e) C200B microcoulometer; and (f) R-100-I recorder with disc integrator.

Reagents. Analytical-grade materials and deionized distilled water were used throughout. Aqueous sulfur stock solutions (1000 mg S l^{-1}) were prepared from sodium sulfate, sodium sulfite, potassium thiocyanate, sodium thiosulfate, potassium pyrosulfate and *o*-aminobenzene sulfonic acid. The aqueous generator electrolyte contains 0.05% potassium iodide, 0.06% sodium azide, and 0.50% acetic acid (all w/v) [3].

Procedure. The Dohrmann analyzer with the sample boat inlet is prepared for operation as recommended by the manufacturer. Sufficient phosphoric acid is added to the sample to give a ca. 1% (v/v) solution. For each analysis, a 25-μl aliquot of sample is injected into the quartz boat via the loading port from a 50-μl syringe. The quartz boat is then introduced half into the entrance of the combustion furnace. After the water has slowly and completely evaporated, the boat is introduced completely into the furnace. Rapid introduction of water causes a disruption of the cell electrolyte which appears as a negative peak on the recorder trace and invalidates the data. During injection of the sample and movement of the boat into the pyrolysis region, argon is swept over the sample. This sweeps all volatile sulfur compounds into the combustion zone where an oxygen flow is maintained. When the recorder indicates a peak and begins to return to the baseline, the oxygen and argon flows are reversed to allow oxidation of any residual sulfur in the sample boat. Should any residual sulfur be present, a second peak will appear. After the return to the baseline, the gas flows are switched to their original positions and the sample boat is withdrawn to the cooling block until the next analysis. The total sulfur is calculated from the integrated areas of the two peaks.

TABLE 1

Sulfur recoveries

Compound	Recovery (%)	Compound	Recovery (%)
Sodium sulfate	93.4	Sodium thiosulfate	95.5
Sodium sulfite	94.6	Potassium pyrosulfate	93.6
Potassium thiocyanate	96.4	*o*-Aminobenzene sulfonic acid	95.5

Results and discussion

Diluted solutions (10 ppm) of the selected sulfur-containing compounds were analyzed. The results (Table 1) show that recoveries do not vary significantly for different sulfur species. These recoveries are similar to those obtained for sulfur in petroleum standards. Although day-to-day recovery on sodium sulfate can vary between 75% and 98%, it is usually 90—95%. The variability is explained by the sensitivity of the equilibrium constant of the reaction $SO_2 + 1/2\ O_2 \rightleftharpoons SO_3$ to temperature changes, e.g., $K(800°C) = 0.93$, $K(827°C) = 0.55$ [5], as well as to variations in oxygen partial pressure. Accordingly, a calibration standard is needed with each set of samples. Sodium sulfate was chosen since it is one of the more difficult sulfur compounds to decompose and does not degrade on storage. High contents of organic halogen compounds (> 100 ppm halogen), except for fluorine compounds, should be avoided as they can form oxyhalogen compounds which interfere with the coulometric determination [3]. To confirm that this interference is a problem with inorganic halogen also, blanks and 10-ppm sodium sulfate samples were doped with 10 ppm, 100 ppm, and 1000 ppm chloride as sodium chloride. Negative peaks or decreased recoveries were not noted for 10 ppm and 100 ppm chloride, but a severe disruption of the cell equilibrium occurred with 1000 ppm chloride. If the sulfur content of a sample exceeds 200—300 ppm, the use of smaller samples or dilution is recommended to insure that the titration time is not extraordinarily long. Precision was found to be ±5% or about 0.1 ppm (whichever is greater).

TABLE 2

Water analyses

Sample	Total sulfur (ppm) (microcoulometry)	Sulfate sulfur (ppm) (turbidimetry)	Sample	Total sulfur (ppm) (microcoulometry)	Sulfate sulfur (ppm) (turbidimetry)
A	8.4	8.7	F	12	12
B	9.8	9.0	G	8.0	8.3
C	13	14.7	H	17	15
D	44	43	I	1.0	0.6
E	28	28	J	570	28

Table 2 shows some representative results on samples from a boiler system where sulfate was expected to be the only sulfur-containing species. The agreement with results obtained by the barium sulfate method is excellent, except for sample J which was suspected to be contaminated by the plasticizer in nylon tubing (*N*-ethyl-*p*-toluenesulfonamide).

The proposed technique provides a rapid measurement of total sulfur in aqueous samples where several species are present. This supplements the conventional applications of the apparatus to organic materials.

REFERENCES

1 Standard Methods for Examination of Water and Waste Water, 14th edn., American Public Health Assoc., 1976, p. 496.
2 M. C. van Grondelle, F. van de Craats, and J. D. van der Laarse, Anal. Chim. Acta, 92 (1977) 267.
3 L. D. Wallace, D. W. Kohlenberger, R. J. Joyce, R. T. Moore, M. E. Riddle and J. A. McNulty, Anal. Chem., 42 (1970) 387.
4 G. de Groot, P. A. Greve and R. A. A. Maes, Anal. Chim. Acta, 79 (1975) 279.
5 Handbook of Chemistry and Physics, R. C. Weast (Ed.), 53rd edn., CRC Press, 1972—73, p. D-45.

Analytica Chimica Acta, 110 (1979) 171—173

Short Communication

DETERMINATION OF ISONICOTINIC ACID HYDRAZIDE (ISONIAZID) BY THE WEISZ RING-OVEN TECHNIQUE

MUHAMMAD HANIF*, FARHAT JAMSHAID and SUMRA PARVEEN

Pakistan Council of Scientific and Industrial Research Laboratories, Lahore-16 (Pakistan)

(Received 28th February 1979)

Summary. A simple precise method is described for the determination of isonicotinic acid hydrazide (isoniazid) alone, and in mixtures with aspirin, paracetamol and streptomycin, by reaction with vanillin in the Weisz ring-oven technique; 0.1—15 μg of isoniazid can be determined with errors of 2—2.7%.

Isonicotinic acid hydrazide (isoniazid) is widely used in the treatment of tuberculosis [1]. In view of its therapeutic importance, rapid simple and sensitive methods for its determination are of interest. The methods normally recommended [2—4] tend to be lengthy or to require rigidly controlled conditions. In the Weisz ring-oven procedure described here, isoniazid reacts with vanillin in acidic media to produce a bright yellow color which has already been utilized photometrically [5].

Experimental

Isonicotinic acid hydrazide solutions. Dissolve 1.0 g of isoniazid (analytical grade, BDH) in 100 ml distilled water and standardize the solution potentiometrically [4]. Prepare working standards (1 μg μl^{-1}) by exact dilution of this stock. For the segment technique, prepare standard isoniazid solutions (0.1, 0.2, 0.4, 0.6, 0.8, and 1.0 μg μl^{-1}) and number these I, II, IV, VI, VIII, and X, respectively.

Other solutions used contained 1% (w/v) vanillin (analytical grade) in ethanol, and 1% (w/v) aspirin or paracetamol (Shazoo Laboratories, Lahore) or Streptomycin (Pfizer Laboratories, Pakistan) in water.

Apparatus. A Weisz ring oven was made in this Institute, according to the prescribed measurements [6] with a working temperature of 110°C. Whatman filter paper no. 41 and automatic capillary pipettes (1 μl and 2 μl; Karl Kolb Scientific and Technical supplies, Buchschlag, Frankfurt) were used. Calibrated grade A glassware was employed.

Procedure. Mark the centre of the filter paper with a pin and apply 1 μl of isoniazid solution and 1 μl of vanillin solution successively. Wash to the ring zone with distilled water; 8—10 washings suffice for complete transference. Remove the paper from the ring oven and immediately fume over concen-

trated hydrochloric acid for 2—3 min. A bright yellow ring appears. For unknown solutions, evaluate the ring against a standard scale prepared in the same way with 1, 2, 4, 6, 8 and 10 drops of the working 1.0 $\mu g\ \mu l^{-1}$ solution, as described by Weisz [6].

Unknown isoniazid solutions were also evaluated by the segment technique [7, 8] with the standard solutions labelled I—X (see below).

Results and discussion

Typical results obtained by the procedures recommended above (Table 1) show that isoniazid can be determined rapidly within the ranges 1.50—15.0 μg and 0.10—15.0 μg with maximum errors of 2—2.7% by the standard scale and segment techniques, respectively.

The standard scale was stable for only one working day; thereafter the color intensity of the rings decreased quickly. Consequently, the segment technique [7, 8] was preferred for evaluation.

Rings placed over hydrochloric acid fumes immediately after perparation, i.e., whilst still moist, became yellow very quickly. When the rings were allowed to dry on the ring oven, color development was slow and tended to be incomplete. Properly prepared rings were clear and distinct and there were no difficulties in evalution.

Isoniazid is normally administered alone, but it was considered worthwhile to examine the effects of aspirin, paracetamol and streptomycin on the determination. Up to 50-fold amounts of each of these drugs caused no interference for either of the evaluation methods and the rate of reaction was not affected. Accordingly, the method may be viable for the analysis of biological fluids.

TABLE 1

Determination of isoniazid by the standard scale and segment techniques

Standard scale method			Segment technique		
Isoniazid taken (μg)	Isoniazid found (μg)	Error (%)	Isoniazid taken (μg)	Isoniazid found (μg)	Error (%)
1.5	1.5	0.0	0.1	0.1	0.0
2.5	2.5	0.0	0.5	0.5	0.0
3.5	3.6	+2.0	1.0	1.0	+2.0
4.0	4.0	0.0	2.0	1.9	−2.5
5.0	5.0	0.0	4.0	4.0	0.0
8.0	8.0	0.0	6.0	6.0	0.0
11.0	10.8	−1.6	8.0	8.2	+2.7
12.0	12.0	0.0	10.0	10.2	+2.5
14.0	14.2	+1.4	12.5	12.3	−1.3
15.0	14.9	−0.9	15.0	14.9	−0.8

REFERENCES

1 Remington's Pharmaceutical Sciences, Mack Publishing, Easton, PA, 14th edn., 1970, p. 1241.
2 U. S. Pharmacopoeia, 19th edn., USPC, Rockville, Md., 1975, p. 273.
3 British Pharmacopoeia H.M.S.O., London, 1973, p. 256.
4 Specifications for the Quality Control of Pharmaceutical Preparations, W.H.O., Geneva, 2nd edn., 1971, p. 20.
5 A. S. Adil and M. Sarwar, private communication.
6 H. Weisz, Microanalysis by the Ring-Oven Technique, Pergamon Press, Oxford, 2nd edn., 1970.
7 H. Weisz, S. Pantel and I. Vereno, Mikrochim. Acta, (1975) 287.
8 H. Weisz and M. Hanif, Anal. Chim. Acta, 81 (1976) 179.

Analytica Chimica Acta, 110 (1979) 175—177

Short Communication

A SPECTROPHOTOMETRIC KINETIC ASSAY FOR ACID PHOSPHATASES WITH AROMATIC PHOSPHATES

K. R. LYNN* and CLAUDIO A. CHUAQUI

Division of Biological Sciences, National Research Council of Canada, Ottawa K1A OR6 (Canada)

(Received 3rd March 1979)

Summary. Acid phosphatases are measured by monitoring the rate of decomposition of various phenolic phosphates and/or production of the phenol at pH 4.8 (acetate buffer). All the substrates tested obey pseudo-first order kinetics; calibration plots are linear over wide ranges.

The activity of phosphatases which have pH optima in the acid range has commonly been measured by reaction with *p*-nitrophenyl phosphate in an acidic medium, followed by spectrophotometric determination of the produced *p*-nitrophenolate ion after adjustment of the pH to about 8.0 [1]. This simultaneously quenches the enzymatic reaction. The method is cumbersome and time-consuming, and is not suited to kinetic studies. Alternative assays for this latter purpose have been used [2] but are as unwieldy.

The spectra of many phenyl phosphates and their parent phenols (which are products of the phosphatase-catalysed hydrolyses) are distinctly different, even at low pH values. Thus it seemed possible directly to determine the rate of production of a phenol from its phosphate ester spectrophotometrically. The method is described here for assays of acid phosphatases with a variety of conventional substrates such as phenyl, *o*-carboxyphenyl, *p*-nitrophenyl and α- and β-naphthyl phosphates. Even when phenol/phenolate production could not be measured unambiguously, it was found that enzyme-catalysed phosphate hydrolysis could be monitored by the disappearance of the substrate.

Experimental

The substrates *p*-nitrophenyl, *o*-carboxyphenyl and α- and β-naphthyl phosphates were used as supplied (Sigma Chemical Co., ICN Pharmaceuticals and Calbiochem, respectively). Phenyl phosphate (Sigma) was purified by the procedure of Salomon et al. [3]. The acid phosphatase was prepared and purified by the method of Hsu et al. [4] after extraction from potatoes. Other reagents used were analytical grade.

Spectra were measured with the cell compartment of the Beckman Model 26 instrument kept at 21°C.

NRCC No. 17602.

Procedure for monitoring the enzyme-catalyzed reaction. To 2.90 ml of buffer (0.1 M sodium acetate at pH 4.8 was used unless specified otherwise) was added 0.1 ml of enzyme solution of suitable concentration in the same buffer. A 5-μl aliquot of the substrate (6×10^{-2} M in the buffer) was added at zero time to one cuvette, the other containing the reference sample, which was identical in all respects except that no substrate was added. Successive spectra were recorded at measured times thereafter, and the "infinity" spectrum (t_∞) was recorded commonly after the reaction had proceeded overnight ($>10\ t_{1/2}$).

Results

A typical experiment with *p*-nitrophenyl phosphate as substrate is recorded in Fig. 1. Under the conditions employed, the substrate concentration greatly exceeds that of the enzyme, and from the data in Fig. 1, a pseudo-first order plot can be prepared from the absorbances at a fixed wavelength. When the formation of the phenol produced was monitored, the rate constant was obtained from a plot of log $(A_\infty - A_t)$ vs. time (where A is the absorbance, and ∞ and t refer to infinite time and time t); log $(A_t - A_\infty)$ vs. time was plotted when the disappearance of the aryl phosphate was followed. The observed

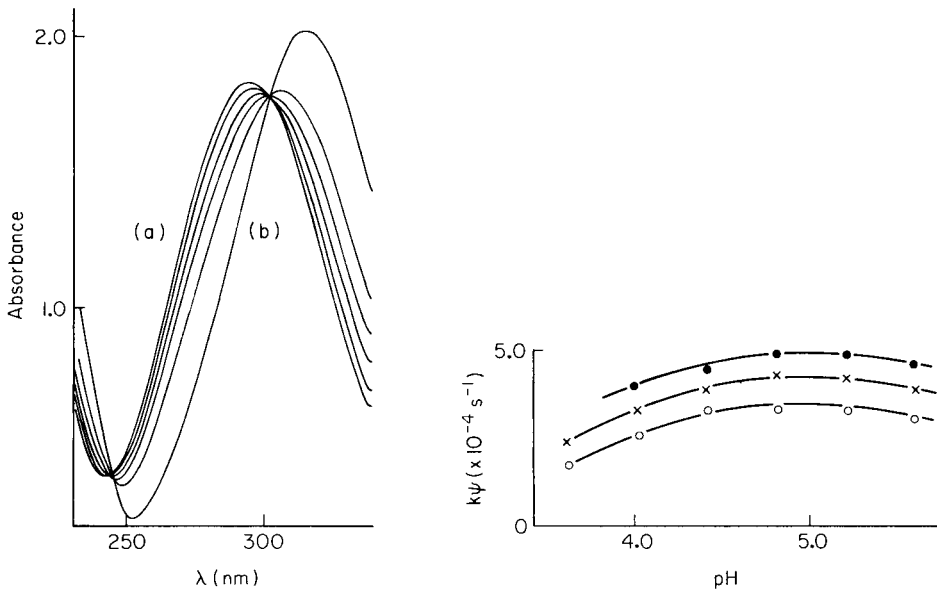

Fig. 1. Spectra measured during acid phosphatase-catalysed hydrolysis of *p*-nitrophenyl phosphate under the conditions described in the text. Successive measurements were made at (a) 30, 210, 540, 900 and 1380 s, (b) t_∞.

Fig. 2. Variation of rate constant with pH for *p*-nitrophenyl phosphate as substrate: (•) 3×10^{-4} M; (×) 1.6×10^{-4} M; (○) 4×10^{-5} M. Displacement of these plots was achieved by using different enzyme concentrations in each set of measurements.

pseudo-first order rate constant k_ψ was calculated as k_ψ = slope × 2.303. All substrates employed here obeyed pseudo-first order kinetics and thus linear plots were produced over at least two half-lives.

As a convenient alternative to this conventional procedure for calculating the rate constants, the method of Schwartz and Gelb [5] for treating first order reactions was applied with completely satisfactory results. In this procedure measurement of A_∞ is no longer required and so the kinetic analysis is facilitated.

The loss of the phosphate ester and the simultaneous production of the phenol could be followed only with *p*-nitrophenyl phosphate; with *o*-carboxyphenyl phosphate and phenyl phosphate only the formation of the product could be monitored, while with the two naphthyl phosphates, assay was restricted to measurements of the disappearance of the substrates, because of the spectra of the relevent species. However, pseudo-first order kinetics were followed with all these substrates. When possible, measurement of A_t at a wavelength between the isosbestic points is to be preferred.

As evidence that the concentration of substrate was in sufficient excess, three experiments in which that concentration was changed from 10^{-4} to 10^{-3} M (in the reaction mixture) gave values of $k_\psi = 13.6\ (\pm 0.2) \times 10^{-4}\ s^{-1}$. A linear relationship between the measured rate and the concentration of the enzyme was found over a sixty-fold range ($k_\psi = 13.6 \times 10^{-4}$ to $2.45 \times 10^{-5}\ s^{-1}$; slope, $4.5 \times 10^{-4}\ s^{-1}$/unit enzyme concentration).

As an application of this procedure, the effects of substrate concentration on the pH of maximum activity (pH_{max}) of potato acid phosphatase were measured. With mammalian alkaline phosphatase, the pH of maximum activity depends on the concentration of the substrate [6]. As can be seen in Fig. 2, a similar variation does not occur in the seven-fold range of substrate concentration investigated here; the pH_{max} is consistently at 5.0.

The procedure described is useful over the pH range 2.4—5.6, and seems to be of general applicability. At the higher pH values employed the hydrolysis product may yield a mixed spectrum of the phenol and phenolate ion, while in more acidic solutions only the phenol spectrum is produced. This change in the product spectrum has no effect on the pseudo-first order constants, because the phenol—phenoxide equilibrium is instantaneous and independent of the rate process studied.

REFERENCES

1 V. P. Hollander in P. D. Boyer (Ed.), The Enzymes, Vol. VI, Academic Press, New York, 1971.
2 G. B. Jorgensen, Acta Chem. Scand., 13 (1959) 900.
3 L. L. Salomon, J. James and P. R. Weaver, Anal. Chem., 36 (1964) 1162.
4 R. Y. Hsu, W. W. Cleland and L. Anderson, Biochemistry, 5 (1966) 799.
5 L. M. Schwartz and R. I. Gelb, Anal. Chem., 50 (1978) 1522.
6 H. N. Fernley in P. D. Boyer (Ed.), The Enzymes, Vol. IV, Academic Press, New York, 1971.

Analytica Chimica Acta, 110 (1979) 179—181

Short Communication

STEPWISE PRECIPITATION OF BARIUM SULPHATE, CHROMATE AND VANADATE BY CATION RELEASE

K. N. UPADHYAYA

Chemistry Department, University of Dar es Salaam, P.O. Box 35061, Dar es Salaam (Tanzania)

(Received 15th November 1978)

Summary. Sulphate is precipitated at pH 4.5—5.0 by adding Ba—EDTA complex. Chromate and vanadate are sequentially precipitated from the filtrate at pH 6—7 and 9, respectively, by adding magnesium to displace barium from its EDTA complex. The analyses are completed gravimetrically.

One way of obtaining controlled precipitation in gravimetric analysis is by replacement of one ion by another from an EDTA complex [1]. Nickel has been precipitated by displacing it from its EDTA complex with zinc, in the presence of dimethylglyoxime [2]. In a similar fashion, if magnesium ions are added to a barium—EDTA complex in the presence of sulphate or chromate, barium sulphate or chromate is precipitated [3]. The same principle has been used to determine thallium as thallium(I) chromate [4]. Firsching [5] has reported the determination of anions forming insoluble silver salts by release of silver from its ammine. The cation-release process has also been used in the separation of silver from lead [6].

Although the method of controlled precipitation has been applied to the determination of cations forming insoluble salts with sulphate and chromate, no attempt appears to have been made to achieve quantitative precipitation of these anions by cation release. The present work, therefore, was undertaken with a view to determining sulphate, chromate and vanadate by stepwise precipitation of their barium salts by release of barium from its EDTA complex.

Experimental

All the chemicals used were of reagent grade. Standardized solutions of sodium sulphate, potassium chromate and sodium metavanadate were used to prepare the solutions for analysis. A 0.02 M solution of barium—EDTA was made by dissolving barium chloride and disodium EDTA (in the ratio 190 mg of the latter to 70 mg of barium) in doubly distilled water.

Sequential determination of sulphate, chromate and vanadate. Take 15—60 ml of solution containing 0.2—0.8 mmol of each anion in a 400-ml beaker, dilute to 150 ml, adjust to pH 4.5—5.0 with acetic acid and ammonia and heat to near boiling. Add a slight excess ($\leqslant$ 48 ml) of the barium—EDTA sol-

ution dropwise with constant stirring and adjust the pH, if necessary, to 4.5—5.0. Heat on a water bath for 40 min, filter through ashless filter paper, wash 2—3 times with hot water and ignite after combustion of the paper. Weigh as $BaSO_4$.

Collect the filtrate and washings from the sulphate determination, and evaporate the solution to nearly 200 ml. Adjust the pH to 6.1, heat to near boiling and add 0.05 M magnesium nitrate solution at 1 drop per 4—6 s with constant stirring. Add rather more magnesium than is equivalent to the excess of EDTA and barium ($\leqslant$ 38 ml), allow the precipitate to settle, filter through a weighed sintered glass crucible, wash the precipitate 3—4 times with small portions of cold distilled water, dry at 105—110°C for 2 h and weigh as $BaCrO_4$.

Collect the filtrate and washings from the chromate determination, adjust the volume to about 200 ml, raise the pH to 9.1, add a further slight excess ($\leqslant$ 24 ml) of the barium—EDTA solution in one portion, if necessary readjust the pH, and heat the solution to near boiling. Add the magnesium solution at the rate of 1 drop per 4—6 s with constant stirring. Add rather more magnesium than that equivalent to the excess of EDTA and barium (e.g. 19 ml), then allow the precipitate to settle, filter, wash 3—4 times with ammoniacal distilled water, dry at 100—105°C for 2 h and weigh as $Ba(VO_3)_2$.

Results and discussion

The stepwise precipitation of sulphate, chromate and vanadate can be successfully carried out in a single solution by the method described (Table 1). The factors which are decisive in these determinations are mainly the difference in the stability constants of the Mg—EDTA ($\log K = 8.69$) and Ba—EDTA ($\log K = 7.76$) complexes and the pH-dependent solubilities of $BaSO_4$, $BaCrO_4$ and $Ba(VO_3)_2$. Barium sulphate is precipitated directly when the barium—EDTA complex is added at pH 4.5—5.0, the chromate is precipitated only when magnesium is added to displace barium from its EDTA complex at pH 6—7, and the precipitation of vanadate takes place only at above pH 9. If magnesium is not added and barium is present as its EDTA complex, the precipitation of barium chromate or barium vanadate does not take place even at pH 10. The extent of replacement of barium from its EDTA complex by magnesium is mainly governed by the insolubility of the particular barium salt at a given pH.

The addition of a slight excess of barium—EDTA is desirable at any stage, but too large an excess must be avoided. The pH ranges for the precipitations are critical. No overlapping precipitation was noticed even when the molar concentrations were in the ratio of 1:2 for any two ions, provided that the pH was accurately controlled. The results obtained were generally within 0.5% of the theoretical values (Table 1). The determination of sulphate was not affected at all by the presence of phosphate, tungstate, molybdate, arsenate, oxalate or fluoride. For chromate determinations, when the pH was maintained just above 6, none of these interfered, but at pH 7, phosphate began to interfere. In the vanadate determination, all these anions interfered seriously, as would be expected from the solubilities of their barium salts.

TABLE 1

Determination of sulphate, chromate and vanadate

Molar ratio (approx.) $SO_4^{2-}:CrO_4^{2-}:VO_3^{-}$[a]	Sulphate (mg)		Chromate (mg)		Vanadate (mg)	
	Taken	Found	Taken	Found	Taken	Found
1:1:1	19.2	19.1	23.2	23.3	19.8	19.9
	38.4	38.3	46.4	46.6	39.6	39.4
	57.6	57.8	69.6	69.4	59.4	59.6
2:1:1	38.4	38.2	23.2	23.3	19.8	19.9
	57.6	57.8	38.8	34.6	29.7	29.8
	76.8	76.5	46.4	46.5	39.6	39.3
1:2:1	19.2	19.3	46.4	46.2	19.8	19.7
	28.8	28.7	69.6	69.8	29.7	29.9
	38.4	38.3	92.8	92.5	39.6	39.4
1:1:2	19.2	19.1	23.2	23.1	39.6	39.8
	28.8	28.9	34.8	34.7	59.4	59.2
	38.4	38.5	46.4	46.6	79.2	78.8

[a]Each set of results is an average of five determinations.

REFERENCES

1 R. Belcher and C. L. Wilson, New Methods of Analytical Chemistry, Chapman and Hall, London, 2nd edn., 1964, p. 243; L. Gordon, M. L. Salutsky and H. H. Willard, Precipitation from Homogeneous Solution, J. Wiley, New York, 1959.
2 R. W. Ramette, private communication, reported by E. D. Salesin and L. Gordon, Talanta, 2 (1959) 392.
3 F. H. Firsching, Anal. Chem., 33 (1961) 1949.
4 K. N. Upadhyaya, Analyst, 103 (1978) 766.
5 F. H. Firsching, Anal. Chem., 32 (1960) 1976.
6 P. F. S. Cartright, Anal. Chem., 40 (1968) 1137.

Analytica Chimica Acta, 110 (1979) 183

Correction

Acid—base equilibria in the mixed solvent 80% dimethylsulfoxide—20% water

M. Georgieva, G. Velinov and O. Budevsky, *Anal. Chim. Acta, 90(1977) 83; 101(1978)139.*

In these publications the pK_a values of some aliphatic and aromatic acids were determined in mixed DMSO—water solvent. Unfortunately, some results of earlier investigators [1, 2] obtained by rather different potentiometric techniques were overlooked. Table 1 lists a number of pK_a values from both sources; agreement is good in most cases. There are some discrepancies (e.g. *o*-methoxybenzoic acid), for which no reasonable explanation is apparent, but the coincidence is sufficient for the purposes of nonaqueous titrations. With the present correction, we would like to point out the priority of the pK_a values obtained by Hallé et al. [1, 2].

TABLE 1

pK_a values of some carboxylic acids

Acid	pK_a^T	
Acetic	8.10 [1]	8.02 [3]
Monochloroacetic	5.66 [1]	5.77 [3]
Benzoic	7.30 [2]	7.32 [4]
o-Chlorobenzoic	6.23 [2]	6.44 [4]
p-Chlorobenzoic	6.65 [2]	6.48 [4]
3,5-Dinitrobenzoic	4.69 [2]	4.59 [4]
o-Methoxybenzoic	7.59 [2]	7.21 [4]

REFERENCES

1 J. C. Hallé and R. Schaal, Anal. Chim. Acta, 60 (1972) 197.
2 J. C. Hallé, R. Gaboriauch and R. Schaal, Bull. Soc. Chim. Fr. (1970) 2047.
3 M. Georgieva, G. Velinov and O. Budevsky, Anal. Chim. Acta, 90 (1977) 83.
4 M. Georgieva, G. Velinov and O. Budevsky, Anal. Chim. Acta, 101 (1978) 139.

(continued from outside of cover)

Short Communications

CONTENTS

(continued on inside page of the cover)

Printed in The Netherlands.